TAL TECH

DOCTORAL THESIS

Influence of Intrinsic and Extrinsic Factors on Mitochondrial Energy Metabolism in the Heart

Jekaterina Aid

TALLINNA TEHNIKAÜLIKOOL
TALLINN UNIVERSITY OF TECHNOLOGY
TALLINN 2024

Influence of Intrinsic and Extrinsic Factors on Mitochondrial Energy Metabolism in the Heart

JEKATERINA AID

**TAL
TECH**
PRESS

TALLINN UNIVERSITY OF TECHNOLOGY
School of Science, Department of Chemistry and Biotechnology
National Institute of Chemical Physics and Biophysics, Laboratory of Chemical Biology

This dissertation was accepted for the defence of the degree of Doctor of Philosophy in Gene Technology on 11/09/2024

Supervisor: Tuuli Käämbre, PhD
Head of the Laboratory of Chemical Biology
National Institute of Chemical Physics and Biophysics
Tallinn, Estonia

Co-supervisors: Kersti Tepp, PhD
National Institute of Chemical Physics and Biophysics
Tallinn, Estonia

Marju Puurand, PhD
National Institute of Chemical Physics and Biophysics
Tallinn, Estonia

Opponents: Prof. Pablo Miguel Garcia-Roves, PhD
Department of Physiological Sciences
University of Barcelona and Bellvitge Biomedical Research Institute
Barcelona, Spain

Prof. Arno Ruusalepp, PhD
Head of the Department of Cardiosurgery
Department of Cardiology
Heart Clinic and Tartu University Clinic
Tartu, Estonia

Defence of the thesis: 05/11/2024, Tallinn

Declaration:
Hereby, I declare that this doctoral thesis, my original investigation and achievement, submitted for the doctoral degree at Tallinn University of Technology, has not been submitted for a doctoral or equivalent academic degree.

Jekaterina Aid

_____
signature

Sisemiste ja väliste tegurite mõju südamelihase mitokondriaalsele energiametabolismile

JEKATERINA AID

Contents

List of Publications

This thesis is based on the following publications:

I   Tepp, K., Puurand, M., Timohhina, N., **Aid-Vanakova, J.**, Reile, I., Shevchuk, I., Chekulayev, V., Eimre, M., Peet, N., Kadaja, L., Paju, K., & Kaambre, T. (2020). Adaptation of striated muscles to Wolframin deficiency in mice: Alterations in cellular bioenergetics. Biochim Biophys Acta Gen Subj, 1864(4), 129523. https://doi.org/10.1016/j.bbagen.2020.129523

II   Tepp, K., **Aid-Vanakova**, J., Puurand, M., Timohhina, N., Reinsalu, L., Tein, K., Plaas, M., Shevchuk, I., Terasmaa, A., & Kaambre, T. (2022). Wolframin deficiency is accompanied with metabolic inflexibility in rat striated muscles. Biochem Biophys Rep, 30, 101250. https://doi.org/10.1016/j.bbrep.2022.101250

III **Aid, J.**, Tanjeko, A. T., Serre, J., Eggelbusch, M., Noort, W., de Wit, G. M. J., van Weeghel, M., Puurand, M., Tepp, K., Gayan-Ramirez, G., Degens, H., Kaambre, T., & Wust, R. C. I. (2024). Smoking cessation only partially reverses cardiac metabolic and structural remodeling in mice. Acta Physiol (Oxf), 240(7), e14145. https://doi.org/10.1111/apha.14145

Author's Contribution to the Publications

Contribution to the papers in this thesis are:

I   The author prepared solutions for experiments, assisted in conducting high-resolution respirometry, helped prepare animals for the experiments, and contributed to writing the manuscript.

II The author contributed to the conceptualization, conducted high-resolution respirometry, prepared solutions, assisted in animal preparation for experiments, developed the methodology, and wrote the original draft.

III The author was involved in the conceptualization, conducted all experiments, handled data analysis and visualization, and was responsible for writing and editing the original draft.

Introduction

Cardiovascular diseases (CVDs) remain a leading cause of morbidity and mortality globally, underscoring the critical need for a deeper understanding of the intricate mechanisms governing cardiac health and disease pathology. Among the myriad factors influencing cardiovascular health, mitochondrial dysfunction has emerged as a significant contributor, impacting cellular bioenergetics, metabolism, and overall cardiac function. Both intrinsic factors, such as genetic mutations, and extrinsic factors, including lifestyle habits like smoking, play pivotal roles in modulating mitochondrial bioenergetics and subsequent cardiac outcomes.

In this thesis, we extensively investigate the intricate influence of intrinsic and extrinsic factors on mitochondrial bioenergetics and inherent cardioprotective mechanisms in cardiac muscle tissue. Our study employs various methodologies, ranging from high-resolution respirometry and enzymatic activity assays to metabolomic profiling and morphological assessments, aiming to unravel the complex interplay between mitochondrial function and cardiovascular health.

Our exploration begins by examining the impact of intrinsic factors, specifically genetic mutations, on mitochondrial bioenergetics using Wolframin-deficient animal models. These models offer a unique opportunity to dissect the role of mitochondrial dysfunction within metabolic disorders, primarily focusing on diabetes. Through meticulous experimentation involving oxygraphic measurement protocols and enzymatic activity assays, we elucidate alterations in mitochondrial kinetics, substrate utilisation patterns, and energy transfer pathways in the cardiac muscle tissue of Wolframin-deficient animals.

Transitioning to extrinsic factors, we investigate the influence of cigarette smoking and subsequent smoking cessation on mitochondrial bioenergetics, metabolism, and structural integrity in cardiac tissue. Utilising a murine model of chronic obstructive pulmonary disease (COPD) exposed to cigarette smoke, followed by a period of smoking cessation, we uncover smoking-induced alterations in mitochondrial function, protein content, supercomplex formation, and metabolic profiles. Our findings illuminate the dynamic interplay between smoking exposure, smoking cessation, mitochondrial dysfunction, and subsequent cardiac pathology.

By synthesising the findings from intrinsic and extrinsic factor studies, we gain comprehensive insights into the intricate mechanisms governing mitochondrial bioenergetics and cardiovascular health. This thesis represents a significant advancement in understanding the multifaceted influences on cardiac muscle tissue, with far-reaching implications for preventing and treating cardiovascular diseases. Additionally, our study underscores the importance of lifestyle modifications and highlights the therapeutic implications of smoking cessation in promoting cardiovascular health and preventing mitochondrial dysfunction-associated cardiovascular diseases.

Abbreviations

ADP	Adenosine diphosphate
AK	Adenylate kinase
AMP	Adenosine monophosphate
ANT	Adenine nucleotide translocase
ATP	Adenosine triphosphate
ATPase	Adenosine triphosphatase
BCAA	Branched-chain amino acid
CI	Complex I, nicotinamide adenine dinucleotide ubiquinone reductase
CII	Complex II, succinate ubiquinone oxidoreductase
CIII	Complex III, ubiquinone cytochrome oxidoreductase
CIV	Complex IV, cytochrome c oxidase
CK	Creatine kinase
Co Q	Coenzyme Q, ubiquinone
CO2	Carbon dioxide
COPD	Chronic obstructive pulmonary disease
Cr	Creatine
CS	Citrate synthase
Cyt c	Cytochrome c
DNA	Deoxyribonucleic acid
DRP1	Dynamin-related protein 1
ER	Endoplasmic reticulum
ETC	Electron transport chain
FA	Fatty acid
FADH2	Flavin adenine dinucleotide
FAO	Fatty acid oxidation
FFA	Free fatty acid
GAPDH	Glutaraldehyde-3-phosphate dehydrogenase
GI	Glucose index
GLUT	Glucose transporter
GTP	Guanosine triphosphate
HBP	Hexosamine biosynthesis pathway
HK	Hexokinase
IAK	Adenylate kinase index
IMM	Inner mitochondrial membrane
IMP	Inosine monophosphate
IMS	Mitochondrial intermembrane space
$K_m(ADP)$	Apparent Michaelis-Menten constant for ADP
MAM	Mitochondria-associated ER membrane
MI	Mitochondrial Interactosome
MtCK	Mitochondrial creatine kinase
mtDNA	Mitochondrial DNA
NADH	Nicotinamide adenine dinucleotide
NADPH	Nicotinamide adenine dinucleotide phosphate
NMNH	Nicotinamide mononucleotide
NTP	Nucleoside diphosphate

Oct	Octanoyl carnitine
OMM	Outer mitochondrial membrane
OPA1	Optic atrophy 1 protein
OXPHOS	Mitochondrial oxidative phosphorylation
PAGE	Polyacrylamide gel electrophoresis
PCr	Phosphocreatine
PEP	Phosphoenolpyruvate
PGK	Phosphoglycerate kinase
Pi	Inorganic phosphate
PK	Pyruvate kinase
PPP	Pentose phosphate pathway
ROS	Reactive oxygen species
SC	Supercomplex
SDH	Succinate dehydrogenase
SERCA	Sarcoplasmic/endoplasmic reticulum Ca^{2+}-ATPase
TCA	Tricarboxylic acid
UPR	Unfolded protein response
VDAC	Voltage-dependent anion channel
WFS1 KO	Wolfram syndrome-1 gene knockout
WS	Wolfram syndrome
WT	Wild type

1 Literature Review

1.1 Cellular Energetics in Cardiomyocytes

The heart, like any other organ, tightly integrates function with metabolism. Cardiomyocyte development and maturation are accompanied by extensive changes in energy metabolism. During the transition from neonate to newborn, cardiomyocytes undergo dramatic metabolic changes, shifting from a glycolytic state to mitochondrial oxidative metabolism (Fisher et al., 1980; Wisneski, Gertz, Neese, Gruenke, Morris, et al., 1985). Cardiac metabolism operates within a dynamic balance to ensure efficient energy transfer at the site of ATP production in the mitochondria and its utilisation at the cross-bridges during contraction and relaxation. The rate of energy turnover, rather than the ATP content of the tissue, serves as the primary determinant of energy metabolism (Balaban, 2002; Balaban et al., 1986; Kupriyanov et al., 1987; Taegtmeyer et al., 1985). As workload increases, so does ATP turnover, leading to elevated oxygen consumption rates and substrate utilisation (Balaban et al., 1986; Katz et al., 1989; Sharma et al., 2005). Key ATP-consuming processes in cardiac muscle include the activity of the actin-myosin ATPase, the sarcoplasmic reticulum calcium ATPase (SERCA) pump, and the sodium-potassium ATPase (Na^+/K^+ ATPase), underscoring the critical need for a continuous energy supply to support muscle function (Tran et al., 2015). Adult cardiomyocytes utilise various substrates, including fatty acids, glucose, lactate, amino acids, and ketone bodies (Chatham, 2002; Gandoy-Fieiras et al., 2020; Stanley et al., 2005), for ATP production through substrate oxidation, ultimately leading to carbon dioxide (CO_2) production.

Fatty acids, esterified as triglycerides, represent the primary fuel source (60–90%) for cardiac contraction (Figure 1) (Bing et al., 1954; Stanley et al., 2005). The pathway of long-chain fatty acid oxidation initiates with the activation of free fatty acids (FFA) in the cytosol with high-energy phosphates, followed by their conversion to acyl-CoA, which is transported into the mitochondrial matrix via the carnitine shuttle where β-oxidation proceeds (van der Vusse et al., 2000). Each cycle of β-oxidation yields one molecule of acetyl-CoA and shortens the acyl-CoA chain by two carbons until the original FFA molecule is fully decomposed into acetyl-CoA. Concurrently, nicotinamide adenine dinucleotide (NADH) and flavin adenine dinucleotide ($FADH_2$) are generated once per cycle (Lopaschuk et al., 2010). Subsequently, 70–90% of fatty acids undergo immediate oxidation, while the remainder is stored in intracellular triglyceride pools (Lopaschuk et al., 1994).

Although long-chain fatty acids serve as the primary energy substrate for the post-natal heart, carbohydrates play this role in the fetal heart (Fisher et al., 1980) and during conditions of exercise or pressure overload in the adult heart (Bishop & Altschuld, 1970; Goodwin & Taegtmeyer, 2000). Glucose enters cardiomyocytes primarily via GLUT-1 and GLUT-4 transporters (Figure 1) (Abel, 2004; Aerni-Flessner et al., 2012; Olson & Pessin, 1996; Razeghi et al., 2001), which undergo translocation to the sarcolemma. Insulin-mediated GLUT-4 predominates as the major glucose transporter in cardiac and skeletal muscle (Abel, 2004). Phosphorylation of glucose by hexokinase (HK) becomes the rate-limiting step for glycolysis during high rates of glucose transport. Hexokinase catalyses the initial phosphorylation of glucose to form glucose-6-phosphate (Roberts & Miyamoto, 2015; Wilson, 2003). This reaction is irreversible since there is no glucose-6-phosphatase in the heart (van Schaftingen & Gerin, 2002). Cardiac HK exists in two isoforms: hexokinase-1 (HK1) and hexokinase-2 (HK2), with the latter being the

predominant isoform (Printz et al., 1993; Wilson, 1995). Despite being a cytosolic enzyme, HK2 exhibits a preference for ATP generated in the mitochondria (Arora & Pedersen, 1988). Hexokinase forms oligomeric complexes through cooperative binding to specific contact points between the mitochondrial inner (IMM) and outer membranes (OMM), thereby accelerating phosphorylation and increasing glycolytic flux (Brdiczka et al., 1998; Russell et al., 1992). While HK demonstrates a high affinity for glucose, it can also utilise fructose or galactose as substrates (Lange & Kohn, 1961; Sols & Crane, 1954). The glycolytic breakdown culminates in the formation of pyruvate, which then undergoes various metabolic fates, including decarboxylation to acetyl-CoA, reduction to lactate, carboxylation to oxaloacetate or malate, or transamination with glutamate to alanine (Peuhkurinen & Hassinen, 1982; Russell & Taegtmeyer, 1991; Taegtmeyer et al., 1977). The fate of pyruvate is determined by metabolic demands and the cellular redox state (Prochownik & Wang, 2021). In well-oxygenated and actively contracting heart muscle, a major portion of pyruvate is transported into the mitochondria through specific transporters, where it is oxidised to acetyl-CoA (Laughlin et al., 1993; McCommis & Finck, 2015; Yiew & Finck, 2022). Acetyl-CoA, the activated two-carbon substrate fragment, initiates the final common pathway for cardiac energy substrates: FFAs, glucose, and lactate. Full oxidation of glucose contributes 10-40% of cardiac energy production (Gertz et al., 1988; Wisneski, Gertz, Neese, Gruenke, & Craig, 1985), with additional pathways like the pentose phosphate pathway (PPP) and the hexosamine biosynthesis pathway (HBP). However, these alternate pathways become more prominent when glycolysis is constrained, such as during elevated levels of FFAs or increased superoxide production (Du et al., 2000; Gupte et al., 2006; Schmitz-Peiffer, 2000).
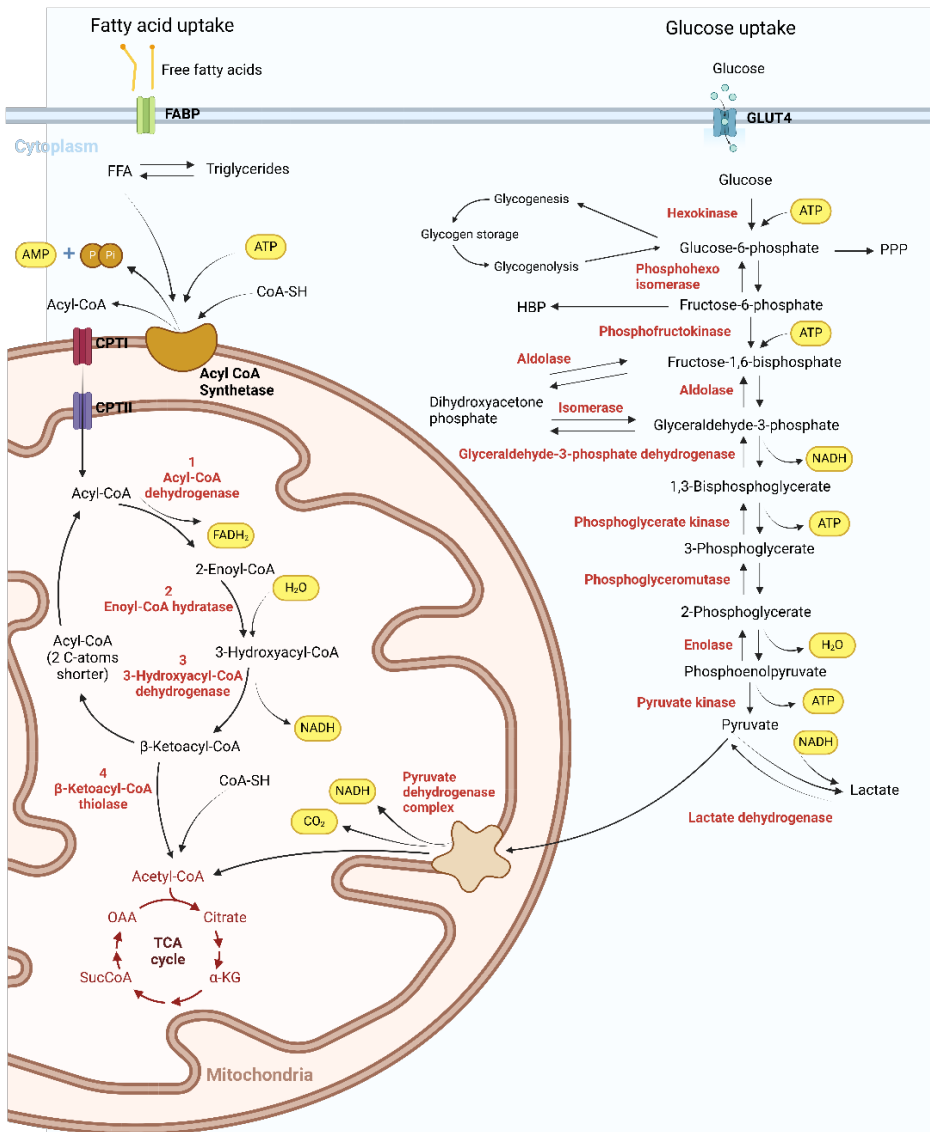
Figure 1. A simplified representation of the mitochondrial fatty acid oxidation and glycolysis in cardiomyocytes. FABP, fatty acid-binding protein, facilitates the transport of fatty acids within the cell; FFA, free fatty acids, enter cardiomyocytes and are transported to mitochondria; CPTI, carnitine palmitoyltransferase I, converts fatty acyl-CoA to fatty acyl-carnitine for transport into mitochondria; CPTII, carnitine palmitoyltransferase II, converts fatty acyl-carnitine back to fatty acyl-CoA inside mitochondria; GLUT4, glucose transporter 4, facilitates glucose entry into the cell; PPP, pentose phosphate pathway, produces NADPH and ribose-5-phosphate for nucleotide synthesis and antioxidant defence; HBP, hexosamine biosynthesis pathway, produces UDP-N-acetylglucosamine for protein glycosylation; TCA cycle, tricarboxylic acid cycle; α-KG, α-ketoglutaric acid; SucCoA, succinyl CoA; OAA, oxaloacetate; ATP, adenosine triphosphate; ADP, adenosine diphosphate; AMP, adenosine monophosphate; FADH$_2$, flavin adenine dinucleotide; NADH, nicotinamide adenine dinucleotide. The figure is created with BioRender.com.

The PPP serves as an alternative pathway for glucose utilisation, encompassing both aerobic and anaerobic segments. The aerobic phase of the PPP yields ribulose-5-phosphate, CO_2, and reduced nicotinamide adenine dinucleotide phosphate (NADPH). One molecule of glucose generates one molecule of ribulose-5-phosphate and two molecules of NADPH. Following the anaerobic conversion of ribulose-5-phosphate, no energy is produced, but it results in the regeneration of glucose-6-phosphate (Stincone et al., 2015). This regenerated glucose-6-phosphate can re-enter other glycolytic pathways, such as glycolysis or the hexosamine biosynthesis pathway. NADPH, a product of the PPP, is primarily utilised for fatty acid synthesis, pyruvate oxidation to malate, and the reduction of glutathione. Ribulose-5-phosphate, derived from the aerobic segment of the PPP, can readily be converted to ribose-5-phosphate, which is integral to the synthesis of nucleotides and nucleic acids (Stincone et al., 2015).

Intracellular glycogen stores also serve as a potential reservoir of glucose in cardiomyocytes, although they are relatively small compared to tissues like the liver or skeletal muscle (Besford et al., 2012). Despite their modest size, cardiac glycogen stores undergo rapid turnover, converting glucose to glycogen for storage and vice versa for substrate supply in glycolysis, thereby maintaining stable glycogen concentrations within cardiomyocytes (Figure 1) (Depre et al., 1999). Increased levels of adenosine monophosphate (AMP), inorganic phosphate, and a decrease in ATP concentration stimulate glycogenolysis, leading to an augmented substrate provision for glycolysis (Depre et al., 1998).

In addition to fatty acids and glucose, the heart can utilise amino acids as substrates for energy production (Banos et al., 1978; Murashige et al., 2020). Among these, the branched-chain amino acids (BCAA) valine, leucine, and isoleucine are metabolised within cardiac muscle (Neinast et al., 2019). These BCAAs are of particular interest in understanding the regulation of cardiac metabolism and the pathogenesis of common diseases such as insulin resistance, diabetes, and cardiovascular diseases (Gao et al., 2021; Karwi & Lopaschuk, 2023; Newgard, 2012). Specifically, leucine and its metabolites, along with valine and isoleucine, have demonstrated inhibitory effects on protein degradation and the promotion of protein synthesis in the heart, potentially influencing protein turnover regulation (Chua et al., 1979).

1.2 Mitochondria

Mitochondria play a pivotal role in maintaining cellular energy balance by efficiently converting adenosine diphosphate (ADP) and inorganic phosphate (P_i) to adenosine triphosphate (ATP) through oxidative phosphorylation (OXPHOS) in response to varying energy demands (Ernster & Schatz, 1981; Kuhlbrandt, 2015). Structurally, mitochondria comprise inner and outer membranes enclosing an intermembrane space (IMS) (Kuhlbrandt, 2015). These membranes feature transporters facilitating the bidirectional transport of metabolites and proteins between the mitochondria and the cytosol, enabling inter-organelle communication. The inner membrane forms cristae, invaginations that augment surface area and serve as sites for electron transport chain (ETC) enzymes (Figure 2), while the matrix houses enzymes, metabolic intermediates, mitochondrial DNA, and ribosomes (Chinnery & Hudson, 2013; Palade, 1953; Protasoni & Zeviani, 2021). The inner mitochondrial membrane (IMM) exhibits selective permeability, inhibiting the passage of most small molecules, including

protons (H^+). In mitochondria with tightly regulated proton gradients, the intact IMM minimises proton backflow, thus ensuring the efficiency of mitochondrial OXPHOS (Nicholls, 1974; Palmieri & Pierri, 2010; van Loon et al., 1987).
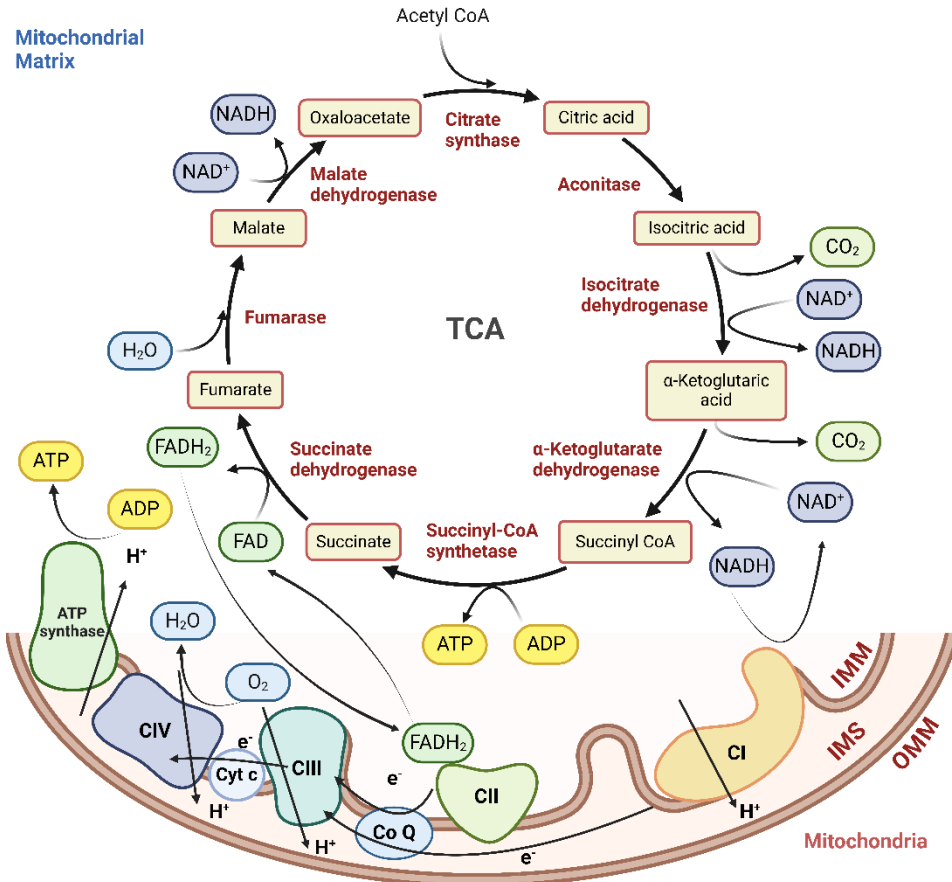
Figure 2. Representation of the TCA cycle and mitochondrial electron transport chain (ETC). The TCA cycle (tricarboxylic acid cycle), known as the Krebs or citric acid cycle, occurs in the mitochondrial matrix and generates high-energy electron carriers (NADH and FADH$_2$) and metabolic intermediates. The electron transport chain (ETC) is located in the IMM and comprises four complexes (CI, CII, CIII, CIV) and ATP synthase. CI transfers electrons from NADH to Co Q, pumping protons into the IMS. CII transfers electrons from FADH$_2$ to Co Q but does not pump protons. Co Q transfers electrons from CI and CII to CIII. CIII transfers electrons from Co Q to Cyt c, pumping protons into the IMS. Cyt c transfers electrons from Complex III to Complex IV. CIV transfers electrons to O$_2$, the final electron acceptor, forming H$_2$O and pumping protons into the IMS. ATP synthase utilises the proton gradient created by the ETC to synthesise ATP from ADP and inorganic phosphate (Pi). IMM, inner mitochondrial membrane; IMS, mitochondrial intermembrane space; OMM, outer mitochondrial membrane; Cyt c, cytochrome c; Co Q, coenzyme Q or ubiquinone. The figure is created with BioRender.com.

In cardiomyocytes, which are characterised by elevated and fluctuating energy demands, mitochondria typically occupy approximately 30–40% of the cellular volume (Barth et al., 1992; Marin-Garcia et al., 2001). Mitochondrial morphology varies across muscle fiber types (oxidative and glycolytic), with oxidative fibers exhibiting a more ordered arrangement between myofibrils, facilitating efficient energy transfer to ATPases (Anmann et al., 2006; Vendelin et al., 2005). This variation is essential for optimising cellular energy metabolism. There is a strong correlation between mitochondrial volume fraction, heart rate, and total body oxygen consumption, with mitochondrial volume fractions varying from 25% in humans to 38% in mice (Barth et al., 1992). Heart muscle mitochondria are plentiful and possess a significantly higher density of cristae than those found in other organs like the liver, brain, or skeletal muscle (Adams et al., 2023). These high cristae density reflects cardiac tissue's specialised metabolic and energy demands. Mitochondria are dynamic organelles that undergo fission and fusion, regulated by proteins like DRP1 and OPA1 (Pernas & Scorrano, 2016). DRP1 orchestrates mitochondrial fission, generating smaller mitochondria and ensuring mitochondrial quality control, distribution, and turnover (Pernas & Scorrano, 2016). Conversely, OPA1 is crucial for mitochondrial fusion, facilitating the merging of multiple mitochondria into a single organelle and maintaining mitochondrial function, integrity, and bioenergetic efficiency (Lin et al., 2022; Yapa et al., 2021). Beyond ATP synthesis, mitochondria play pivotal roles in various cellular processes, including thermogenesis, cellular signalling, and the maintenance of ion homeostasis (Bertholet & Kirichok, 2022; Rossi et al., 2019; Tait & Green, 2012). Additionally, they are involved in signalling pathways related to cell death, highlighting their central role in metabolic regulation, particularly in conditions like diabetes and heart failure (Chakrabarty & Chandel, 2022; Green et al., 2011; Takeda et al., 2023).

Inside the mitochondrial matrix, the tricarboxylic acid (TCA) cycle orchestrates the degradation of acetyl CoA to CO_2 while concurrently generating the reducing equivalents nicotinamide adenine dinucleotide (NADH) and flavin adenine dinucleotide ($FADH_2$) (Figure 2) (Fernie et al., 2004; Martinez-Reyes & Chandel, 2020). These electron carriers subsequently fuel the electron transport chain, catalysing the translocation of hydrogen ions outside the inner mitochondrial membrane and establishing a proton gradient. This gradient drives ATP synthesis via OXPHOS, wherein protons derived from NADH and $FADH_2$ combine with oxygen to yield water (Fernie et al., 2004). This fundamental process interconnects glycolysis, fatty acid oxidation, and amino acid oxidation pathways. It connects all catabolic pathways for substrate oxidation with respiration and serves as a primary source of biosynthetic precursors for numerous anabolic processes (Doenst et al., 2013).

1.2.1 Respiratory Chain

The complexes comprising the mitochondrial respiratory chain are localised within the inner mitochondrial membrane and encompass a nicotinamide adenine dinucleotide ubiquinone reductase (Complex I, CI), a succinate ubiquinone oxidoreductase (Complex II, CII), ubiquinone cytochrome oxidoreductase (Complex III, CIII), and cytochrome c oxidase (Complex IV, CIV) (Figure 2). Additionally, two mobile electron carriers, ubiquinone (Coenzyme Q, Co Q) and cytochrome c (Cyt c), participate in electron transfer between these complexes (Sousa et al., 2018). Ubiquinone undergoes diffusion within the IMM, migrating from CI to CIII as part of the electron transport chain process (Lenaz & Genova, 2009; Schneider et al., 1982).

Complex I, recognised as one of the largest, L-shaped enzymes in mammalian cells, facilitates the simultaneous transfer of two electrons from NADH to ubiquinone while translocating four protons across the membrane into intermembrane space, thereby establishing a proton gradient (Wirth et al., 2016). This complex plays a crucial role in NADH oxidation within the mitochondrial matrix, contributing to the regeneration of NAD^+ for sustaining the TCA cycle and fatty acid oxidation (Arnold & Finley, 2023).

Complex II facilitates the transfer of electrons from succinate to ubiquinone within the mitochondrial respiratory chain (Cecchini, 2003). Additionally, fatty acids and glycerol-3-phosphate can channel electrons into the ubiquinone pool. While CII does not directly contribute to establishing the proton gradient, it plays a crucial role in the oxidation of succinate to fumarate (Arnold & Finley, 2023). This process reduces ubiquinone to ubiquinol, thereby increasing the pool of electrons available to CIII and CIV for further electron transport (Cecchini, 2003).

Complex III occupies a central position within the respiratory chain, facilitating the transfer of electrons from ubiquinone, supplied by both CI and CII, to cytochrome c within CIV. This process is integral to establishing the proton gradient across the mitochondrial membrane and crucial for ATP synthesis (Rich & Marechal, 2010).

Complex IV, also referred to as cytochrome c oxidase, stands out as the sole OXPHOS complex documented to possess tissue-specific subunits, suggesting a potential role in modulating enzyme activity to suit the requirements of distinct tissues (Sinkler et al., 2017). Functionally, CIV facilitates the oxidation of reduced cytochrome c by molecular oxygen, serving as the terminal electron acceptor within the electron transport chain.

Electron transport through CI, CIII, and CIV drives the expulsion of protons from the mitochondrial matrix into the intermembrane space, culminating in establishing an electrochemical gradient across the IMM. Upon its release through Complex V (the F_0F_1-ATPase; CV), this proton motive force drives the synthesis of ATP from ADP and inorganic phosphate (Walker, 2013).

The reduction of molecular oxygen (O_2) within CIV must proceed without the release of partially reduced intermediates, such as hydrogen peroxide and hydroxyl free radicals, which have the potential to cause damage to cellular components (Turrens, 2003). Additionally, recent research suggests a dynamic interconversion between CIV's monomeric and dimeric states via reversible phosphorylation. Specifically, under elevated ATP/ADP ratios, the dimeric form of CIV is induced, inhibiting respiration and serving as a mechanism to prevent the generation of reactive oxygen species (ROS) (Ramzan et al., 2019).

1.2.2 Supercomplexes

Through the utilisation of cryo-electron microscopy and blue native PAGE analysis on digitonin-extracted mitochondria, it has been shown that CI, CII, CIII, and CIV are involved in the formation of larger higher-order structural units known as supercomplexes (SCs) (Schagger & Pfeiffer, 2000, 2001). Existing evidence indicates that the mitochondrial respiratory chain consists of individual complexes and SCs, co-localized within the IMM, both contributing to electron transfer and OXPHOS functions (Acin-Perez et al., 2008; Lapuente-Brun et al., 2013; Mourier et al., 2014). The balance of free complexes and SCs can be dynamically adjusted to accommodate internal environmental cues (Acin-Perez et al., 2008; Lapuente-Brun et al., 2013). Notably, in mammalian cell lines, elevated galactose levels have been shown to promote SC assembly, ensuring optimal functionality of the electron transport chain (Acin-Perez & Enriquez, 2014).

SCs exhibit two primary categories: those incorporating CI and those lacking it. Among SCs containing CI are CI/III, CI/III/IV, and CI/II/III/IV, while CI is absent in SCs such as CIII/IV and CII/III/IV (Acin-Perez et al., 2008; Cogliati et al., 2016; Lapuente-Brun et al., 2013). SCs display considerable heterogeneity across species, tissue types, and physiological conditions. In mammals, the majority of CI is bound within SCs, with 54% consisting of $CI/III_2/IV$ and 17% of CI/III_2 configurations (Letts et al., 2016; Schagger & Pfeiffer, 2000). Various SC combinations exist, including CI/III_2, $CI/III_2/IV_n$ (n = 1–4), and $CIII_2/IV_n$ (n = 1 or 2) (Acin-Perez et al., 2008). The predominant SC assembly observed through native electrophoresis techniques is $CI/III_2/IV_n$, which encompasses all complexes required to transfer electrons from NADH to oxygen (Letts et al., 2016; Schagger & Pfeiffer, 2000). These structures, which contain all essential components for electron transmission from NADH to oxygen, are referred to as respirasomes (Acin-Perez et al., 2008; Schagger & Pfeiffer, 2000; Shinzawa-Itoh et al., 2016). In 2017, Yang et al. identified a higher-order assembly termed a megacomplex composed of $CI_2/III_2/IV_2$ (Guo et al., 2017).

The formation of SCs facilitates the diffusion of ubiquinone and cytochrome c by reducing the intercomplex distance and enhancing electron transfer efficiency. Additionally, the assembly of SCs has been demonstrated to promote efficient energy production (Genova & Lenaz, 2014; Ikeda et al., 2013; Lapuente-Brun et al., 2013), stabilise CI (Schagger et al., 2004), facilitate substrate channelling (Wheeldon et al., 2016), stabilise individual complexes (Bianchi et al., 2004; Letts et al., 2016; Protasoni et al., 2020; Stroh et al., 2004), and provide protection against reactive oxygen species (ROS) (Genova & Lenaz, 2015; Lopez-Fabuel et al., 2016; Maranzana et al., 2013). ROS production, primarily originating from CI and CIII, may decrease with enhanced electron flux between complexes (Lenaz, 2012; Maranzana et al., 2013). $CIII_2/IV$, compared to free CIII and CIV, enhances mitochondrial respiration and ATP synthesis efficiency (Lapuente-Brun et al., 2013). Moreover, studies have revealed that CIII acts as the central hub for the assembly of SCs. A central role of CIII was evidenced by the observation that the physical deletion of CIII led to a decrease in CI assembly, while inhibition of CIII activity did not have the same effect (Acin-Perez et al., 2004; Protasoni et al., 2020). Thus, the dynamic assembly and disassembly of SCs play a pivotal role in regulating mitochondrial respiratory chain activity. It is noteworthy that CII is notably absent in most reported SC structures, except for one instance – $CI/II/III_2/IV_2$ (Muhleip et al., 2023). When present, CII's asymmetrical shape induces curvature in the SC, leading to a hypothesis that its inclusion may stabilise cristae folds. However, the absence of CII in most SCs suggests a lower affinity, possibly due to its limited protein-protein interactions with other complexes, implying that a significant portion of CII exists outside these SCs (Iverson et al., 2023; Muhleip et al., 2023).

Studies over the past decade have presented evidence showing the interconnected relationship between mitochondrial dynamics, cristae morphology, and respiratory function. For instance, observations of mitochondrial elongation and cristae remodelling during nutrient deprivation or ischemic episodes highlighted the role of these structural adaptations in preserving mitochondrial ATP production efficiency under challenging conditions (Gomes & Scorrano, 2011; Khacho et al., 2014; Patten et al., 2014). The remodelling processes occurring in mitochondria and cristae under such stressors can modulate mitochondrial efficiency by promoting the assembly of SCs and enhancing the respiratory reserve capacity (Cogliati et al., 2013; Khacho et al., 2014; Patten et al., 2014). The assembly of mitochondrial SCs is regulated by various factors, including mitochondrial cristae morphology, phospholipids, assembly factors, and others. OPA1,

a protein crucial for maintaining mitochondrial cristae morphology, has been implicated in the formation of respiratory chain SCs (Azuma et al., 2020; Cogliati et al., 2013). Depletion of OPA1 results in the disarray of cristae structure, leading to the disturbance of SC assembly and impairment of respiratory capacity (Cogliati et al., 2013; Patten et al., 2014). Furthermore, even a modest increase in OPA1 levels can promote cristae constriction, enhance the activity of respiratory enzymes, and improve mitochondrial respiration efficiency (Cogliati et al., 2013).

The disruption of SC assembly can significantly contribute to the pathogenesis of various diseases. Evidence suggests that impaired SC assembly is implicated in a range of disease models, including neurodegenerative diseases, genetic disorders, heart failure, and cancer (Baertling et al., 2017; Kim et al., 2018; Novack et al., 2020; Vercellino & Sazanov, 2022). Additionally, studies have demonstrated that ageing is associated with a decline in SC formation in rat hearts (Gomez et al., 2009). However, preserving SC organisation during ageing may exhibit tissue-specific differences (Lombardi et al., 2009).

1.3 Phosphotransfer Networks and Mitochondrial Interactosome

Phosphotransfer networks, including creatine kinase (CK), adenylate kinase (AK), and glycolytic/glycogenolytic enzymes, constitute the cardiac bioenergetic infrastructure. These networks catalyse reactions that drive high-energy phosphoryl flux, maintaining a rapid turnover rate of ATP and ADP at sites of energy generation and consumption (Figure 3) (Chung et al., 2010; Dzeja & Terzic, 2003; Guzun et al., 2015; Saks et al., 2006). In a healthy heart, the majority of newly synthesised ATP molecules undergo processing by CK (80–88%), AK phosphotransferases (15%), and glycolytic transfer systems (5–7%) before utilisation (Aliev et al., 2011; Dzeja, Hoyer, et al., 2011; Nemutlu et al., 2012; Pucar et al., 2001). These phosphotransfer networks play critical roles in cells and tissues experiencing high and intermittent energy fluctuations (Dzeja & Terzic, 2003; Gruno et al., 2006; Wallimann et al., 2011; Wallimann et al., 1992). Directly transferring phosphoryl groups through enzymatic reactions from mitochondria to energy consumption sites, such as ATPases, is essential for efficient energy utilisation (Dzeja & Terzic, 2003). ADP diffusion towards mitochondria holds regulatory significance as a limiting factor for ATPase activity. Maintaining a high ATP/ADP ratio near ATPases is crucial for their efficiency, necessitating the removal of ADP from the ATPases' microenvironment (Figure 3) (Wallimann et al., 1992; Zala et al., 2017). Moreover, the produced ADP serves as a signal for sufficient ATP synthesis in mitochondria.

Mitochondrial affinity to exogenous ADP varies among cell types and can be characterised by the apparent Michaelis-Menten constant K_m(ADP) (Kuznetsov et al., 1996). The K_m (ADP) reflects the substrate concentration required to achieve half of the maximum respiration rate in mitochondria (Wong et al., 2017). It represents a measure of the affinity of mitochondria for ADP during OXPHOS, reflecting how effectively ADP stimulates mitochondrial respiration. A lower K_m(ADP) value indicates a higher affinity of mitochondria for ADP, meaning that mitochondrial respiration is stimulated even at lower concentrations of ADP. Conversely, a higher K_m(ADP) value indicates a lower affinity for ADP, requiring higher concentrations of ADP to achieve the same level of stimulation in mitochondrial respiration (Appaix et al., 2003). Changes in K_m(ADP) values can reflect alterations in the regulation of cellular energy production and diffusion restrictions of energy metabolites through OMM (Tepp et al., 2017). Thus, the K_m(ADP) serves as an important parameter for assessing mitochondrial function and cellular bioenergetics (Kuznetsov et al., 2022). In permeabilised cardiac muscle, the K_m(ADP) is

approximately 400 µM, whereas, for isolated mitochondria, it is significantly lower, around 20 µM (Guzun et al., 2012; Guzun et al., 2009; Saks, Belikova, & Kuznetsov, 1991; Saks, Belikova, Kuznetsov, et al., 1991). This difference arises from the voltage-dependent anion channel (VDAC) located on the OMM, which selectively facilitates the flux of various metabolites essential for cellular metabolism, including ATP, ADP, AMP, NADH, and NADPH (Colombini, 2016; Noskov et al., 2016; Rostovtseva & Bezrukov, 2008; Rostovtseva et al., 2008). The isolation steps affect this property of mitochondria to restrict adenine nucleotide diffusion and disrupt mitochondrial intracellular position and assembly, as well as their interactions with other organelles and proteins (Kuznetsov et al., 1996; Kuznetsov et al., 2008). In contrast, in permeabilised cells, this mitochondrial function remains unchanged, as well as preserving essential interactions with the cytoskeleton, nucleus, and endoplasmic reticulum (ER) (Appaix et al., 2003; Kunz et al., 1993; Kuznetsov et al., 2008; Saks et al., 1998). Besides analysing the affinity for ADP, the permeabilisation technique enables the investigation of adenine nucleotide exchange between mitochondria and cellular ATPases via phosphotransfer networks, in situ analysis of respiratory chain complexes, and the study of tiny biological specimens (Kuznetsov et al., 2008).

Limitations on the diffusion of ATP and ADP lead to forming metabolic micro-compartments and non-uniform distribution of metabolite concentrations across cellular regions (Colombini, 2016; Noskov et al., 2016; Puurand et al., 2019). In contrast to the restrictions on adenine nucleotides, VDAC allows unhindered passage of phosphocreatine (PCr) and creatine (Cr) (Timohhina et al., 2009), establishing PCr as the primary carrier of high-energy phosphate bonds within the cell (Figure 3). This selective permeability of VDAC is instrumental in ensuring efficient energy transfer and utilisation within mitochondria and other cellular compartments, thereby playing a significant role in cellular bioenergetics and maintaining metabolic homeostasis.
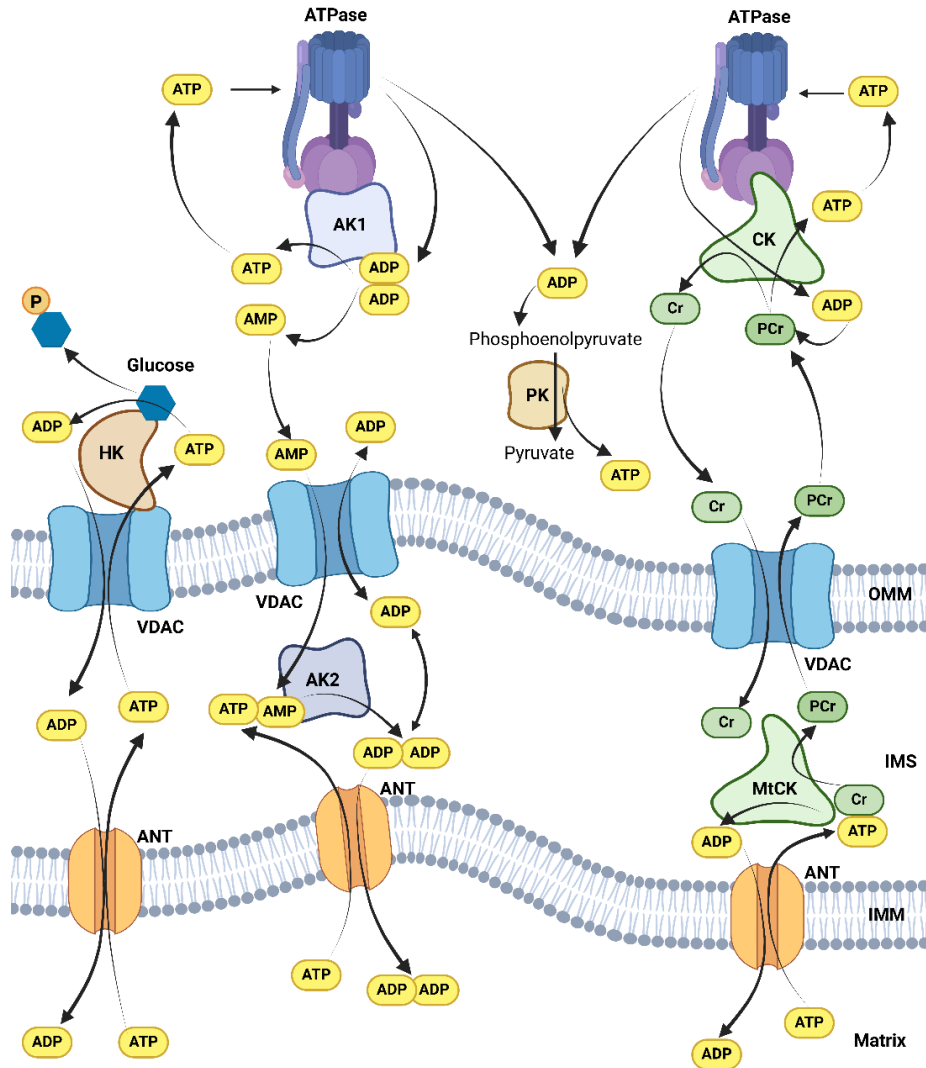
Figure 3. Phosphotransfer networks of CK, AK and HK, and phosphoenolpyruvate/pyruvate kinase (PEP/PK) system. Mitochondrial creatine kinase (MtCK) is located in IMS and catalyses the generation of phosphocreatine (PCr) from creatine (Cr) and ATP, which is transported through the adenine nucleotide translocase (ANT) from the mitochondrial matrix to the IMS. PCr passes through the voltage-dependent anion channel (VDAC) to the cytoplasm, where it is utilised by cytosolic CK to generate ATP and Cr from PCr and ADP near cytosolic ATPases (such as SERCA). Pyruvate kinase (PK) generates pyruvate and ATP from phosphoenolpyruvate (PEP) and ADP produced by ATPases. Adding PK and PEP to the medium with permeabilised cells or tissue traps cytosolic ADP that is not associated with the energy transport system. Mitochondrial adenylate kinase (AK2), located in the IMS, catalyses the formation of two molecules of ADP from ATP and AMP. These ADP molecules are transported to the cytoplasm via VDAC and back to the mitochondrial matrix via ANT. Cytosolic adenylate kinase (AK1) generates ATP and AMP from two molecules of ADP near ATPases. Hexokinase (HK), bound to VDAC, directs newly synthesised mitochondrial ATP to the glycolysis pathway to form glycose-6-phosphate. The figure is created with BioRender.com.

1.3.1 Creatine Kinase Pathway

Creatine kinase enzymes are pivotal in cellular energy transfer and storage (Wallimann et al., 1992). These enzymes catalyse the reversible phosphorylation of creatine to form phosphocreatine, acting as an energy buffer and preventing abrupt declines in total ATP concentrations (Schlattner et al., 2006). There are five major CK isoforms, including cytosolic isoforms (CK-BB, CK-MM, CK-MB) and mitochondrial isoforms (uMtCK, sMtCK), expressed in various tissues, with higher expression observed in tissues with elevated energy demands, such as the heart, skeletal muscle, and nerve cells (McLeish & Kenyon, 2005; Wallimann & Hemmer, 1994; Wallimann et al., 1992). MtCK isoforms are functionally coupled to the adenine nucleotide translocase (ANT) in IMM, while cytosolic CK isoforms create micro-compartments for efficient substrate exchange near ATPases (Figure 3). This spatial organisation enables effective metabolite channelling and regulation of the CK reaction in specific directions based on ATP levels (Schlattner et al., 2016; Wallimann et al., 1992). In the presence of creatine, MtCK regulates phosphocreatine production in collaboration with ANT, which acts as an ATP/ADP antiporter (Saks et al., 2012). ANT directs ADP produced from the PCr/Cr reaction into the mitochondrial matrix, accelerating the respiration rate and maintaining a tight coupling between mitochondrial respiration and ATP synthesis in cardiac cells under normal physiological conditions (Tepp et al., 2011).

Fluctuations in concentrations of ADP and creatine in the mitochondrial IMS regulate the OXPHOS rate (Saks et al., 2000). Respirometric studies of permeabilised cells have revealed that the addition of creatine into the experimental medium increases the OXPHOS rate due to the activation of CK (Saks et al., 2000). The addition of pyruvate kinase (PK) and phosphoenolpyruvate (PEP) to the medium traps ADP produced by cytosolic ATPases and lower respiration; however, subsequent addition of creatine activates MtCK, accelerating the ATP/ADP turnover rate in the IMS and increase OXPHOS (Saks et al., 2001). The phosphocreatine/creatine kinase (PCr/CK) network is pivotal in overcoming the limitations imposed by ATP and ADP diffusion restriction (Saks, Belikova, & Kuznetsov, 1991). This network acts as an intracellular energy transfer system, facilitating the rapid regeneration of ATP from phosphocreatine during periods of high energy demand in striated muscle cells (Dzeja et al., 1996; Guzun et al., 2015; Saks et al., 2007).

In different muscle types, the affinity of mitochondria for ADP varies significantly, resulting in different K_m(ADP) values (Kuznetsov et al., 1996). This variation reflects tissue-specific regulation of the OMM permeability (Kuznetsov et al., 1996). In fast-twitch glycolytic muscles, the affinity for ADP is high, with a low K_m(ADP) value. Conversely, in slow-twitch muscles such as the heart and soleus muscle, the affinity for ADP is low, resulting in a high K_m(ADP) value (Kuznetsov et al., 1996). Additionally, in fast-twitch muscles, CK primarily serves as an energy buffer, and the K_m(ADP) value does not change with activation of the PCr/CK network by adding creatine in permeabilised cells medium (Burelle & Hochachka, 2002; Kay et al., 1997; Kuznetsov et al., 1996). The CK pathway facilitates compartmentalised energy transfer in slow-twitch muscles, ensuring a stable energy supply for myofibrils and ion channel ATPases (Wallimann et al., 1992). The effective functional coupling of OXPHOS to the CK pathway in slow-twitch muscles with high K_m(ADP) is confirmed by a significantly lower value in the presence of creatine (Guzun et al., 2011; Saks et al., 2007; Tepp et al., 2011; Timohhina et al., 2009; Varikmaa et al., 2014).

To support the high energy need of cardiac muscle cells, mitochondrial respiration is regulated by the Mitochondrial Interactosome (MI) supercomplex, formed by ATP-syntasome (Chen et al., 2004; Ko et al., 2003), MtCK, ANT, VDAC and tubulin that regulates effective ATP formation and its extrusion from mitochondria to the cytoplasm in the form of PCr (Figure 4) (Guzun et al., 2011; Timohhina et al., 2009). Notably, creatine's impact on OXPHOS varies between rat ventricular cardiomyocytes and atrial fibers (Anflous et al., 1997), yet in human atria, MtCK is functionally coupled to OXPHOS as observed in ventricular muscle (Seppet et al., 2005).
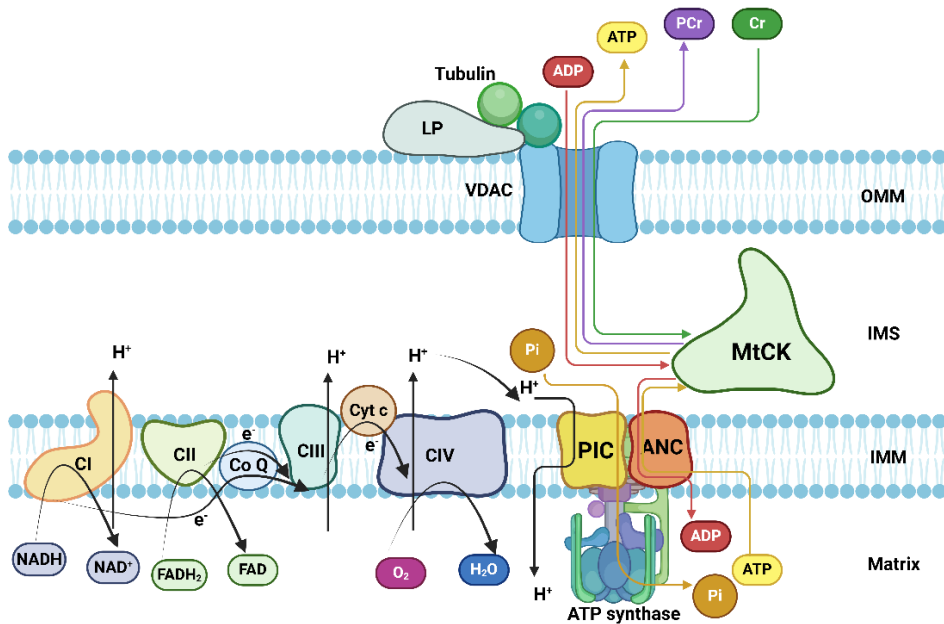
Figure 4. Mitochondrial Interactosome (MI) model. MI consists of ATP synthasome (formed by ATP synthase, adenine nucleotide carrier (ANC) and inorganic phosphate carrier (PIC) as proposed by P. Pedersen (Pedersen, 2007)), mitochondrial creatine kinase (MtCK), and Voltage-dependent anion channel (VDAC) with regulatory proteins tubulin and linker protein (LP). Cr, creatine; PCr, phosphocreatine; Pi, inorganic phosphate; OMM, outer mitochondrial membrane; IMS, intermembrane space; IMM, inner mitochondrial membrane; mitochondrial respiratory complexes CI, CII, CIII, CIV; Co Q, Coenzyme Q; Cyt c, cytochrome c. The figure is created with BioRender.com.

In adult mammalian heart muscle cells, the CK pathway exerts robust control over energy transport and OXPHOS. Conversely, postnatal heart cells typically display undetectable activation of respiration with creatine, likely due to the underdeveloped CK pathway at that stage (Anmann et al., 2014). In pathology, the activation rate of the CK pathway generally diminishes, often serving as an early indicator preceding profound changes in energy metabolism (Anmann et al., 2014; Dzeja, Hoyer, et al., 2011; Schlattner et al., 2006). CK deficiency has been identified as a crucial factor compromising energy delivery and resulting in impaired cellular functioning (Dzeja, Hoyer, et al., 2011). This deficiency prompts compensatory mechanisms wherein glycolytic enzymes and AK partially substitute for CK's phosphotransfer functions (Dzeja et al., 2004). Additionally, an increase in mitochondrial density has been observed as part of these compensatory mechanisms (Wiesner et al., 1999), thereby rescuing cellular bioenergetics.

1.3.2 Adenylate Kinase Pathway

Adenylate kinase is an enzyme involved in the reversible interconversion of adenine nucleotides (2 ADP → ATP + AMP), regulating nucleotide ratios in various cellular compartments (Figure 3) (Dzeja & Terzic, 2009). It influences the activity of AMP-sensitive metabolic enzymes, participates in purine nucleotide synthesis, and aids in regenerating other nucleoside diphosphates from NTP using AMP as a preferred phosphate substrate (Dzeja & Terzic, 2009; Panayiotou et al., 2014). Notably, AK's unique ability to transfer both β- and γ-phosphoryl groups of ATP enhances the energetic potential of ATP (Dzeja & Terzic, 2009).

In vertebrates, nine AK isoforms (AK1–AK9) have distinct sub-cellular locations, forming an intracellular network for transporting energy-rich phosphoryls between compartments (Dzeja & Terzic, 2009; Dzeja & Terzic, 2003; Noma, 2005; Panayiotou et al., 2014). AK1 and AK2, located in the cytoplasm and mitochondria, respectively, specifically bind AMP and prefer ATP over other nucleotide triphosphates. AK3, specific for AMP phosphorylation, utilises guanosine triphosphate (GTP) or inositol triphosphate (ITP) as phosphoryl donors (Dzeja & Terzic, 2009).

AK's signalling function amplifies small changes in the ATP/ADP ratio into a significant increase in the AMP/ATP ratio, activating various AMP-sensitive components, including those in glycolytic pathways, glycogenolysis, and metabolic sensors like ATP-sensitive potassium channels and AMP-activated protein kinase (Chung et al., 2010; Dzeja & Terzic, 2009; Selivanov et al., 2004).

AK2, located in the IMS, generates ADP from ATP and AMP, which then channels into the mitochondrial matrix through the ANT, stimulating OXPHOS (Gellerich, 1992). Its significant expression in various tissues, such as the liver, heart, skeletal muscle, pancreas, kidney, placenta, brain, testis, lung, and gastrointestinal wall, underscores its role in energy metabolism and transfer (Gruno et al., 2006; Kaldma et al., 2014; Khoo & Russell, 1972; Noma et al., 1998; Tanimura et al., 2014). AK2 also plays a crucial role in differentiating cardiac, neural, and hematopoietic stem cells (Dzeja, Chung, et al., 2011; Inouye et al., 1998; Tanimura et al., 2014).

The cytosolic partner of AK2 in the energy-transfer circuit is AK1, the most abundant isoform in the cytosol. AK1 is highly expressed in tissues with high energy demand, including the brain, skeletal and heart muscles, and erythrocytes (Khoo & Russell, 1972; Noma, 2005). Interestingly, AK1-knockout muscles in mice adapt by up-regulating glycolytic, CK, and guanine nucleotide phosphotransfer systems but exhibit lower energetic efficiency than wild type (Janssen et al., 2000).

1.3.3 Glycolytic Pathway

The energy generated through glycolysis sustains various cellular functions, including muscle contraction, cell motility, and nuclear processes (Masters et al., 1987; Ottaway & Mowbray, 1977). Glycolytic enzymes play a pivotal role in intracellular high-phosphoryl transfer. Proximal to mitochondria, HK utilises energy-rich phosphoryl groups from ATP to phosphorylate glucose to glucose-6-phosphate (Roberts & Miyamoto, 2015; Wilson, 2003). Conversely, pyruvate kinase phosphorylates ADP in the cytosol, supplying ATP for cellular utilisation (Dzeja & Terzic, 2003). Furthermore, the glutaraldehyde-3-phosphate dehydrogenase and phosphoglycerate kinase (GAPDH/PGK) networks facilitate the transfer of energy-rich phosphoryls, exchanging them for NADH and ADP (Dzeja & Terzic, 2003).

Mammalian tissues exhibit four isoforms of HKs (HK1-HK4). HK1 and HK2 bind to VDAC through their hydrophobic N-terminus (Figure 3) (Pedersen, 2008; Wilson, 2003). This interaction is thought to enhance kinase access to newly generated ATP, overcoming the OMM permeability restrictions on adenine nucleotides (Pedersen, 2008; Puurand et al., 2019). It also prevents product inhibition by glucose-6-phosphate. The activity and subcellular localisation of HK isoenzymes dictate the metabolic fate (anabolic or catabolic) of glucose-6-phosphate, influencing diverse intracellular roles of glucose (John et al., 2011). The stringent regulation of HK binding to the OMM is contingent on cellular energetic demands, particularly in skeletal muscle (Parra et al., 1997). A decrease in HK2-mitochondrial interaction has been associated with adverse outcomes in ischemia-reperfusion injury of the heart (Nederlof et al., 2016; Wu et al., 2011).

1.4 Cardiac Metabolism in Cardiac Pathologies

Metabolic fluxes within the myocardium serve as the initial responders to changes in the physiological environment of the heart, subsequently triggering and sustaining functional and structural remodelling processes (Young et al., 2002). Assessments of myocardial metabolism utilising [^{11}C] tracers, which are oxidised by the heart, have revealed alterations in substrate preference among patients with idiopathic dilated cardiomyopathy. Specifically, there is a noted decrease in fatty acid metabolism accompanied by an increase in glucose metabolism (Davila-Roman et al., 2002), indicative of the expression of fetal metabolic gene programs within the failing human heart (Razeghi et al., 2001). Both hypertrophy and atrophy are associated with elevated glucose oxidation rates despite diminished insulin responsiveness of the heart (Doenst et al., 2001). Alongside an increase in glycolysis, hypertrophied hearts typically exhibit a reduction in fatty acid oxidation (Allard et al., 1994; el Alaoui-Talibi et al., 1992).

During ischemic events, the accumulation of glycolytic intermediates may exacerbate contractile dysfunction (Neely & Grotyohann, 1984). Additionally, acute hyperglycaemia has been shown to abolish ischemic preconditioning in vivo (Kersten et al., 1998), whereas the provision of glucose, insulin, and potassium together improves contractile function in acutely ischemic, reperfused myocardium (Gradinac et al., 1989; Howell et al., 2011). Glucose holds therapeutic relevance for several reasons: firstly, glycolysis offers an immediate source of cytosolic ATP during acute oxygen deficit; secondly, glycolytically derived ATP may serve as a preferential source for membrane ion transport processes; and thirdly, high glucose oxidation rates are crucial for restoring normal myocardial function following ischemia-reperfusion (Depre et al., 1999; Mallet et al., 1990).

Myocardial glucose transport, glycolysis, and glucose oxidation are directly or indirectly insulin-dependent. Therefore, in the insulin-deficient diabetic state, these processes are diminished due to insulin resistance, impaired pyruvate dehydrogenase activity, and reduced glucose transporter (GLUT1 and GLUT4) levels (Camps et al., 1992; Lopaschuk, 1996; Randle et al., 1963). Elevated fatty acid oxidation (FAO) levels in diabetic states contribute to an overall reduction in glucose metabolism rates (Hafstad et al., 2009; Hallsten et al., 2004) and lead to increased cardiac fatty acid uptake, storage, and metabolism (Herrero et al., 2006; Malfitano et al., 2015). Consequently, the heart predominantly relies on FAO to meet its energy demands, utilising either exogenous sources or the turnover of stored triacylglycerol (Saddik & Lopaschuk, 1994; Wall & Lopaschuk, 1989). This reliance on FAO is detrimental to mitochondrial function because it induces increased oxygen consumption (Mjos, 1971), mitochondrial uncoupling between

respiration and ATP production (Banke & Lewandowski, 2015; Boudina et al., 2007; Cole et al., 2011; Vettor et al., 2002), and generates more reactive oxygen species (Tsushima et al., 2018). Mitochondrial uncoupling results in elevated proton leak through the mitochondrial inner membrane to the matrix (Boudina et al., 2007) and decreased ATP synthesis (Malfitano et al., 2015; Petersen et al., 2004). The increased oxygen consumption associated with predominant FAO also reduces cardiac efficiency (Hafstad et al., 2009; Mather et al., 2016) and may contribute to cardiac dysfunction in diabetic conditions (Boudina et al., 2005; Mazumder et al., 2004; Rijzewijk et al., 2009). Furthermore, an increase in FAO inhibits the ANT in the mitochondrial membrane, which is responsible for transporting ATP from the mitochondria to the cytosol (Shug et al., 1975; Woldegiorgis et al., 1982). Under normal conditions, the heart is metabolically flexible and can switch its substrate preference based on workload and substrate availability (Karwi et al., 2018). However, this metabolic flexibility is impaired when FAO predominates, and glucose oxidation decreases in diabetes.

Metabolic dysregulation, when the rate of fatty acid uptake surpasses the rate of oxidation, leads to a spectrum of disturbances commonly associated with mitochondrial dysfunction (Petersen et al., 2004; Shulman, 2000), including triglyceride accumulation (Schaffer, 2003; Unger & Orci, 2001). In failing human hearts, lipid accumulation emerges as a characteristic feature, accompanied by a diverse array of cellular and metabolic disruptions collectively termed lipotoxicity (Schaffer, 2003; Sharma et al., 2004; Unger, 2005). Increased net triglyceride synthesis in the heart has been observed under conditions of starvation, diabetes, ischemia, and heart failure (Sharma et al., 2004), yet whether elevated triglyceride levels stem from heightened esterification rates or diminished lipolysis rates remains unknown (Schaffer, 2003). Enzymatic deficiencies affecting long and very long-chain fatty acids (C14 or greater), or impairments in cellular carnitine import or enzymes participating in the carnitine shuttle, result in more severe manifestations of heart failure compared to defects involving the metabolism of shorter-chain fatty acids (Hale & Bennett, 1992). Notably, impaired FAO and the subsequent accumulation of triglycerides within cardiomyocytes are hallmark features of contractile dysfunction observed in diabetic patients (McGavock et al., 2007).

1.5 Wolfram Syndrome

Wolfram syndrome (WS), also known as DIDMOAD syndrome (Diabetes Insipidus, Diabetes Mellitus, Optic Atrophy, and Deafness), is a rare autosomal recessive neurodegenerative disorder characterised by a diverse array of clinical manifestations (Barrett & Bundey, 1997; Minton et al., 2003). These features encompass diabetes mellitus, optic atrophy, diabetes insipidus, sensorineural hearing loss, and various neurological abnormalities. The clinical presentation of WS displays significant variation, with the DIDMOAD complex being crucial for diagnosis (Cremers et al., 1977). While the exact prevalence of Wolfram syndrome varies among different populations, it is estimated to affect approximately 1 in 160,000–770,000 individuals worldwide (Barrett & Bundey, 1997; Urano, 2016).

Typically, WS emerges during childhood or adolescence and progresses relentlessly, leading to severe disability and premature mortality. On average, individuals with WS have a shortened lifespan, with death occurring around 30 years of age, often attributed to central respiratory failure resulting from massive brain atrophy (Barrett & Bundey, 1997; Barrett et al., 1995). The onset of WS symptoms usually begins in childhood, with diabetes mellitus typically arising around six years of age, followed by optic atrophy at

approximately 11 years of age, and subsequently, the development of diabetes insipidus and deafness (Barrett & Bundey, 1997; Barrett et al., 1995).

Despite its clinical significance, WS is frequently underdiagnosed, with clinical attention often focusing on managing diabetes and its associated complications once symptoms become apparent (Medlej et al., 2004). Despite the apparent simplicity of its autosomal recessive inheritance pattern, WS exhibits complex penetrance and expression of traits, resulting in a heterogeneous clinical phenotype. In addition to the classical symptoms, WS is associated with a spectrum of neurological and psychiatric disorders, reproductive abnormalities, restricted joint mobility, cardiovascular and gastrointestinal autonomic neuropathy, and diabetic microvascular complications (Rohayem et al., 2011; Saran et al., 2012). These diverse clinical manifestations pose significant challenges in the clinical management of WS.

Wolfram syndrome primarily results from biallelic mutations in the WFS1 gene on chromosome 4p16.1. The WFS1 gene consists of eight exons, with mutations predominantly observed within exon 8, and can generate 15 different transcripts (Hardy et al., 1999; Strom et al., 1998). These mutations, often homozygous or compound heterozygous, disrupt the coding sequence of the WFS1 gene, which encodes the wolframin endoplasmic reticulum (ER) transmembrane glycoprotein (Inoue et al., 1998; Lee et al., 2022; Rigoli et al., 2018; Tanizawa et al., 2000). Wolframin features nine transmembrane domains, with its C-terminus residing in the ER lumen and the N-terminus in the cytoplasm (Hofmann et al., 2003). It is primarily localised in pancreatic beta-cells, neurons, cells of the optic nerve, and tissues such as the internal ear, heart, placenta, lung, and liver. Notably, mutations on both alleles are necessary for the complete manifestation of Wolfram syndrome. However, single-allele mutations significantly increase the risk of type 2 diabetes, hearing loss, depression, suicide, and other complex diseases (Cryns et al., 2003; Koido et al., 2005; Minton et al., 2002; Must et al., 2009; Sandhu et al., 2007; Swift et al., 1998).

Wolframin plays a pivotal role in modulating calcium homeostasis within the ER, influencing the formation of mitochondria-associated ER membrane (MAM) structures and regulating calcium transport between the ER and mitochondria (Delprat et al., 2018; La Morgia et al., 2020). Dysfunctional wolframin results in ER stress and activation of the Unfolded Protein Response (UPR) pathway (Fonseca et al., 2005; Morikawa et al., 2017; Samara et al., 2019). The UPR serves as an adaptive cellular mechanism aimed to restore ER homeostasis in response to disruptions in protein folding and the accumulation of misfolded proteins within the ER lumen. Nevertheless, chronic or severe ER stress, characteristic of WS, can overwhelm the UPR machinery, leading to cellular dysfunction, apoptosis, and neurodegeneration.

Recent investigations have identified occurrences of heart diseases among individuals with WS, primarily attributed to structural abnormalities (Ganie et al., 2011; Korkmaz et al., 2016; Medlej et al., 2004). A study conducted in the Lebanese population disclosed five cases of cardiac abnormalities among 31 WS patients, indicating a prevalence significantly higher than that observed in the general population (Medlej et al., 2004). However, despite the structural defects noted in cardiac muscle in a somewhat higher percentage of WS patients compared to the general population, such abnormalities are not universally prevalent among all affected individuals (Barrett et al., 1993; Ganie et al., 2011; Korkmaz et al., 2016; Medlej et al., 2004). Furthermore, studies examining WFS1-deficient rat left ventricle cardiomyocytes have revealed increased contractility due to prolonged cytosolic calcium transients (Cagalinec et al., 2019). Additionally, a higher

relative incidence of sinus tachycardia and atrioventricular arrhythmias has been observed in WS patients (Kinsley et al., 1995). These findings underscore the complexity of cardiac involvement in WS and highlight the need for further research to elucidate cardiovascular manifestations' underlying mechanisms and clinical implications in this rare genetic disorder.

As WS manifests with diabetes as its initial symptom, it presents a promising genetic model for investigating the cardiovascular complications associated with diabetes mellitus. Given the established association between diabetes mellitus and cardiovascular complications (Htay et al., 2019), the study of WS offers valuable insights into the underlying mechanisms contributing to diabetic cardiomyopathy, coronary artery disease, and other cardiovascular diseases. By elucidating the molecular and mitochondrial bioenergetic pathways involved in the pathogenesis of cardiovascular complications in individuals with WS, novel therapeutic targets and strategies can be identified for mitigating the adverse effects of diabetes on the heart. Furthermore, using WS as a genetic model allows the identification of specific genetic variants that predispose individuals with WS to cardiovascular complications. Also, this approach may lead to the development of personalised interventions aimed at preventing or attenuating the progression of cardiovascular disease in individuals with diabetes.

1.6 Smoking and Cardiovascular Diseases

Despite intensified public awareness campaigns, regulatory measures on tobacco marketing, and taxation policies, cigarette smoking has persisted as a risk factor for chronic obstructive pulmonary disease (COPD) (Laniado-Laborin, 2009), cardiovascular diseases (CVD) (Banks et al., 2019), and various cancers (Macacu et al., 2015; Samet, 2013; Sasco et al., 2004) since the mid-20th century. These diseases significantly elevate the mortality rate among current smokers. Smoking exerts a synergistic effect with other conventional cardiovascular risk factors, including hypertension, dyslipidaemia, diabetes, and obesity, thereby magnifying the overall cardiovascular risk (Fagard, 2009; Prakash et al., 2021). Individuals who smoke and concurrently present with these risk factors face a markedly augmented likelihood of developing CVD compared to non-smokers or those with a single risk factor. This heightened risk is evident not only among active smokers but also extends to individuals exposed to second-hand smoke (Flor et al., 2024). Moreover, the elevated risk for cardiovascular complications persists among ex-smokers for an extended duration, potentially attributable to irreversible cumulative alterations induced by prolonged exposure to cigarette smoke (Ahmed et al., 2015; Gopal et al., 2012; Lee & Son, 2019). Former heavy smokers exhibit a heightened prevalence of type 2 diabetes mellitus, left ventricular systolic dysfunction, coronary artery disease, and peripheral arterial disease, alongside elevated circulating levels of serum C-reactive protein and interleukin-6 compared to individuals who have never smoked (Ahmed et al., 2015). These observations underscore the profound and enduring impact of smoking on cardiovascular health, suggesting that the risk for cardiovascular complications remains elevated long after smoking cessation.

The detrimental impacts of smoking on cardiovascular health encompass a spectrum of pathological mechanisms, predominantly attributed to the toxic constituents inherent in cigarette smoke, notably nicotine, carbon monoxide (CO), and various chemical compounds (Astrup & Kjeldsen, 1974; Cheng et al., 2010; Petsophonsakul et al., 2022; Wang et al., 2023; Whitehead et al., 2021). These substances detrimentally affect oxygen transport to tissues and cellular metabolism (Caliri et al., 2021; Sagone et al., 1973).

Carbon monoxide exhibits a higher affinity for haemoglobin than oxygen, resulting in the formation of carboxyhaemoglobin and impaired tissue oxygenation (Aronow, 1976; Wald et al., 1981). This chronic hypoxemia fosters endothelial dysfunction, oxidative stress, and the development of atherosclerotic plaques, thereby accelerating coronary artery disease (CAD) progression and elevating the risk of myocardial infarction and ischemic stroke. Nicotine, a potent addictive agent in tobacco, elicits sympathomimetic effects, culminating in heightened heart rate, blood pressure, and myocardial oxygen demand. Additionally, nicotine stimulates the release of catecholamines, thereby promoting vasoconstriction and platelet aggregation, which exacerbate cardiovascular susceptibility (D'Alessandro et al., 2012; Fox, 1988). Moreover, nicotine, carbon monoxide, and other smoke constituents disrupt nitric oxide synthesis, a pivotal mediator of endothelium-dependent vasodilation, inducing endothelial dysfunction and vasoconstriction (Messner & Bernhard, 2014).

Chronic smoking disrupts lipid metabolism, culminating in unfavourable alterations in lipid profiles typified by elevated low-density lipoprotein cholesterol levels and diminished high-density lipoprotein cholesterol levels (Ambrose & Barua, 2004; Freeman et al., 1993; Schuitemaker et al., 2002). Furthermore, smoking induces lipoprotein oxidation and glycation, rendering them more atherogenic and susceptible to endothelial injury (Ferretti et al., 2006). Long-term smoking leads to detrimental structural and functional alterations in the myocardium, which include left ventricular hypertrophy, impaired myocardial contractility, and reduced coronary flow reserve (Deanfield et al., 1986; Hendriks et al., 2020; Park et al., 2021).

Smoking exerts significant effects on mitochondrial function, primarily through alterations in molecular mechanisms associated with oxidative stress, inflammation, and mitochondrial DNA (mtDNA) damage (Dikalov et al., 2019; Giordano et al., 2022; Liu et al., 2023; Rom et al., 2013; Ueda et al., 2023). Studies have demonstrated that smoking diminishes mitochondrial respiration in murine skeletal muscles, resulting in skeletal muscle atrophy (Ajime et al., 2021; Chan et al., 2020; Ding et al., 2019), as well as increases macrophage infiltration in bronchoalveolar lavage fluid, with values returning to baseline upon smoking cessation (Ajime et al., 2021; Darabseh et al., 2021). Furthermore, smoking has been linked to capillary rarefaction (Nogueira et al., 2018), indicating potential broader impacts beyond skeletal muscle, likely affecting mitochondria in various tissues, including the brain and heart. The generation of ROS during smoking induces oxidative stress and compromises the body's antioxidant defence mechanisms (Michaud et al., 2006). ROS directly target mitochondrial components, leading to dysfunction by damaging proteins, lipids, and DNA and by inducing the opening of the mitochondrial permeability transition pore (mPTP), disrupting mitochondrial membrane potential and ATP production (Cadenas, 2018; Juan et al., 2021; Redza-Dutordoir & Averill-Bates, 2016). Smoking-induced oxidative stress also triggers inflammatory responses within the vascular wall, characterised by releasing pro-inflammatory cytokines, chemokines, and adhesion molecules, which can further impact mitochondrial function by activating pro-inflammatory pathways (Dahdah et al., 2022). Chronic exposure to cigarette smoke also disrupts the balance between mitochondrial biogenesis and degradation, resulting in reduced mitochondrial mass and impaired function (Tulen et al., 2022). Smoking-induced mitochondrial dysfunction extends to programmed cell death pathways, leading to dysregulated apoptosis, thereby contributing to tissue damage and disease progression (Aoshiba & Nagai, 2003; Redza-Dutordoir & Averill-Bates, 2016).

2 Aims of the Study

The principal aim of this study was to investigate the influence of intrinsic and extrinsic factors on mitochondrial bioenergetics and to evaluate inherent cardioprotective mechanisms in cardiac muscle tissue, thereby advancing our understanding of cardiovascular health and disease pathology.

Intrinsic factors, such as gene mutations, were evaluated using Wolframin-deficient mice and rats as experimental models. These models were chosen to explore alterations in mitochondrial bioenergetics and energy transfer pathways in animals affected by metabolic disorders, focusing on diabetes as the primary disease of interest.

Our specific aims were as follows:

1. Evaluate mitochondrial kinetics, OXPHOS function and dynamic substrate utilisation patterns in cardiac muscle tissue.

2. Investigate changes in phosphotransfer pathways, including creatine kinase, adenylate kinase and glycolytic pathways, within cardiac muscle tissue.

3. Compare metabolic differences between Wolframin-deficient and control cardiac tissues to understand the impact of WFS deficiency on mitochondrial function.

In the second phase of our study, we aimed to evaluate the impact of extrinsic factors on cardiac muscle bioenergetics and the recovery potential of cardiac tissue. To achieve this, we utilised a mouse model of chronic obstructive pulmonary disease (COPD) exposed to cigarette smoke. Following this exposure, the mice underwent a smoking cessation period lasting up to two weeks. The objectives related to extrinsic factors were:

1. Explore changes in mitochondrial bioenergetics resulting from exposure to cigarette smoke and subsequent smoking cessation.

2. Investigate structural and metabolic modifications in cardiac muscle tissue triggered by exposure to cigarette smoke and subsequent smoking cessation.

3. Evaluate the inflammatory response within cardiac muscle tissue following exposure to cigarette smoke and subsequent cessation of smoking.

3 Materials and Methods

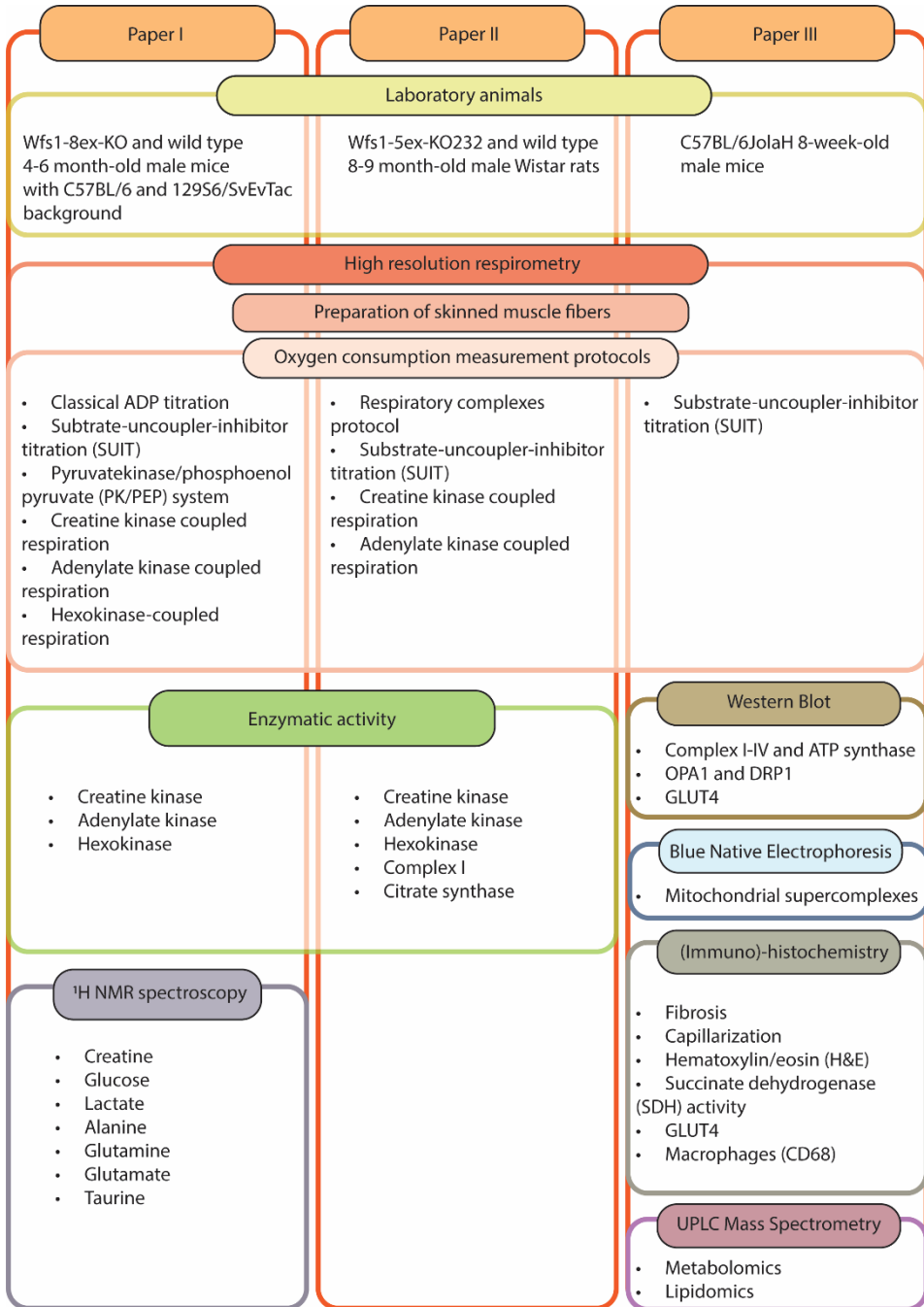The summary of the applied approaches and techniques is illustrated in the figure.

Figure 5. Design of the study.

4 Results

4.1 The Genetic Mutation in Wolframin Gene as an Intrinsic Factor Influencing Mitochondrial Bioenergetics in Cardiac Muscle: Insights from Wolframin-Deficient Models (Paper I and Paper II)

To investigate the influence of intrinsic factors on mitochondrial bioenergetics in cardiac muscle, we utilised two models featuring metabolic syndrome caused by genetic modifications in the Wolframin gene: mice with a 129S6/SvEvTac and C57BL/6 mixed background and Wistar rats (hereafter referred to as WFS1 KO). Their wild-type (WT) littermates were used as controls.

To evaluate the variations in mitochondrial respiration and ATP generation between Wolframin-deficient and control animals, we utilised oxygraphic measurement protocols: (1) SUIT (substrate-uncoupler-inhibitor-titration); (2) Respiratory Chain (RC) protocol, which aimed to ascertain the individual capacity of CI-, CII-, and CIV-linked electron transport to support ADP-dependent oxygen consumption; (3) the ADP-titration protocol, employed to determine kinetic constants such as the apparent K_m constant for ADP (K_m(ADP)) and the maximal respiration rate (V_{max}); (4) three distinct protocols for coupling assessment of CK, AK, and HK to OXPHOS. These protocols facilitated the simultaneous monitoring of the respiration of different ETC complexes and the preference of pathways for specific substrates.

4.1.1 Impact of Wolframin Deficiency on Mitochondrial Kinetics in Cardiac Muscle (Paper I) and OXPHOS Function (Paper I and Paper II)

We employed the classical ADP-titration protocol to elucidate the impact of Wolframin gene deficiency on the regulation of the outer mitochondrial membrane in cardiac muscle (Figure 6A). A K_m(ADP) value reduction was observed in the cardiac muscle fibers of WFS1-deficient mice when glutamate and malate served as CI-linked substrates without adding pyruvate and creatine. Specifically, in WT and WFS1 KO mice, the K_m(ADP) values were 100 and 50 μM ADP, respectively (Figure 6B). Additionally, a significant reduction in the maximal oxygen consumption rate (V_{max}) was observed in WFS1 KO cardiac cells (Figure 6C). In contrast, no differences in K_m(ADP) and V_{max} were observed in WFS1 KO animals when using a combination of malate and pyruvate without glutamate.

Figure 6. Kinetic analysis of the regulation of ADP-activated respiration with malate and glutamate in mouse model. (A) Representative trace of oxygraphic measurement of ADP-titration (until saturation). CI-linked substrates malate and glutamate. The respiration rate is represented in nmol $O_2*min^{-1}*mg\ dw^{-1}$ (red line; right axis); O_2 concentration is represented in µM (blue line; left axis). (B) The corresponding apparent Michaelis-Menten constant (K_m) values for exogenously added ADP were determined for WFS1 KO and WT mice. (C) The maximal oxygen consumption rate (V_{max}) was determined from the measurements for the Michaelis-Menten coefficient calculation. The respiration rate is represented in nmol $O_2*min^{-1}*mg\ dw^{-1}$; *p-value < 0.05, **p-value < 0.01, ***p-value < 0. 001. Results are expressed as mean ± SEM.

To determine which of the two main ETC electron feeding sites (CI and CII) could be limiting for OXPHOS in WFS1 KO animals, we conducted several experiments employing SUIT and RC protocols.

Employing the SUIT protocol (Figure 7A), we observed that leak respiration (oxygen consumption without adenylates) did not differ between groups in cardiac muscle. Following the SUIT protocol, we initiated the activation of CI by sequentially introducing malate and pyruvate, followed by adding ADP to stimulate OXPHOS within the mitochondria, and subsequently adding glutamate to augment the maximal activity of CI-linked respiration. After that, we initiated the CII-linked respiration by introducing CII substrate succinate. Respiratory activity of cardiac muscle driven simultaneously by CI and CII exhibited no differences between WFS1-deficient and control mice.

The RC protocol enabled the individual assessment of ADP-dependent respiration for complexes CI, CII, and CIV (Figure 7B). This was achieved by initially activating CI, then inhibiting it with rotenone, followed by activating CII. Subsequently, CIII was inhibited using Antimycin A, allowing for the measurement of CIV maximal capacity after adding an artificial substrate. In both WFS1-deficient animal models used, no differences in

parameters were obtained with the RC protocol compared to WT animals. In the rat model, two alternative CI-linked substrate combinations, malate with glutamate or pyruvate, were used to activate CI. Our findings indicated no statistically significant alterations in WFS1 KO cardiac muscles compared to WT animals for either substrate combination.
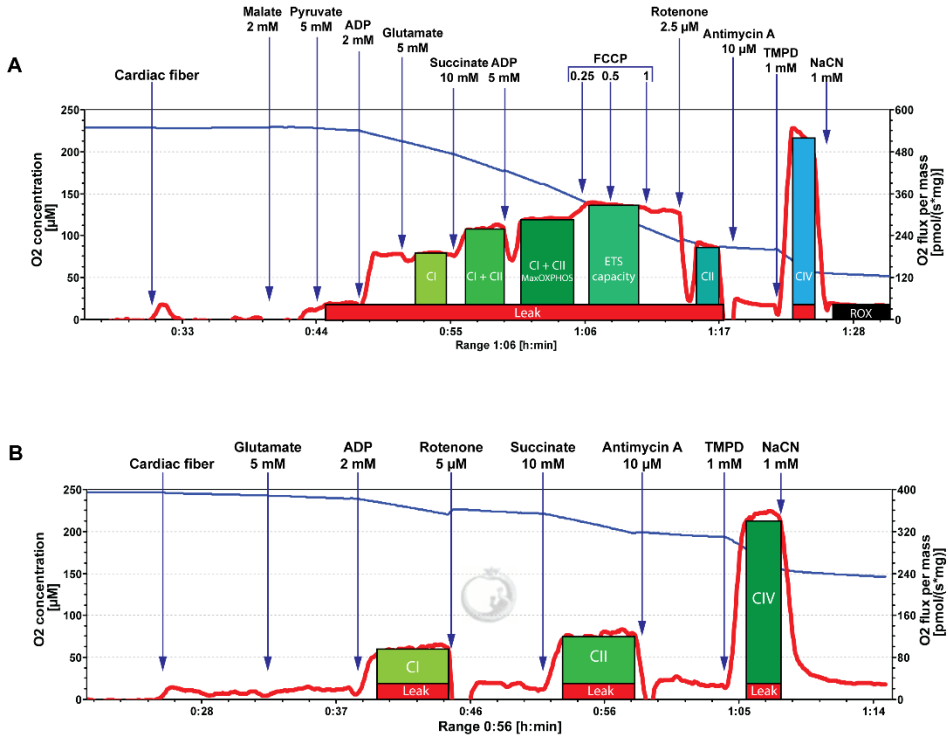

Figure 7. Representative traces of oxygraphic measurements corresponding to SUIT (A) and Respiratory chain (B) protocols. The respiration rate is represented in nmol O_2*min^{-1}*mg dw^{-1} (red line; right axis); O_2 concentration is expressed in µM (blue line; left axis). A leak means uncoupled and non-phosphorylating oxygen consumption without adenylates; CI means the oxygen consumption rate with CI-linked substrates (malate, glutamate, and pyruvate); CI+CII means the oxygen consumption rate with CI- and CII-linked substrates (malate, glutamate, and pyruvate; succinate, respectively); CI+CII MaxOXPHOS means the oxygen consumption rate after the addition of 5 mM ADP (saturated state); ETC capacity means maximal oxygen consumption rate after addition of uncoupler; CII means oxygen consumption rate with CII-linked substrates after inhibition of CI; CIV means oxygen consumption rate with artificial CIV substrate TMPD and inhibition of CI, CII and CIII; ROX is residual oxygen consumption rate due to oxidative side reactions remaining after addition of ETC inhibitors.

4.1.2 Substrate Preferences and Mitochondrial Function in Wolframin-Deficient Cardiac Muscle (Paper II)

In our investigation, we evaluated substrate preferences and the flexibility of OXPHOS with different substrate combinations to switch between glucose-linked (pyruvate) and fatty acid oxidation (octanoyl carnitine) substrates in the cardiac muscle of WFS1-deficient rats.

We employed SUIT protocols, which involve the simultaneous activation of mitochondrial ETC complexes, providing a condition more akin to physiological circumstances. Following the SUIT-1 protocol (Figure 8A), respiration was initially sustained solely by malate, concurrently with the activation of the fatty acid (FA) pathway using octanoyl carnitine (Oct). We observed no differences in FA-linked respiration rates in cardiac muscle between the experimental groups. Then, pyruvate was introduced to complement the system with a substrate from the glycolytic pathway. Following this, maximal CI-linked respiration was activated using glutamate. Notably, maximal CI-linked respiration and maximal OXPHOS, involving the activation of both CI and CII, were markedly diminished in WFS1 KO animals compared to WT counterparts (Figure 8B,C). In normal cardiac muscle, the sequential addition of substrates typically increases the respiration rate, reaching its peak in the presence of an uncoupler.
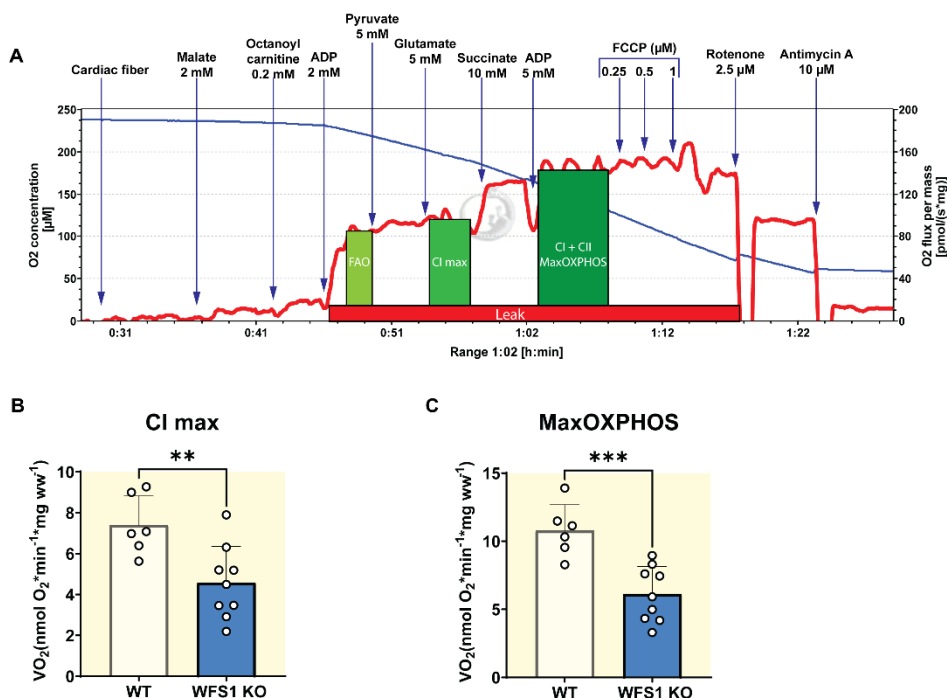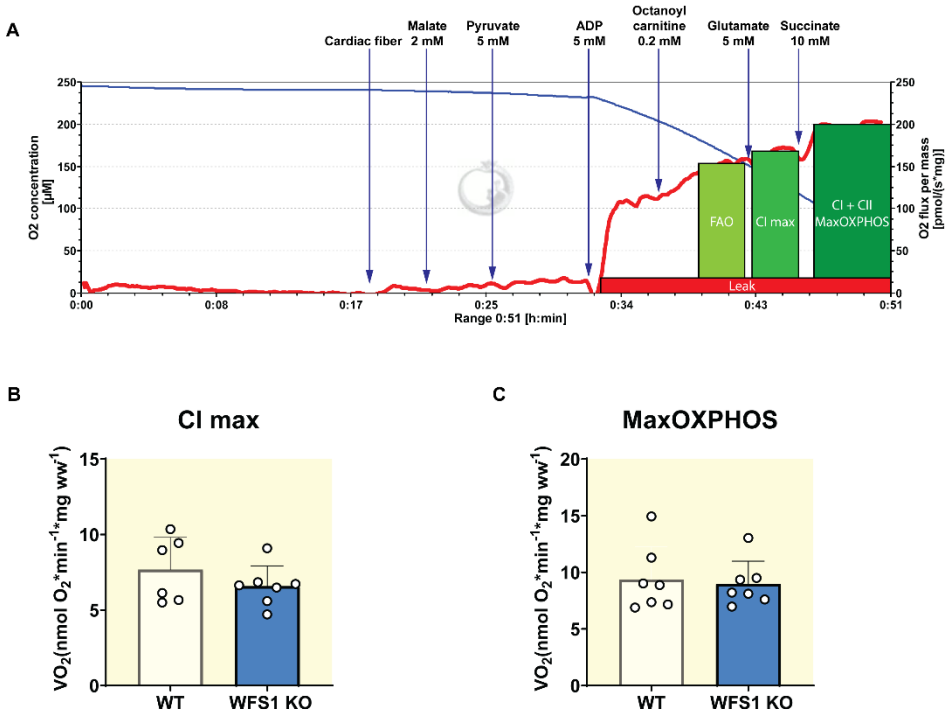

Figure 8. The influence of consecutive activation of FA and glycolytic pathways on mitochondrial respiratory capacity in the rat model. (A) Representative trace of oxygraphic measurement corresponding to SUIT-1 protocol with activation of FA and glycolytic pathways in permeabilised cardiac muscle tissue in rats, where FAO is oxygen consumption rate with fatty acid oxidation, CI max is maximal oxygen consumption rate with CI-linked substrates (malate, glutamate, and pyruvate), CI+CII MaxOXPHOS is maximal oxygen consumption rate with CI- and CII-linked substrates (malate, glutamate, and pyruvate; succinate, respectively). The respiration rate is represented in nmol $O_2*min^{-1}*mg\ ww^{-1}$ (red line; right axis); O_2 concentration is represented in µM (blue line; left axis). (B) The maximal oxygen consumption rate with CI-linked substrates (CI max) was decreased in WFS1 KO rats compared to the WT group. (C) The maximal oxygen consumption rate with CI- and CII-linked substrates was decreased in WFS1 KO rats compared to the WT group. The respiration rate is represented in nmol $O_2*min^{-1}*mg\ ww^{-1}$; *p-value < 0.05, **p-value < 0.01, ***p-value < 0. 001; n = 6–9. Results are expressed as mean ± SEM.

To test the hypothesis that the decrease in the respiration rate observed in previous experiments was caused by the activation of the FA pathway, thereby inhibiting the utilisation of other CI-linked substrates, we devised the SUIT-2 protocol (Figure 9A). In the SUIT-2 protocol, substrates were added in reverse order to activate pathways, with glucose-linked substrates, malate and pyruvate, introduced first. Subsequently, the FA pathway was activated, and the maximum CI-linked oxygen consumption rate was measured by adding glutamate. Our results demonstrated no significant alterations in WFS1KO cardiac muscle (Figure 9B,C), indicating that only the activated FA pathway could inhibit the glucose-linked pathway in the SUIT-1 protocol.

Figure 9. The influence of the consecutive activation of glycolytic and FA pathways on mitochondrial respiratory capacity in the rat model. (A) Representative trace of oxygraphic measurement corresponding to SUIT-2 protocol with activation of glycolytic and FA pathways in permeabilised cardiac muscle tissue in rats, where FAO is oxygen consumption rate with fatty acid oxidation, CI max is maximal oxygen consumption rate with CI-linked substrates (malate, glutamate, and pyruvate), CI+CII MaxOXPHOS is maximal oxygen consumption rate with CI- and CII-linked substrates (malate, glutamate, and pyruvate; succinate, respectively). The respiration rate is represented in $nmol\ O_2*min^{-1}*mg\ ww^{-1}$ (red line; right axis); O_2 concentration is expressed in μM (blue line; left axis). The maximal oxygen consumption rate with CI-linked substrates (B) and CI- and CII-linked substrates (C) did not differ between WFS1 KO and WT groups. The respiration rate is represented in $nmol\ O_2*min^{-1}*mg\ ww^{-1}$; n = 6–8. Results are expressed as mean ± SEM.

To investigate potential impairments in using glucose-linked substrates, we implemented the SUIT-3 protocol (Figure 10A). According to this protocol, exclusively malate, glutamate, and pyruvate were used as substrates to activate pathways without adding octanoyl carnitine. Our findings revealed no significant differences in the ETC capacity between WFS1 KO and WT in cardiac muscle when the glucose-linked pathway

was evaluated independently from the FA pathway (Figure 10B,C). Furthermore, comparing different substrate introduction orders in WT cardiac muscle demonstrated that the maximal OXPHOS capacity and CI-linked respiration rates were higher when SUIT-1 and SUIT-2 protocols were employed. Conversely, in WFS1 KO cardiac muscle, the highest oxygen consumption rate was observed with the SUIT-2 protocol (pyruvate added first) compared to SUIT-1 and SUIT-3, suggesting alterations in the fatty acid pathway.
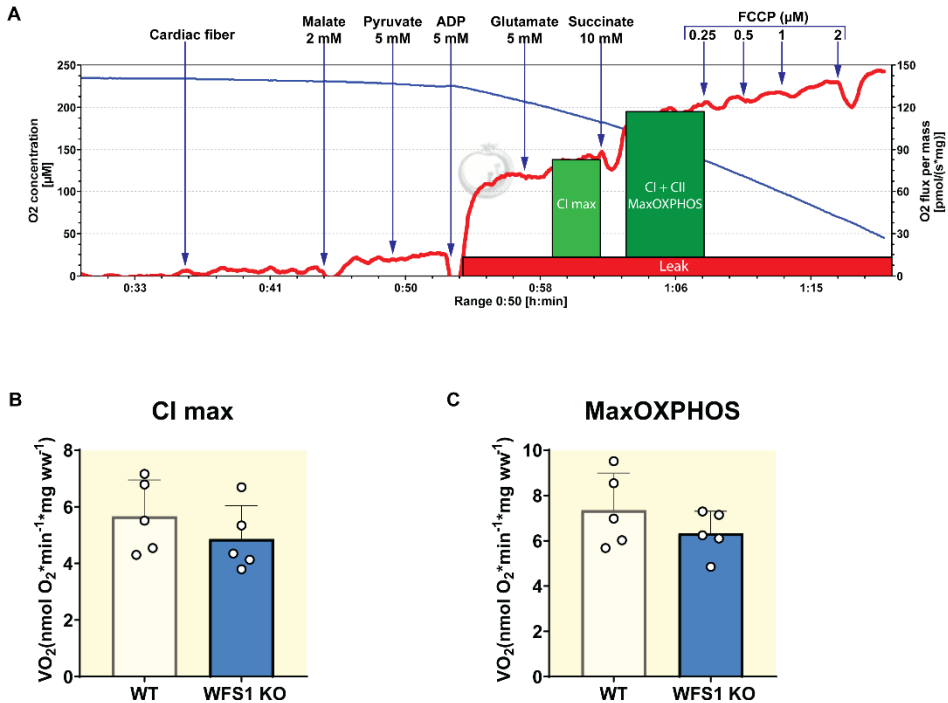
Figure 10. The influence of glycose-linked pathway activation on mitochondrial respiratory capacity in the rat model. (A) Representative trace of oxygraphic measurement corresponding to SUIT-3 protocol with activation of glycolytic pathways in permeabilised cardiac muscle tissue in rats, CI max is maximal oxygen consumption rate with CI-linked substrates (malate, glutamate, and pyruvate), CI+CII MaxOXPHOS is maximal oxygen consumption rate with CI- and CII-linked substrates (malate, glutamate, and pyruvate; succinate, respectively). The respiration rate is represented in $nmol\ O_2*min^{-1}*mg\ ww^{-1}$ (red line; right axis); O_2 concentration is expressed in μM (blue line; left axis). The maximal oxygen consumption rate with CI-linked substrates (B) and CI- and CII-linked substrates (C) did not differ between WFS1 KO and WT groups. The respiration rate is represented in $nmol\ O_2*min^{-1}*mg\ ww^{-1}$; n = 5. Results are expressed as mean ± SEM.

4.1.3 Impact of Energy Transfer Pathways on Oxidative Phosphorylation in Cardiac Muscle: Experimental Insights from Mouse and Rat Models (Paper I and Paper II)

The continuous transfer of intracellular ATP from mitochondria to ATPases and the supply of metabolites to mitochondria is significant in cardiac cells, where mitochondria serve as the primary energy producers. Our study investigated how three critical energy facilitation systems influenced OXPHOS in muscles: the Cr/PCr, AK, and glycolytic pathways. Alteration in these pathways can exert immediate influences on cellular metabolism.

4.1.3.1 Assessment of Creatine Kinase/Phosphocreatine Pathway Activity and its Impact on Oxidative Phosphorylation in Cardiac Muscle

A distinguishing feature of the creatine kinase pathway's efficacy in oxidative muscle cells is the heightened affinity of mitochondria towards ADP, as indicated by decreased K_m(ADP) value upon pathway activation with creatine. Accordingly, activating the CK pathway in the mouse model using the ADP-titration protocol reduced the K_m(ADP) value in WT cardiac muscle fibers, as expected (Table 1).

Previous experiments conducted without creatine using the ADP-titration protocol had demonstrated a significantly lower K_m(ADP) value in cardiac fibers of WFS1 KO mice. However, when creatine was introduced to mimic physiological conditions more accurately, the K_m(ADP) value for WFS1 KO animals remained unaltered (Table 1). Consequently, upon activating the CK pathway, the K_m(ADP) values in the study and control animals were comparable, with the decrease observed only in the control group. Consequently, no further significant decrease was detected in response to CK pathway activation with creatine in WFS1 KO mice.

Table 1. Michaelis-Menten constant K_m(ADP) values in the cardiac muscle of WFS1-deficient (WFS1 KO) and wild-type (WT) mice with and without activation of creatine kinase pathway by adding creatine.

	CARDIAC MUSCLE K_M(ADP) VALUE	
MOUS MODEL	**WITHOUT CREATINE**	**WITH CREATINE**
WT	101.6 ± 21.3	42.7 ± 5.0
WFS1 KO	54.2 ± 5.2	41.4 ± 3.0

Conversely, in a rat model, no pathological alterations were detected in WFS1 KO animals following CK pathway activation.

The CK/PCr pathway serves as cardiac muscle's primary energy transport system. We employed the PK/PEP system protocol to assess CK pathway activity to capture all ADP generated by ATPases in the cell's cytosol of the mouse model.

The PK/PEP system was activated by adding pyruvate kinase (PK), which traps all extramitochondrial ADP generated by ATPases (Figure 11A). In these conditions, energy flux through the CK pathway was measured, where registered oxygen consumption depended solely on the ADP/ATP circulation incorporated in the MI and CK transfer system. Activation of the PK/PEP system led to the rephosphorylation of ADP produced by ATPases to ATP in the cytosol. This resulted in decreased mitochondrial oxygen consumption by OXPHOS due to reduced ADP transport to mitochondria. The respiration started to increase after activation of the CK transfer system by stepwise addition of creatine, and the maximal respiration rate (V_{cr}) was determined upon achieving saturation. In the mouse model, the maximal creatine-activated OXPHOS rate (V_{cr}) in WFS1 KO cardiac muscle fibers was significantly lower compared to WT (Figure 11B). However, no difference in V_{cr} was observed between WFS1 KO and WT in a rat model.
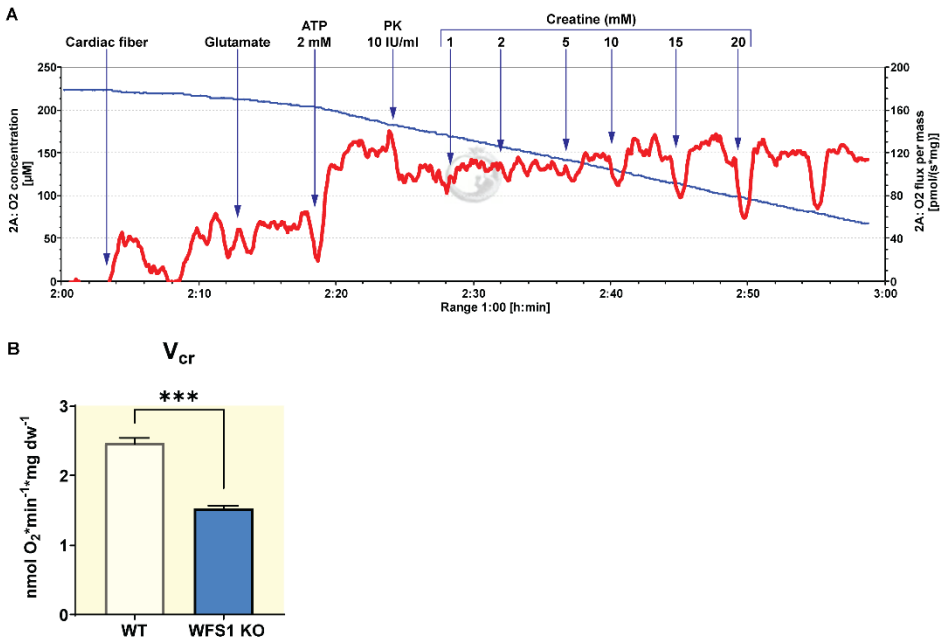
Figure 11. Functional coupling between OXPHOS and creatine kinase pathway in the mouse model. (A) Representative trace of oxygraphic measurement corresponding to PK/PEP system protocol to estimate CK coupling with OXPHOS in permeabilised cardiac muscle tissue in mice. The respiration rate is represented in nmol O_2*min^{-1}*mg dw^{-1} (red line; right axis); O_2 concentration is represented in μM (blue line; left axis). (B) The oxygen consumption rate is measured with the maximal activation of the creatine kinase pathway, and V_{cr} is the maximal oxygen consumption rate determined from the measurements for the Michaelis-Menten coefficient calculation. Respiration rate is represented in nmol O_2*min^{-1}*mg dw^{-1}; *p-value < 0.05, **p-value < 0.01, ***p-value < 0. 001. Results are expressed as mean ± SEM.

4.1.3.2 Investigating the Role of Adenylate Kinase Isoforms in Cardiac Muscle Energy Transfer

The adenylate kinase pathway represents another significant energy pathway in muscle cells, characterised by various AK enzyme isoforms. Our investigation focused on measuring the activity of the cytosolic adenylate kinase isoform AK1 and the mitochondrial adenylate kinase isoform AK2 using an oxygraphic method. These isoforms facilitate the transfer of high-energy phosphates from mitochondria to ATPases. AK2 is situated in the intermembrane space of mitochondria and facilitates both ATP production and its translocation from mitochondria to the cytosol. Conversely, AK1 is crucial in maintaining the ATP/ADP ratio at ATP-utilization sites by interconverting various adenosine phosphates (ATP, ADP, and AMP).

To assess the functional coupling of cytosolic and mitochondrial AKs with OXPHOS, we employed the adenylate kinase index (IAK) (Figure 12A,B). In the mouse model, we observed a significant increase in the AK index value in the heart fibers of WFS1 KO animals compared to the WT (Figure 12B). However, we did not reveal the same effect in the WFS1 KO rat model.
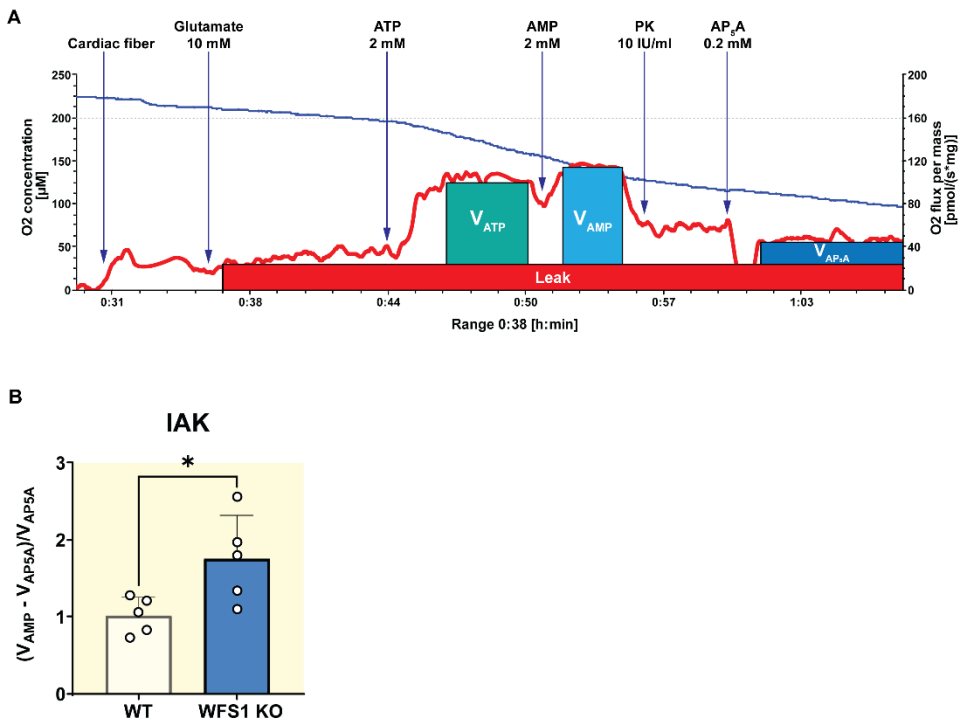
Figure 12. Functional coupling between OXPHOS and adenylate kinase (AK) pathway in the mouse model. (A) Representative trace of oxygraphic measurement of AK coupling with OXPHOS in permeabilised cardiac muscle tissue in mice. V_{ATP} is the oxygen consumption rate after activation of ATPases and production of endogenous ADP; V_{AMP} is the oxygen consumption rate at the maximal activation of the AK system; V_{AP5A} is the oxygen consumption rate in the presence of an AK inhibitor. The respiration rate is represented in nmol $O_2*min^{-1}*mg\ dw^{-1}$ (red line; right axis); O_2 concentration is expressed in µM (blue line; left axis). (B) Functional coupling of oxygen consumption with the AK pathway is represented as AK index (IAK) calculated as IAK = $(V_{AMP} - V_{AP5A})/V_{AP5A}$; *p-value < 0.05, **p-value < 0.01, ***p-value < 0. 001; n = 5. Results are expressed as mean ± SEM.

4.1.3.3 Assessing Hexokinase Activity and Functional Coupling of Oxidative Phosphorylation with Glycolysis in Cardiac Muscle

In our investigation of the glycolytic pathway, mainly focusing on the role of hexokinase in regulating cellular respiration, we calculated the glucose index (GI) as a metric to assess the functional coupling of OXPHOS with glycolysis (Figure 13A,B). The GI was determined as the ratio of the relative increase in OXPHOS rate following glucose addition to the maximal respiration rate with exogenous ADP.

Hexokinases catalyse the initial and irreversible step of glycolysis by phosphorylating glucose to glucose-6-phosphate. In our study, we sought to elucidate the impact of HK activity on cellular respiration dynamics. Our results revealed a higher GI in cardiac muscle tissues obtained from WFS1 KO mice compared to those from WT mice (Figure 13B). This observation suggests an enhanced functional coupling between OXPHOS and glycolysis in the cardiac muscle of WFS1 KO mice.
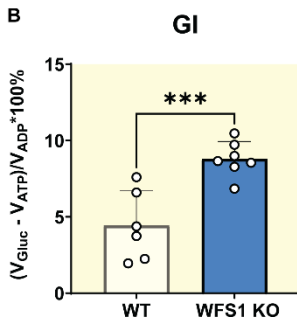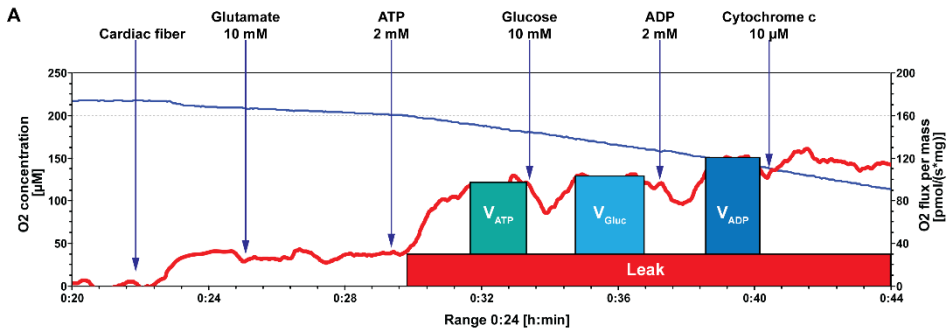
Figure 13. Functional coupling between OXPHOS and hexokinase in a mouse model. (A) Representative trace of oxygraphic measurement to estimate mitochondrial-associated HK coupling with OXPHOS in permeabilised cardiac muscle tissue in mice. V_{ATP} is the oxygen consumption rate with endogenous ADP; V_{Gluc} is the oxygen consumption rate with activated HK; V_{ADP} is the maximal ADP-dependent respiration rate. The respiration rate is represented in nmol $O_2*min^{-1}*mg$ dw^{-1} (red line; right axis); O_2 concentration is expressed in µM (blue line; left axis). (B) The glucose index (GI) is calculated as $(V_{Gluc} − V_{ATP})/(V_{ADP})*100\%$ where $(V_{Gluc} − V_{ATP})$ is the increase in the oxygen consumption rate in response to an addition of 10 mM glucose and V_{ADP} is the respiration rate in the presence of 2 mM ADP; *p-value < 0.05, **p-value < 0.01, ***p-value < 0. 001; n = 6–7. Results are expressed as mean ± SEM.

However, in contrast to the findings in the mouse model, our experiments conducted on a rat model did not yield similar results. Specifically, the GI did not exhibit significant differences between WFS1 KO animals and the WT group in the rat model.

4.1.4 Assessment of Enzymatic Activity in Cardiac Muscles of Wolframin-deficient Mice and Rats

Enzymatic activity measurements were employed in our investigation to elucidate the observed alterations in energy transfer pathways in the mouse model. Specifically, we assessed the activity levels of critical enzymes involved in energy transfer and metabolism: CK, AK, and HK. Our analysis indicated no significant differences in the enzymatic activity of these three enzymes between WFS1 KO animals and the control group. However, our findings revealed a decrease in the CK energy transfer system concurrent with an increase in the functional coupling of mitochondria with AK and HK in the cardiac muscles of WFS1 KO mice.

In the rat model, enzymatic activity measurements of CK, AK, and HK showed no significant differences between WFS1 KO and WT groups, consistent with the results

obtained from energy transfer pathway experiments. Furthermore, assessment of CI enzymatic activity in rat cardiac muscle revealed no differences between WFS1 KO and WT animals. Additionally, we investigated citrate synthase (CS) activity to explore potential alterations in mitochondrial abundance in WFS1 KO and WT animals. Our analysis did not detect any changes in CS activity between WFS1 KO and WT rat cardiac muscle samples.

4.1.5 Assessment of Cardiac Tissue Metabolite Composition in WFS1 Knockout Mice using ^{1}H NMR Spectroscopy (Paper I)

In this study, we conducted ^{1}H NMR spectroscopy analysis to assess the metabolite levels in water-soluble cardiac tissue extracts obtained from mice aged 4-6 months. Principal component analysis of proton NMR spectra revealed no systematic differences between the two mouse genotypes, indicating overall similarity in the metabolic profiles of WFS1 KO and WT groups.

Furthermore, we quantified the total creatine content and determined the concentrations of six abundant metabolites: glucose, lactate, alanine, glutamine, glutamate, and taurine. Our findings indicated no statistically significant differences in the levels of these metabolites between the WFS1 KO and WT groups in mice.

These results suggest that, at the metabolic level assessed by ^{1}H NMR spectroscopy, there are no discernible variations in cardiac tissue metabolite composition between WFS1 KO mice and their WT counterparts.

4.2 Impact of Cigarette Smoking and Smoking Cessation as Extrinsic Factor on Mitochondrial Bioenergetics, Metabolism, and Structural Changes in Cardiac Tissue: Insights from Murine Studies (Paper III)

In the second segment of our study, we delved into the impact of smoking and smoking cessation as extrinsic factors on mitochondrial bioenergetics, cellular metabolism, and structural changes in murine cardiac tissue. Our objectives were to elucidate the alterations on the molecular level in cardiac tissue induced by extrinsic factors and to examine the recovery process.

4.2.1 Impact of Cigarette Smoking and Smoking Cessation on Mitochondrial Function in Cardiac Tissue

To elucidate smoking-induced alterations in cardiac metabolism, we assessed mitochondrial respiration in the apex of the heart. Leak respiration with NADH substrates, NADH (CI)-linked respiration, and CII-linked respiration showed no significant differences between groups (Figure 14A-C). However, oxidative phosphorylation capacity tended to decrease after smoking compared to the control, subsequently returning to control values after smoking cessation (Figure 14D). Notably, uncoupling respiration (Figure 14E) demonstrated a significant decrease after smoking, returning to control levels after smoking cessation. Succinate dehydrogenase (SDH) activity declined post-smoking and continued to diminish after one week of smoking cessation yet returned to smoking levels following a two-week cessation period (Figure 14F,G).
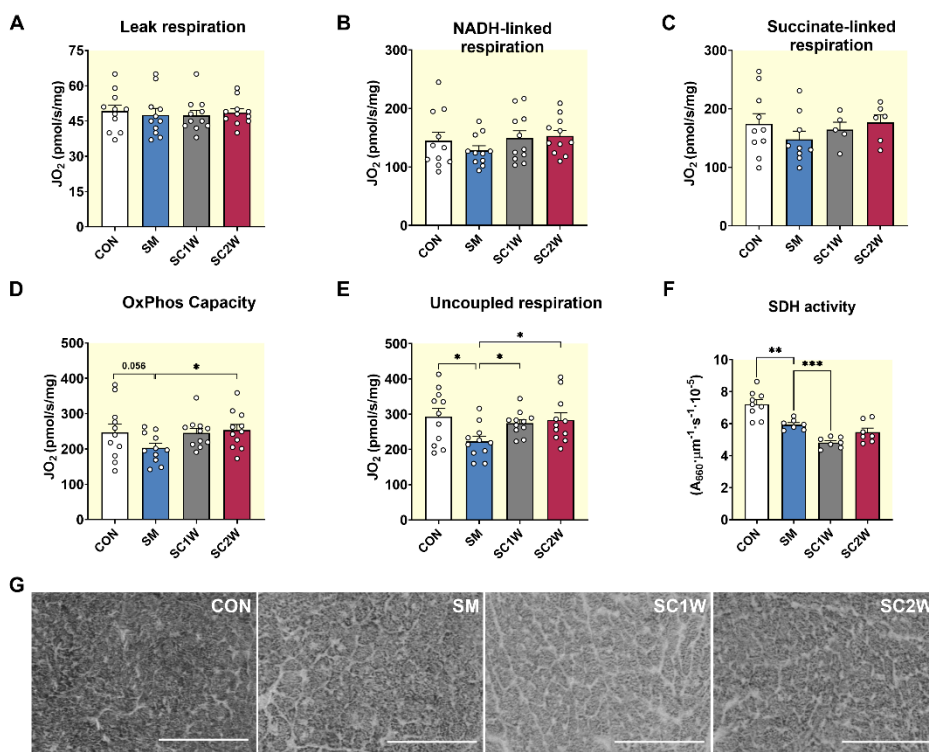
Figure 14. Cardiac uncoupling respiration is reduced with smoking and restored after smoking cessation. Succinate dehydrogenase activity depression in smoking and smoking cessation groups in mice. (A) Leak respiration, (B) NADH (complex I)-linked with pyruvate, malate, and glutamate, and (C) complex II-linked respiration (with succinate/rotenone) were not significantly different among control (CON), smoking (SM), and after 1–2 weeks smoking cessation (SC1W and SC2W). (D) Oxidative phosphorylation and (E) uncoupled respiration were lower in smoking compared to 2-week smoking cessation (CON n = 11, SM n = 11, SC1W n = 11, SC2W n = 11). (F) Lower succinate dehydrogenase (SDH) activity after smoking and both groups of smoking cessation compared to control (CON n = 9, SM n = 7, SC1W n = 7, SC2W n = 7). (G) Representative images of succinate dehydrogenase (SDH) activity staining. The scale bar is 100 µm. Results are expressed as mean ± SEM. SM vs. CON and SC2W vs. CON (unpaired two-tailed t-test); SC1W vs. SM and SC2W vs. SM (one-way ANOVA).

4.2.2 Effects of Smoking and Smoking Cessation on Mitochondrial Protein Content and Supercomplex Formation

The content of mitochondrial CI subunit NDUFB8 was observed to be diminished after smoking compared to the control group, persisting at lower levels even after two weeks of smoking cessation (Figure 15 A,B). Conversely, no notable differences were detected in the protein levels of subunits pertaining to CII, CIII, and ATP synthase (Figure 15 C,D,F), although a reduction in CIV subunit MTCO1 was evident after smoking (Figure 15 E). Protein content analysis of critical regulators of mitochondrial fusion (OPA1) and fission (DRP1) revealed no significant alterations across experimental groups (Figure 15 G-I).
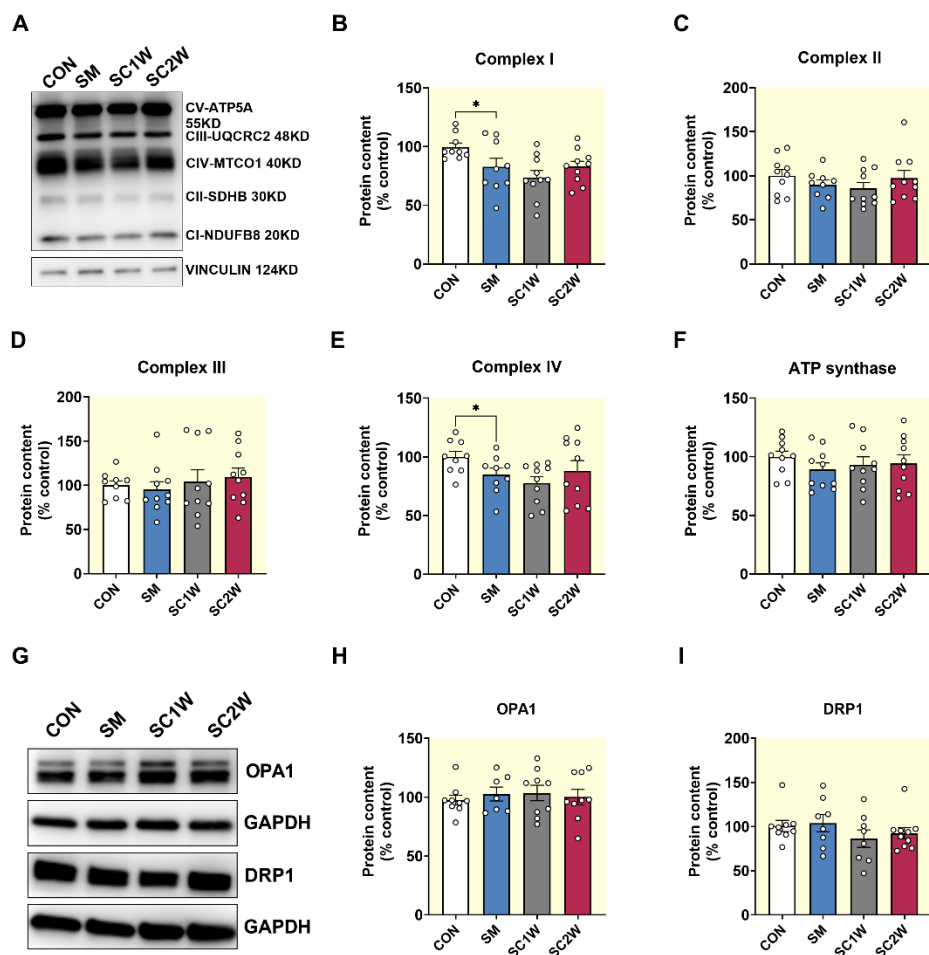
Figure 15. Effect of smoking and smoking cessation on the abundance of complex I and complex IV subunits and mitochondrial dynamics (fusion and fission) in the heart of mice. (A) A typical example is showing bands of the mitochondrial complex subunits. (B-F) Protein content of mitochondrial complex I-IV and ATP synthase subunits (CON n = 9–10, SM n = 9–10, SC1W n = 10, SC2W n = 10). Vinculin was used as a loading control. (G) Typical example of Western immunoblotting showing bands of the OPA1 (CON n = 9, SM n = 7, SC1W n = 9, SC2W n = 9) and DRP1 proteins in control (CON n = 9), smoking (SM n = 8), 1–2-week smoking cessation (SC1W n = 8, SC2W n = 10). (H-I) The protein content of markers for mitochondrial fusion OPA1 (H) and fission DRP1 (I) were not significantly different between groups. Results are expressed as mean ± SEM. SM vs. CON and SC2W vs. CON (unpaired two-tailed t-test); SC1W vs. SM and SC2W vs. SM (one-way ANOVA).

Following the isolation of mitochondria, we conducted blue-native electrophoresis to assess mitochondrial supercomplex (SC) formation (Figure 16A-D). Notably, smoking was associated with a decreased abundance of high-molecular-weight mitochondrial SCs, which was rectified to control levels after a two-week smoking cessation period (Figure 16A). Additionally, the content of free mitochondrial complexes tended to decrease after smoking, persisting at lower levels post-smoking cessation (Figure 16B). Interestingly, the normalised mitochondrial supercomplex content, relative to total

complexes (Figure 16C), remained consistent between smoking and control conditions, indicating a proportional reduction in SCs and free complexes after smoking. Furthermore, the normalised mitochondrial SC content gradually increased following smoking cessation, indicating a transition of free complexes to SCs.
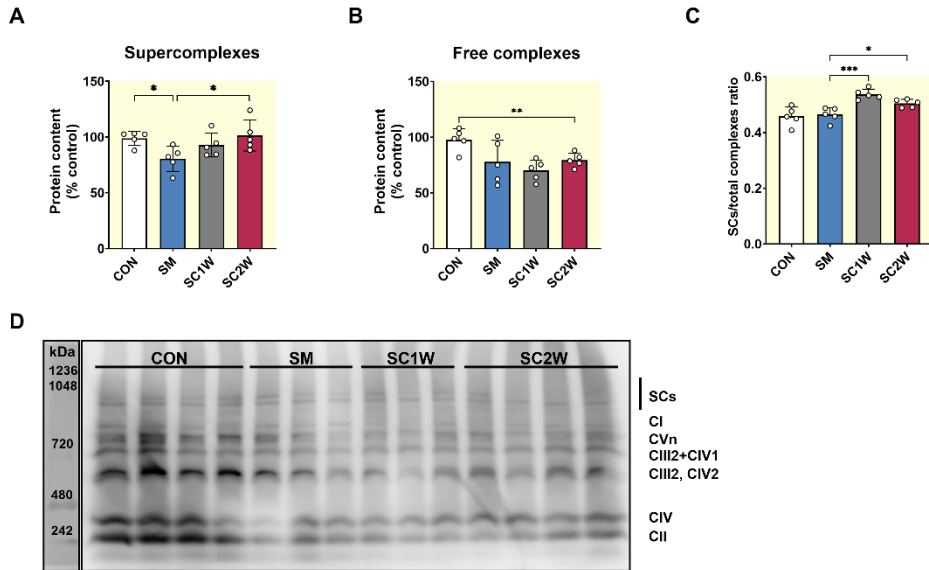

Figure 16. Supercomplex formation in the heart after smoking and smoking cessation in mice. (A) The protein content of high-molecular-weight supercomplexes was lower after smoking and recovered after smoke cessation (CON n = 5, SM n = 5, SC1W n = 5, SC2W n = 5). (B) The content of free or low-molecular-weight complexes of CI-IV and ATPase synthase were lower in SC1W and SC2W. (C) Normalised supercomplex relative to total complex increased after smoke cessation. (D) Representative examples of free mitochondrial complexes and complexes assembled in the supercomplex (SCs: $I+III_2+II_n$, $I+III_2+IV_1$). Results are expressed as mean ± SEM. SM vs. CON and SC2W vs. CON (unpaired two-tailed t-test); SC1W vs. SM and SC2W vs. SM (one-way ANOVA).

4.2.3 Metabolic and Lipidomic Profiling Reveals the Impact of Cigarette Smoking and Smoking Cessation on Cardiac Metabolism and Lipid Composition

Metabolomics analyses were conducted to elucidate the impact of cigarette smoking and cessation on cardiac metabolism. Metabolites with variable importance in projection (VIP) score exceeding 1.4 were subjected to enrichment pathway analysis. This analysis unveiled notable alterations in various metabolic pathways, including nicotinate and nicotinamide metabolism, glycolysis, pentose phosphate metabolism, gluconeogenesis, branched-chain amino acid degradation, nucleotide metabolism, mitochondrial beta-oxidation, and other lipid metabolism pathways (Figure 17).

Figure 17. Top 30 metabolic pathways altered after smoking and smoking cessation in mice. The enrichment plot depicts several metabolic pathway alterations induced by smoking and smoking cessation. Metabolites were used with variable importance in projection (VIP) score > 1.4 for control (CON n = 5), smoking (SM n = 5), and 1 to 2 weeks of smoking cessation (SC1W n = 5 and SC2W n = 5). The dot size represents the enrichment ratio (metabolite count enriched in the pathway), and the colour presents significance.

Cigarette smoking and subsequent cessation exerted notable effects on the nicotinamide adenine dinucleotide (NAD$^+$) pathway, specifically leading to a decrease in the reduced form of nicotinamide mononucleotide (NMNH) (Figure 18). Following a two-week smoking cessation period, levels of NAD$^+$ and NADH were observed to increase in comparison to active smoking conditions.
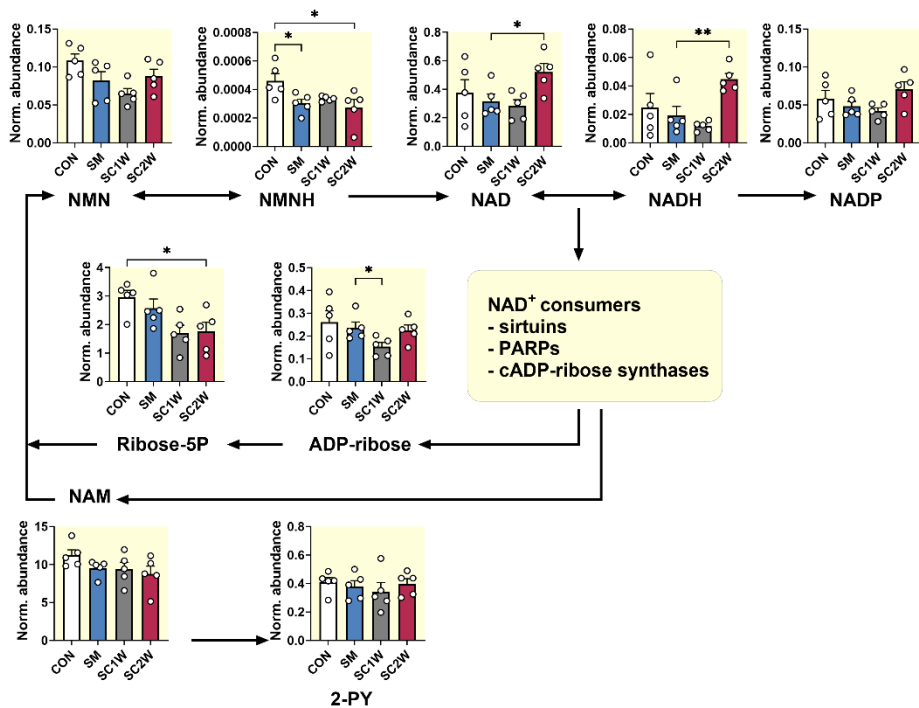
Figure 18. Smoking- and smoking-cessation-induced alterations in metabolites related to NAD+ metabolism in the mouse heart. A simplified diagram describes the route from nicotinamide mononucleotide (NMN) and reduced form of nicotinamide mononucleotide (NMNH), the precursors of NAD biosynthesis, to nicotinamide (NAM) through nicotinamide adenine dinucleotide (NAD) and reduced form of nicotinamide adenine dinucleotide (NADH). NADP indicates nicotinamide adenine dinucleotide phosphate; 2-PY indicates N-methyl-2-pyridone-5-carboxamide. Control (CON n = 5), smoking (SM n = 5), 1-week smoking cessation (SC1W n = 5), and 2-week smoking cessation (SC2W n = 5). Results are expressed as mean ± SEM. SM vs. CON and SC2W vs. CON (unpaired two-tailed t-test); SC1W vs. SM and SC2W vs. SM (one-way ANOVA).

Additionally, elevated concentrations of metabolites associated with glycolysis and gluconeogenesis indicated an increased rate of glucose catabolism following two weeks of smoking cessation compared to control conditions (Figure 19). Conversely, metabolites involved in the pentose phosphate pathway, such as ribose-5 phosphate and sedoheptulose-7 phosphate, exhibited lower levels after two weeks of smoking cessation compared to control conditions (Figure 19). Notably, ophthalmic acid, a biomarker associated with oxidative stress, demonstrated elevated levels both after smoking and following the two-week cessation period (Figure 19).
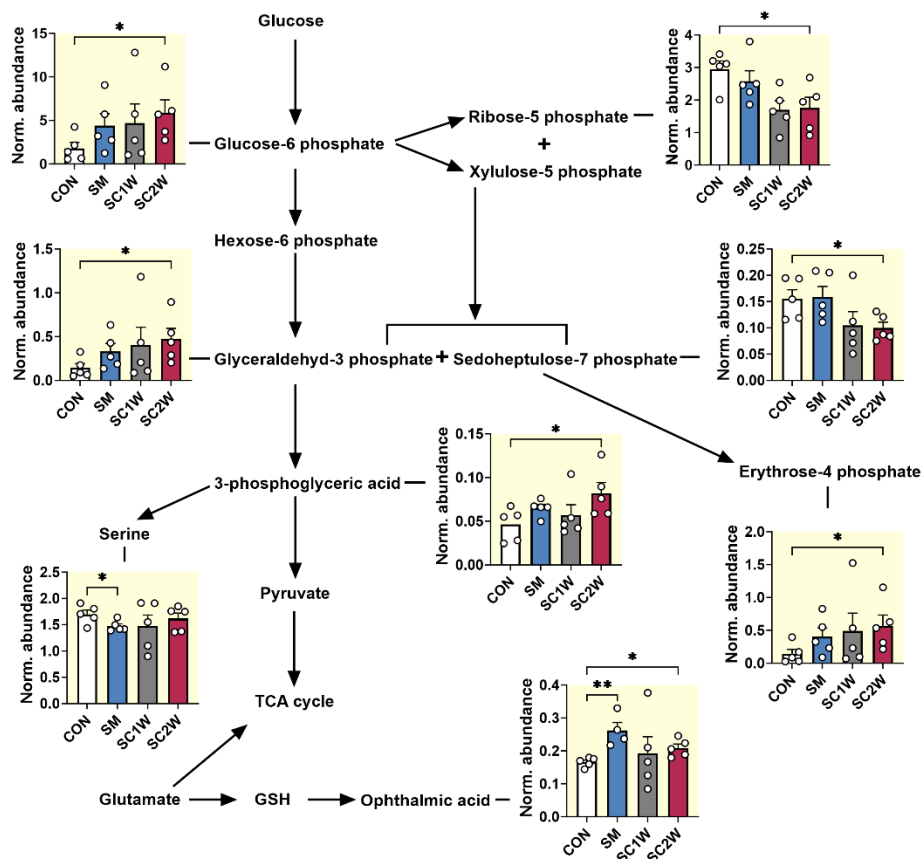
Figure 19. Smoking- and smoking-cessation-induced changes in the levels of metabolites of the glycolysis, pentose phosphate pathway, and cell stress pathway in the mouse heart. A simplified diagram of the glycolysis, the pentose phosphate pathway, the tricarboxylic acid (TCA) cycle, and cell stress pathway. The pentose phosphate pathway is linked to glycolysis through glucose 6-phosphate. In reversible reaction of ribose-5 phosphate and xylulose-5 phosphate form glyceraldehyde-3 phosphate and sedoheptulose-7 phosphate. In the reversible reaction of glyceraldehyde-3 phosphate and sedoheptulose-7 phosphate form hexose-6 phosphate and erythrose-4 phosphate. Ophthalmic acid is a metabolite produced by the same enzymatic reactions as glutathione (GSH) but without the reactive cysteine. It can be used as a marker for (increased) GSH synthesis. Control (CON n = 5), smoking (SM n = 5), 1-week smoking cessation (SC1W n = 5), and 2-week smoking cessation (SC2W n = 5). Results are expressed as mean ± SEM. SM vs. CON and SC2W vs. CON (unpaired two-tailed t-test); SC1W vs. SM and SC2W vs. SM (one-way ANOVA).

Upon one week of smoking cessation, concentrations of the branched-chain amino acids isoleucine, leucine, and valine (Figure 20A-C) decreased compared to levels observed during smoking. However, restoration of branched-chain amino acid content to control levels did not occur after two weeks of smoke cessation.
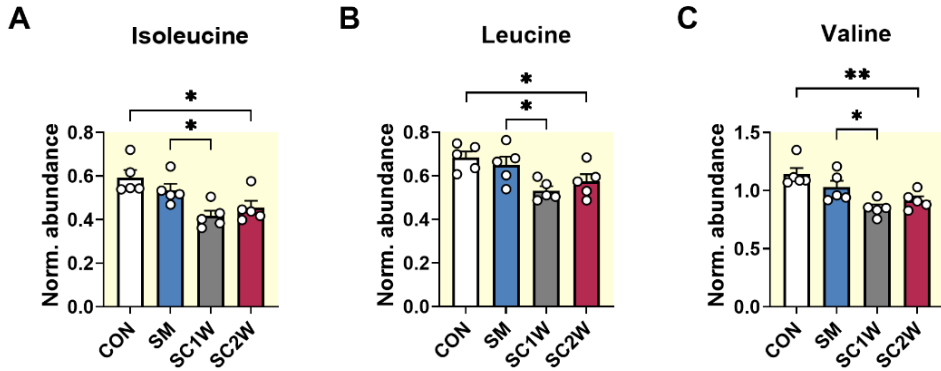
Figure 20. Smoking- and smoking-cessation-induced decrease in branched-chain amino acids (BCAAs) content in the mouse heart. Abundance of BCAAs (A) isoleucine, (B) leucine and (C) valine in mice heart in control (CON n = 5), smoking (SM n = 5), 1-week smoking cessation (SC1W n = 5) and 2-week smoking cessation (SC2W n = 5) groups. Results are expressed as mean ± SEM. SM vs. CON and SC2W vs. CON (unpaired two-tailed t-test); SC1W vs. SM and SC2W vs. SM (one-way ANOVA).

Although cardiac purine and pyrimidine contents remained unaffected by smoking, their levels were elevated after two weeks of smoke cessation compared to control conditions (Figure 21). Metabolites involved in purine biosynthesis, such as inosinic acid (IMP) and hypoxanthine, were unaltered by smoking but displayed decreased levels following two weeks of smoke cessation (Figure 21).
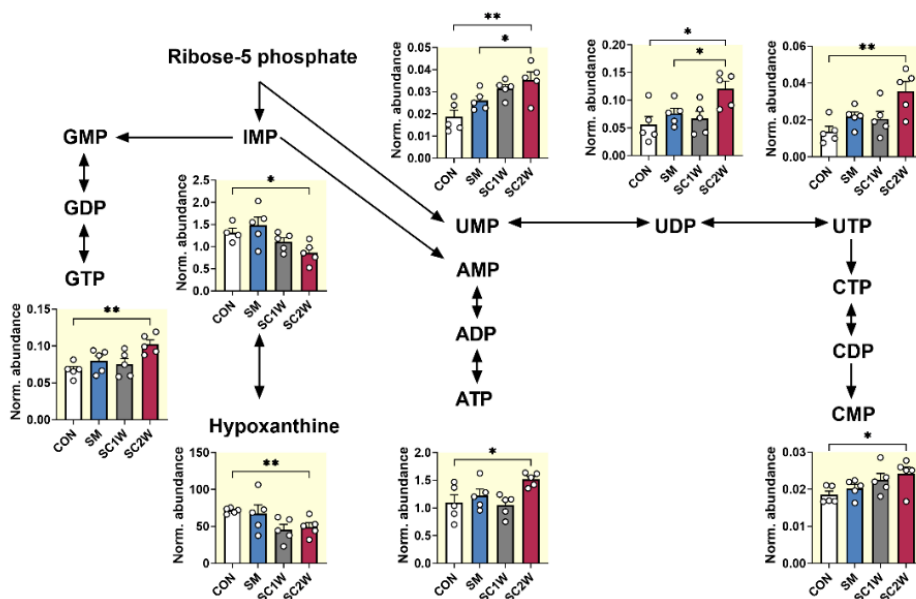
Figure 21. Simplified schematic representation of purine and pyrimidine metabolism in the heart of smoking and smoking-cessation mice. Ribose-5 phosphate is the starting point of the two de novo biosynthesis pathways. Abbreviations: IMP, inosine monophosphate; UMP, uridine monophosphate; UDP, uridine diphosphate; UTP, uridine triphosphate; CTP, cytidine triphosphate; CDP, cytidine diphosphate; CMP, cytidine monophosphate; AMP, adenine monophosphate; ADP, adenine diphosphate; ATP, adenine triphosphate; GMP, guanosine monophosphate; GDP, guanosine diphosphate; GTP, guanosine triphosphate. Control (CON n = 5), smoking (SM n = 5), 1-week smoking cessation (SC1W n = 5), and 2-week smoking cessation (SC2W n = 5). Results are expressed as mean ± SEM. SM vs. CON and SC2W vs. CON (unpaired two-tailed t-test); SC1W vs. SM and SC2W vs. SM (one-way ANOVA).

Lipid profiling of the cardiac apex was conducted to investigate potential alterations in lipid content and species induced by smoking. Enrichment analysis revealed a differential abundance of various lipid classes between experimental groups (Figure 22A-D). Despite total triacylglycerol concentration in heart tissue remaining unchanged after both smoking and smoking cessation, concentrations of long-chain and very-long-chain highly unsaturated triacylglycerols were elevated following two weeks of smoke cessation compared to both control and smoking conditions (Figure 22E-H). This suggests a potential reduction in triacylglycerol breakdown or an increase in their production after smoke cessation.
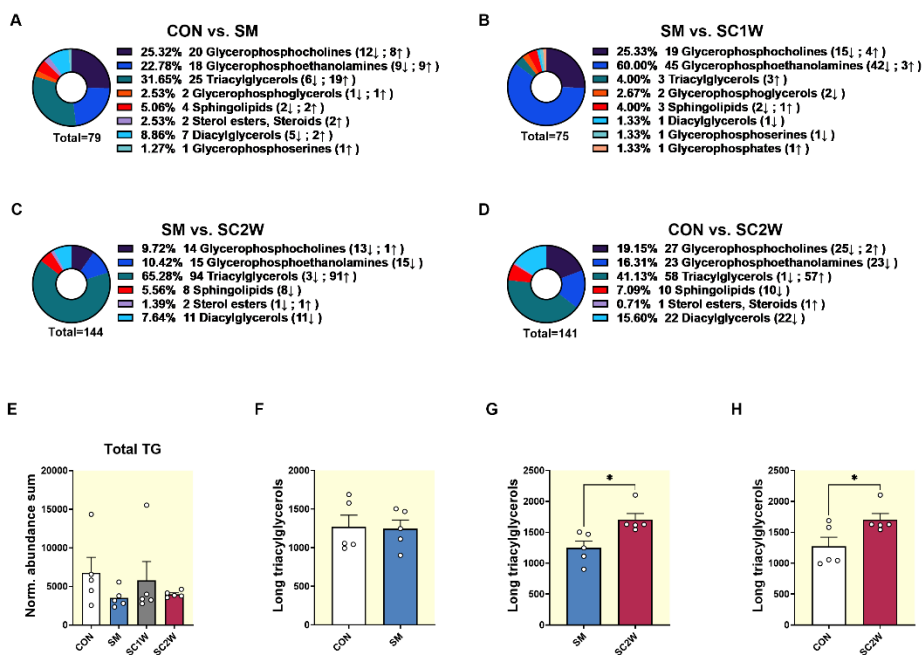
Figure 22. Lipids analysis of the mouse heart after smoking and smoking cessation. Pie charts depicting the lipidomic data of comparison (A) control and smoking (CON vs SM), (B) smoking and 1-week smoking cessation (SM vs. SC1W), (C) smoking and 2-week smoking cessation (SM vs. SC2W), and (D) control and 2-week smoking cessation groups (CON vs. SC2W). The pie chart depicts the main lipid classes different between groups; lipid species with p-value < 0.05 were used for this analysis. CON n = 5, SM n = 5, SC1W n = 5, SC2W n = 5. (E) Total triacylglycerols concentration in control (CON n = 5), smoking (SM n = 5), and 1- or 2-week smoking cessation groups (SC1W n = 5 and SC2W n = 5, respectively). SM vs. CON and SC2W vs. CON (unpaired two-tailed t-test); SC1W vs. SM and SC2W vs. SM (one-way ANOVA). (F-H) Comparison of long- and very-long-chain highly unsaturated triacylglycerols among control, smoking, and two weeks of smoking cessation. Triacylglycerols TG (51:5) – TG (84:18) were chosen for comparison. CON vs. SM, SM vs. SC2W, and CON vs. SC2W (unpaired two-tailed t-test). Results are expressed as mean ± SEM.

4.2.4 Effects of Smoking and Smoking Cessation on Glucose Transport: Investigation of GLUT4 Translocation and Protein Concentration in Cardiac Tissue

Our comprehensive metabolomic and lipidomic analyses unveiled a notable metabolic shift induced by smoking cessation, characterised by a transition from fatty acid oxidation to glucose oxidation. This alteration in metabolic substrate preference suggested a potential modulation in the cellular trafficking of glucose transporter type 4 (GLUT4) from the cytosol to the cell membrane. To investigate this phenomenon further, we assessed membrane-associated GLUT4 in mice subjected to a fasting period exceeding three hours.

Surprisingly, our observations revealed that smoking did not exert any significant influence on the fraction of GLUT4 associated with the cell membrane (Figure 23A-D). However, following smoking cessation, there was a discernible increase in the translocation of GLUT4 towards the cell membrane (Figure 23A,C), indicating a potential regulatory

mechanism associated with smoking cessation. Interestingly, no differences were observed in the amount of cell membrane that contained GLUT4 (Figure 23D).

To complement our findings, we employed western immunoblotting to examine whether there were alterations in the overall concentration of GLUT4 protein. However, no significant differences in the overall GLUT4 protein concentration were observed between groups (Figure 23B). These results suggest that while smoking cessation may influence the translocation of GLUT4 to the cell membrane, it does not significantly affect the total abundance of GLUT4 protein in cardiac tissue.
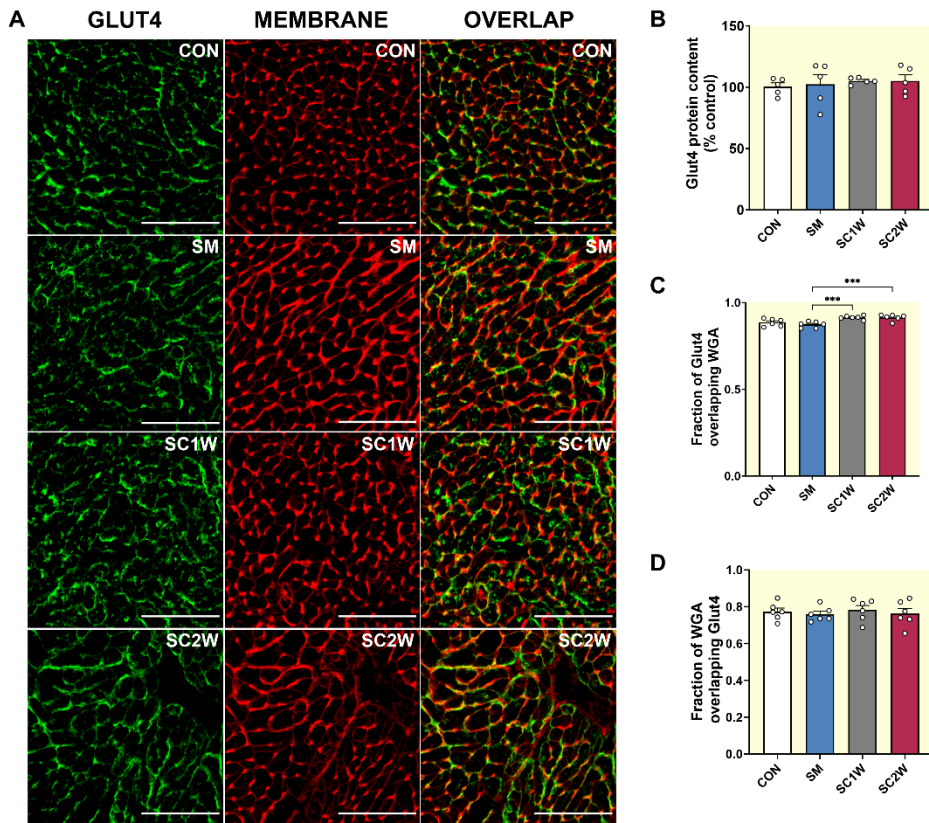

Figure 23. More glucose transporter type 4 (GLUT4) translocation at the cell membrane after smoking and smoking cessation in mice. (A) Representative images of heart sections stained with GLUT4 antibody. The left panel shows GLUT4 protein staining with GLUT4 antibody; the middle panel shows membrane staining with WGA antibody; and the right panel shows GLUT4 and membrane staining overlapping. The scale bar is 100 μm. (B) Western blot analysis was used to measure the protein content of GLUT4 (CON n = 5, SM n = 5, SC1W n = 5, SC2W n = 5). (C) The fraction of GLUT4 localised at the cell membrane increased after smoke cessation. (D) Fraction of membrane overlapping with GLUT4 in control (CON n = 6), smoking (SM n = 6), and 1- or 2-week smoking cessation (SC1W n = 6, SC2W n = 6). Results are expressed as mean ± SEM. SM vs. SM vs. CON and SC2W vs. CON (unpaired two-tailed t-test); SC1W vs. SM and SC2W vs. SM (one-way ANOVA).

4.2.5 Effects of Smoking and Smoking Cessation on Body Mass, Heart Mass, Cardiomyocyte Size, Collagen Content, Capillary Density, and Cardiac Nuclear Density in a Murine Model

Our study observed distinct alterations in body mass, heart mass, and cardiomyocyte size associated with smoking and smoking cessation (Figure 24A-D). Specifically, body mass exhibited a reduction following smoking (SM) compared to the control (CON) group, with a gradual increase noted after smoking cessation (Figure 24A). Conversely, while heart mass did not significantly differ between the smoking and control groups, it demonstrated an elevation following two weeks of smoking cessation (SC2W) compared to the smoking cohort (Figure 24B). Interestingly, the heart-to-body mass ratio exhibited an increase following smoking, which persisted unchanged after smoking cessation. Furthermore, assessment of the cardiomyocyte cross-sectional area revealed a tendency towards lower values after smoking (Figure 24C,D), albeit without a subsequent increase following smoking cessation.

We observed that collagen content was elevated in smoking groups compared to controls and further increased after one week of smoking cessation (Figure 24E,F). Interestingly, while there was no significant difference in collagen content between two weeks of smoking cessation (SC2W) and smoking groups, the collagen content in SC2W remained higher compared to the control group.

Regarding capillary density (Figure 24G,H), we found no significant differences between smoking and control groups. However, capillary density notably increased after smoking cessation and remained elevated compared to the control group.
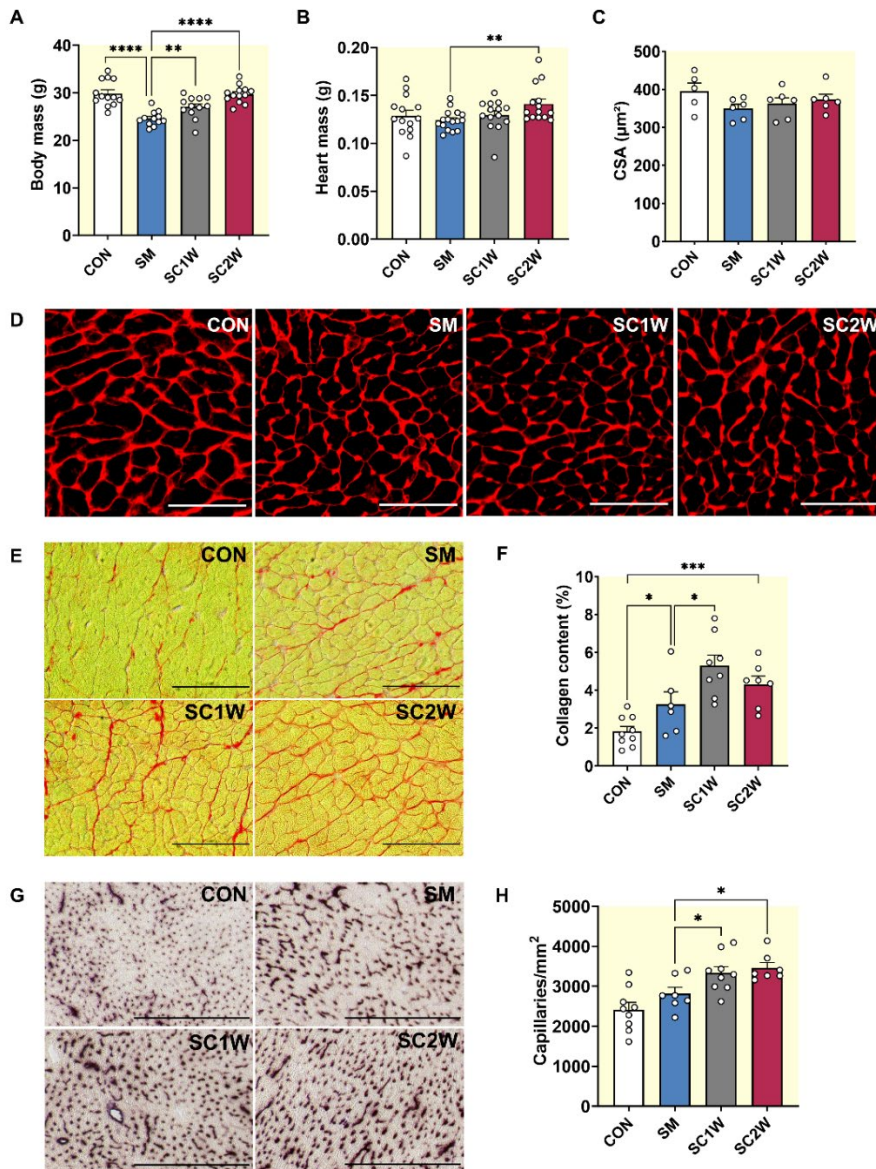
Figure 24. Body mass, heart mass, cross-sectional area of cardiomyocytes, fibrosis, and capillary density after smoking and smoking cessation in mice. (A) Body (CON n = 13, SM n = 12, SC1W n = 12, SC2W n = 13) and heart mass (B) of mice exposed to cigarette smoke (SM n = 16) and after 1–2 weeks of smoking cessation (SC1W n = 14, SC2W n = 14), compared to control (CON n = 14). (C) The cardiomyocyte cross-sectional area was not significantly different between groups (CON n = 5, SM n = 6, SC1W n = 6, SC2W n = 6). (D) Representative images of cell membranes (wheat germ agglutinin antibody). (E) Representative images of collagen. (F) Collagen content was higher after smoking and further increased after smoking cessation (CON n = 9, SM n = 6, SC1W n = 8, SC2W n = 7). (G) Representative images of cardiac capillaries. (H) Capillary density increased after 1 and 2 weeks of smoking cessation (CON n = 9, SM n = 7, SC1W n = 9, SC2W n = 7). Results are expressed as mean ± SEM. The corresponding significant p values are shown in the figures. The scale bar represents 100 μm (D, E) or 250 μm (G). SM vs. CON and SC2W vs. CON (unpaired two-tailed t-test); SC1W vs. SM and SC2W vs. SM (one-way ANOVA).

Our investigation used a hematoxylin and eosin stain to visualise cells and nuclei in cardiac tissue samples (Figure 25 A,B). Our analysis revealed no significant differences in cardiac nuclear density between smoking and control groups. However, nuclear density increased after one week of smoking cessation, although this effect was not sustained after two weeks of cessation compared to smoking. Notably, no signs of cardiac cell necrosis or cell death were observed in any of the experimental groups.

Further examination suggested that the additional nuclei observed after one week of smoking cessation may represent infiltrated immune cells, particularly macrophages. Cigarette smoke exposure notably elevated the concentration of infiltrated macrophages compared to the control group (Figure 25 C,D). Importantly, this elevation persisted above control levels even after smoking cessation.
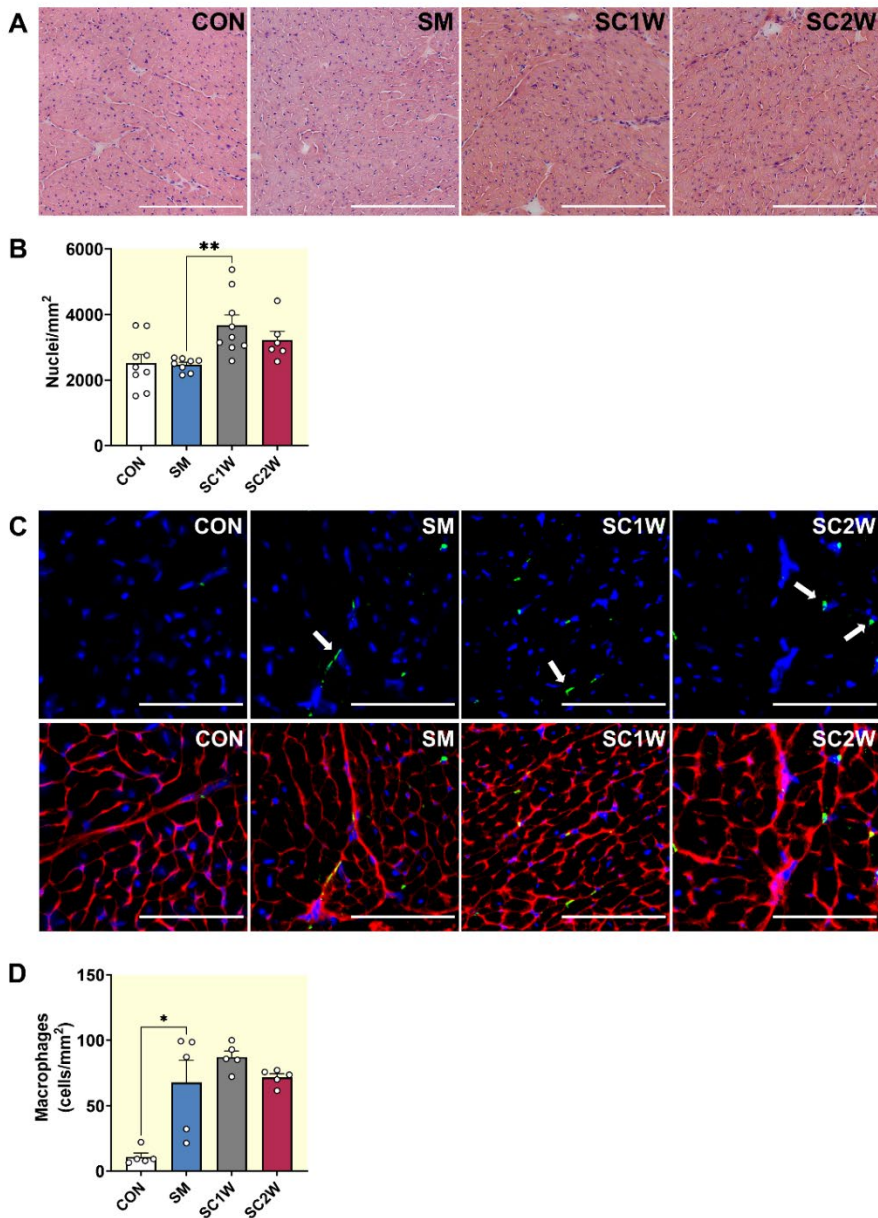
Figure 25. Nuclear density and macrophage infiltration of cardiac tissue after smoking and smoking cessation in mice. (A) Representative examples for hematoxylin and eosin staining in control (CON), smoking (SM), and 1-2 weeks of smoking cessation (SC1W and SC2W). (B) Nuclear density in cardiac tissue increased after smoking cessation (CON n = 9, SM n = 8, SC1W n = 9, SC2W n = 6). (C) Representative examples of macrophages (green), membranes (red), and nuclei (blue). The upper panel shows staining of cardiomyocyte nuclei and macrophages, and the lower panel shows staining of cardiomyocyte membranes and nuclei and macrophages. White arrows show macrophages (upper panel). (D) Macrophage density was higher after smoking and smoking cessation. (CON n = 5, SM n = 5, SC1W n = 5, SC2W n = 5). Results are expressed as the mean ± SEM. The scale bar is 250 (A) or 50 µm (C). SM vs. CON and SC2W vs. CON (unpaired two-tailed t-test); SC1W vs. SM and SC2W vs. SM (one-way ANOVA).

5 Discussion

5.1 Metabolic Flexibility and Compensatory Mechanisms in Cardiac Tissue of WFS1 Deficient Animal Models: Insights into Gene Mutations as Intrinsic Factors

The WFS1 gene exhibits high expression levels within cardiac tissue, yet cardiac manifestations are notably absent from the core complications of WS (Barrett & Bundey, 1997; Minton et al., 2003). While the functional repercussions of WFS1 deficiency in the heart remain understudied, sporadic reports indicate cardiac anomalies in WS patients, including occurrences of cardiac murmurs, cardiomyopathy, disrupted cardiac calcium signalling, and compromised cardiac function (Cagalinec et al., 2019; Ganie et al., 2011; Korkmaz et al., 2016; Medlej et al., 2004). Based on various publications, it is suggested that the WFS1 gene plays a significant role in modulating calcium homeostasis, regulating calcium transport between the ER and mitochondria, and participating in the formation of MAM structures (Delprat et al., 2018; La Morgia et al., 2020). However, the absence of severe cardiological complications resulting from mutations in this gene is perplexing.

The primary objective of this investigation is to characterise the bioenergetic profile of cardiomyocytes and explore the potential existence of inherent cardioprotective mechanisms associated with intrinsic factors, notably the deletion of the highly expressed WFS1 gene in cardiac tissue and the subsequent development of early-stage diabetes. Given the known functions of the WFS1 gene in cellular processes, the expected changes in cardiac function and metabolism are anticipated to be more significant than what has been observed in WS patients and animal models. Notably, the absence of specific cardiac pathologies upon WFS1 gene deletion presents an opportunity to explore compensatory mechanisms regulating cardiac bioenergetics. This investigation is unique and has not been previously conducted in the context of WS. To this end, we utilised two distinct models of WFS1-deficient animals: mice lacking the 8th exon of WFS1 and rats with deletion of the 5th exon. Given WFS1's cellular functions, it is hypothesised that WFS1 deficiency would impact cardiac bioenergetics, yet compensatory mechanisms may mitigate these alterations, thereby accounting for the infrequent cardiac complications observed in WS patients. To minimise the potential confounding effects of diabetes and other early symptoms of WS on cardiac bioenergetics, experimental animals were deliberately chosen from an age cohort preceding the manifestation of most symptoms associated with WS (Ivask et al., 2016; Koks, 2023; Plaas et al., 2017). This strategic selection aims to isolate the influence of WFS1 deficiency on cardiac energetics, independent of any secondary effects resulting from other complications, particularly late-stage diabetic complications. Through a series of experiments, we evaluated the influence of intrinsic factors on mitochondrial function and substrate preferences, shedding light on the complex interplay between genetic mutations, cellular metabolism, and cardiac physiology.

In the initial phase of our study, we employed WFS1 deficient mice with a deletion of the 8th exon and their WT littermates, aged between 4 and 6 months. This model is well-established to mirror various facets of WS, including growth retardation, diabetes, infertility, ocular complications, and notably, neurological and behavioural abnormalities, alongside a shortened lifespan (Ivask et al., 2016; Koks, 2023; Koks et al., 2009; Luuk et al., 2008; Luuk et al., 2009; Noormets et al., 2009).

Our investigation revealed significant kinetic alterations in the apparent affinity of exogenous ADP to mitochondria in WFS1 KO mice compared to WT counterparts. Notable changes were also observed in the functional characteristics of the electron transport chain and phosphotransfer networks, which play pivotal roles in facilitating the transport of high-energy bonds to ATPases. These findings underscore the intricate regulatory mechanisms governing mitochondrial function in the absence of WFS1 expression and provide insights into potential disruptions in cellular energy metabolism pathways associated with WFS1 deficiency.

Specifically, we noted a reduced maximal ADP-dependent respiration rate in WFS1 deficient animals when utilising glutamate and malate as substrates, albeit in the absence of pyruvate. Additionally, we observed a reduced K_m(ADP) value for WFS1 KO animals compared to controls under these conditions. This suggests that WFS1 deficiency may impact glutamate metabolism pathways without significantly affecting pyruvate metabolism. Given the known association of WS with increased ER stress, decreased mitochondria-ER connectivity, and disturbances in calcium homeostasis, we speculate that these alterations may influence the activity of mitochondrial proteins involved in glutamate metabolism, such as the glutamate/aspartate antiporter (AGC) (Del Arco et al., 2016; Rueda et al., 2016; Yuan et al., 2023).

Furthermore, our study revealed several alterations in energy trafficking pathways within cardiac muscle cells of WFS1 KO mice. Despite observing an unchanged oxygen consumption rate in WFS1-deficient mice under activated creatine kinase (CK) pathway conditions, a lower rate was noted in the absence of pathway activation compared to control animals. This discrepancy may suggest weakened interactions between mitochondrial CK and adenine nucleotide translocase (ANT), potentially compromising the function of the Mitochondrial Interactosome (MI) (Saks et al., 2010). These findings imply that WFS1 deficiency could disrupt the coordination between CK and ANT, crucial components of the MI complex, which is integral to regulating mitochondrial energy metabolism. Further investigation into the molecular mechanisms underlying these disruptions is warranted to elucidate their impact on overall mitochondrial function and cellular energy homeostasis in WFS1-deficient mice.

The observed decrease in creatine kinase pathway activity in WFS1 KO mice corresponds with an increased functional coupling between mitochondria and the adenylate kinase and hexokinase pathways. Furthermore, the heightened glycolytic activity indicated by the increase in the glycolytic index value in the cardiac muscle cells of WFS1 KO mice resembles age-related changes observed in rat heart cardiomyocytes (Tepp et al., 2016). These findings suggest the presence of a compensatory mechanism wherein the AK and HK pathways assume greater responsibility in managing energy flow from mitochondria to ATPases, particularly in situations where CK pathway function is compromised. This adaptive response likely plays a crucial role in maintaining cellular energy homeostasis and underscores the dynamic interplay between different metabolic pathways to ensure efficient ATP production and utilisation in cardiac muscle cells.

Previous research has indicated that WFS1 mutant mice exhibit glucose intolerance and diminished insulin secretion, although they do not display fasting hyperglycemia. Thus, the WS mouse model only partially manifests diabetes and other symptoms of WS, according to reports by Plaas et al. (Plaas et al., 2017). In contrast, the WFS1 KO rats utilised in the second part of our experiments, aged 8–9 months with a deletion of the 5th exon of the WFS1 gene, better mimic the human condition of WS (Plaas et al., 2017). Disease progression in these rats begins with a defect in glucose-stimulated insulin

release at three months of age, followed by glucose intolerance and decreased basal serum insulin levels at six months. By ten months, WFS1 deficient rats exhibit signs of glycosuria, which worsens by 13 months, preceding the development of hyperglycemia. While WFS1 KO rats exhibit insulin deficiency, insulin sensitivity remains unaltered at the age during our experiments. Additionally, experiments by Cagalinec et al. showed increased contractility of cardiomyocytes derived from WFS1 KO rats at four months, mainly due to prolonged cytosolic calcium transients (Cagalinec et al., 2019). These findings suggest an extended duration of calcium release in ventricular cardiomyocytes of WFS1 KO animals. Therefore, cardiac complications in this model develop independently of insulin deficiency and before the onset of hyperglycemia. Thus, changes in heart muscle bioenergetics may be attributed to WFS1 deficiency.

The bioenergetic profile of tissue is characterised by measuring mitochondrial oxygen consumption, which depends on two main substrate delivery pathways: FAO and the glycolysis-linked pathway. While cells typically prefer specific substrate pathways, healthy tissue can usually shift between substrates as required. However, inflexibility in these pathways is a hallmark of several metabolic disorders, including sarcopenia, type 2 diabetes, obesity, heart failure, and atrial fibrillation (Goodpaster & Sparks, 2017; Karwi et al., 2018; Prior et al., 2014; Qin et al., 2022; Shoemaker et al., 2022). Similarly, decreased activity in some respiratory system complexes can be partially compensated by others, such as the increased activity of CII accompanied by reduced activity of CI is described in various tissues during ageing and pathology (Gruno et al., 2008; Koit et al., 2017; Tepp et al., 2017; Weber et al., 2018).

In WFS1 KO rat cardiac muscle, the primary alteration observed was the inhibitory effect of the activated FA pathway on glucose-linked pathway usage. Our results align with previous knowledge that energy production in insulin-resistant heart cells cannot effectively switch from FA to glucose-linked metabolism and primarily rely on FA oxidation, even in a hyperglycemic state (Buchanan et al., 2005). When substrates were introduced in reverse order, and the glucose-linked substrate pathway was activated before the FA pathway, no difference was observed between WFS1 KO and WT heart muscle fibers. In normal cardiac muscle, the sequential addition of substrates typically induces an increase in respiration rate, reflecting mitochondrial adaptability in utilising different substrates to maintain energy metabolism (Lemieux et al., 2017). However, this function appears compromised in WFS1-deficient animals, resulting in inefficiency in utilising glucose-linked carbon sources when FAO is already activated in mitochondria.

Our study did not detect a significant increase in Leak oxygen consumption in cardiac tissue in both mouse and rat models, indicating that functionality of the inner mitochondrial membrane of the heart is not extensively altered in WFS1 deficiency. Additionally, there were no significant alterations in the maximal oxygen consumption capacity of individual respiratory complexes in cardiac muscle cells.

In contrast to cardiac tissue, in the glycolytic rectus femoris muscle of WFS1 KO rats, the activation of glucose-linked pathways inhibits FA usage (Tepp et al., 2022). Interestingly, higher CS activity in the glycolytic gastrocnemius white muscle preserves OXPHOS capacity in the WFS1 KO muscle. A similar trend is observed in the glycolytic rectus femoris muscle, where the WFS1 KO muscle exhibits higher CI activity than the WT muscle. However, in the oxidative soleus muscle, a significant decrease in respiratory capacity is noted in WFS1 KO animals across all substrate combinations, regardless of the order in which substrates were presented (Tepp et al., 2022). The higher CS activity in the WFS1 KO soleus muscle suggests an adaptive increase in mitochondrial number in

response to decreased ETC capacity. Nevertheless, these adaptations do not seem sufficient to maintain OXPHOS levels comparable to WT. Overall, changes in skeletal muscles have been more pronounced than in cardiac muscle, where the heart retains its functional and metabolic capacity, as evidenced by an unchanged V_{max}.

In summary, metabolic inflexibility in substrate usage is the primary alteration observed in the rat cardiac muscle cell bioenergetics due to WFS1 deficiency. WFS protein deficiency contributes to the development of this inflexibility in the heart, impairing the ability of mitochondria to utilise different substrates simultaneously.

The variations in mitochondrial bioenergetics between the two models of WFS1 deficiency may stem from different deletions in the WFS1 gene. Notably, cardiac complications have been documented in WS patients with a deletion in the 8th exon of the WFS1 gene (Ganie et al., 2011; Korkmaz et al., 2016). It is well-established that different mutations in the WFS1 gene result in distinct phenotypes of WS (Koks, 2023).

5.2 Effects of Smoking and Smoking Cessation as Extrinsic Factor on Cardiac Bioenergetics, Metabolism, and Structure in a Mouse Model of COPD

The investigation into the impact of cigarette smoking and smoking cessation on mitochondrial bioenergetics, metabolism, and structural changes in cardiac tissue using the mouse model of Chronic Obstructive Pulmonary Disease (COPD) has provided valuable insights into the molecular responses to these extrinsic factors. Through a comprehensive analysis of mitochondrial function, protein content, metabolite composition, glucose transport, and cardiac morphology, we have elucidated the multifaceted effects of smoking and smoking cessation on cardiac health.

We discovered that smoking induced a reduction in maximal mitochondrial capacity, which reverted to control levels following two weeks of smoking cessation. This change was associated with differences in mitochondrial protein content, succinate dehydrogenase (SDH) activity, and mitochondrial supercomplex formation. Metabolomic and lipidomic analyses revealed a shift from fatty acid to glucose oxidation upon smoking cessation, indicating partial restoration of cardiac metabolism. Additionally, smoking led to macrophage infiltration and fibrosis in the heart, with partial recovery observed after cessation. Intriguingly, smoking cessation prompted extensive capillary proliferation, leading to increased capillary density.

Uncoupled respiration was lower after smoking but returned to control levels after cessation. This was likely due to decreased mitochondrial protein content and impairments in mitochondrial respiration and electron transport caused by cigarette smoke compounds (Cardellach et al., 2003; Miro et al., 1999). Smoking cessation improved mitochondrial function, potentially through alterations in mitochondrial SC formation. We propose that smoking and cessation influence the balance between the disassembly and re-assembly of mitochondrial SCs and protein synthesis, explaining alterations in SC content and mitochondrial respiration without evident mitochondrial biogenesis. Nollet et al. (2023) recently demonstrated that augmenting the integration of CI into respiratory supercomplexes enhanced the ability to oxidise NADH, consequently leading to increased NADH-linked respiration (Nollet et al., 2023). Moreover, alterations in nicotinamide metabolism and increased ophthalmic acid concentration were observed, potentially contributing to improved mitochondrial function and redox signalling post-cessation (Soga et al., 2006; Yaku et al., 2018).

Cardiomyocytes demonstrate metabolic flexibility (Smith et al., 2018), primarily utilising FA and glucose for ATP production (Makrecka-Kuka et al., 2020; Smith et al., 2018). Our metabolomic analysis revealed a transition from fatty acid to glucose oxidation in cardiomyocytes following smoking cessation, accompanied by enhanced colocalisation of GLUT4 at the plasma membrane. Elevated levels of various glycolytic intermediates suggested an increased reliance on glucose oxidation post-smoking cessation, akin to observations in cardiovascular pathologies characterised by metabolic inflexibility (Makrecka-Kuka et al., 2020; McGarrah et al., 2018; Smith et al., 2018). However, according to recent studies on FAO inhibition, the transition from FAO to glycolysis could also play a cardioprotective role in cardiomyocyte function (Li et al., 2023). Furthermore, smoking cessation led to heightened concentrations of long-chain and very-long-chain highly unsaturated triacylglycerols, indicating diminished fatty acid oxidation. Excessive triacylglycerol accumulation is linked to insulin resistance, mitochondrial anomalies (Eggelbusch et al., 2024; Kelley & Goodpaster, 2001), cardiac hypertrophy (Makrecka-Kuka et al., 2020), and eventual ventricular dysfunction (Ge et al., 2012). In patients with COPD, elevated serum triacylglycerol levels are noted (Xuan et al., 2018), with negative associations between serum diacylglycerols/triacylglycerols and skeletal muscle oxidative capacity in severe COPD cases (Li et al., 2021). Concurrently, lower tissue concentrations of sphingomyelin SM(t33:0) and ceramide Cer(d44:3) were observed in smoking versus control conditions, with several ceramides and hexosylceramides displaying significantly reduced concentrations post-smoking cessation compared to controls.

Regarding smoking-induced structural changes, such as cardiac atrophy and fibrosis, they showed only partial recovery post-cessation. Local and systemic inflammation likely contributed to these changes, as evidenced by macrophage infiltration into the heart, persisting even after smoking cessation. These infiltrations, primarily around endothelial cells, may elevate endothelial permeability in smoke-exposed mice (Mazzone et al., 2010). Tissue-infiltrating macrophages, involved in cellular clearance, tissue remodelling, and angiogenesis, elevate local pro-inflammatory cytokine concentrations, such as TNF-α, various interleukins, and TGF-β, potentially affecting cardiac metabolism, collagen production, and fibrosis (Eggelbusch et al., 2022; McDonald et al., 2018; Oishi & Manabe, 2018; Shi et al., 2021). Smoking-induced fibrosis persisted post-cessation, alongside increased cardiac macrophage infiltration and capillary density. These findings suggest that local inflammation drove structural alterations in the heart, associated with stiffening and diastolic dysfunction, commonly observed in COPD patients with preserved ejection fraction (Gonzalez et al., 2019).

Decreased cytosolic concentrations of branched-chain amino acids post-smoking cessation may reflect heightened protein synthesis (Petersen et al., 2007), although cardiomyocyte size did not enlarge. The contradiction between increased heart weight and unchanged cardiomyocyte size post-smoking cessation likely involves factors beyond elevated protein synthesis, possibly involving increased cell infiltration and blood volume. Elevated circulating inflammatory cytokines, such as tumour necrosis factor-α (TNF-α), may also contribute to reduced BCAA content post-smoking cessation (Holecek, 2018), owing to continued local inflammation rather than solely reflecting protein synthesis.

Elevated purine and pyrimidine levels post-smoking cessation may contribute to metabolic aberrations and ventricular dysfunction akin to observations in pulmonary arterial hypertension and myocardial hypertrophy (Prisco et al., 2020; Swain et al., 1982).

Metabolites associated with uridine metabolism, implicated in protein O-GlcNAcylation and insulin resistance (Yki-Jarvinen et al., 1998), exhibited alterations post-smoking cessation. Although GLUT4 translocation to the cell membrane was altered, further studies are warranted to elucidate the impact of smoking and smoking cessation on whole-body insulin resistance.

Regarding angiogenesis, despite smoking being linked to endothelial damage and decreased capillary-to-fiber ratio in skeletal muscle (Nogueira et al., 2018), no such decrease in capillary density was observed in the hearts of smoke-exposed mice. Instead, capillary density increased post-smoking cessation, possibly driven by elevated circulating endothelial progenitor cells (Kondo et al., 2004) and sustained local inflammation and cytokine release by macrophages. This discrepancy between smoking-induced changes in capillary density in skeletal muscle and cardiac muscle is perhaps due to the unceasing demand for oxygen and nutrients in the beating heart, while skeletal muscles have intermittent activities.

6 Conclusions

Intrinsic Factors: Wolframin Deficiency

Aim 1: Evaluate mitochondrial kinetics, OXPHOS function, and dynamic substrate utilization in cardiac tissue.

Conclusion: WFS1 KO mice exhibited a decrease in apparent K_m(ADP) and no increase in mitochondrial affinity for ADP after CK system activation, indicating compromised mitochondrial interactome function and weakened interactions between CK and ANT. Additionally, the reduced maximal oxygen consumption rate when using glutamate (but not pyruvate) as a substrate suggests that WFS1 deficiency impacts glutamate metabolism pathways.

Aim 2: Investigate changes in phosphotransfer pathways within cardiac muscle tissue.

Conclusion: The CK energy transfer pathway was impaired in WFS1 KO mice, evidenced by reduced creatine-activated respiration and non-altered mitochondrial affinity to ADP after creatine supplementation. However, compensatory mechanisms, such as increased coupling between mitochondria and alternate pathways (e.g., AK and HK pathways), allowed these mice to maintain energy flow despite the CK system impairment.

Aim 3: Compare metabolic differences between Wolframin-deficient and control cardiac tissues.

Conclusion: Significant metabolic differences were observed in WFS1 KO mice, including a shift from FAO to glucose oxidation. The activation of the fatty acid pathway in the WFS1 KO rat model inhibited glucose-linked substrate utilisation, leading to diminished CI-linked respiration and OXPHOS capacity compared to wild-type animals.

Extrinsic Factors: Impact of Smoking and Smoking Cessation

Aim 1: Explore changes in mitochondrial bioenergetics due to cigarette smoke exposure and smoking cessation.

Conclusion: Cigarette smoke exposure transiently reduced OXPHOS capacity and uncoupled respiration in cardiac tissue. These effects were reversible after smoking cessation, indicating that cessation may mitigate smoking-induced mitochondrial impairments. Smoking also reduced levels of mitochondrial respiratory chain complexes I and IV, disrupting supercomplex formation, which was restored after cessation. The balance between disassembly and reassembly of supercomplexes contributed to improved mitochondrial respiration post-smoking cessation. However, succinate dehydrogenase activity decreased after cessation, suggesting a prolonged impact on this aspect of mitochondrial function.

Aim 2: Investigate structural and metabolic modifications in cardiac muscle tissue caused by smoking and subsequent cessation.

Conclusion: Smoking and smoking cessation caused structural changes in cardiac tissue, such as alterations in collagen content and capillary density. Metabolic shifts, including lipidomic changes and increased GLUT4 transfer to the plasma membrane, suggest a switch from fatty acid oxidation to glucose oxidation post-smoking cessation.

Aim 3: Evaluate the inflammatory response in cardiac tissue following smoking and cessation.

Conclusion: Smoking-induced inflammation, reflected by macrophage infiltration and changes in cardiac tissue morphology (collagen content, capillary density, nuclear density), showed signs of remodelling associated with smoking and smoking cessation. These findings imply a dynamic response to environmental stressors, which may offer insights into how cessation can reverse smoking-induced damage.

Common Influences of Intrinsic and Extrinsic Factors

- Both intrinsic (Wolframin deficiency) and extrinsic (smoking and cessation) factors led to metabolic inflexibility, with a marked shift from FAO to glycolysis in cardiac tissue. In WFS1-deficient mice, this shift was linked to compensatory mechanisms, while in smoke-exposed mice, it suggested a protective adaptation during smoking cessation.
- The heightened glycolytic activity observed in both models indicates that metabolic reprogramming, involving increased glucose utilization, may represent a cardioprotective response to stress. This highlights new mechanisms of mitochondrial resilience in cardiac tissue under various conditions.

List of Figures

References

Abel, E. D. (2004). Glucose transport in the heart. *Front Biosci*, *9*, 201-215. https://doi.org/10.2741/1216

Acin-Perez, R., Bayona-Bafaluy, M. P., Fernandez-Silva, P., Moreno-Loshuertos, R., Perez-Martos, A., Bruno, C., Moraes, C. T., & Enriquez, J. A. (2004). Respiratory complex III is required to maintain complex I in mammalian mitochondria. *Mol Cell*, *13*(6), 805-815. https://doi.org/10.1016/s1097-2765(04)00124-8

Acin-Perez, R., & Enriquez, J. A. (2014). The function of the respiratory supercomplexes: the plasticity model. *Biochim Biophys Acta*, *1837*(4), 444-450. https://doi.org/10.1016/j.bbabio.2013.12.009

Acin-Perez, R., Fernandez-Silva, P., Peleato, M. L., Perez-Martos, A., & Enriquez, J. A. (2008). Respiratory active mitochondrial supercomplexes. *Mol Cell*, *32*(4), 529-539. https://doi.org/10.1016/j.molcel.2008.10.021

Adams, R. A., Liu, Z., Hsieh, C., Marko, M., Lederer, W. J., Jafri, M. S., & Mannella, C. (2023). Structural Analysis of Mitochondria in Cardiomyocytes: Insights into Bioenergetics and Membrane Remodeling. *Curr Issues Mol Biol*, *45*(7), 6097-6115. https://doi.org/10.3390/cimb45070385

Aerni-Flessner, L., Abi-Jaoude, M., Koenig, A., Payne, M., & Hruz, P. W. (2012). GLUT4, GLUT1, and GLUT8 are the dominant GLUT transcripts expressed in the murine left ventricle. *Cardiovasc Diabetol*, *11*, 63. https://doi.org/10.1186/1475-2840-11-63

Ahmed, A. A., Patel, K., Nyaku, M. A., Kheirbek, R. E., Bittner, V., Fonarow, G. C., Filippatos, G. S., Morgan, C. J., Aban, I. B., Mujib, M., Desai, R. V., Allman, R. M., White, M., Deedwania, P., Howard, G., Bonow, R. O., Fletcher, R. D., Aronow, W. S., & Ahmed, A. (2015). Risk of Heart Failure and Death After Prolonged Smoking Cessation: Role of Amount and Duration of Prior Smoking. *Circ Heart Fail*, *8*(4), 694-701. https://doi.org/10.1161/circheartfailure.114.001885

Ajime, T. T., Serre, J., Wust, R. C. I., Messa, G. A. M., Poffe, C., Swaminathan, A., Maes, K., Janssens, W., Troosters, T., Degens, H., & Gayan-Ramirez, G. (2021). Two Weeks of Smoking Cessation Reverse Cigarette Smoke-Induced Skeletal Muscle Atrophy and Mitochondrial Dysfunction in Mice. *Nicotine Tob Res*, *23*(1), 143-151. https://doi.org/10.1093/ntr/ntaa016

Aliev, M., Guzun, R., Karu-Varikmaa, M., Kaambre, T., Wallimann, T., & Saks, V. (2011). Molecular system bioenergics of the heart: experimental studies of metabolic compartmentation and energy fluxes versus computer modeling. *Int J Mol Sci*, *12*(12), 9296-9331. https://doi.org/10.3390/ijms12129296

Allard, M. F., Schonekess, B. O., Henning, S. L., English, D. R., & Lopaschuk, G. D. (1994). Contribution of oxidative metabolism and glycolysis to ATP production in hypertrophied hearts. *Am J Physiol*, *267*(2 Pt 2), H742-750. https://doi.org/10.1152/ajpheart.1994.267.2.H742

Ambrose, J. A., & Barua, R. S. (2004). The pathophysiology of cigarette smoking and cardiovascular disease: an update. *J Am Coll Cardiol*, *43*(10), 1731-1737. https://doi.org/10.1016/j.jacc.2003.12.047

Anflous, K., Veksler, V., Mateo, P., Samson, F., Saks, V., & Ventura-Clapier, R. (1997). Mitochondrial creatine kinase isoform expression does not correlate with its mode of action. *Biochem J*, *322 (Pt 1)*, 73-78. https://doi.org/10.1042/bj3220073

Anmann, T., Guzun, R., Beraud, N., Pelloux, S., Kuznetsov, A. V., Kogerman, L., Kaambre, T., Sikk, P., Paju, K., Peet, N., Seppet, E., Ojeda, C., Tourneur, Y., & Saks, V. (2006). Different kinetics of the regulation of respiration in permeabilized cardiomyocytes and in HL-1 cardiac cells. Importance of cell structure/organization for respiration regulation. *Biochim Biophys Acta*, *1757*(12), 1597-1606. https://doi.org/10.1016/j.bbabio.2006.09.008

Anmann, T., Varikmaa, M., Timohhina, N., Tepp, K., Shevchuk, I., Chekulayev, V., Saks, V., & Kaambre, T. (2014). Formation of highly organized intracellular structure and energy metabolism in cardiac muscle cells during postnatal development of rat heart. *Biochim Biophys Acta*, *1837*(8), 1350-1361. https://doi.org/10.1016/j.bbabio.2014.03.015

Aoshiba, K., & Nagai, A. (2003). Oxidative stress, cell death, and other damage to alveolar epithelial cells induced by cigarette smoke. *Tob Induc Dis*, *1*(3), 219-226. https://doi.org/10.1186/1617-9625-1-3-219

Appaix, F., Kuznetsov, A. V., Usson, Y., Kay, L., Andrienko, T., Olivares, J., Kaambre, T., Sikk, P., Margreiter, R., & Saks, V. (2003). Possible role of cytoskeleton in intracellular arrangement and regulation of mitochondria. *Exp Physiol*, *88*(1), 175-190. https://doi.org/10.1113/eph8802511

Arnold, P. K., & Finley, L. W. S. (2023). Regulation and function of the mammalian tricarboxylic acid cycle. *J Biol Chem*, *299*(2), 102838. https://doi.org/10.1016/j.jbc.2022.102838

Aronow, W. S. (1976). Effect of cigarette smoking and of carbon monoxide on coronary heart disease. *Chest*, *70*(4), 514-518. https://doi.org/10.1378/chest.70.4.514

Arora, K. K., & Pedersen, P. L. (1988). Functional significance of mitochondrial bound hexokinase in tumor cell metabolism. Evidence for preferential phosphorylation of glucose by intramitochondrially generated ATP. *J Biol Chem*, *263*(33), 17422-17428.

Astrup, P., & Kjeldsen, K. (1974). Carbon monoxide, smoking, and atherosclerosis. *Med Clin North Am*, *58*(2), 323-350. https://doi.org/10.1016/s0025-7125(16)32161-7

Azuma, K., Ikeda, K., & Inoue, S. (2020). Functional Mechanisms of Mitochondrial Respiratory Chain Supercomplex Assembly Factors and Their Involvement in Muscle Quality. *Int J Mol Sci*, *21*(9). https://doi.org/10.3390/ijms21093182

Baertling, F., Sanchez-Caballero, L., van den Brand, M. A. M., Wintjes, L. T., Brink, M., van den Brandt, F. A., Wilson, C., Rodenburg, R. J. T., & Nijtmans, L. G. J. (2017). NDUFAF4 variants are associated with Leigh syndrome and cause a specific mitochondrial complex I assembly defect. *Eur J Hum Genet*, *25*(11), 1273-1277. https://doi.org/10.1038/ejhg.2017.133

Balaban, R. S. (2002). Cardiac energy metabolism homeostasis: role of cytosolic calcium. *J Mol Cell Cardiol*, *34*(10), 1259-1271. https://doi.org/10.1006/jmcc.2002.2082

Balaban, R. S., Kantor, H. L., Katz, L. A., & Briggs, R. W. (1986). Relation between work and phosphate metabolite in the in vivo paced mammalian heart. *Science*, *232*(4754), 1121-1123. https://doi.org/10.1126/science.3704638

Banke, N. H., & Lewandowski, E. D. (2015). Impaired cytosolic NADH shuttling and elevated UCP3 contribute to inefficient citric acid cycle flux support of postischemic cardiac work in diabetic hearts. *J Mol Cell Cardiol*, *79*, 13-20. https://doi.org/10.1016/j.yjmcc.2014.10.015

Banks, E., Joshy, G., Korda, R. J., Stavreski, B., Soga, K., Egger, S., Day, C., Clarke, N. E., Lewington, S., & Lopez, A. D. (2019). Tobacco smoking and risk of 36 cardiovascular disease subtypes: fatal and non-fatal outcomes in a large prospective Australian study. *BMC Med*, *17*(1), 128. https://doi.org/10.1186/s12916-019-1351-4

Banos, G., Daniel, P. M., Moorhouse, S. R., Pratt, O. E., & Wilson, P. A. (1978). The influx of amino acids into the heart of the rat. *J Physiol*, *280*, 471-486. https://doi.org/10.1113/jphysiol.1978.sp012395

Barrett, T., Tranebjaerg, L., Gupta, R., McCarthy, L., Rendtorff, N. D., Williams, D., Wright, B., & Dias, R. (1993). WFS1 Spectrum Disorder. In M. P. Adam, J. Feldman, G. M. Mirzaa, R. A. Pagon, S. E. Wallace, L. J. H. Bean, K. W. Gripp, & A. Amemiya (Eds.), *GeneReviews((R))*. University of Washington, Seattle. GeneReviews is a registered trademark of the University of Washington, Seattle. All rights reserved.

Barrett, T. G., & Bundey, S. E. (1997). Wolfram (DIDMOAD) syndrome. *J Med Genet*, *34*(10), 838-841. https://doi.org/10.1136/jmg.34.10.838

Barrett, T. G., Bundey, S. E., & Macleod, A. F. (1995). Neurodegeneration and diabetes: UK nationwide study of Wolfram (DIDMOAD) syndrome. *Lancet*, *346*(8988), 1458-1463. https://doi.org/10.1016/s0140-6736(95)92473-6

Barth, E., Stammler, G., Speiser, B., & Schaper, J. (1992). Ultrastructural quantitation of mitochondria and myofilaments in cardiac muscle from 10 different animal species including man. *J Mol Cell Cardiol*, *24*(7), 669-681. https://doi.org/10.1016/0022-2828(92)93381-s

Bertholet, A. M., & Kirichok, Y. (2022). Mitochondrial H(+) Leak and Thermogenesis. *Annu Rev Physiol*, *84*, 381-407. https://doi.org/10.1146/annurev-physiol-021119-034405

Besford, Q. A., Sullivan, M. A., Zheng, L., Gilbert, R. G., Stapleton, D., & Gray-Weale, A. (2012). The structure of cardiac glycogen in healthy mice. *Int J Biol Macromol*, *51*(5), 887-891. https://doi.org/10.1016/j.ijbiomac.2012.06.037

Bianchi, C., Genova, M. L., Parenti Castelli, G., & Lenaz, G. (2004). The mitochondrial respiratory chain is partially organized in a supercomplex assembly: kinetic evidence using flux control analysis. *J Biol Chem*, *279*(35), 36562-36569. https://doi.org/10.1074/jbc.M405135200

Bing, R. J., Siegel, A., Ungar, I., & Gilbert, M. (1954). Metabolism of the human heart. II. Studies on fat, ketone and amino acid metabolism. *Am J Med*, *16*(4), 504-515. https://doi.org/10.1016/0002-9343(54)90365-4

Bishop, S. P., & Altschuld, R. A. (1970). Increased glycolytic metabolism in cardiac hypertrophy and congestive failure. *Am J Physiol*, *218*(1), 153-159. https://doi.org/10.1152/ajplegacy.1970.218.1.153

Boudina, S., Sena, S., O'Neill, B. T., Tathireddy, P., Young, M. E., & Abel, E. D. (2005). Reduced mitochondrial oxidative capacity and increased mitochondrial uncoupling impair myocardial energetics in obesity. *Circulation*, *112*(17), 2686-2695. https://doi.org/10.1161/circulationaha.105.554360

Boudina, S., Sena, S., Theobald, H., Sheng, X., Wright, J. J., Hu, X. X., Aziz, S., Johnson, J. I., Bugger, H., Zaha, V. G., & Abel, E. D. (2007). Mitochondrial energetics in the heart in obesity-related diabetes: direct evidence for increased uncoupled respiration and activation of uncoupling proteins. *Diabetes*, *56*(10), 2457-2466. https://doi.org/10.2337/db07-0481

Brdiczka, D., Beutner, G., Ruck, A., Dolder, M., & Wallimann, T. (1998). The molecular structure of mitochondrial contact sites. Their role in regulation of energy metabolism and permeability transition. *Biofactors*, *8*(3-4), 235-242. https://doi.org/10.1002/biof.5520080311

Buchanan, J., Mazumder, P. K., Hu, P., Chakrabarti, G., Roberts, M. W., Yun, U. J., Cooksey, R. C., Litwin, S. E., & Abel, E. D. (2005). Reduced cardiac efficiency and altered substrate metabolism precedes the onset of hyperglycemia and contractile dysfunction in two mouse models of insulin resistance and obesity. *Endocrinology*, *146*(12), 5341-5349. https://doi.org/10.1210/en.2005-0938

Burelle, Y., & Hochachka, P. W. (2002). Endurance training induces muscle-specific changes in mitochondrial function in skinned muscle fibers. *J Appl Physiol (1985)*, *92*(6), 2429-2438. https://doi.org/10.1152/japplphysiol.01024.2001

Cadenas, S. (2018). ROS and redox signaling in myocardial ischemia-reperfusion injury and cardioprotection. *Free Radic Biol Med*, *117*, 76-89. https://doi.org/10.1016/j.freeradbiomed.2018.01.024

Cagalinec, M., Zahradnikova, A., Zahradnikova, A., Jr., Kovacova, D., Paulis, L., Kurekova, S., Hot'ka, M., Pavelkova, J., Plaas, M., Novotova, M., & Zahradnik, I. (2019). Calcium Signaling and Contractility in Cardiac Myocyte of Wolframin Deficient Rats. *Front Physiol*, *10*, 172. https://doi.org/10.3389/fphys.2019.00172

Caliri, A. W., Tommasi, S., & Besaratinia, A. (2021). Relationships among smoking, oxidative stress, inflammation, macromolecular damage, and cancer. *Mutat Res Rev Mutat Res*, *787*, 108365. https://doi.org/10.1016/j.mrrev.2021.108365

Camps, M., Castello, A., Munoz, P., Monfar, M., Testar, X., Palacin, M., & Zorzano, A. (1992). Effect of diabetes and fasting on GLUT-4 (muscle/fat) glucose-transporter expression in insulin-sensitive tissues. Heterogeneous response in heart, red and white muscle. *Biochem J*, *282 (Pt 3)*, 765-772. https://doi.org/10.1042/bj2820765

Cardellach, F., Alonso, J. R., Lopez, S., Casademont, J., & Miro, O. (2003). Effect of smoking cessation on mitochondrial respiratory chain function. *J Toxicol Clin Toxicol*, *41*(3), 223-228. https://doi.org/10.1081/clt-120021102

Cecchini, G. (2003). Function and structure of complex II of the respiratory chain. *Annu Rev Biochem*, *72*, 77-109. https://doi.org/10.1146/annurev.biochem.72.121801.161700

Chakrabarty, R. P., & Chandel, N. S. (2022). Beyond ATP, new roles of mitochondria. *Biochem (Lond)*, *44*(4), 2-8. https://doi.org/10.1042/bio_2022_119

Chan, S. M. H., Cerni, C., Passey, S., Seow, H. J., Bernardo, I., van der Poel, C., Dobric, A., Brassington, K., Selemidis, S., Bozinovski, S., & Vlahos, R. (2020). Cigarette Smoking Exacerbates Skeletal Muscle Injury without Compromising Its Regenerative Capacity. *Am J Respir Cell Mol Biol*, *62*(2), 217-230. https://doi.org/10.1165/rcmb.2019-0106OC

Chatham, J. C. (2002). Lactate -- the forgotten fuel! *J Physiol*, *542*(Pt 2), 333. https://doi.org/10.1113/jphysiol.2002.020974

Chen, C., Ko, Y., Delannoy, M., Ludtke, S. J., Chiu, W., & Pedersen, P. L. (2004). Mitochondrial ATP synthasome: three-dimensional structure by electron microscopy of the ATP synthase in complex formation with carriers for Pi and ADP/ATP. *J Biol Chem*, *279*(30), 31761-31768. https://doi.org/10.1074/jbc.M401353200

Cheng, S., Lyass, A., Massaro, J. M., O'Connor, G. T., Keaney, J. F., Jr., & Vasan, R. S. (2010). Exhaled carbon monoxide and risk of metabolic syndrome and cardiovascular disease in the community. *Circulation*, *122*(15), 1470-1477. https://doi.org/10.1161/circulationaha.110.941013

Chinnery, P. F., & Hudson, G. (2013). Mitochondrial genetics. *Br Med Bull*, *106*, 135-159. https://doi.org/10.1093/bmb/ldt017

Chua, B., Siehl, D. L., & Morgan, H. E. (1979). Effect of leucine and metabolites of branched chain amino acids on protein turnover in heart. *J Biol Chem*, *254*(17), 8358-8362.

Chung, S., Arrell, D. K., Faustino, R. S., Terzic, A., & Dzeja, P. P. (2010). Glycolytic network restructuring integral to the energetics of embryonic stem cell cardiac differentiation. *J Mol Cell Cardiol*, *48*(4), 725-734. https://doi.org/10.1016/j.yjmcc.2009.12.014

Cogliati, S., Calvo, E., Loureiro, M., Guaras, A. M., Nieto-Arellano, R., Garcia-Poyatos, C., Ezkurdia, I., Mercader, N., Vazquez, J., & Enriquez, J. A. (2016). Mechanism of super-assembly of respiratory complexes III and IV. *Nature*, *539*(7630), 579-582. https://doi.org/10.1038/nature20157

Cogliati, S., Frezza, C., Soriano, M. E., Varanita, T., Quintana-Cabrera, R., Corrado, M., Cipolat, S., Costa, V., Casarin, A., Gomes, L. C., Perales-Clemente, E., Salviati, L., Fernandez-Silva, P., Enriquez, J. A., & Scorrano, L. (2013). Mitochondrial cristae shape determines respiratory chain supercomplexes assembly and respiratory efficiency. *Cell*, *155*(1), 160-171. https://doi.org/10.1016/j.cell.2013.08.032

Cole, M. A., Murray, A. J., Cochlin, L. E., Heather, L. C., McAleese, S., Knight, N. S., Sutton, E., Jamil, A. A., Parassol, N., & Clarke, K. (2011). A high fat diet increases mitochondrial fatty acid oxidation and uncoupling to decrease efficiency in rat heart. *Basic Res Cardiol*, *106*(3), 447-457. https://doi.org/10.1007/s00395-011-0156-1

Colombini, M. (2016). The VDAC channel: Molecular basis for selectivity. *Biochim Biophys Acta*, *1863*(10), 2498-2502. https://doi.org/10.1016/j.bbamcr.2016.01.019

Cremers, C. W., Wijdeveld, P. G., & Pinckers, A. J. (1977). Juvenile diabetes mellitus, optic atrophy, hearing loss, diabetes insipidus, atonia of the urinary tract and bladder, and other abnormalities (Wolfram syndrome). A review of 88 cases from the literature with personal observations on 3 new patients. *Acta Paediatr Scand Suppl*(264), 1-16. https://doi.org/10.1111/j.1651-2227.1977.tb15069.x

Cryns, K., Sivakumaran, T. A., Van den Ouweland, J. M., Pennings, R. J., Cremers, C. W., Flothmann, K., Young, T. L., Smith, R. J., Lesperance, M. M., & Van Camp, G. (2003). Mutational spectrum of the WFS1 gene in Wolfram syndrome, nonsyndromic hearing impairment, diabetes mellitus, and psychiatric disease. *Hum Mutat*, *22*(4), 275-287. https://doi.org/10.1002/humu.10258

D'Alessandro, A., Boeckelmann, I., Hammwhoner, M., & Goette, A. (2012). Nicotine, cigarette smoking and cardiac arrhythmia: an overview. *Eur J Prev Cardiol*, *19*(3), 297-305. https://doi.org/10.1177/1741826711411738

Dahdah, A., Jaggers, R. M., Sreejit, G., Johnson, J., Kanuri, B., Murphy, A. J., & Nagareddy, P. R. (2022). Immunological Insights into Cigarette Smoking-Induced Cardiovascular Disease Risk. *Cells*, *11*(20). https://doi.org/10.3390/cells11203190

Darabseh, M. Z., Maden-Wilkinson, T. M., Welbourne, G., Wust, R. C. I., Ahmed, N., Aushah, H., Selfe, J., Morse, C. I., & Degens, H. (2021). Fourteen days of smoking cessation improves muscle fatigue resistance and reverses markers of systemic inflammation. *Sci Rep*, *11*(1), 12286. https://doi.org/10.1038/s41598-021-91510-x

Davila-Roman, V. G., Vedala, G., Herrero, P., de las Fuentes, L., Rogers, J. G., Kelly, D. P., & Gropler, R. J. (2002). Altered myocardial fatty acid and glucose metabolism in idiopathic dilated cardiomyopathy. *J Am Coll Cardiol*, *40*(2), 271-277. https://doi.org/10.1016/s0735-1097(02)01967-8

Deanfield, J. E., Shea, M. J., Wilson, R. A., Horlock, P., de Landsheere, C. M., & Selwyn, A. P. (1986). Direct effects of smoking on the heart: silent ischemic disturbances of coronary flow. *Am J Cardiol*, *57*(13), 1005-1009. https://doi.org/10.1016/0002-9149(86)90665-x

Del Arco, A., Contreras, L., Pardo, B., & Satrustegui, J. (2016). Calcium regulation of mitochondrial carriers. *Biochim Biophys Acta*, *1863*(10), 2413-2421. https://doi.org/10.1016/j.bbamcr.2016.03.024

Delprat, B., Maurice, T., & Delettre, C. (2018). Wolfram syndrome: MAMs' connection? *Cell Death Dis*, *9*(3), 364. https://doi.org/10.1038/s41419-018-0406-3

Depre, C., Rider, M. H., & Hue, L. (1998). Mechanisms of control of heart glycolysis. *Eur J Biochem*, *258*(2), 277-290. https://doi.org/10.1046/j.1432-1327.1998.2580277.x

Depre, C., Vanoverschelde, J. L., & Taegtmeyer, H. (1999). Glucose for the heart. *Circulation*, *99*(4), 578-588. https://doi.org/10.1161/01.cir.99.4.578

Dikalov, S., Itani, H., Richmond, B., Vergeade, A., Rahman, S. M. J., Boutaud, O., Blackwell, T., Massion, P. P., Harrison, D. G., & Dikalova, A. (2019). Tobacco smoking induces cardiovascular mitochondrial oxidative stress, promotes endothelial dysfunction, and enhances hypertension. *Am J Physiol Heart Circ Physiol*, *316*(3), H639-h646. https://doi.org/10.1152/ajpheart.00595.2018

Ding, J., Li, F., Cong, Y., Miao, J., Wu, D., Liu, B., & Wang, L. (2019). Trichostatin A inhibits skeletal muscle atrophy induced by cigarette smoke exposure in mice. *Life Sci*, *235*, 116800. https://doi.org/10.1016/j.lfs.2019.116800

Doenst, T., Goodwin, G. W., Cedars, A. M., Wang, M., Stepkowski, S., & Taegtmeyer, H. (2001). Load-induced changes in vivo alter substrate fluxes and insulin responsiveness of rat heart in vitro. *Metabolism*, *50*(9), 1083-1090. https://doi.org/10.1053/meta.2001.25605

Doenst, T., Nguyen, T. D., & Abel, E. D. (2013). Cardiac metabolism in heart failure: implications beyond ATP production. *Circ Res*, *113*(6), 709-724. https://doi.org/10.1161/circresaha.113.300376

Du, X. L., Edelstein, D., Rossetti, L., Fantus, I. G., Goldberg, H., Ziyadeh, F., Wu, J., & Brownlee, M. (2000). Hyperglycemia-induced mitochondrial superoxide overproduction activates the hexosamine pathway and induces plasminogen activator inhibitor-1 expression by increasing Sp1 glycosylation. *Proc Natl Acad Sci U S A*, *97*(22), 12222-12226. https://doi.org/10.1073/pnas.97.22.12222

Dzeja, P., & Terzic, A. (2009). Adenylate kinase and AMP signaling networks: metabolic monitoring, signal communication and body energy sensing. *Int J Mol Sci*, *10*(4), 1729-1772. https://doi.org/10.3390/ijms10041729

Dzeja, P. P., Chung, S., Faustino, R. S., Behfar, A., & Terzic, A. (2011). Developmental enhancement of adenylate kinase-AMPK metabolic signaling axis supports stem cell cardiac differentiation. *PLoS One*, *6*(4), e19300. https://doi.org/10.1371/journal.pone.0019300

Dzeja, P. P., Hoyer, K., Tian, R., Zhang, S., Nemutlu, E., Spindler, M., & Ingwall, J. S. (2011). Rearrangement of energetic and substrate utilization networks compensate for chronic myocardial creatine kinase deficiency. *J Physiol*, *589*(Pt 21), 5193-5211. https://doi.org/10.1113/jphysiol.2011.212829

Dzeja, P. P., & Terzic, A. (2003). Phosphotransfer networks and cellular energetics. *J Exp Biol*, *206*(Pt 12), 2039-2047. https://doi.org/10.1242/jeb.00426

Dzeja, P. P., Terzic, A., & Wieringa, B. (2004). Phosphotransfer dynamics in skeletal muscle from creatine kinase gene- deleted mice. *Mol Cell Biochem*, *256-257*(1-2), 13-27. https://doi.org/10.1023/b:mcbi.0000009856.23646.38

Dzeja, P. P., Zeleznikar, R. J., & Goldberg, N. D. (1996). Suppression of creatine kinase-catalyzed phosphotransfer results in increased phosphoryl transfer by adenylate kinase in intact skeletal muscle. *J Biol Chem*, *271*(22), 12847-12851. https://doi.org/10.1074/jbc.271.22.12847

Eggelbusch, M., Charlton, B. T., Bosutti, A., Ganse, B., Giakoumaki, I., Grootemaat, A. E., Hendrickse, P. W., Jaspers, Y., Kemp, S., Kerkhoff, T. J., Noort, W., van Weeghel, M., van der Wel, N. N., Wesseling, J. R., Frings-Meuthen, P., Rittweger, J., Mulder, E. R., Jaspers, R. T., Degens, H., & Wust, R. C. I. (2024). The impact of bed rest on human skeletal muscle metabolism. *Cell Rep Med*, *5*(1), 101372. https://doi.org/10.1016/j.xcrm.2023.101372

Eggelbusch, M., Shi, A., Broeksma, B. C., Vazquez-Cruz, M., Soares, M. N., de Wit, G. M. J., Everts, B., Jaspers, R. T., & Wust, R. C. I. (2022). The NLRP3 inflammasome contributes to inflammation-induced morphological and metabolic alterations in skeletal muscle. *J Cachexia Sarcopenia Muscle*, *13*(6), 3048-3061. https://doi.org/10.1002/jcsm.13062

el Alaoui-Talibi, Z., Landormy, S., Loireau, A., & Moravec, J. (1992). Fatty acid oxidation and mechanical performance of volume-overloaded rat hearts. *Am J Physiol*, *262*(4 Pt 2), H1068-1074. https://doi.org/10.1152/ajpheart.1992.262.4.H1068

Ernster, L., & Schatz, G. (1981). Mitochondria: a historical review. *J Cell Biol*, *91*(3 Pt 2), 227s-255s. https://doi.org/10.1083/jcb.91.3.227s

Fagard, R. H. (2009). Smoking amplifies cardiovascular risk in patients with hypertension and diabetes. *Diabetes Care*, *32 Suppl 2*, S429-431. https://doi.org/10.2337/dc09-S354

Fernie, A. R., Carrari, F., & Sweetlove, L. J. (2004). Respiratory metabolism: glycolysis, the TCA cycle and mitochondrial electron transport. *Curr Opin Plant Biol*, *7*(3), 254-261. https://doi.org/10.1016/j.pbi.2004.03.007

Ferretti, G., Bacchetti, T., Negre-Salvayre, A., Salvayre, R., Dousset, N., & Curatola, G. (2006). Structural modifications of HDL and functional consequences. *Atherosclerosis*, *184*(1), 1-7. https://doi.org/10.1016/j.atherosclerosis.2005.08.008

Fisher, D. J., Heymann, M. A., & Rudolph, A. M. (1980). Myocardial oxygen and carbohydrate consumption in fetal lambs in utero and in adult sheep. *Am J Physiol*, *238*(3), H399-405. https://doi.org/10.1152/ajpheart.1980.238.3.H399

Flor, L. S., Anderson, J. A., Ahmad, N., Aravkin, A., Carr, S., Dai, X., Gil, G. F., Hay, S. I., Malloy, M. J., McLaughlin, S. A., Mullany, E. C., Murray, C. J. L., O'Connell, E. M., Okereke, C., Sorensen, R. J. D., Whisnant, J., Zheng, P., & Gakidou, E. (2024). Health effects associated with exposure to secondhand smoke: a Burden of Proof study. *Nat Med*, *30*(1), 149-167. https://doi.org/10.1038/s41591-023-02743-4

Fonseca, S. G., Fukuma, M., Lipson, K. L., Nguyen, L. X., Allen, J. R., Oka, Y., & Urano, F. (2005). WFS1 is a novel component of the unfolded protein response and maintains homeostasis of the endoplasmic reticulum in pancreatic beta-cells. *J Biol Chem*, *280*(47), 39609-39615. https://doi.org/10.1074/jbc.M507426200

Fox, K. M. (1988). Smoking, catecholamines, and the ischemic myocardium. *Postgrad Med*, *Spec No*, 148-151.

Freeman, D. J., Griffin, B. A., Murray, E., Lindsay, G. M., Gaffney, D., Packard, C. J., & Shepherd, J. (1993). Smoking and plasma lipoproteins in man: effects on low density lipoprotein cholesterol levels and high density lipoprotein subfraction distribution. *Eur J Clin Invest*, *23*(10), 630-640. https://doi.org/10.1111/j.1365-2362.1993.tb00724.x

Gandoy-Fieiras, N., Gonzalez-Juanatey, J. R., & Eiras, S. (2020). Myocardium Metabolism in Physiological and Pathophysiological States: Implications of Epicardial Adipose Tissue and Potential Therapeutic Targets. *Int J Mol Sci*, *21*(7). https://doi.org/10.3390/ijms21072641

Ganie, M. A., Laway, B. A., Nisar, S., Wani, M. M., Khurana, M. L., Ahmad, F., Ahmed, S., Gupta, P., Ali, I., Shabir, I., Shadan, A., Ahmed, A., & Tufail, S. (2011). Presentation and clinical course of Wolfram (DIDMOAD) syndrome from North India. *Diabet Med*, *28*(11), 1337-1342. https://doi.org/10.1111/j.1464-5491.2011.03377.x

Gao, C., Yu, J., & Wang, Y. (2021). Branched chain amino acids in cardiac growth and pathology - timing is everything. *J Mol Cell Cardiol*, *159*, 14-15. https://doi.org/10.1016/j.yjmcc.2021.05.020

Ge, F., Hu, C., Hyodo, E., Arai, K., Zhou, S., Lobdell, H. t., Walewski, J. L., Homma, S., & Berk, P. D. (2012). Cardiomyocyte triglyceride accumulation and reduced ventricular function in mice with obesity reflect increased long chain Fatty Acid uptake and de novo Fatty Acid synthesis. *J Obes*, *2012*, 205648. https://doi.org/10.1155/2012/205648

Gellerich, F. N. (1992). The role of adenylate kinase in dynamic compartmentation of adenine nucleotides in the mitochondrial intermembrane space. *FEBS Lett*, *297*(1-2), 55-58. https://doi.org/10.1016/0014-5793(92)80326-c

Genova, M. L., & Lenaz, G. (2014). Functional role of mitochondrial respiratory supercomplexes. *Biochim Biophys Acta*, *1837*(4), 427-443. https://doi.org/10.1016/j.bbabio.2013.11.002

Genova, M. L., & Lenaz, G. (2015). The Interplay Between Respiratory Supercomplexes and ROS in Aging. *Antioxid Redox Signal*, *23*(3), 208-238. https://doi.org/10.1089/ars.2014.6214

Gertz, E. W., Wisneski, J. A., Stanley, W. C., & Neese, R. A. (1988). Myocardial substrate utilization during exercise in humans. Dual carbon- labeled carbohydrate isotope experiments. *J Clin Invest*, *82*(6), 2017-2025. https://doi.org/10.1172/jci113822

Giordano, L., Gregory, A. D., Perez Verdaguer, M., Ware, S. A., Harvey, H., DeVallance, E., Brzoska, T., Sundd, P., Zhang, Y., Sciurba, F. C., Shapiro, S. D., & Kaufman, B. A. (2022). Extracellular Release of Mitochondrial DNA: Triggered by Cigarette Smoke and Detected in COPD. *Cells*, *11*(3). https://doi.org/10.3390/cells11030369

Gomes, L. C., & Scorrano, L. (2011). Mitochondrial elongation during autophagy: a stereotypical response to survive in difficult times. *Autophagy*, *7*(10), 1251-1253. https://doi.org/10.4161/auto.7.10.16771

Gomez, L. A., Monette, J. S., Chavez, J. D., Maier, C. S., & Hagen, T. M. (2009). Supercomplexes of the mitochondrial electron transport chain decline in the aging rat heart. *Arch Biochem Biophys*, *490*(1), 30-35. https://doi.org/10.1016/j.abb.2009.08.002

Gonzalez, A., Lopez, B., Ravassa, S., San Jose, G., & Diez, J. (2019). The complex dynamics of myocardial interstitial fibrosis in heart failure. Focus on collagen cross-linking. *Biochim Biophys Acta Mol Cell Res*, *1866*(9), 1421-1432. https://doi.org/10.1016/j.bbamcr.2019.06.001

Goodpaster, B. H., & Sparks, L. M. (2017). Metabolic Flexibility in Health and Disease. *Cell Metab*, *25*(5), 1027-1036. https://doi.org/10.1016/j.cmet.2017.04.015

Goodwin, G. W., & Taegtmeyer, H. (2000). Improved energy homeostasis of the heart in the metabolic state of exercise. *Am J Physiol Heart Circ Physiol*, *279*(4), H1490-1501. https://doi.org/10.1152/ajpheart.2000.279.4.H1490

Gopal, D. M., Kalogeropoulos, A. P., Georgiopoulou, V. V., Smith, A. L., Bauer, D. C., Newman, A. B., Kim, L., Bibbins-Domingo, K., Tindle, H., Harris, T. B., Tang, W. W., Kritchevsky, S. B., & Butler, J. (2012). Cigarette smoking exposure and heart failure risk in older adults: the Health, Aging, and Body Composition Study. *Am Heart J*, *164*(2), 236-242. https://doi.org/10.1016/j.ahj.2012.05.013

Gradinac, S., Coleman, G. M., Taegtmeyer, H., Sweeney, M. S., & Frazier, O. H. (1989). Improved cardiac function with glucose-insulin-potassium after aortocoronary bypass grafting. *Ann Thorac Surg*, *48*(4), 484-489. https://doi.org/10.1016/s0003-4975(10)66844-0

Green, D. R., Galluzzi, L., & Kroemer, G. (2011). Mitochondria and the autophagy-inflammation-cell death axis in organismal aging. *Science*, *333*(6046), 1109-1112. https://doi.org/10.1126/science.1201940

Gruno, M., Peet, N., Seppet, E., Kadaja, L., Paju, K., Eimre, M., Orlova, E., Peetsalu, M., Tein, A., Soplepmann, J., Schlattner, U., Peetsalu, A., & Seppet, E. K. (2006). Oxidative phosphorylation and its coupling to mitochondrial creatine and adenylate kinases in human gastric mucosa. *Am J Physiol Regul Integr Comp Physiol*, *291*(4), R936-946. https://doi.org/10.1152/ajpregu.00162.2006

Gruno, M., Peet, N., Tein, A., Salupere, R., Sirotkina, M., Valle, J., Peetsalu, A., & Seppet, E. K. (2008). Atrophic gastritis: deficient complex I of the respiratory chain in the mitochondria of corpus mucosal cells. *J Gastroenterol*, *43*(10), 780-788. https://doi.org/10.1007/s00535-008-2231-4

Guo, R., Zong, S., Wu, M., Gu, J., & Yang, M. (2017). Architecture of Human Mitochondrial Respiratory Megacomplex I2III2IV2. *Cell*, *170*(6), 1247-1257.e1212. https://doi.org/10.1016/j.cell.2017.07.050

Gupte, S. A., Levine, R. J., Gupte, R. S., Young, M. E., Lionetti, V., Labinskyy, V., Floyd, B. C., Ojaimi, C., Bellomo, M., Wolin, M. S., & Recchia, F. A. (2006). Glucose-6-phosphate dehydrogenase-derived NADPH fuels superoxide production in the failing heart. *J Mol Cell Cardiol*, *41*(2), 340-349. https://doi.org/10.1016/j.yjmcc.2006.05.003

Guzun, R., Gonzalez-Granillo, M., Karu-Varikmaa, M., Grichine, A., Usson, Y., Kaambre, T., Guerrero-Roesch, K., Kuznetsov, A., Schlattner, U., & Saks, V. (2012). Regulation of respiration in muscle cells in vivo by VDAC through interaction with the cytoskeleton and MtCK within Mitochondrial Interactosome. *Biochim Biophys Acta*, *1818*(6), 1545-1554. https://doi.org/10.1016/j.bbamem.2011.12.034

Guzun, R., Kaambre, T., Bagur, R., Grichine, A., Usson, Y., Varikmaa, M., Anmann, T., Tepp, K., Timohhina, N., Shevchuk, I., Chekulayev, V., Boucher, F., Dos Santos, P., Schlattner, U., Wallimann, T., Kuznetsov, A. V., Dzeja, P., Aliev, M., & Saks, V. (2015). Modular organization of cardiac energy metabolism: energy conversion, transfer and feedback regulation. *Acta Physiol (Oxf)*, *213*(1), 84-106. https://doi.org/10.1111/apha.12287

Guzun, R., Timohhina, N., Tepp, K., Gonzalez-Granillo, M., Shevchuk, I., Chekulayev, V., Kuznetsov, A. V., Kaambre, T., & Saks, V. A. (2011). Systems bioenergetics of creatine kinase networks: physiological roles of creatine and phosphocreatine in regulation of cardiac cell function. *Amino Acids*, *40*(5), 1333-1348. https://doi.org/10.1007/s00726-011-0854-x

Guzun, R., Timohhina, N., Tepp, K., Monge, C., Kaambre, T., Sikk, P., Kuznetsov, A. V., Pison, C., & Saks, V. (2009). Regulation of respiration controlled by mitochondrial creatine kinase in permeabilized cardiac cells in situ. Importance of system level properties. *Biochim Biophys Acta*, *1787*(9), 1089-1105. https://doi.org/10.1016/j.bbabio.2009.03.024

Hafstad, A. D., Khalid, A. M., Hagve, M., Lund, T., Larsen, T. S., Severson, D. L., Clarke, K., Berge, R. K., & Aasum, E. (2009). Cardiac peroxisome proliferator-activated receptor-alpha activation causes increased fatty acid oxidation, reducing efficiency and post- ischaemic functional loss. *Cardiovasc Res*, *83*(3), 519-526. https://doi.org/10.1093/cvr/cvp132

Hale, D. E., & Bennett, M. J. (1992). Fatty acid oxidation disorders: a new class of metabolic diseases. *J Pediatr*, *121*(1), 1-11. https://doi.org/10.1016/s0022-3476(05)82532-6

Hallsten, K., Virtanen, K. A., Lonnqvist, F., Janatuinen, T., Turiceanu, M., Ronnemaa, T., Viikari, J., Lehtimaki, T., Knuuti, J., & Nuutila, P. (2004). Enhancement of insulin-stimulated myocardial glucose uptake in patients with Type 2 diabetes treated with rosiglitazone. *Diabet Med*, *21*(12), 1280-1287. https://doi.org/10.1111/j.1464-5491.2004.01332.x

Hardy, C., Khanim, F., Torres, R., Scott-Brown, M., Seller, A., Poulton, J., Collier, D., Kirk, J., Polymeropoulos, M., Latif, F., & Barrett, T. (1999). Clinical and molecular genetic analysis of 19 Wolfram syndrome kindreds demonstrating a wide spectrum of mutations in WFS1. *Am J Hum Genet*, *65*(5), 1279-1290. https://doi.org/10.1086/302609

Hendriks, T., van Dijk, R., Alsabaan, N. A., & van der Harst, P. (2020). Active Tobacco Smoking Impairs Cardiac Systolic Function. *Sci Rep*, *10*(1), 6608. https://doi.org/10.1038/s41598-020-63509-3

Herrero, P., Peterson, L. R., McGill, J. B., Matthew, S., Lesniak, D., Dence, C., & Gropler, R. J. (2006). Increased myocardial fatty acid metabolism in patients with type 1 diabetes mellitus. *J Am Coll Cardiol*, *47*(3), 598-604. https://doi.org/10.1016/j.jacc.2005.09.030

Hofmann, S., Philbrook, C., Gerbitz, K. D., & Bauer, M. F. (2003). Wolfram syndrome: structural and functional analyses of mutant and wild- type wolframin, the WFS1 gene product. *Hum Mol Genet*, *12*(16), 2003-2012. https://doi.org/10.1093/hmg/ddg214

Holecek, M. (2018). Branched-chain amino acids in health and disease: metabolism, alterations in blood plasma, and as supplements. *Nutr Metab (Lond)*, *15*, 33. https://doi.org/10.1186/s12986-018-0271-1

Howell, N. J., Ashrafian, H., Drury, N. E., Ranasinghe, A. M., Contractor, H., Isackson, H., Calvert, M., Williams, L. K., Freemantle, N., Quinn, D. W., Green, D., Frenneaux, M., Bonser, R. S., Mascaro, J. G., Graham, T. R., Rooney, S. J., Wilson, I. C., & Pagano, D. (2011). Glucose-insulin-potassium reduces the incidence of low cardiac output episodes after aortic valve replacement for aortic stenosis in patients with left ventricular hypertrophy: results from the Hypertrophy, Insulin, Glucose, and Electrolytes (HINGE) trial. *Circulation*, *123*(2), 170-177. https://doi.org/10.1161/circulationaha.110.945170

Htay, T., Soe, K., Lopez-Perez, A., Doan, A. H., Romagosa, M. A., & Aung, K. (2019). Mortality and Cardiovascular Disease in Type 1 and Type 2 Diabetes. *Curr Cardiol Rep*, *21*(6), 45. https://doi.org/10.1007/s11886-019-1133-9

Ikeda, K., Shiba, S., Horie-Inoue, K., Shimokata, K., & Inoue, S. (2013). A stabilizing factor for mitochondrial respiratory supercomplex assembly regulates energy metabolism in muscle. *Nat Commun*, *4*, 2147. https://doi.org/10.1038/ncomms3147

Inoue, H., Tanizawa, Y., Wasson, J., Behn, P., Kalidas, K., Bernal-Mizrachi, E., Mueckler, M., Marshall, H., Donis-Keller, H., Crock, P., Rogers, D., Mikuni, M., Kumashiro, H., Higashi, K., Sobue, G., Oka, Y., & Permutt, M. A. (1998). A gene encoding a transmembrane protein is mutated in patients with diabetes mellitus and optic atrophy (Wolfram syndrome). *Nat Genet*, *20*(2), 143-148. https://doi.org/10.1038/2441

Inouye, S., Seo, M., Yamada, Y., & Nakazawa, A. (1998). Increase of adenylate kinase isozyme 1 protein during neuronal differentiation in mouse embryonal carcinoma P19 cells and in rat brain primary cultured cells. *J Neurochem*, *71*(1), 125-133. https://doi.org/10.1046/j.1471-4159.1998.71010125.x

Ivask, M., Hugill, A., & Koks, S. (2016). RNA-sequencing of WFS1-deficient pancreatic islets. *Physiol Rep*, *4*(7). https://doi.org/10.14814/phy2.12750

Iverson, T. M., Singh, P. K., & Cecchini, G. (2023). An evolving view of complex II-noncanonical complexes, megacomplexes, respiration, signaling, and beyond. *J Biol Chem*, *299*(6), 104761. https://doi.org/10.1016/j.jbc.2023.104761

Janssen, E., Dzeja, P. P., Oerlemans, F., Simonetti, A. W., Heerschap, A., de Haan, A., Rush, P. S., Terjung, R. R., Wieringa, B., & Terzic, A. (2000). Adenylate kinase 1 gene deletion disrupts muscle energetic economy despite metabolic rearrangement. *Embo j*, *19*(23), 6371-6381. https://doi.org/10.1093/emboj/19.23.6371

John, S., Weiss, J. N., & Ribalet, B. (2011). Subcellular localization of hexokinases I and II directs the metabolic fate of glucose. *PLoS One*, *6*(3), e17674. https://doi.org/10.1371/journal.pone.0017674

Juan, C. A., Perez de la Lastra, J. M., Plou, F. J., & Perez-Lebena, E. (2021). The Chemistry of Reactive Oxygen Species (ROS) Revisited: Outlining Their Role in Biological Macromolecules (DNA, Lipids and Proteins) and Induced Pathologies. *Int J Mol Sci*, *22*(9). https://doi.org/10.3390/ijms22094642

Kaldma, A., Klepinin, A., Chekulayev, V., Mado, K., Shevchuk, I., Timohhina, N., Tepp, K., Kandashvili, M., Varikmaa, M., Koit, A., Planken, M., Heck, K., Truu, L., Planken, A., Valvere, V., Rebane, E., & Kaambre, T. (2014). An in situ study of bioenergetic properties of human colorectal cancer: the regulation of mitochondrial respiration and distribution of flux control among the components of ATP synthasome. *Int J Biochem Cell Biol*, *55*, 171-186. https://doi.org/10.1016/j.biocel.2014.09.004

Karwi, Q. G., & Lopaschuk, G. D. (2023). Branched-Chain Amino Acid Metabolism in the Failing Heart. *Cardiovasc Drugs Ther*, *37*(2), 413-420. https://doi.org/10.1007/s10557-022-07320-4

Karwi, Q. G., Uddin, G. M., Ho, K. L., & Lopaschuk, G. D. (2018). Loss of Metabolic Flexibility in the Failing Heart. *Front Cardiovasc Med*, *5*, 68. https://doi.org/10.3389/fcvm.2018.00068

Katz, L. A., Swain, J. A., Portman, M. A., & Balaban, R. S. (1989). Relation between phosphate metabolites and oxygen consumption of heart in vivo. *Am J Physiol*, *256*(1 Pt 2), H265-274. https://doi.org/10.1152/ajpheart.1989.256.1.H265

Kay, L., Li, Z., Mericskay, M., Olivares, J., Tranqui, L., Fontaine, E., Tiivel, T., Sikk, P., Kaambre, T., Samuel, J. L., Rappaport, L., Usson, Y., Leverve, X., Paulin, D., & Saks, V. A. (1997). Study of regulation of mitochondrial respiration in vivo. An analysis of influence of ADP diffusion and possible role of cytoskeleton. *Biochim Biophys Acta*, *1322*(1), 41-59. https://doi.org/10.1016/s0005-2728(97)00071-6

Kelley, D. E., & Goodpaster, B. H. (2001). Skeletal muscle triglyceride. An aspect of regional adiposity and insulin resistance. *Diabetes Care*, *24*(5), 933-941. https://doi.org/10.2337/diacare.24.5.933

Kersten, J. R., Schmeling, T. J., Orth, K. G., Pagel, P. S., & Warltier, D. C. (1998). Acute hyperglycemia abolishes ischemic preconditioning in vivo. *Am J Physiol*, *275*(2), H721-725. https://doi.org/10.1152/ajpheart.1998.275.2.H721

Khacho, M., Tarabay, M., Patten, D., Khacho, P., MacLaurin, J. G., Guadagno, J., Bergeron, R., Cregan, S. P., Harper, M. E., Park, D. S., & Slack, R. S. (2014). Acidosis overrides oxygen deprivation to maintain mitochondrial function and cell survival. *Nat Commun*, *5*, 3550. https://doi.org/10.1038/ncomms4550

Khoo, J. C., & Russell, P. J. (1972). Isoenzymes of adenylate kinase in human tissue. *Biochim Biophys Acta*, *268*(1), 98-101. https://doi.org/10.1016/0005-2744(72)90202-1

Kim, J., Lee, K., Fujioka, H., Tandler, B., & Hoppel, C. L. (2018). Cardiac mitochondrial structure and function in tafazzin-knockdown mice. *Mitochondrion*, *43*, 53-62. https://doi.org/10.1016/j.mito.2018.10.005

Kinsley, B. T., Swift, M., Dumont, R. H., & Swift, R. G. (1995). Morbidity and mortality in the Wolfram syndrome. *Diabetes Care*, *18*(12), 1566-1570. https://doi.org/10.2337/diacare.18.12.1566

Ko, Y. H., Delannoy, M., Hullihen, J., Chiu, W., & Pedersen, P. L. (2003). Mitochondrial ATP synthasome. Cristae-enriched membranes and a multiwell detergent screening assay yield dispersed single complexes containing the ATP synthase and carriers for Pi and ADP/ATP. *J Biol Chem*, *278*(14), 12305-12309. https://doi.org/10.1074/jbc.C200703200

Koido, K., Koks, S., Nikopensius, T., Maron, E., Altmae, S., Heinaste, E., Vabrit, K., Tammekivi, V., Hallast, P., Kurg, A., Shlik, J., Vasar, V., Metspalu, A., & Vasar, E. (2005). Polymorphisms in wolframin (WFS1) gene are possibly related to increased risk for mood disorders. *Int J Neuropsychopharmacol*, *8*(2), 235-244. https://doi.org/10.1017/s1461145704004791

Koit, A., Shevchuk, I., Ounpuu, L., Klepinin, A., Chekulayev, V., Timohhina, N., Tepp, K., Puurand, M., Truu, L., Heck, K., Valvere, V., Guzun, R., & Kaambre, T. (2017). Mitochondrial Respiration in Human Colorectal and Breast Cancer Clinical Material Is Regulated Differently. *Oxid Med Cell Longev*, *2017*, 1372640. https://doi.org/10.1155/2017/1372640

Koks, S. (2023). Genomics of Wolfram Syndrome 1 (WFS1). *Biomolecules*, *13*(9). https://doi.org/10.3390/biom13091346

Koks, S., Soomets, U., Paya-Cano, J. L., Fernandes, C., Luuk, H., Plaas, M., Terasmaa, A., Tillmann, V., Noormets, K., Vasar, E., & Schalkwyk, L. C. (2009). Wfs1 gene deletion causes growth retardation in mice and interferes with the growth hormone pathway. *Physiol Genomics*, *37*(3), 249-259. https://doi.org/10.1152/physiolgenomics.90407.2008

Kondo, T., Hayashi, M., Takeshita, K., Numaguchi, Y., Kobayashi, K., Iino, S., Inden, Y., & Murohara, T. (2004). Smoking cessation rapidly increases circulating progenitor cells in peripheral blood in chronic smokers. *Arterioscler Thromb Vasc Biol*, *24*(8), 1442-1447. https://doi.org/10.1161/01.ATV.0000135655.52088.c5

Korkmaz, H. A., Demir, K., Hazan, F., Yildiz, M., Elmas, O. N., & Ozkan, B. (2016). Association of Wolfram syndrome with Fallot tetralogy in a girl. *Arch Argent Pediatr*, *114*(3), e163-166. https://doi.org/10.5546/aap.2016.eng.e163 (Asociacion entre el sindrome de Wolfram y la tetralogia de Fallot en una nina.)

Kuhlbrandt, W. (2015). Structure and function of mitochondrial membrane protein complexes. *BMC Biol*, *13*, 89. https://doi.org/10.1186/s12915-015-0201-x

Kunz, W. S., Kuznetsov, A. V., Schulze, W., Eichhorn, K., Schild, L., Striggow, F., Bohnensack, R., Neuhof, S., Grasshoff, H., Neumann, H. W., & Gellerich, F. N. (1993). Functional characterization of mitochondrial oxidative phosphorylation in saponin-skinned human muscle fibers. *Biochim Biophys Acta*, *1144*(1), 46-53. https://doi.org/10.1016/0005-2728(93)90029-f

Kupriyanov, V. V., Lakomkin, V. L., Kapelko, V. I., Steinschneider, A., Ruuge, E. K., & Saks, V. A. (1987). Dissociation of adenosine triphosphate levels and contractile function in isovolumic hearts perfused with 2-deoxyglucose. *J Mol Cell Cardiol*, *19*(8), 729-740. https://doi.org/10.1016/s0022-2828(87)80384-x

Kuznetsov, A. V., Javadov, S., Margreiter, R., Hagenbuchner, J., & Ausserlechner, M. J. (2022). Analysis of Mitochondrial Function, Structure, and Intracellular Organization In Situ in Cardiomyocytes and Skeletal Muscles. *Int J Mol Sci*, *23*(4). https://doi.org/10.3390/ijms23042252

Kuznetsov, A. V., Tiivel, T., Sikk, P., Kaambre, T., Kay, L., Daneshrad, Z., Rossi, A., Kadaja, L., Peet, N., Seppet, E., & Saks, V. A. (1996). Striking differences between the kinetics of regulation of respiration by ADP in slow-twitch and fast-twitch muscles in vivo. *Eur J Biochem*, *241*(3), 909-915. https://doi.org/10.1111/j.1432-1033.1996.00909.x

Kuznetsov, A. V., Veksler, V., Gellerich, F. N., Saks, V., Margreiter, R., & Kunz, W. S. (2008). Analysis of mitochondrial function in situ in permeabilized muscle fibers, tissues and cells. *Nat Protoc*, *3*(6), 965-976. https://doi.org/10.1038/nprot.2008.61

La Morgia, C., Maresca, A., Amore, G., Gramegna, L. L., Carbonelli, M., Scimonelli, E., Danese, A., Patergnani, S., Caporali, L., Tagliavini, F., Del Dotto, V., Capristo, M., Sadun, F., Barboni, P., Savini, G., Evangelisti, S., Bianchini, C., Valentino, M. L., Liguori, R., . . . Carelli, V. (2020). Calcium mishandling in absence of primary mitochondrial dysfunction drives cellular pathology in Wolfram Syndrome. *Sci Rep*, *10*(1), 4785. https://doi.org/10.1038/s41598-020-61735-3

Lange, C. F., Jr., & Kohn, P. (1961). Substrate specificity of hexokinases. *J Biol Chem*, *236*, 1-5.

Laniado-Laborin, R. (2009). Smoking and chronic obstructive pulmonary disease (COPD). Parallel epidemics of the 21 century. *Int J Environ Res Public Health*, *6*(1), 209-224. https://doi.org/10.3390/ijerph6010209

Lapuente-Brun, E., Moreno-Loshuertos, R., Acin-Perez, R., Latorre-Pellicer, A., Colas, C., Balsa, E., Perales-Clemente, E., Quiros, P. M., Calvo, E., Rodriguez-Hernandez, M. A., Navas, P., Cruz, R., Carracedo, A., Lopez-Otin, C., Perez-Martos, A., Fernandez-Silva, P., Fernandez-Vizarra, E., & Enriquez, J. A. (2013). Supercomplex assembly determines electron flux in the mitochondrial electron transport chain. *Science*, *340*(6140), 1567-1570. https://doi.org/10.1126/science.1230381

Laughlin, M. R., Taylor, J., Chesnick, A. S., DeGroot, M., & Balaban, R. S. (1993). Pyruvate and lactate metabolism in the in vivo dog heart. *Am J Physiol*, *264*(6 Pt 2), H2068-2079. https://doi.org/10.1152/ajpheart.1993.264.6.H2068

Lee, H., & Son, Y. J. (2019). Influence of Smoking Status on Risk of Incident Heart Failure: A Systematic Review and Meta-Analysis of Prospective Cohort Studies. *Int J Environ Res Public Health*, *16*(15). https://doi.org/10.3390/ijerph16152697

Lee, J., Iwasaki, T., Kaida, T., Chuman, H., Yoshimura, A., Okamoto, Y., Takashima, H., & Miyata, K. (2022). A case of adult-onset Wolfram syndrome with compound heterozygous mutations of the WFS1 gene. *Am J Ophthalmol Case Rep*, *25*, 101315. https://doi.org/10.1016/j.ajoc.2022.101315

Lemieux, H., Blier, P. U., & Gnaiger, E. (2017). Remodeling pathway control of mitochondrial respiratory capacity by temperature in mouse heart: electron flow through the Q-junction in permeabilized fibers. *Sci Rep*, *7*(1), 2840. https://doi.org/10.1038/s41598-017-02789-8

Lenaz, G. (2012). Mitochondria and reactive oxygen species. Which role in physiology and pathology? *Adv Exp Med Biol*, *942*, 93-136. https://doi.org/10.1007/978-94-007-2869-1_5

Lenaz, G., & Genova, M. L. (2009). Mobility and function of coenzyme Q (ubiquinone) in the mitochondrial respiratory chain. *Biochim Biophys Acta*, *1787*(6), 563-573. https://doi.org/10.1016/j.bbabio.2009.02.019

Letts, J. A., Fiedorczuk, K., & Sazanov, L. A. (2016). The architecture of respiratory supercomplexes. *Nature*, *537*(7622), 644-648. https://doi.org/10.1038/nature19774

Li, R., Adami, A., Chang, C. C., Tseng, C. H., Hsiai, T. K., & Rossiter, H. B. (2021). Serum Acylglycerols Inversely Associate with Muscle Oxidative Capacity in Severe COPD. *Med Sci Sports Exerc*, *53*(1), 10-18. https://doi.org/10.1249/mss.0000000000002441

Li, X., Wu, F., Gunther, S., Looso, M., Kuenne, C., Zhang, T., Wiesnet, M., Klatt, S., Zukunft, S., Fleming, I., Poschet, G., Wietelmann, A., Atzberger, A., Potente, M., Yuan, X., & Braun, T. (2023). Inhibition of fatty acid oxidation enables heart regeneration in adult mice. *Nature*, *622*(7983), 619-626. https://doi.org/10.1038/s41586-023-06585-5

Lin, J., Duan, J., Wang, Q., Xu, S., Zhou, S., & Yao, K. (2022). Mitochondrial Dynamics and Mitophagy in Cardiometabolic Disease. *Front Cardiovasc Med*, *9*, 917135. https://doi.org/10.3389/fcvm.2022.917135

Liu, Y., Lu, L., Yang, H., Wu, X., Luo, X., Shen, J., Xiao, Z., Zhao, Y., Du, F., Chen, Y., Deng, S., Cho, C. H., Li, Q., Li, X., Li, W., Wang, F., Sun, Y., Gu, L., Chen, M., & Li, M. (2023). Dysregulation of immunity by cigarette smoking promotes inflammation and cancer: A review. *Environ Pollut*, *339*, 122730. https://doi.org/10.1016/j.envpol.2023.122730

Lombardi, A., Silvestri, E., Cioffi, F., Senese, R., Lanni, A., Goglia, F., de Lange, P., & Moreno, M. (2009). Defining the transcriptomic and proteomic profiles of rat ageing skeletal muscle by the use of a cDNA array, 2D- and Blue native-PAGE approach. *J Proteomics*, *72*(4), 708-721. https://doi.org/10.1016/j.jprot.2009.02.007

Lopaschuk, G. D. (1996). Abnormal mechanical function in diabetes: relationship to altered myocardial carbohydrate/lipid metabolism. *Coron Artery Dis*, *7*(2), 116-123. https://doi.org/10.1097/00019501-199602000-00004

Lopaschuk, G. D., Belke, D. D., Gamble, J., Itoi, T., & Schonekess, B. O. (1994). Regulation of fatty acid oxidation in the mammalian heart in health and disease. *Biochim Biophys Acta*, *1213*(3), 263-276. https://doi.org/10.1016/0005-2760(94)00082-4

Lopaschuk, G. D., Ussher, J. R., Folmes, C. D., Jaswal, J. S., & Stanley, W. C. (2010). Myocardial fatty acid metabolism in health and disease. *Physiol Rev*, *90*(1), 207-258. https://doi.org/10.1152/physrev.00015.2009

Lopez-Fabuel, I., Le Douce, J., Logan, A., James, A. M., Bonvento, G., Murphy, M. P., Almeida, A., & Bolanos, J. P. (2016). Complex I assembly into supercomplexes determines differential mitochondrial ROS production in neurons and astrocytes. *Proc Natl Acad Sci U S A*, *113*(46), 13063-13068. https://doi.org/10.1073/pnas.1613701113

Luuk, H., Koks, S., Plaas, M., Hannibal, J., Rehfeld, J. F., & Vasar, E. (2008). Distribution of Wfs1 protein in the central nervous system of the mouse and its relation to clinical symptoms of the Wolfram syndrome. *J Comp Neurol*, *509*(6), 642-660. https://doi.org/10.1002/cne.21777

Luuk, H., Plaas, M., Raud, S., Innos, J., Sutt, S., Lasner, H., Abramov, U., Kurrikoff, K., Koks, S., & Vasar, E. (2009). Wfs1-deficient mice display impaired behavioural adaptation in stressful environment. *Behav Brain Res*, *198*(2), 334-345. https://doi.org/10.1016/j.bbr.2008.11.007

Macacu, A., Autier, P., Boniol, M., & Boyle, P. (2015). Active and passive smoking and risk of breast cancer: a meta-analysis. *Breast Cancer Res Treat*, *154*(2), 213-224. https://doi.org/10.1007/s10549-015-3628-4

Makrecka-Kuka, M., Liepinsh, E., Murray, A. J., Lemieux, H., Dambrova, M., Tepp, K., Puurand, M., Kaambre, T., Han, W. H., de Goede, P., O'Brien, K. A., Turan, B., Tuncay, E., Olgar, Y., Rolo, A. P., Palmeira, C. M., Boardman, N. T., Wust, R. C. I., & Larsen, T. S. (2020). Altered mitochondrial metabolism in the insulin-resistant heart. *Acta Physiol (Oxf)*, *228*(3), e13430. https://doi.org/10.1111/apha.13430

Malfitano, C., de Souza Junior, A. L., Carbonaro, M., Bolsoni-Lopes, A., Figueroa, D., de Souza, L. E., Silva, K. A., Consolim-Colombo, F., Curi, R., & Irigoyen, M. C. (2015). Glucose and fatty acid metabolism in infarcted heart from streptozotocin- induced diabetic rats after 2 weeks of tissue remodeling. *Cardiovasc Diabetol*, *14*, 149. https://doi.org/10.1186/s12933-015-0308-y

Mallet, R. T., Hartman, D. A., & Bunger, R. (1990). Glucose requirement for postischemic recovery of perfused working heart. *Eur J Biochem*, *188*(2), 481-493. https://doi.org/10.1111/j.1432-1033.1990.tb15426.x

Maranzana, E., Barbero, G., Falasca, A. I., Lenaz, G., & Genova, M. L. (2013). Mitochondrial respiratory supercomplex association limits production of reactive oxygen species from complex I. *Antioxid Redox Signal*, *19*(13), 1469-1480. https://doi.org/10.1089/ars.2012.4845

Marin-Garcia, J., Goldenthal, M. J., & Moe, G. W. (2001). Mitochondrial pathology in cardiac failure. *Cardiovasc Res*, *49*(1), 17-26. https://doi.org/10.1016/s0008-6363(00)00241-8

Martinez-Reyes, I., & Chandel, N. S. (2020). Mitochondrial TCA cycle metabolites control physiology and disease. *Nat Commun*, *11*(1), 102. https://doi.org/10.1038/s41467-019-13668-3

Masters, C. J., Reid, S., & Don, M. (1987). Glycolysis--new concepts in an old pathway. *Mol Cell Biochem*, *76*(1), 3-14. https://doi.org/10.1007/bf00219393

Mather, K. J., Hutchins, G. D., Perry, K., Territo, W., Chisholm, R., Acton, A., Glick-Wilson, B., Considine, R. V., Moberly, S., & DeGrado, T. R. (2016). Assessment of myocardial metabolic flexibility and work efficiency in human type 2 diabetes using 16-[18F]fluoro-4-thiapalmitate, a novel PET fatty acid tracer. *Am J Physiol Endocrinol Metab*, *310*(6), E452-460. https://doi.org/10.1152/ajpendo.00437.2015

Mazumder, P. K., O'Neill, B. T., Roberts, M. W., Buchanan, J., Yun, U. J., Cooksey, R. C., Boudina, S., & Abel, E. D. (2004). Impaired cardiac efficiency and increased fatty acid oxidation in insulin-resistant ob/ob mouse hearts. *Diabetes*, *53*(9), 2366-2374. https://doi.org/10.2337/diabetes.53.9.2366

Mazzone, P., Tierney, W., Hossain, M., Puvenna, V., Janigro, D., & Cucullo, L. (2010). Pathophysiological impact of cigarette smoke exposure on the cerebrovascular system with a focus on the blood-brain barrier: expanding the awareness of smoking toxicity in an underappreciated area. *Int J Environ Res Public Health*, *7*(12), 4111-4126. https://doi.org/10.3390/ijerph7124111

McCommis, K. S., & Finck, B. N. (2015). Mitochondrial pyruvate transport: a historical perspective and future research directions. *Biochem J*, *466*(3), 443-454. https://doi.org/10.1042/bj20141171

McDonald, L. T., Zile, M. R., Zhang, Y., Van Laer, A. O., Baicu, C. F., Stroud, R. E., Jones, J. A., LaRue, A. C., & Bradshaw, A. D. (2018). Increased macrophage-derived SPARC precedes collagen deposition in myocardial fibrosis. *Am J Physiol Heart Circ Physiol*, *315*(1), H92-h100. https://doi.org/10.1152/ajpheart.00719.2017

McGarrah, R. W., Crown, S. B., Zhang, G. F., Shah, S. H., & Newgard, C. B. (2018). Cardiovascular Metabolomics. *Circ Res*, *122*(9), 1238-1258. https://doi.org/10.1161/circresaha.117.311002

McGavock, J. M., Lingvay, I., Zib, I., Tillery, T., Salas, N., Unger, R., Levine, B. D., Raskin, P., Victor, R. G., & Szczepaniak, L. S. (2007). Cardiac steatosis in diabetes mellitus: a 1H-magnetic resonance spectroscopy study. *Circulation*, *116*(10), 1170-1175. https://doi.org/10.1161/circulationaha.106.645614

McLeish, M. J., & Kenyon, G. L. (2005). Relating structure to mechanism in creatine kinase. *Crit Rev Biochem Mol Biol*, *40*(1), 1-20. https://doi.org/10.1080/10409230590918577

Medlej, R., Wasson, J., Baz, P., Azar, S., Salti, I., Loiselet, J., Permutt, A., & Halaby, G. (2004). Diabetes mellitus and optic atrophy: a study of Wolfram syndrome in the Lebanese population. *J Clin Endocrinol Metab*, *89*(4), 1656-1661. https://doi.org/10.1210/jc.2002-030015

Messner, B., & Bernhard, D. (2014). Smoking and cardiovascular disease: mechanisms of endothelial dysfunction and early atherogenesis. *Arterioscler Thromb Vasc Biol*, *34*(3), 509-515. https://doi.org/10.1161/atvbaha.113.300156

Michaud, S. E., Dussault, S., Groleau, J., Haddad, P., & Rivard, A. (2006). Cigarette smoke exposure impairs VEGF-induced endothelial cell migration: role of NO and reactive oxygen species. *J Mol Cell Cardiol*, *41*(2), 275-284. https://doi.org/10.1016/j.yjmcc.2006.05.004

Minton, J. A., Hattersley, A. T., Owen, K., McCarthy, M. I., Walker, M., Latif, F., Barrett, T., & Frayling, T. M. (2002). Association studies of genetic variation in the WFS1 gene and type 2 diabetes in U.K. populations. *Diabetes*, *51*(4), 1287-1290. https://doi.org/10.2337/diabetes.51.4.1287

Minton, J. A., Rainbow, L. A., Ricketts, C., & Barrett, T. G. (2003). Wolfram syndrome. *Rev Endocr Metab Disord*, *4*(1), 53-59. https://doi.org/10.1023/a:1021875403463

Miro, O., Alonso, J. R., Jarreta, D., Casademont, J., Urbano-Marquez, A., & Cardellach, F. (1999). Smoking disturbs mitochondrial respiratory chain function and enhances lipid peroxidation on human circulating lymphocytes. *Carcinogenesis*, *20*(7), 1331-1336. https://doi.org/10.1093/carcin/20.7.1331

Mjos, O. D. (1971). Effect of free fatty acids on myocardial function and oxygen consumption in intact dogs. *J Clin Invest*, *50*(7), 1386-1389. https://doi.org/10.1172/jci106621

Morikawa, S., Tajima, T., Nakamura, A., Ishizu, K., & Ariga, T. (2017). A novel heterozygous mutation of the WFS1 gene leading to constitutive endoplasmic reticulum stress is the cause of Wolfram syndrome. *Pediatr Diabetes*, *18*(8), 934-941. https://doi.org/10.1111/pedi.12513

Mourier, A., Matic, S., Ruzzenente, B., Larsson, N. G., & Milenkovic, D. (2014). The respiratory chain supercomplex organization is independent of COX7a2l isoforms. *Cell Metab*, *20*(6), 1069-1075. https://doi.org/10.1016/j.cmet.2014.11.005

Muhleip, A., Flygaard, R. K., Baradaran, R., Haapanen, O., Gruhl, T., Tobiasson, V., Marechal, A., Sharma, V., & Amunts, A. (2023). Structural basis of mitochondrial membrane bending by the I-II-III2-IV2 supercomplex. *Nature*, *615*(7954), 934-938. https://doi.org/10.1038/s41586-023-05817-y

Murashige, D., Jang, C., Neinast, M., Edwards, J. J., Cowan, A., Hyman, M. C., Rabinowitz, J. D., Frankel, D. S., & Arany, Z. (2020). Comprehensive quantification of fuel use by the failing and nonfailing human heart. *Science*, *370*(6514), 364-368. https://doi.org/10.1126/science.abc8861

Must, A., Koks, S., Vasar, E., Tasa, G., Lang, A., Maron, E., & Vali, M. (2009). Common variations in 4p locus are related to male completed suicide. *Neuromolecular Med*, *11*(1), 13-19. https://doi.org/10.1007/s12017-008-8056-8

Nederlof, R., Gurel-Gurevin, E., Eerbeek, O., Xie, C., Deijs, G. S., Konkel, M., Hu, J., Weber, N. C., Schumacher, C. A., Baartscheer, A., Mik, E. G., Hollmann, M. W., Akar, F. G., & Zuurbier, C. J. (2016). Reducing mitochondrial bound hexokinase II mediates transition from non- injurious into injurious ischemia/reperfusion of the intact heart. *J Physiol Biochem*, *73*(3), 323-333. https://doi.org/10.1007/s13105-017-0555-3

Neely, J. R., & Grotyohann, L. W. (1984). Role of glycolytic products in damage to ischemic myocardium. Dissociation of adenosine triphosphate levels and recovery of function of reperfused ischemic hearts. *Circ Res*, *55*(6), 816-824. https://doi.org/10.1161/01.res.55.6.816

Neinast, M., Murashige, D., & Arany, Z. (2019). Branched Chain Amino Acids. *Annu Rev Physiol*, *81*, 139-164. https://doi.org/10.1146/annurev-physiol-020518-114455

Nemutlu, E., Zhang, S., Gupta, A., Juranic, N. O., Macura, S. I., Terzic, A., Jahangir, A., & Dzeja, P. (2012). Dynamic phosphometabolomic profiling of human tissues and transgenic models by 18O-assisted (3)(1)P NMR and mass spectrometry. *Physiol Genomics*, *44*(7), 386-402. https://doi.org/10.1152/physiolgenomics.00152.2011

Newgard, C. B. (2012). Interplay between lipids and branched-chain amino acids in development of insulin resistance. *Cell Metab*, *15*(5), 606-614. https://doi.org/10.1016/j.cmet.2012.01.024

Nicholls, D. G. (1974). The influence of respiration and ATP hydrolysis on the proton-electrochemical gradient across the inner membrane of rat-liver mitochondria as determined by ion distribution. *Eur J Biochem*, *50*(1), 305-315. https://doi.org/10.1111/j.1432-1033.1974.tb03899.x

Nogueira, L., Trisko, B. M., Lima-Rosa, F. L., Jackson, J., Lund-Palau, H., Yamaguchi, M., & Breen, E. C. (2018). Cigarette smoke directly impairs skeletal muscle function through capillary regression and altered myofibre calcium kinetics in mice. *J Physiol*, *596*(14), 2901-2916. https://doi.org/10.1113/jp275888

Nollet, E. E., Duursma, I., Rozenbaum, A., Eggelbusch, M., Wust, R. C. I., Schoonvelde, S. A. C., Michels, M., Jansen, M., van der Wel, N. N., Bedi, K. C., Margulies, K. B., Nirschl, J., Kuster, D. W. D., & van der Velden, J. (2023). Mitochondrial dysfunction in human hypertrophic cardiomyopathy is linked to cardiomyocyte architecture disruption and corrected by improving NADH- driven mitochondrial respiration. *Eur Heart J*, *44*(13), 1170-1185. https://doi.org/10.1093/eurheartj/ehad028

Noma, T. (2005). Dynamics of nucleotide metabolism as a supporter of life phenomena. *J Med Invest*, *52*(3-4), 127-136. https://doi.org/10.2152/jmi.52.127

Noma, T., Song, S., Yoon, Y. S., Tanaka, S., & Nakazawa, A. (1998). cDNA cloning and tissue-specific expression of the gene encoding human adenylate kinase isozyme 2. *Biochim Biophys Acta*, *1395*(1), 34-39. https://doi.org/10.1016/s0167-4781(97)00193-0

Noormets, K., Koks, S., Kavak, A., Arend, A., Aunapuu, M., Keldrimaa, A., Vasar, E., & Tillmann, V. (2009). Male mice with deleted Wolframin (Wfs1) gene have reduced fertility. *Reprod Biol Endocrinol*, *7*, 82. https://doi.org/10.1186/1477-7827-7-82

Noskov, S. Y., Rostovtseva, T. K., Chamberlin, A. C., Teijido, O., Jiang, W., & Bezrukov, S. M. (2016). Current state of theoretical and experimental studies of the voltage-dependent anion channel (VDAC). *Biochim Biophys Acta*, *1858*(7 Pt B), 1778-1790. https://doi.org/10.1016/j.bbamem.2016.02.026

Novack, G. V., Galeano, P., Castano, E. M., & Morelli, L. (2020). Mitochondrial Supercomplexes: Physiological Organization and Dysregulation in Age-Related Neurodegenerative Disorders. *Front Endocrinol (Lausanne)*, *11*, 600. https://doi.org/10.3389/fendo.2020.00600

Oishi, Y., & Manabe, I. (2018). Macrophages in inflammation, repair and regeneration. *Int Immunol*, *30*(11), 511-528. https://doi.org/10.1093/intimm/dxy054

Olson, A. L., & Pessin, J. E. (1996). Structure, function, and regulation of the mammalian facilitative glucose transporter gene family. *Annu Rev Nutr*, *16*, 235-256. https://doi.org/10.1146/annurev.nu.16.070196.001315

Ottaway, J. H., & Mowbray, J. (1977). The role of compartmentation in the control of glycolysis. *Curr Top Cell Regul*, *12*, 107-208. https://doi.org/10.1016/b978-0-12-152812-6.50010-x

Palade, G. E. (1953). An electron microscope study of the mitochondrial structure. *J Histochem Cytochem*, *1*(4), 188-211. https://doi.org/10.1177/1.4.188

Palmieri, F., & Pierri, C. L. (2010). Mitochondrial metabolite transport. *Essays Biochem*, *47*, 37-52. https://doi.org/10.1042/bse0470037

Panayiotou, C., Solaroli, N., & Karlsson, A. (2014). The many isoforms of human adenylate kinases. *Int J Biochem Cell Biol*, *49*, 75-83. https://doi.org/10.1016/j.biocel.2014.01.014

Park, S. K., Ryoo, J. H., Kang, J. G., & Jung, J. Y. (2021). Smoking Status, Intensity of Smoking, and Their Relation to Left Ventricular Hypertrophy in Working Aged Korean Men. *Nicotine Tob Res*, *23*(7), 1176-1182. https://doi.org/10.1093/ntr/ntab020

Parra, J., Brdiczka, D., Cusso, R., & Pette, D. (1997). Enhanced catalytic activity of hexokinase by work-induced mitochondrial binding in fast-twitch muscle of rat. *FEBS Lett*, *403*(3), 279-282. https://doi.org/10.1016/s0014-5793(97)00047-1

Patten, D. A., Wong, J., Khacho, M., Soubannier, V., Mailloux, R. J., Pilon-Larose, K., MacLaurin, J. G., Park, D. S., McBride, H. M., Trinkle-Mulcahy, L., Harper, M. E., Germain, M., & Slack, R. S. (2014). OPA1-dependent cristae modulation is essential for cellular adaptation to metabolic demand. *Embo j*, *33*(22), 2676-2691. https://doi.org/10.15252/embj.201488349

Pedersen, P. L. (2007). Warburg, me and Hexokinase 2: Multiple discoveries of key molecular events underlying one of cancers' most common phenotypes, the "Warburg Effect", i.e., elevated glycolysis in the presence of oxygen. *J Bioenerg Biomembr*, *39*(3), 211-222. https://doi.org/10.1007/s10863-007-9094-x

Pedersen, P. L. (2008). Voltage dependent anion channels (VDACs): a brief introduction with a focus on the outer mitochondrial compartment's roles together with hexokinase-2 in the "Warburg effect" in cancer. *J Bioenerg Biomembr*, *40*(3), 123-126. https://doi.org/10.1007/s10863-008-9165-7

Pernas, L., & Scorrano, L. (2016). Mito-Morphosis: Mitochondrial Fusion, Fission, and Cristae Remodeling as Key Mediators of Cellular Function. *Annu Rev Physiol*, *78*, 505-531. https://doi.org/10.1146/annurev-physiol-021115-105011

Petersen, A. M., Magkos, F., Atherton, P., Selby, A., Smith, K., Rennie, M. J., Pedersen, B. K., & Mittendorfer, B. (2007). Smoking impairs muscle protein synthesis and increases the expression of myostatin and MAFbx in muscle. *Am J Physiol Endocrinol Metab*, *293*(3), E843-848. https://doi.org/10.1152/ajpendo.00301.2007

Petersen, K. F., Dufour, S., Befroy, D., Garcia, R., & Shulman, G. I. (2004). Impaired mitochondrial activity in the insulin-resistant offspring of patients with type 2 diabetes. *N Engl J Med*, *350*(7), 664-671. https://doi.org/10.1056/NEJMoa031314

Petsophonsakul, P., Burgmaier, M., Willems, B., Heeneman, S., Stadler, N., Gremse, F., Reith, S., Burgmaier, K., Kahles, F., Marx, N., Natour, E., Bidar, E., Jacobs, M., Mees, B., Reutelingsperger, C., Furmanik, M., & Schurgers, L. (2022). Nicotine promotes vascular calcification via intracellular Ca2+-mediated, Nox5-induced oxidative stress, and extracellular vesicle release in vascular smooth muscle cells. *Cardiovasc Res*, *118*(9), 2196-2210. https://doi.org/10.1093/cvr/cvab244

Peuhkurinen, K. J., & Hassinen, I. E. (1982). Pyruvate carboxylation as an anaplerotic mechanism in the isolated perfused rat heart. *Biochem J*, *202*(1), 67-76. https://doi.org/10.1042/bj2020067

Plaas, M., Seppa, K., Reimets, R., Jagomae, T., Toots, M., Koppel, T., Vallisoo, T., Nigul, M., Heinla, I., Meier, R., Kaasik, A., Piirsoo, A., Hickey, M. A., Terasmaa, A., & Vasar, E. (2017). Wfs1- deficient rats develop primary symptoms of Wolfram syndrome: insulin-dependent diabetes, optic nerve atrophy and medullary degeneration. *Sci Rep*, *7*(1), 10220. https://doi.org/10.1038/s41598-017-09392-x

Prakash, V., Jaker, S., Burgan, A., Jacques, A., Fluck, D., Sharma, P., Fry, C. H., & Han, T. S. (2021). The smoking-dyslipidaemia dyad: A potent synergistic risk for atherosclerotic coronary artery disease. *JRSM Cardiovasc Dis*, *10*, 2048004020980945. https://doi.org/10.1177/2048004020980945

Printz, R. L., Koch, S., Potter, L. R., O'Doherty, R. M., Tiesinga, J. J., Moritz, S., & Granner, D. K. (1993). Hexokinase II mRNA and gene structure, regulation by insulin, and evolution. *J Biol Chem*, *268*(7), 5209-5219.

Prior, S. J., Ryan, A. S., Stevenson, T. G., & Goldberg, A. P. (2014). Metabolic inflexibility during submaximal aerobic exercise is associated with glucose intolerance in obese older adults. *Obesity (Silver Spring)*, *22*(2), 451-457. https://doi.org/10.1002/oby.20609

Prisco, S. Z., Rose, L., Potus, F., Tian, L., Wu, D., Hartweck, L., Al-Qazazi, R., Neuber-Hess, M., Eklund, M., Hsu, S., Thenappan, T., Archer, S. L., & Prins, K. W. (2020). Excess Protein O-GlcNAcylation Links Metabolic Derangements to Right Ventricular Dysfunction in Pulmonary Arterial Hypertension. *Int J Mol Sci*, *21*(19). https://doi.org/10.3390/ijms21197278

Prochownik, E. V., & Wang, H. (2021). The Metabolic Fates of Pyruvate in Normal and Neoplastic Cells. *Cells*, *10*(4). https://doi.org/10.3390/cells10040762

Protasoni, M., Perez-Perez, R., Lobo-Jarne, T., Harbour, M. E., Ding, S., Penas, A., Diaz, F., Moraes, C. T., Fearnley, I. M., Zeviani, M., Ugalde, C., & Fernandez-Vizarra, E. (2020). Respiratory supercomplexes act as a platform for complex III-mediated maturation of human mitochondrial complexes I and IV. *Embo j*, *39*(3), e102817. https://doi.org/10.15252/embj.2019102817

Protasoni, M., & Zeviani, M. (2021). Mitochondrial Structure and Bioenergetics in Normal and Disease Conditions. *Int J Mol Sci*, *22*(2). https://doi.org/10.3390/ijms22020586

Pucar, D., Dzeja, P. P., Bast, P., Juranic, N., Macura, S., & Terzic, A. (2001). Cellular energetics in the preconditioned state: protective role for phosphotransfer reactions captured by 18O-assisted 31P NMR. *J Biol Chem*, *276*(48), 44812-44819. https://doi.org/10.1074/jbc.M104425200

Puurand, M., Tepp, K., Timohhina, N., Aid, J., Shevchuk, I., Chekulayev, V., & Kaambre, T. (2019). Tubulin betaII and betaIII Isoforms as the Regulators of VDAC Channel Permeability in Health and Disease. *Cells*, *8*(3). https://doi.org/10.3390/cells8030239

Qin, X., Zhang, Y., & Zheng, Q. (2022). Metabolic Inflexibility as a Pathogenic Basis for Atrial Fibrillation. *Int J Mol Sci*, *23*(15). https://doi.org/10.3390/ijms23158291

Ramzan, R., Rhiel, A., Weber, P., Kadenbach, B., & Vogt, S. (2019). Reversible dimerization of cytochrome c oxidase regulates mitochondrial respiration. *Mitochondrion*, *49*, 149-155. https://doi.org/10.1016/j.mito.2019.08.002

Randle, P. J., Garland, P. B., Hales, C. N., & Newsholme, E. A. (1963). The glucose fatty-acid cycle. Its role in insulin sensitivity and the metabolic disturbances of diabetes mellitus. *Lancet*, *1*(7285), 785-789. https://doi.org/10.1016/s0140-6736(63)91500-9

Razeghi, P., Young, M. E., Alcorn, J. L., Moravec, C. S., Frazier, O. H., & Taegtmeyer, H. (2001). Metabolic gene expression in fetal and failing human heart. *Circulation*, *104*(24), 2923-2931. https://doi.org/10.1161/hc4901.100526

Redza-Dutordoir, M., & Averill-Bates, D. A. (2016). Activation of apoptosis signalling pathways by reactive oxygen species. *Biochim Biophys Acta*, *1863*(12), 2977-2992. https://doi.org/10.1016/j.bbamcr.2016.09.012

Rich, P. R., & Marechal, A. (2010). The mitochondrial respiratory chain. *Essays Biochem*, *47*, 1-23. https://doi.org/10.1042/bse0470001

Rigoli, L., Bramanti, P., Di Bella, C., & De Luca, F. (2018). Genetic and clinical aspects of Wolfram syndrome 1, a severe neurodegenerative disease. *Pediatr Res*, *83*(5), 921-929. https://doi.org/10.1038/pr.2018.17

Rijzewijk, L. J., van der Meer, R. W., Lamb, H. J., de Jong, H. W., Lubberink, M., Romijn, J. A., Bax, J. J., de Roos, A., Twisk, J. W., Heine, R. J., Lammertsma, A. A., Smit, J. W., & Diamant, M. (2009). Altered myocardial substrate metabolism and decreased diastolic function in nonischemic human diabetic cardiomyopathy: studies with cardiac positron emission tomography and magnetic resonance imaging. *J Am Coll Cardiol*, *54*(16), 1524-1532. https://doi.org/10.1016/j.jacc.2009.04.074

Roberts, D. J., & Miyamoto, S. (2015). Hexokinase II integrates energy metabolism and cellular protection: Akting on mitochondria and TORCing to autophagy. *Cell Death Differ*, *22*(2), 248-257. https://doi.org/10.1038/cdd.2014.173

Rohayem, J., Ehlers, C., Wiedemann, B., Holl, R., Oexle, K., Kordonouri, O., Salzano, G., Meissner, T., Burger, W., Schober, E., Huebner, A., & Lee-Kirsch, M. A. (2011). Diabetes and neurodegeneration in Wolfram syndrome: a multicenter study of phenotype and genotype. *Diabetes Care*, *34*(7), 1503-1510. https://doi.org/10.2337/dc10-1937

Rom, O., Avezov, K., Aizenbud, D., & Reznick, A. Z. (2013). Cigarette smoking and inflammation revisited. *Respir Physiol Neurobiol*, *187*(1), 5-10. https://doi.org/10.1016/j.resp.2013.01.013

Rossi, A., Pizzo, P., & Filadi, R. (2019). Calcium, mitochondria and cell metabolism: A functional triangle in bioenergetics. *Biochim Biophys Acta Mol Cell Res*, *1866*(7), 1068-1078. https://doi.org/10.1016/j.bbamcr.2018.10.016

Rostovtseva, T. K., & Bezrukov, S. M. (2008). VDAC regulation: role of cytosolic proteins and mitochondrial lipids. *J Bioenerg Biomembr*, *40*(3), 163-170. https://doi.org/10.1007/s10863-008-9145-y

Rostovtseva, T. K., Sheldon, K. L., Hassanzadeh, E., Monge, C., Saks, V., Bezrukov, S. M., & Sackett, D. L. (2008). Tubulin binding blocks mitochondrial voltage-dependent anion channel and regulates respiration. *Proc Natl Acad Sci U S A*, *105*(48), 18746-18751. https://doi.org/10.1073/pnas.0806303105

Rueda, C. B., Llorente-Folch, I., Traba, J., Amigo, I., Gonzalez-Sanchez, P., Contreras, L., Juaristi, I., Martinez-Valero, P., Pardo, B., Del Arco, A., & Satrustegui, J. (2016). Glutamate excitotoxicity and Ca2+-regulation of respiration: Role of the Ca2+ activated mitochondrial transporters (CaMCs). *Biochim Biophys Acta*, *1857*(8), 1158-1166. https://doi.org/10.1016/j.bbabio.2016.04.003

Russell, R. R., 3rd, Mrus, J. M., Mommessin, J. I., & Taegtmeyer, H. (1992). Compartmentation of hexokinase in rat heart. A critical factor for tracer kinetic analysis of myocardial glucose metabolism. *J Clin Invest*, *90*(5), 1972-1977. https://doi.org/10.1172/jci116076

Russell, R. R., 3rd, & Taegtmeyer, H. (1991). Pyruvate carboxylation prevents the decline in contractile function of rat hearts oxidizing acetoacetate. *Am J Physiol*, *261*(6 Pt 2), H1756-1762. https://doi.org/10.1152/ajpheart.1991.261.6.H1756

Saddik, M., & Lopaschuk, G. D. (1994). Triacylglycerol turnover in isolated working hearts of acutely diabetic rats. *Can J Physiol Pharmacol*, *72*(10), 1110-1119. https://doi.org/10.1139/y94-157

Sagone, A. L., Jr., Lawrence, T., & Balcerzak, S. P. (1973). Effect of smoking on tissue oxygen supply. *Blood*, *41*(6), 845-851.

Saks, V., Dzeja, P., Schlattner, U., Vendelin, M., Terzic, A., & Wallimann, T. (2006). Cardiac system bioenergetics: metabolic basis of the Frank-Starling law. *J Physiol*, *571*(Pt 2), 253-273. https://doi.org/10.1113/jphysiol.2005.101444

Saks, V., Guzun, R., Timohhina, N., Tepp, K., Varikmaa, M., Monge, C., Beraud, N., Kaambre, T., Kuznetsov, A., Kadaja, L., Eimre, M., & Seppet, E. (2010). Structure-function relationships in feedback regulation of energy fluxes in vivo in health and disease: mitochondrial interactosome. *Biochim Biophys Acta*, *1797*(6-7), 678-697. https://doi.org/10.1016/j.bbabio.2010.01.011

Saks, V., Kaambre, T., Guzun, R., Anmann, T., Sikk, P., Schlattner, U., Wallimann, T., Aliev, M., & Vendelin, M. (2007). The creatine kinase phosphotransfer network: thermodynamic and kinetic considerations, the impact of the mitochondrial outer membrane and modelling approaches. *Subcell Biochem*, *46*, 27-65. https://doi.org/10.1007/978-1-4020-6486-9_3

Saks, V., Kuznetsov, A. V., Gonzalez-Granillo, M., Tepp, K., Timohhina, N., Karu-Varikmaa, M., Kaambre, T., Dos Santos, P., Boucher, F., & Guzun, R. (2012). Intracellular Energetic Units regulate metabolism in cardiac cells. *J Mol Cell Cardiol*, *52*(2), 419-436. https://doi.org/10.1016/j.yjmcc.2011.07.015

Saks, V. A., Belikova, Y. O., & Kuznetsov, A. V. (1991). In vivo regulation of mitochondrial respiration in cardiomyocytes: specific restrictions for intracellular diffusion of ADP. *Biochim Biophys Acta*, *1074*(2), 302-311. https://doi.org/10.1016/0304-4165(91)90168-g

Saks, V. A., Belikova, Y. O., Kuznetsov, A. V., Khuchua, Z. A., Branishte, T. H., Semenovsky, M. L., & Naumov, V. G. (1991). Phosphocreatine pathway for energy transport: ADP diffusion and cardiomyopathy. *Am J Physiol*, *261*(4 Suppl), 30-38. https://doi.org/10.1152/ajplung.1991.261.4.L30

Saks, V. A., Kaambre, T., Sikk, P., Eimre, M., Orlova, E., Paju, K., Piirsoo, A., Appaix, F., Kay, L., Regitz-Zagrosek, V., Fleck, E., & Seppet, E. (2001). Intracellular energetic units in red muscle cells. *Biochem J*, *356*(Pt 2), 643-657. https://doi.org/10.1042/0264-6021:3560643

Saks, V. A., Kongas, O., Vendelin, M., & Kay, L. (2000). Role of the creatine/phosphocreatine system in the regulation of mitochondrial respiration. *Acta Physiol Scand*, *168*(4), 635-641. https://doi.org/10.1046/j.1365-201x.2000.00715.x

Saks, V. A., Veksler, V. I., Kuznetsov, A. V., Kay, L., Sikk, P., Tiivel, T., Tranqui, L., Olivares, J., Winkler, K., Wiedemann, F., & Kunz, W. S. (1998). Permeabilized cell and skinned fiber techniques in studies of mitochondrial function in vivo. *Mol Cell Biochem*, *184*(1-2), 81-100.

Samara, A., Rahn, R., Neyman, O., Park, K. Y., Samara, A., Marshall, B., Dougherty, J., & Hershey, T. (2019). Developmental hypomyelination in Wolfram syndrome: new insights from neuroimaging and gene expression analyses. *Orphanet J Rare Dis*, *14*(1), 279. https://doi.org/10.1186/s13023-019-1260-9

Samet, J. M. (2013). Tobacco smoking: the leading cause of preventable disease worldwide. *Thorac Surg Clin*, *23*(2), 103-112. https://doi.org/10.1016/j.thorsurg.2013.01.009

Sandhu, M. S., Weedon, M. N., Fawcett, K. A., Wasson, J., Debenham, S. L., Daly, A., Lango, H., Frayling, T. M., Neumann, R. J., Sherva, R., Blech, I., Pharoah, P. D., Palmer, C. N., Kimber, C., Tavendale, R., Morris, A. D., McCarthy, M. I., Walker, M., Hitman, G., . . . Barroso, I. (2007). Common variants in WFS1 confer risk of type 2 diabetes. *Nat Genet*, *39*(8), 951-953. https://doi.org/10.1038/ng2067

Saran, S., Philip, R., Patidar, P., Gutch, M., Agroiya, P., Agarwal, P., & Gupta, K. (2012). Atypical presentations of Wolframs syndrome. *Indian J Endocrinol Metab*, *16*(Suppl 2), S504-505. https://doi.org/10.4103/2230-8210.104148

Sasco, A. J., Secretan, M. B., & Straif, K. (2004). Tobacco smoking and cancer: a brief review of recent epidemiological evidence. *Lung Cancer*, *45 Suppl 2*, S3-9. https://doi.org/10.1016/j.lungcan.2004.07.998

Schaffer, J. E. (2003). Lipotoxicity: when tissues overeat. *Curr Opin Lipidol*, *14*(3), 281-287. https://doi.org/10.1097/00041433-200306000-00008

Schagger, H., de Coo, R., Bauer, M. F., Hofmann, S., Godinot, C., & Brandt, U. (2004). Significance of respirasomes for the assembly/stability of human respiratory chain complex I. *J Biol Chem*, *279*(35), 36349-36353. https://doi.org/10.1074/jbc.M404033200

Schagger, H., & Pfeiffer, K. (2000). Supercomplexes in the respiratory chains of yeast and mammalian mitochondria. *Embo j*, *19*(8), 1777-1783. https://doi.org/10.1093/emboj/19.8.1777

Schagger, H., & Pfeiffer, K. (2001). The ratio of oxidative phosphorylation complexes I-V in bovine heart mitochondria and the composition of respiratory chain supercomplexes. *J Biol Chem*, *276*(41), 37861-37867. https://doi.org/10.1074/jbc.M106474200

Schlattner, U., Klaus, A., Ramirez Rios, S., Guzun, R., Kay, L., & Tokarska-Schlattner, M. (2016). Cellular compartmentation of energy metabolism: creatine kinase microcompartments and recruitment of B-type creatine kinase to specific subcellular sites. *Amino Acids*, *48*(8), 1751-1774. https://doi.org/10.1007/s00726-016-2267-3

Schlattner, U., Tokarska-Schlattner, M., & Wallimann, T. (2006). Mitochondrial creatine kinase in human health and disease. *Biochim Biophys Acta*, *1762*(2), 164-180. https://doi.org/10.1016/j.bbadis.2005.09.004

Schmitz-Peiffer, C. (2000). Signalling aspects of insulin resistance in skeletal muscle: mechanisms induced by lipid oversupply. *Cell Signal*, *12*(9-10), 583-594. https://doi.org/10.1016/s0898-6568(00)00110-8

Schneider, H., Lemasters, J. J., & Hackenbrock, C. R. (1982). Lateral diffusion of ubiquinone during electron transfer in phospholipid- and ubiquinone-enriched mitochondrial membranes. *J Biol Chem*, *257*(18), 10789-10793.

Schuitemaker, G. E., Dinant, G. J., van der Pol, G. A., & van Wersch, J. W. (2002). Relationship between smoking habits and low-density lipoprotein-cholesterol, high-density lipoprotein-cholesterol, and triglycerides in a hypercholesterolemic adult cohort, in relation to gender and age. *Clin Exp Med*, *2*(2), 83-88. https://doi.org/10.1007/s102380200011

Selivanov, V. A., Alekseev, A. E., Hodgson, D. M., Dzeja, P. P., & Terzic, A. (2004). Nucleotide-gated KATP channels integrated with creatine and adenylate kinases: amplification, tuning and sensing of energetic signals in the compartmentalized cellular environment. *Mol Cell Biochem*, *256-257*(1-2), 243-256. https://doi.org/10.1023/b:mcbi.0000009872.35940.7d

Seppet, E. K., Eimre, M., Anmann, T., Seppet, E., Peet, N., Kaambre, T., Paju, K., Piirsoo, A., Kuznetsov, A. V., Vendelin, M., Gellerich, F. N., Zierz, S., & Saks, V. A. (2005). Intracellular energetic units in healthy and diseased hearts. *Exp Clin Cardiol*, *10*(3), 173-183.

Sharma, N., Okere, I. C., Brunengraber, D. Z., McElfresh, T. A., King, K. L., Sterk, J. P., Huang, H., Chandler, M. P., & Stanley, W. C. (2005). Regulation of pyruvate dehydrogenase activity and citric acid cycle intermediates during high cardiac power generation. *J Physiol*, *562*(Pt 2), 593-603. https://doi.org/10.1113/jphysiol.2004.075713

Sharma, S., Adrogue, J. V., Golfman, L., Uray, I., Lemm, J., Youker, K., Noon, G. P., Frazier, O. H., & Taegtmeyer, H. (2004). Intramyocardial lipid accumulation in the failing human heart resembles the lipotoxic rat heart. *Faseb j*, *18*(14), 1692-1700. https://doi.org/10.1096/fj.04-2263com

Shi, A., Hillege, M. M. G., Wust, R. C. I., Wu, G., & Jaspers, R. T. (2021). Synergistic short-term and long-term effects of TGF-beta1 and 3 on collagen production in differentiating myoblasts. *Biochem Biophys Res Commun*, *547*, 176-182. https://doi.org/10.1016/j.bbrc.2021.02.007

Shinzawa-Itoh, K., Shimomura, H., Yanagisawa, S., Shimada, S., Takahashi, R., Oosaki, M., Ogura, T., & Tsukihara, T. (2016). Purification of Active Respiratory Supercomplex from Bovine Heart Mitochondria Enables Functional Studies. *J Biol Chem*, *291*(8), 4178-4184. https://doi.org/10.1074/jbc.M115.680553

Shoemaker, M. E., Pereira, S. L., Mustad, V. A., Gillen, Z. M., McKay, B. D., Lopez-Pedrosa, J. M., Rueda, R., & Cramer, J. T. (2022). Differences in muscle energy metabolism and metabolic flexibility between sarcopenic and nonsarcopenic older adults. *J Cachexia Sarcopenia Muscle*, *13*(2), 1224-1237. https://doi.org/10.1002/jcsm.12932

Shug, A. L., Shrago, E., Bittar, N., Folts, J. D., & Koke, J. R. (1975). Acyl-CoA inhibition of adenine nucleotide translocation in ischemic myocardium. *Am J Physiol*, *228*(3), 689-692. https://doi.org/10.1152/ajplegacy.1975.228.3.689

Shulman, G. I. (2000). Cellular mechanisms of insulin resistance. *J Clin Invest*, *106*(2), 171-176. https://doi.org/10.1172/jci10583

Sinkler, C. A., Kalpage, H., Shay, J., Lee, I., Malek, M. H., Grossman, L. I., & Huttemann, M. (2017). Tissue- and Condition-Specific Isoforms of Mammalian Cytochrome c Oxidase Subunits: From Function to Human Disease. *Oxid Med Cell Longev*, *2017*, 1534056. https://doi.org/10.1155/2017/1534056

Smith, R. L., Soeters, M. R., Wust, R. C. I., & Houtkooper, R. H. (2018). Metabolic Flexibility as an Adaptation to Energy Resources and Requirements in Health and Disease. *Endocr Rev*, *39*(4), 489-517. https://doi.org/10.1210/er.2017-00211

Soga, T., Baran, R., Suematsu, M., Ueno, Y., Ikeda, S., Sakurakawa, T., Kakazu, Y., Ishikawa, T., Robert, M., Nishioka, T., & Tomita, M. (2006). Differential metabolomics reveals ophthalmic acid as an oxidative stress biomarker indicating hepatic glutathione consumption. *J Biol Chem*, *281*(24), 16768-16776. https://doi.org/10.1074/jbc.M601876200

Sols, A., & Crane, R. K. (1954). Substrate specificity of brain hexokinase. *J Biol Chem*, *210*(2), 581-595.

Sousa, J. S., D'Imprima, E., & Vonck, J. (2018). Mitochondrial Respiratory Chain Complexes. *Subcell Biochem*, *87*, 167-227. https://doi.org/10.1007/978-981-10-7757-9_7

Stanley, W. C., Recchia, F. A., & Lopaschuk, G. D. (2005). Myocardial substrate metabolism in the normal and failing heart. *Physiol Rev*, *85*(3), 1093-1129. https://doi.org/10.1152/physrev.00006.2004

Stincone, A., Prigione, A., Cramer, T., Wamelink, M. M., Campbell, K., Cheung, E., Olin-Sandoval, V., Gruning, N. M., Kruger, A., Tauqeer Alam, M., Keller, M. A., Breitenbach, M., Brindle, K. M., Rabinowitz, J. D., & Ralser, M. (2015). The return of metabolism: biochemistry and physiology of the pentose phosphate pathway. *Biol Rev Camb Philos Soc*, *90*(3), 927-963. https://doi.org/10.1111/brv.12140

Stroh, A., Anderka, O., Pfeiffer, K., Yagi, T., Finel, M., Ludwig, B., & Schagger, H. (2004). Assembly of respiratory complexes I, III, and IV into NADH oxidase supercomplex stabilizes complex I in Paracoccus denitrificans. *J Biol Chem*, *279*(6), 5000-5007. https://doi.org/10.1074/jbc.M309505200

Strom, T. M., Hortnagel, K., Hofmann, S., Gekeler, F., Scharfe, C., Rabl, W., Gerbitz, K. D., & Meitinger, T. (1998). Diabetes insipidus, diabetes mellitus, optic atrophy and deafness (DIDMOAD) caused by mutations in a novel gene (wolframin) coding for a predicted transmembrane protein. *Hum Mol Genet*, *7*(13), 2021-2028. https://doi.org/10.1093/hmg/7.13.2021

Swain, J. L., Sabina, R. L., Peyton, R. B., Jones, R. N., Wechsler, A. S., & Holmes, E. W. (1982). Derangements in myocardial purine and pyrimidine nucleotide metabolism in patients with coronary artery disease and left ventricular hypertrophy. *Proc Natl Acad Sci U S A*, *79*(2), 655-659. https://doi.org/10.1073/pnas.79.2.655

Swift, R. G., Polymeropoulos, M. H., Torres, R., & Swift, M. (1998). Predisposition of Wolfram syndrome heterozygotes to psychiatric illness. *Mol Psychiatry*, *3*(1), 86-91. https://doi.org/10.1038/sj.mp.4000344

Taegtmeyer, H., Peterson, M. B., Ragavan, V. V., Ferguson, A. G., & Lesch, M. (1977). De novo alanine synthesis in isolated oxygen-deprived rabbit myocardium. *J Biol Chem*, *252*(14), 5010-5018.

Taegtmeyer, H., Roberts, A. F., & Raine, A. E. (1985). Energy metabolism in reperfused heart muscle: metabolic correlates to return of function. *J Am Coll Cardiol*, *6*(4), 864-870. https://doi.org/10.1016/s0735-1097(85)80496-4

Tait, S. W., & Green, D. R. (2012). Mitochondria and cell signalling. *J Cell Sci*, *125*(Pt 4), 807-815. https://doi.org/10.1242/jcs.099234

Takeda, Y., Harada, Y., Yoshikawa, T., & Dai, P. (2023). Mitochondrial Energy Metabolism in the Regulation of Thermogenic Brown Fats and Human Metabolic Diseases. *Int J Mol Sci*, *24*(2). https://doi.org/10.3390/ijms24021352

Tanimura, A., Horiguchi, T., Miyoshi, K., Hagita, H., & Noma, T. (2014). Differential expression of adenine nucleotide converting enzymes in mitochondrial intermembrane space: a potential role of adenylate kinase isozyme 2 in neutrophil differentiation. *PLoS One*, *9*(2), e89916. https://doi.org/10.1371/journal.pone.0089916

Tanizawa, Y., Inoue, H., & Oka, Y. (2000). [Positional cloning of the gene(WFS1) for Wolfram syndrome]. *Rinsho Byori*, *48*(10), 941-947.

Tepp, K., Aid-Vanakova, J., Puurand, M., Timohhina, N., Reinsalu, L., Tein, K., Plaas, M., Shevchuk, I., Terasmaa, A., & Kaambre, T. (2022). Wolframin deficiency is accompanied with metabolic inflexibility in rat striated muscles. *Biochem Biophys Rep*, *30*, 101250. https://doi.org/10.1016/j.bbrep.2022.101250

Tepp, K., Puurand, M., Timohhina, N., Adamson, J., Klepinin, A., Truu, L., Shevchuk, I., Chekulayev, V., & Kaambre, T. (2017). Changes in the mitochondrial function and in the efficiency of energy transfer pathways during cardiomyocyte aging. *Mol Cell Biochem*, *432*(1-2), 141-158. https://doi.org/10.1007/s11010-017-3005-1

Tepp, K., Shevchuk, I., Chekulayev, V., Timohhina, N., Kuznetsov, A. V., Guzun, R., Saks, V., & Kaambre, T. (2011). High efficiency of energy flux controls within mitochondrial interactosome in cardiac intracellular energetic units. *Biochim Biophys Acta*, *1807*(12), 1549-1561. https://doi.org/10.1016/j.bbabio.2011.08.005

Tepp, K., Timohhina, N., Puurand, M., Klepinin, A., Chekulayev, V., Shevchuk, I., & Kaambre, T. (2016). Bioenergetics of the aging heart and skeletal muscles: Modern concepts and controversies. *Ageing Res Rev*, *28*, 1-14. https://doi.org/10.1016/j.arr.2016.04.001

Timohhina, N., Guzun, R., Tepp, K., Monge, C., Varikmaa, M., Vija, H., Sikk, P., Kaambre, T., Sackett, D., & Saks, V. (2009). Direct measurement of energy fluxes from mitochondria into cytoplasm in permeabilized cardiac cells in situ: some evidence for Mitochondrial Interactosome. *J Bioenerg Biomembr*, *41*(3), 259-275. https://doi.org/10.1007/s10863-009-9224-8

Tran, K., Loiselle, D. S., & Crampin, E. J. (2015). Regulation of cardiac cellular bioenergetics: mechanisms and consequences. *Physiol Rep*, *3*(7). https://doi.org/10.14814/phy2.12464

Tsushima, K., Bugger, H., Wende, A. R., Soto, J., Jenson, G. A., Tor, A. R., McGlauflin, R., Kenny, H. C., Zhang, Y., Souvenir, R., Hu, X. X., Sloan, C. L., Pereira, R. O., Lira, V. A., Spitzer, K. W., Sharp, T. L., Shoghi, K. I., Sparagna, G. C., Rog-Zielinska, E. A., . . . Abel, E. D. (2018). Mitochondrial Reactive Oxygen Species in Lipotoxic Hearts Induce Post- Translational Modifications of AKAP121, DRP1, and OPA1 That Promote Mitochondrial Fission. *Circ Res*, *122*(1), 58-73. https://doi.org/10.1161/circresaha.117.311307

Tulen, C. B. M., Wang, Y., Beentjes, D., Jessen, P. J. J., Ninaber, D. K., Reynaert, N. L., van Schooten, F. J., Opperhuizen, A., Hiemstra, P. S., & Remels, A. H. V. (2022). Dysregulated mitochondrial metabolism upon cigarette smoke exposure in various human bronchial epithelial cell models. *Dis Model Mech*, *15*(3). https://doi.org/10.1242/dmm.049247

Turrens, J. F. (2003). Mitochondrial formation of reactive oxygen species. *J Physiol*, *552*(Pt 2), 335-344. https://doi.org/10.1113/jphysiol.2003.049478

Ueda, K., Sakai, C., Ishida, T., Morita, K., Kobayashi, Y., Horikoshi, Y., Baba, A., Okazaki, Y., Yoshizumi, M., Tashiro, S., & Ishida, M. (2023). Cigarette smoke induces mitochondrial DNA damage and activates cGAS-STING pathway: application to a biomarker for atherosclerosis. *Clin Sci (Lond)*, *137*(2), 163-180. https://doi.org/10.1042/cs20220525

Unger, R. H. (2005). Longevity, lipotoxicity and leptin: the adipocyte defense against feasting and famine. *Biochimie*, *87*(1), 57-64. https://doi.org/10.1016/j.biochi.2004.11.014

Unger, R. H., & Orci, L. (2001). Diseases of liporegulation: new perspective on obesity and related disorders. *Faseb j*, *15*(2), 312-321. https://doi.org/10.1096/fj.00-0590

Urano, F. (2016). Wolfram Syndrome: Diagnosis, Management, and Treatment. *Curr Diab Rep*, *16*(1), 6. https://doi.org/10.1007/s11892-015-0702-6

van der Vusse, G. J., van Bilsen, M., & Glatz, J. F. (2000). Cardiac fatty acid uptake and transport in health and disease. *Cardiovasc Res*, *45*(2), 279-293. https://doi.org/10.1016/s0008-6363(99)00263-1

van Loon, A. P., Brandli, A. W., Pesold-Hurt, B., Blank, D., & Schatz, G. (1987). Transport of proteins to the mitochondrial intermembrane space: the 'matrix-targeting' and the 'sorting' domains in the cytochrome c1 presequence. *Embo j*, *6*(8), 2433-2439. https://doi.org/10.1002/j.1460-2075.1987.tb02522.x

van Schaftingen, E., & Gerin, I. (2002). The glucose-6-phosphatase system. *Biochem J*, *362*(Pt 3), 513-532. https://doi.org/10.1042/0264-6021:3620513

Varikmaa, M., Bagur, R., Kaambre, T., Grichine, A., Timohhina, N., Tepp, K., Shevchuk, I., Chekulayev, V., Metsis, M., Boucher, F., Saks, V., Kuznetsov, A. V., & Guzun, R. (2014). Role of mitochondria-cytoskeleton interactions in respiration regulation and mitochondrial organization in striated muscles. *Biochim Biophys Acta*, *1837*(2), 232-245. https://doi.org/10.1016/j.bbabio.2013.10.011

Vendelin, M., Beraud, N., Guerrero, K., Andrienko, T., Kuznetsov, A. V., Olivares, J., Kay, L., & Saks, V. A. (2005). Mitochondrial regular arrangement in muscle cells: a "crystal-like" pattern. *Am J Physiol Cell Physiol*, *288*(3), C757-767. https://doi.org/10.1152/ajpcell.00281.2004

Vercellino, I., & Sazanov, L. A. (2022). The assembly, regulation and function of the mitochondrial respiratory chain. *Nat Rev Mol Cell Biol*, *23*(2), 141-161. https://doi.org/10.1038/s41580-021-00415-0

Vettor, R., Fabris, R., Serra, R., Lombardi, A. M., Tonello, C., Granzotto, M., Marzolo, M. O., Carruba, M. O., Ricquier, D., Federspil, G., & Nisoli, E. (2002). Changes in FAT/CD36, UCP2, UCP3 and GLUT4 gene expression during lipid infusion in rat skeletal and heart muscle. *Int J Obes Relat Metab Disord*, *26*(6), 838-847. https://doi.org/10.1038/sj.ijo.0802005

Wald, N. J., Idle, M., Boreham, J., & Bailey, A. (1981). Carbon monoxide in breath in relation to smoking and carboxyhaemoglobin levels. *Thorax*, *36*(5), 366-369. https://doi.org/10.1136/thx.36.5.366

Walker, J. E. (2013). The ATP synthase: the understood, the uncertain and the unknown. *Biochem Soc Trans*, *41*(1), 1-16. https://doi.org/10.1042/bst20110773

Wall, S. R., & Lopaschuk, G. D. (1989). Glucose oxidation rates in fatty acid-perfused isolated working hearts from diabetic rats. *Biochim Biophys Acta*, *1006*(1), 97-103. https://doi.org/10.1016/0005-2760(89)90328-7

Wallimann, T., & Hemmer, W. (1994). Creatine kinase in non-muscle tissues and cells. *Mol Cell Biochem*, *133-134*, 193-220. https://doi.org/10.1007/bf01267955

Wallimann, T., Tokarska-Schlattner, M., & Schlattner, U. (2011). The creatine kinase system and pleiotropic effects of creatine. *Amino Acids*, *40*(5), 1271-1296. https://doi.org/10.1007/s00726-011-0877-3

Wallimann, T., Wyss, M., Brdiczka, D., Nicolay, K., & Eppenberger, H. M. (1992). Intracellular compartmentation, structure and function of creatine kinase isoenzymes in tissues with high and fluctuating energy demands: the 'phosphocreatine circuit' for cellular energy homeostasis. *Biochem J*, *281 (Pt 1)*, 21-40. https://doi.org/10.1042/bj2810021

Wang, C., Liu, C., Shi, J., Li, H., Jiang, S., Zhao, P., Zhang, M., Du, G., Fu, S., Li, S., Wang, Z., Wang, X., Gao, F., Sun, P., & Tian, J. (2023). Nicotine exacerbates endothelial dysfunction and drives atherosclerosis via extracellular vesicle-miRNA. *Cardiovasc Res*, *119*(3), 729-742. https://doi.org/10.1093/cvr/cvac140

Weber, A., Klocker, H., Oberacher, H., Gnaiger, E., Neuwirt, H., Sampson, N., & Eder, I. E. (2018). Succinate Accumulation Is Associated with a Shift of Mitochondrial Respiratory Control and HIF-1alpha Upregulation in PTEN Negative Prostate Cancer Cells. *Int J Mol Sci*, *19*(7). https://doi.org/10.3390/ijms19072129

Wheeldon, I., Minteer, S. D., Banta, S., Barton, S. C., Atanassov, P., & Sigman, M. (2016). Substrate channelling as an approach to cascade reactions. *Nat Chem*, *8*(4), 299-309. https://doi.org/10.1038/nchem.2459

Whitehead, A. K., Erwin, A. P., & Yue, X. (2021). Nicotine and vascular dysfunction. *Acta Physiol (Oxf)*, *231*(4), e13631. https://doi.org/10.1111/apha.13631

Wiesner, R. J., Hornung, T. V., Garman, J. D., Clayton, D. A., O'Gorman, E., & Wallimann, T. (1999). Stimulation of mitochondrial gene expression and proliferation of mitochondria following impairment of cellular energy transfer by inhibition of the phosphocreatine circuit in rat hearts. *J Bioenerg Biomembr*, *31*(6), 559-567. https://doi.org/10.1023/a:1005417011436

Wilson, J. E. (1995). Hexokinases. *Rev Physiol Biochem Pharmacol*, *126*, 65-198. https://doi.org/10.1007/BFb0049776

Wilson, J. E. (2003). Isozymes of mammalian hexokinase: structure, subcellular localization and metabolic function. *J Exp Biol*, *206*(Pt 12), 2049-2057. https://doi.org/10.1242/jeb.00241

Wirth, C., Brandt, U., Hunte, C., & Zickermann, V. (2016). Structure and function of mitochondrial complex I. *Biochim Biophys Acta*, *1857*(7), 902-914. https://doi.org/10.1016/j.bbabio.2016.02.013

Wisneski, J. A., Gertz, E. W., Neese, R. A., Gruenke, L. D., & Craig, J. C. (1985). Dual carbon-labeled isotope experiments using D-[6-14C] glucose and L-[1,2,3-13C3] lactate: a new approach for investigating human myocardial metabolism during ischemia. *J Am Coll Cardiol*, *5*(5), 1138-1146. https://doi.org/10.1016/s0735-1097(85)80016-4

Wisneski, J. A., Gertz, E. W., Neese, R. A., Gruenke, L. D., Morris, D. L., & Craig, J. C. (1985). Metabolic fate of extracted glucose in normal human myocardium. *J Clin Invest*, *76*(5), 1819-1827. https://doi.org/10.1172/jci112174

Woldegiorgis, G., Yousufzai, S. Y., & Shrago, E. (1982). Studies on the interaction of palmitoyl coenzyme A with the adenine nucleotide translocase. *J Biol Chem*, *257*(24), 14783-14787.

Wong, J. F., Simmons, C. A., & Young, E. W. K. (2017). Chapter 3 - Modeling and Measurement of Biomolecular Transport and Sensing in Microfluidic Cell Culture and Analysis Systems. In S. M. Becker (Ed.), *Modeling of Microscale Transport in Biological Processes* (pp. 41-75). Academic Press. https://doi.org/https://doi.org/10.1016/B978-0-12-804595-4.00003-1

Wu, R., Smeele, K. M., Wyatt, E., Ichikawa, Y., Eerbeek, O., Sun, L., Chawla, K., Hollmann, M. W., Nagpal, V., Heikkinen, S., Laakso, M., Jujo, K., Wasserstrom, J. A., Zuurbier, C. J., & Ardehali, H. (2011). Reduction in hexokinase II levels results in decreased cardiac function and altered remodeling after ischemia/reperfusion injury. *Circ Res*, *108*(1), 60-69. https://doi.org/10.1161/circresaha.110.223115

Xuan, L., Han, F., Gong, L., Lv, Y., Wan, Z., Liu, H., Zhang, D., Jia, Y., Yang, S., Ren, L., & Liu, L. (2018). Association between chronic obstructive pulmonary disease and serum lipid levels: a meta-analysis. *Lipids Health Dis*, *17*(1), 263. https://doi.org/10.1186/s12944-018-0904-4

Yaku, K., Okabe, K., & Nakagawa, T. (2018). NAD metabolism: Implications in aging and longevity. *Ageing Res Rev*, *47*, 1-17. https://doi.org/10.1016/j.arr.2018.05.006

Yapa, N. M. B., Lisnyak, V., Reljic, B., & Ryan, M. T. (2021). Mitochondrial dynamics in health and disease. *FEBS Lett*, *595*(8), 1184-1204. https://doi.org/10.1002/1873-3468.14077

Yiew, N. K. H., & Finck, B. N. (2022). The mitochondrial pyruvate carrier at the crossroads of intermediary metabolism. *Am J Physiol Endocrinol Metab*, *323*(1), E33-e52. https://doi.org/10.1152/ajpendo.00074.2022

Yki-Jarvinen, H., Virkamaki, A., Daniels, M. C., McClain, D., & Gottschalk, W. K. (1998). Insulin and glucosamine infusions increase O-linked N-acetyl-glucosamine in skeletal muscle proteins in vivo. *Metabolism*, *47*(4), 449-455. https://doi.org/10.1016/s0026-0495(98)90058-0

Young, M. E., McNulty, P., & Taegtmeyer, H. (2002). Adaptation and maladaptation of the heart in diabetes: Part II: potential mechanisms. *Circulation*, *105*(15), 1861-1870. https://doi.org/10.1161/01.cir.0000012467.61045.87

Yuan, F., Li, Y., Hu, R., Gong, M., Chai, M., Ma, X., Cha, J., Guo, P., Yang, K., Li, M., Xu, M., Ma, Q., Su, Q., Zhang, C., Sheng, Z., Wu, H., Wang, Y., Yuan, W., Bian, S., . . . Li, W. (2023). Modeling disrupted synapse formation in wolfram syndrome using hESCs- derived neural cells and cerebral organoids identifies Riluzole as a therapeutic molecule. *Mol Psychiatry*, *28*(4), 1557-1570. https://doi.org/10.1038/s41380-023-01987-3

Zala, D., Schlattner, U., Desvignes, T., Bobe, J., Roux, A., Chavrier, P., & Boissan, M. (2017). The advantage of channeling nucleotides for very processive functions. *F1000Res*, *6*, 724. https://doi.org/10.12688/f1000research.11561.2

Acknowledgements

This thesis was realised at the National Institute of Chemical Physics and Biophysics in the Laboratory of Chemical Biology, Tallinn, Estonia, and at the Department of Human Movement Sciences, Vrije University, Amsterdam, Netherlands, with the support of the Dora Plus scholarship. It would not have been possible without the collective brilliance and kindness of many remarkable people with whom I had the fortune to work.

First and foremost, I extend my heartfelt gratitude to my supervisors, Tuuli Käämbre, Kersti Tepp, and Marju Puurand. Your meticulous guidance and steadfast support have been crucial in shaping my professional path and this thesis. Thank you for your enduring patience and belief in my abilities.

A special thank you to Rob Wust, Natalja Timohhina, and Vladimir Chekulayev, who were not only exceptional mentors but also became dear friends, generously sharing your wisdom and support. Your endless well of knowledge and friendship have enriched my experience immeasurably.

To my lab-mates in Tallinn and Amsterdam – Igor Shevchuk, Anton Terasmaa, Ljudmila Klepinina, Aleksandr Klepinin, Indrek Reile, Rutt Taba, Wendy Noort, Gerard M.J. de Wit, Moritz Eggelbusch, and Richie Goulding – thank you for the warm and welcoming atmosphere, for sharing your methods and insights, and for the friendships that I treasure. You made our labs feel like a second home. I look forward to our paths crossing again, both in science and life.

Special thanks to Hans Degens and Ghislaine Gayan-Ramirez for your insightful comments in preparing our manuscript regarding smoking and smoking cessation. Your expertise helped immensely in refining our work.

Additionally, I want to thank my first supervisor, Koit Reimand, who shared his extensive knowledge and inspired me to continue this challenging journey in research.

Lastly, I must express my deepest gratitude to my mom and my sister Tamara, whose love and support have been my foundation throughout everything and to my two beautiful daughters, Sofia and Vasilisa. You have inspired and motivated me every step of the way as I pursued this doctoral degree. I also want to thank my dearest ex-husband, Kirill, who supported me all these years, no matter the cost.

Thank you all for your large and small contributions to this significant chapter of my life.

Abstract

Influence of Intrinsic and Extrinsic Factors on Mitochondrial Bioenergetics in the Heart

Both intrinsic factors, such as genetic mutations, and extrinsic factors, including lifestyle habits like smoking, play pivotal roles in modulating mitochondrial bioenergetics and subsequent cardiac outcomes.

This study aims to extensively investigate the influence of intrinsic and extrinsic factors on mitochondrial bioenergetics and inherent cardioprotective mechanisms in cardiac muscle tissue. Various methodologies were employed, including high-resolution respirometry, enzymatic activity assays, metabolomic profiling with NMR and UPLC-MS, protein content assessment with Western blot and blue native gel electrophoresis, and morphological assessments by histochemistry and immunohistochemistry. These approaches were used to unravel the complex interplay between mitochondrial function and cardiovascular health.

Wolframin-deficient animal models were employed to investigate the effects of intrinsic factors, specifically genetic mutations, on mitochondrial bioenergetics. Results demonstrated that WFS1 deficiency alters the regulation of the outer mitochondrial membrane, impacts glutamate metabolism pathways, and limits substrate utilisation flexibility. Compensatory mechanisms were observed through the activation of adenylate kinase and hexokinase pathways to mitigate alterations in the creatine kinase pathway.

A mouse model of chronic obstructive pulmonary disease (COPD) exposed to cigarette smoke, followed by a period of smoking cessation, was used to investigate the effects of cigarette smoking and subsequent smoking cessation on mitochondrial bioenergetics, metabolism, and structural integrity in cardiac tissue. Findings revealed that cigarette smoking led to a transient decrease in oxidative phosphorylation capacity and uncoupling respiration in cardiac tissue, which was restored to control levels following smoking cessation. Smoking reduced mitochondrial respiratory chain complexes I and IV levels and disrupted supercomplex (SC) formation. These effects were reversed after smoking cessation, indicating potential recovery of mitochondrial protein content and SC formation. The balance between disassembly and reassembly of SCs contributed to improved mitochondrial respiration post-smoking cessation. Despite the recovery, succinate dehydrogenase activity remained decreased, suggesting a prolonged impact on this aspect of mitochondrial function. Significant changes in metabolic and lipidomic pathways, along with increased GLUT4 transfer to the plasma membrane, indicated a shift in metabolic substrate preference from fatty acid oxidation to glucose oxidation following smoking cessation. Additionally, changes in collagen content, capillary density, cardiac nuclear density, and macrophage infiltration associated with smoking and smoking cessation were identified, indicating potential remodelling processes in response to these conditions.

Impaired substrate utilisation and a shift from fatty acid oxidation to glycolysis emerged as a common feature in both WFS1 deficiency and smoking- and smoking cessation-induced cardiac alterations. However, this shift from fatty acid oxidation to glycolysis may play a potential role in cardioprotection.

Lühikokkuvõte

Sisemiste ja väliste tegurite mõju südamelihase mitokondriaalsele bioenergeetikale

Nii sisemised tegurid, näiteks geneetilised mutatsioonid, kui ka välised tegurid, sealhulgas elustiil ja harjumused nagu suitsetamine, mängivad olulist rolli mitokondriaalse bioenergeetika ja sellest tulenevate südamefunktsioonide moduleerimisel. Käesoleva teadustöö eesmärk oli põhjalikult uurida sisemiste ja väliste tegurite mõju mitokondri metabolismile ning loomulikele kaitsemehhanismidele südamelihase koes. Uurimistöös kasutati kõrglahutusega respiromeetriat, ensüümaktiivsuste mõõtmist, metaboolset profileerimist NMR ja UPLC-MS abil, valgu sisalduse hindamist Western bloti ja Blue native geel-elektroforeesi abil ning morfoloogilisi hindamist histokeemia ja immunohistokeemia abil. Need lähenemisviisid võimaldasid selgitada südamelihase rakkude mitokondriaalse funktsionaalsuse ja südame tervise vahelisi interaktsioone.

Selleks, et uurida endogeensete tegurite, eelkõige geneetiliste mutatsioonide, mõju mitokondriaalsele energiametabolismile kasutati Wolframiini geeni puudulikkusega loommudeleid. Tulemused näitasid, et WFS1 puudulikkus muudab mitokondri välismembraani regulatsiooni, mõjutab glutamaadi metabolismi ning vähendab substraadi kasutamise paindlikkust. Samal ajal aktiveerusid kompensatsioonimehhanismid adenülaatkinaasi ja heksokinaasi radade näol, et leevendada kreatiinkinaasi raja funktsiooni langust.

Selleks, et uurida kuidas tubaka suitsetamine ja sellele järgnev suitsetamisest loobumine mõjutab mitokondri ainevahetust ja südamekoe struktuuri, kasutati kroonilise obstruktiivse kopsuhaigusega hiiremudelit. Hiiri eksponeeriti sigaretisuitsule, millele järgnes suitsetamisest loobumise periood. Uuringu tulemused näitasid, et sigareti suitsetamine langetas oksüdatiivse fosforüülimise võimekust ja ATP sünteesist lahti sidestatud hapniku tarbimise kiirust südamekoe rakkudes, kuid need taastusid kontrolltasemele pärast suitsetamisest loobumist. Suitsetamine vähendas ka mitokondriaalse hingamisahela komplekside I ja IV suhtelist sisaldust koes, millega mõjutas ka hingamisahela superkompleksi moodustumist. Samas saavutasid need näitajad pärast suitsetamisest loobumist esialgse taseme, viidates et mitokondriaalse valgu sisaldus ja SC moodustumise regulatsioon mitokondri sisemembraanis on võimelised taastuma. Tasakaal superkomplekside pidevas reorganiseerumises parandas mitokondriaalset hapniku tarbimist pärast suitsetamisest loobumist. Vaatamata eelnevale jäi suktsinaadi dehüdrogenaasi aktiivsus madalamaks, mis näitab, et muutused selle ensüümi aktiivsuses mõjutavad mitokondri ainevahetust pikema aja jooksul. Olulised muutused metaboolsetes ja lipiidiega seotud radades, samuti suurenenud GLUT4 transport rakumembraani viitasid nihkele substraadi eelistuses rasvhapete oksüdatsioonilt glükoosi oksüdatsioonile pärast suitsetamisest loobumist. Lisaks tuvastati suitsetamise ja suitsetamisest loobumisega seotud muutused koe kollageeni sisalduses, kapillaaride tiheduses, südameraku tuumade tiheduses ja makrofaagide infiltratsioonis, mis viitavad võimalikele ümberkujundamisprotsessidele vastusena nendele tingimustele.

Häired mitmete substraatide kasutamisel ja energiametabolismi ümberlülitamises rasvhapete oksüdatsioonilt glükolüüsile ilmnesid ühise omadusena südamelihase rakkudes nii WFS1 puudulikkuse kui ka suitsetamise ja suitsetamisest loobumise mõjul.

Samas võib see nihe rasvhapete oksüdatsioonilt glükolüüsile mängida potentsiaalset rolli ka südamelihase adaptatsioonimehhanismides molekulaarsel tasemel.

Kokkuvõtteks, lähtudes selles töös tehtud uuringute tulemustest, saame üksikasjaliku ülevaate sisemiste ja väliste tegurite mõjust mitokondriaalsele bioenergeetikale ning südame-veresoonkonna tervise keerulisele regulatsioonile. Käesolev doktoritöö annab märkimisväärse panuse südame lihaskudet mõjutavate tegurite mõistmisel, millel on oluline sisend südamehaiguste ennetamisel ja ravis. Lisaks rõhutab meie uuring elustiili muutuste tähtsust ning toob esile suitsetamisest loobumise olulisuse südame-veresoonkonna tervise säilitamisel ning mitokondriaalse düsfunktsiooniga seotud südamehaiguste ennetamisel.

Appendix 1

Publication I

Tepp, K., Puurand, M., Timohhina, N., Aid-Vanakova, J., Reile, I., Shevchuk, I., Chekulayev, V., Eimre, M., Peet, N., Kadaja, L., Paju, K., & Kaambre, T. (2020). Adaptation of striated muscles to Wolframin deficiency in mice: Alterations in cellular bioenergetics. Biochim Biophys Acta Gen Subj, 1864(4), 129523. https://doi.org/10.1016/j.bbagen.2020.129523

Adaptation of striated muscles to Wolframin deficiency in mice: Alterations in cellular bioenergetics

Kersti Tepp[a,*], Marju Puurand[a], Natalja Timohhina[a], Jekaterina Aid-Vanakova[a], Indrek Reile[b], Igor Shevchuk[a], Vladimir Chekulayev[a], Margus Eimre[c], Nadežda Peet[c], Lumme Kadaja[c], Kalju Paju[c], Tuuli Käämbre[a]

[a] Laboratory of Chemical Biology, National Institute of Chemical Physics and Biophysics, Akadeemia tee 23, 12618 Tallinn, Estonia
[b] Laboratory of Chemical Physics, National Institute of Chemical Physics and Biophysics, Akadeemia tee 23, 12618 Tallinn, Estonia
[c] Department of Pathophysiology, Institute of Biomedicine and Translational Medicine, University of Tartu, Ravila 19, 50411 Tartu, Estonia

A B S T R A C T

Background: Wolfram syndrome (WS), caused by mutations in WFS1 gene, is a
multi-targeting disease affecting multiple organ systems. Wolframin is localized in the membrane of the endoplasmic reticulum (ER), influencing Ca^{2+} metabolism and ER interaction with mitochondria, but the exact role of the protein remains unclear. In this study we aimed to characterize alterations in energy metabolism in the cardiac and in the oxidative and glycolytic skeletal muscles in Wfs1-deficiency.
Methods: Alterations in the bioenergetic profiles in the cardiac and skeletal muscles of *Wfs1*-knock-out (KO) male mice and their wild type male littermates were determined using high resolution respirometry, quantitative RT-PCR, NMR spectroscopy, and immunofluorescence confocal microscopy.
Results: Oxygen consumption without ATP synthase activation (leak) was significantly higher in the glycolytic muscles of Wfs1 KO mice compared to wild types. ADP-stimulated respiration with glutamate and malate was reduced in the Wfs1-deficient cardiac as well as oxidative and glycolytic skeletal muscles.
Conclusions: Wfs1-deficiency in both cardiac and skeletal muscles results in functional alterations of energy transport from mitochondria to ATP-ases. There was a substrate-dependent decrease in the maximal Complex I –linked respiratory capacity of the electron transport system in muscles of Wfs1 KO mice. Moreover, in cardiac and gastrocnemius white muscles a decrease in the function of one pathway were balanced by the increase in the activity of the parallel pathway.
General significance: This work provides new insights to the muscle involvement at early stages of metabolic syndrome like WS as well as developing glucose intolerance.

1. Introduction

1.1. Wolfram syndrome as a metabolic syndrome simultaneously affecting multiple tissues

Wolfram syndrome (WS) also known as DIDMOAD is an autosomal recessive disorder, caused by mutations in the WFS1 gene which encodes for the protein wolframin [1–3]. It is a multi-targeting disease, having influence on a number of organ systems simultaneously, and causes neuronal degeneration, ataxia and alterations in the performance of cardiac and skeletal muscles [4,5]. The first symptoms of WS are diabetes mellitus (mean age of onset 6 years) and optic atrophy (mean onset at 11 years), followed by diabetes insipidus and deafness. WS is a rare but probably underdiagnosed condition; for example, in a study of 589 diabetic patients in Lebanon 31 new WS cases were found [6].

The Wfs1 gene product wolframin is a transmembrane protein localized in the membrane of the endoplasmic reticulum (ER) [7,8]. The exact cellular role of wolframin is still under debate. Most current studies report that wolframin directly or indirectly regulates Ca^{2+} homeostasis and has an influence on the ER stress response [9–13]. Other studies have additionally demonstrated that wolframin participates in the Mitochondria-Associated ER Membrane (MAM) formation and Ca^{2+} transport between mitochondria and ER [5,14].

It has been suggested that the development of glucose intolerance in Wfs1 KO mice and WS patients is related to the insufficient insulin secretion which, in turn, is caused by the progressive loss of pancreatic β-cells due to alterations in cellular Ca^{2+} signaling [15] and increased ER stress response with the activation of Unfolded Protein Response (UPR) pathways [16–19]. The intracellular mechanisms for progressive loss of the β-cells and neurodegeneration in Wfs1-deficient animals could be similar. A recent study of mitochondrial function of Wfs1-deficient primary rat neuronal cultures revealed that these cells have ER stress, disturbed calcium homeostasis which in turn affects mitochondrial fusion and fission dynamics, decreased mitochondrial membrane potential and cellular ATP content [14]. At the same time, however, the levels of wolframin are high in the cardiac, skeletal

muscles, lungs and brown adipose tissue in WT animals, no UPR alterations have been detected in these tissues of Wfs1-deficient mice [17]. Furthermore, compared to changes in the pancreas and neurons that are apparent relatively early in the disease process, functional alterations in the lung and heart tissue emerge later, if at all in WS patients [20,21]. Therefore, the study of cardiac and skeletal muscles of Wfs1 KO animals could be a valuable model to better understand the function of the wolframin, but also diabetes and metabolic syndrome mechanisms in these tissues as well as clarify why these cells are not affected by Wfs1-deficiency related progressive degradation as it occurs in the pancreatic β-cells and neurons. Currently, the pathways of the differential effects of wolframin deficiency on different organs remain unclear. Studies have demonstrated multiple interacting partners to wolframin and several distinct theories have been proposed about the pathways and timescale of how wolframin deficiency leads to alterations in different organ systems [17,22–25].

Several lines of evidence indicate that WS has common features with mitochondrial diseases. Alterations in mitochondrial DNA (mtDNA) have been found in various tissues, including the skeletal muscles, of several WS patients with conflicting results concerning mitochondrial respiratory system function [26–30]. In addition, silencing of *Wfs1* gene in HEK cells has been shown to cause significant changes in the transcription of several genes related to mitochondrial dysfunction and apoptosis [25]. However, in a study of seven Spanish WS patients no mtDNA abnormalities were found in blood samples [31].

Alterations in skeletal muscle energy metabolism in Wfs1-deficient animals and in WS-patients are poorly described. Human muscles comprise approximately 40% of the body mass. Skeletal muscles contribute significantly to basal energy metabolism and serve as storage for important substrates such as amino acids and carbohydrates. In addition, skeletal muscles are responsible for a great majority of insulin-mediated glucose uptake [32]. During hyperglycemia, muscles are the main tissue responsible for non-insulin mediated glucose uptake. Therefore, disruptions of glucose metabolism, that are associated with WS, could also be present in skeletal muscles.

Recently, there have been some descriptions of heart diseases among WS patients, mostly due to structural alterations [6,33,34]. In a study of Lebanese population, out of the 31 WS patients, 5 cases with cardiac abnormalities were found [6], which is significantly higher than in normal population. At the cellular level, Cagalinec et al. (2019) described altered Ca^{2+} metabolism in the cardiomyocytes of the Wfs1-deficient rats. They found that myocytes of the left ventricle had increased contractility (both amplitude and duration of the contraction) due to the prolonged cytosolic calcium transients. The authors proposed that this is caused by the upregulation of RyR2 receptors which is related to the wolframin deficiency [23]. Furthermore, sinus tachycardia and atrial and ventricular arrhythmias have been reported in some patients in an extensive case study of WS patients [35].

To fully understand the function of wolframin, it is important to clarify the mechanisms of varying offset of the disease in different tissues; describe the alterations in skeletal and cardiac muscles in Wfs1 deficiency and determine the mechanisms by which muscles are less affected compared to pancreatic β-cells and neurons even though Wfs1 gene is highly expressed in the heart. As described above, there is ample evidence that wolframin influences the mitochondrial metabolism either directly or indirectly through altered ER, Ca^{2+} homeostasis and MAM. The study of oxidative and glycolytic muscles in Wfs1 KO mice enables to estimate the extent of the alterations in the bioenergetic profile in muscles with wolframin deficiency.

1.2. Regulation of energy metabolism in muscle tissues

As the energy demand of the oxidative skeletal muscles is permanent but intermittent in intensity, the performance and flexible regulation of energy metabolism is crucial for muscle function. In oxidative skeletal and cardiac muscle cells the oxidative phosphorylation (OXPHOS) in mitochondria is the main energy source. Therefore, alterations in OXPHOS and transport of high-energy compounds to ATPases have a direct influence on the tissue performance. In muscle cells, the phenomenon called "macromolecular crowding", i.e. high concentrations of macromolecules in the cells, results in extensive diffusion restrictions for metabolites [36,37]. Thus, despite the seemingly close proximity of mitochondria and ATPases, specific phosphotransfer networks are needed for the effective energy transfer from the ATP-generating sites (mainly mitochondrial matrix) to the ATP-utilizing locations (cytosol, myofibrils) [38]. A key link in high-energy phosphate transport system is the supercomplex Mitochondrial Interactosome (MI) (Fig. 1) that consists of ATP Synthasome (electron transport system, ATP-synthase and inorganic phosphate carrier), Adenine Nucleotide Translocase (ANT), mitochondrial creatine kinase (MtCK) and mitochondrial voltage dependent anion channel (VDAC) [39,40]. The movement of the adenine nucleotides through outer mitochondrial membrane (OMM) is impeded due to the functional interactions of VDAC with specific proteins including hexokinase (HK), beta-tubulin component of free αβ-tubulin heterodimer and other cytoskeletal components such as plectin [41–44]. However, there are no restrictions for the transfer of creatine (Cr) and phosphocreatine (PCr) through the VDAC, so the cytosolic and mitochondrial creatine kinase (CK) isoforms create an opportunity for facilitated energy transport without ADP and ATP free diffusion into the cytoplasm (Fig. 1). In the adenylate kinase (AK) pathway, the mitochondrial AK2 isoform, present in the inter-membrane space, facilitates both production and export of ATP by mitochondria. In turn, the cytosolic AK1 isoform, through sequential phosphotransfers, is responsible for the transmission of ATP and the maintenance of the ATP/ADP ratio at ATP-utilization sites [38]. Moreover, compartmentalization of high-energy phosphate carriers between cellular micro-compartments ensures more efficient energy transfer compared to ATP/ADP free diffusion in the cytoplasm [45,46]. In the inner mitochondrial membrane (IMM) an electron transport system (ETS), consisting of four complexes, creates the proton gradient to drive ATP synthase. The contribution of each ETS complex to OXPHOS depends on the tissue type; activities of the complexes change during development and aging but alterations in ETS function could be also a sign of disease. For example, in cancer cells there is an increase in Complex II (CII)-linked oxygen consumption rate in comparison with corresponding healthy tissue [47–49].

The role of MI supercomplex together with CK and AK phosphotransfer pathways is to increase the efficiency of the ATP synthesis by the generation of two circuits: (1) transport of the energy to ATPases and (2) quick metabolic feedback signaling (information flux in the form of ADP) back toward mitochondria to fulfill the energy requirement of the cell. Alterations in MI and energy transfer pathways have a direct influence on the muscle performance.

In this study we aimed to assess whether mitochondrial function is impaired in the developing glucose intolerance in Wfs1 KO mice. Using permeabilized muscle fibers, we measured the oxygen consumption rate of ETS with two different protocols, recorded the ADP-dependency of respiration with and without creatine, evaluated the contribution of AK and CK energy transfer pathway, and the role of HK to regulate the cellular respiration. We additionally assessed the levels of metabolites, structural integrity of the cytoskeleton and the location of cytoskeletal proteins relative to mitochondria using ^1H NMR and immunofluorescent confocal microscopy. To our knowledge this is a first study to show functional alterations in intracellular energy transfer networks in the cardiac and skeletal muscles of Wfs1 KO animals.

2. Methods

2.1. Laboratory animals and chemicals

In all experiments the wild type (WT) male mice and their Wfs1-deficient male littermates (age 4–6 months) with 129S6/SvEvTac and
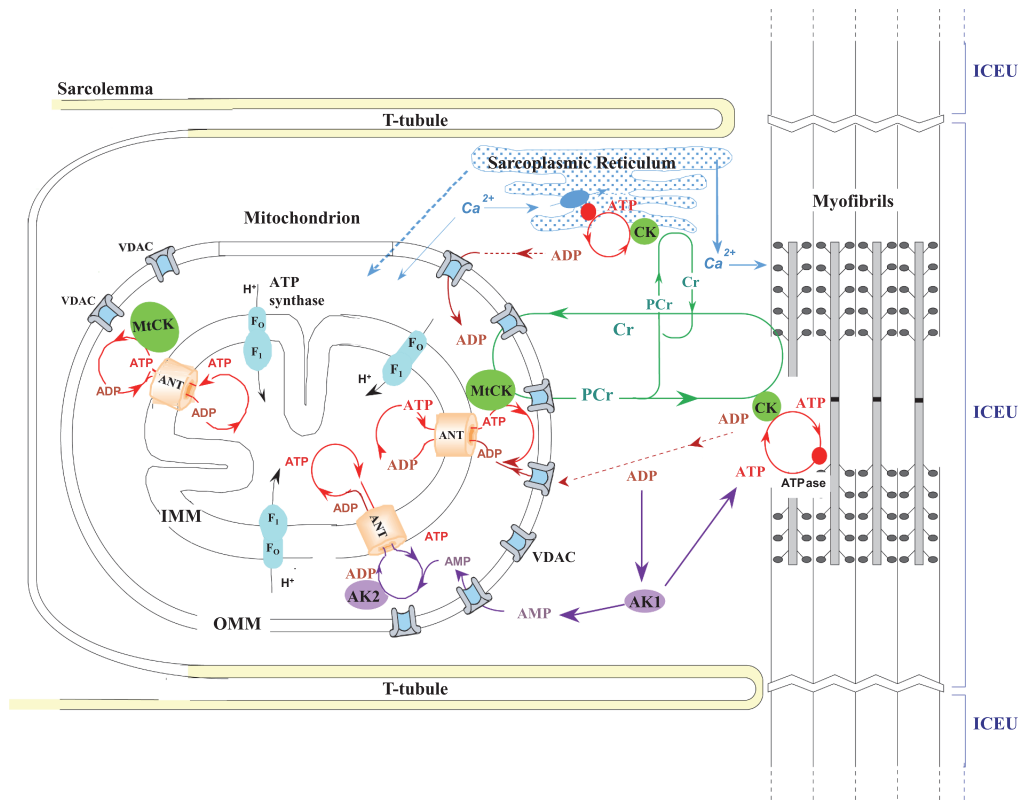
Fig. 1. Regulation of energy metabolism of striated muscle tissues
Oxidative muscle cells are divided into functional sections called Intracellular Energetic Units (ICEU) where mitochondria are in fixed position between the T-tubules in respect of myofibrils. Movement of the adenine nucleotides through outer mitochondrial membrane (OMM) voltage dependent anion channel (VDAC) is impeded due to the functional interactions of VDAC with cytoskeletal protein(s). However, there are no restrictions for movement of creatine (Cr) and phosphocreatine (PCr), so the cytosolic and mitochondrial creatine kinase (CK) isoforms create a circuit for facilitated energy transport without ADP and ATP free diffusion into the cytoplasm. This transport is regulated by supercomplex Mitochondrial Interactosome consisting of ATP Synthase, Adenine Nucleotide Translocase (ANT), mitochondrial CK (MtCK) and VDAC. MtCK transfers phosphate group from ATP to Cr. Produced PCr is moving toward ATPases via CK pathway and ADP is transported directly back to ATP- synthase via ANT. In the adenylate kinase (AK) pathway the mitochondrial AK2 isoform, present in the intermembrane space, facilitates both production and export of ATP by mitochondria. In turn, the cytosolic AK1 isoform, through sequential phosphotransfers, is responsible for the transmission of ATP and maintenance of the ATP/ADP ratio at the ATP-utilization sites. (Modified from [44])

C57BL/6 mixed genetic background were used. Wfs1-deficient mice were generated by replacing most of the coding region of the Wfs1 gene as previously described [50]. Breeding and genotyping of the mice were performed at the Laboratory Animal Centre of the Institute of Biomedicine and Translational Medicine, University of Tartu. The mice were housed under standard laboratory conditions (at constant temperature 22 °C and a 12:12 h light/dark cycle with free access to food and water) in the vivarium of the Department of Chemistry and Biotechnology, Tallinn University of Technology. Animal experiments were approved by the Estonian National Board of Animal Experiments in accordance with the European Communities Directive (86/609/EEC).

Only ultra-pure chemicals suitable for molecular biology and work with cell cultures were used in experiments. All chemicals were purchased from Fluka and Sigma-Aldrich (Saint Louis, MO, USA).

2.2. Preparation of skinned muscle fibers

For fiber preparation animals were anaesthetized by intraperitoneal injection of ketamine (75 mg/kg) and dexmedetomidine (1 mg/kg), decapitated and skinned fibers were prepared from the heart, *m. soleus*,

m. gastrocnemius white (GW) and *M. rectus femoris* (RF) according to the methods described previously [51]. In order to study the regulation of mitochondrial respiration in muscle fibers, the cells' sarcolemma was permeabilized by saponin treatment (50μg/mL) for 30 min keeping the mitochondrial membranes intact. Skinned fibers were washed in Mitomedium B solution: (EGTA (0.5 mM), MgCl$_2$.6H$_2$O (3.0 mM), K-lactobionate (60 mM), KH$_2$PO$_4$ (3.0 mM), taurine (20 mM), HEPES (20 mM), sucrose (110 mM), dithiothreitol (DTT, 0.5 mM), bovine serum albumin (BSA, 5 mg/mL) at pH 7.1 supplemented with leupeptin (1 μM) for the protection of cytoskeletal proteins from lysosomal proteolysis and kept in the same solution at 4 °C until used for experiments.

2.3. Measurements of oxygen consumption

All experimental measurements of oxygen consumption were determined by a high-resolution respirometry instrument Oxygraph-2 K (OROBOROS Instruments, Innsbruck, Austria). Measurements were carried out at 25 °C in the Mitomedium B solution [51], supplemented with BSA (5 mg/mL) under continuous magnetic stirring. The permeabilized fiber was weighted and inserted into the oxygraphic chamber

with respiration media (Mitomedium B solution) supplemented with 0.2 μM free Ca^{2+} and respiratory substrates according to the protocol. The measured oxygen consumption rates are presented as nmol O_2/min per mg dry weight.

2.3.1. Measurement of oxygen consumption kinetics

The apparent affinity of mitochondria to exogenous ADP (Km(ADP)) characterizes intracellular diffusion restrictions for ADP and varies significantly between different cell types. These differences are caused by specific structural and functional organization of cells' energy metabolism [52,53]. In these experiments glutamate (G, 5 mM) and malate (M, 2 mM) were used as respiratory substrates. In order to determine the kinetic constants of exogenous ADP stimulated respiration, the oxygen consumption rates with cumulative addition of ADP was measured. From these data the Km(ADP) values and maximal respiration rates (V_{max}) were calculated using Michaelis-Menten equation. In this study we determined Km(ADP) value for oxidative *m. soleus* and heart muscles in parallel with and without activated CK pathway; Km(ADP) for glycolytic RF and GW muscles was determined without creatine. If a Km(ADP) in the presence of creatine is significantly lower than the corresponding value without creatine, there exists an effective functional coupling of OXPHOS to CK pathway [39,52,54].

2.3.2. Determination of the coupled state of mitochondrial creatine kinase

In order to measure energy flux through CK pathway, the pyruvate kinase/phosphoenol pyruvate (PK/PEP) system was added to trap extramitochondrial ADP. In these conditions we measure only the OXPHOS activated by intramitochondrial ADP/ATP and directly connected with the CK system [39,52,54]. The respiratory solution was supplemented with the following substrates: G + M with addition of PEP (5 mM). After addition of MgATP (2 mM) to activate ATPases, the injected PK (10 IU/mL) activates PK/PEP system. While the PK/PEP system rephosphorylates the ADP produced by cytosolic ATPases, the backflow of the ADP to mitochondria is smaller, and the oxygen consumption rate by the OXPHOS inside the mitochondria decreases. Thereafter, creatine was added stepwise until saturation was reached and the maximal respiration rate (V_{Cr}) was detected.

2.3.3. Estimation the role of cytosolic and mitochondrial adenylate kinase

For this experiment the respiratory solution was supplemented with respiratory substrates G + M with addition of PEP (5 mM). In order to assess the influence of the AK system on the mitochondrial respiration and to distinguish the mitochondrial AK2-dependent respiration rate from the respiration stimulated by the cytosolic AK1, we first added MgATP (2 mM) to activate ATPases and induce maximal endogenous ADP production. Thereafter, AMP (2 mM) was added in order to activate the AK reaction coupled with OXPHOS, involving AK1 and AK2 and to register the maximal AMP stimulated respiration (VAMP). Meanwhile, injection of PK decreases the respiration to the level of coupled reaction between AK2 and ANT inside mitochondria which is demonstrated by V_{PK}. In order to determine the proportion of respiration independent of AK, the AK inhibitor diadenosine pentaphosphate (AP5A) was used (V_{AP5A}).

The AK functional coupling with OXPHOS is represented as AK index (IAK) and was calculated as IAK = ($V_{AMP} − V_{AP5A}$)/V_{AP5A}. The AK1 portion of the AK-dependent respiration (IAK1) was calculated as IAK1 = (($V_{AMP} − V_{PK}$) / ($V_{AMP} − V_{AP5A}$))*100% [55].

2.3.4. Coupling of hexokinases to OXPHOS

Hexokinases catalyze the first and irreversible step of glycolysis, phosphorylating glucose to glucose-6-phosphate (G6P). In order to measure the ability of HK to stimulate OXPHOS by locally generated ADP in the vicinity of VDAC channel, MgATP was added into the medium supplemented with respiratory substrates G + M. The addition of MgATP (0.1 mM and 2 mM in case of glycolytic and oxidative muscle, respectively) allowed achieving maximal stimulation of

mitochondria with endogenous ADP produced by ATPases. Supplementation of glucose (10 mM) activates the HK reaction and V_{GLUC} could be registered. Then, the maximal ADP-dependent respiration rate (V_{ADP}) is achieved in the presence of ADP (2 mM). Addition of cytochrome *c* (10 μM) allowed controlling the quality of the OMM. The glucose index (GI) was calculated as ($V_{GLUC} − V_{ATP}$) / (V_{ADP})*100% [52].

2.3.5. Substrate-uncoupler-inhibitor titration (SUIT) protocols

In order to reconstitute the TCA cycle function and sequential separate branches of mitochondrial pathways for OXPHOS analysis a modified SUIT protocols were used [56]. Permeabilized muscle fibers were added into a chamber where respiration was observed in Mitomedium B solution.

Protocol 1. Titration of substrates, uncouplers and inhibitors were added in sequence. Malate and pyruvate (P, 5 mM), providing electrons for Complex I (CI) were injected into the chamber to register basal leak oxygen consumption in the absence of adenylates. The addition of ADP (2 mM) stimulated respiration and represented coupled work of CI and phosphorylation system. In order to detect substrates' preference and determine limiting factor for CI, G (5 mM) was added into the chamber and the maximal CI-dependent respiration rate was registered. Succinate (S) supports electron transport through CII, thus addition of S (10 mM) allowed determining the ADP-dependent respiration when electrons are fed to the ETS via CI and CII. Subsequent addition of ADP (final concentration of 5 mM) stimulated respiration and allowed to control the limitations in the efficiency of ATP synthase [57]. The theoretical maximal capacity of the ETS was evaluated with titration of uncoupler carbonyl cyanide-4-(trifluoromethoxy)phenylhydrazone (FCCP) until saturation of respiration was reached. Subsequent inhibition of CI by rotenone (2.5 μM) allowed to determine the CII-linked electron transfer (ET) capacity. Inhibition of Complex III (CIII) by antimycin A (10 μM) allowed to determine the residual oxygen consumption. Addition of *N,N,N′,N′*-tetramethyl-*p*-phenylenediamine (TMPD; 1 mM) demonstrates maximal capacity of complex IV (CIV). Addition of NaCN (1 mM) inhibited cytochrome oxidase (COX) and blocked electron transport, as a result it allowed to detect residual oxygen consumption due to TMPD oxidation reactions [56].

Protocol 2. In the second protocol the contribution of CI and CII to oxygen consumption in skinned muscle fibers was evaluated. First, the mitochondrial respiration rates under nonphosphorylating conditions (basal respiration rate (V_0)) with G and M in the oxygraphic chamber were registered. Second, after addition of 2 mM ADP the maximum rate of NADH-linked ADP-dependent respiration was detected; subsequently, CI was inhibited by rotenone (5 μM). Last, the substrate S (10 mM) was added to activate ETS CII-dependent respiration. From these results the ratio of CII versus CI can be calculated.

2.4. Immunofluorescence confocal microscopy

To examine cell architecture and colocalization of mitochondrial VDAC with βII-tubulin and plectin in WT and Wfs1 KO mice fibers, confocal microscopy imaging was used. The tissue samples (fibers) were washed with Ca/Mg free phosphate buffered saline (PBS) and fixed in 4% paraformaldehyde (PFA) at 37 °C for 15 min. After washing step with PBS, the samples were treated with Antigen Retrieval Buffer (Tris (100 mM), urea (5%), pH 9.5) at 95 °C for 5 min. The fibers were washed with PBS and permeabilized with 1% Triton X-100 at room temperature for 15 min, washed again with PBS and blocked in PBS solution containing 2% fatty acid free BSA for 1 h at room temperature. In order to detect VDAC with βII-tubulin the samples were incubated at 4 °C overnight with primary antibodies: goat polyclonal antibodies for VDAC (sc-32,064) at 1:50 or 1:70 and rabbit monoclonal antibody for βII-tubulin (ab170931) at 1:200 or 1:250. After incubation, the samples were washed with 2% BSA solution and secondary antibodies were used for visualization (Cy3 donkey anti-goat IgG (Abcam, ab97115) at 1:200

Table 1
Primers for real-time PCR analysis.

Primer	Sequence 5 > 3
ACTB	F: AGCCATGTACGTAGCCATCCA
	R: GACTTTGCTTTCCTTGGTCAGG
CKB	F: TCGTGGCATATGGCACAATG
	R: CGGGTGAACACTTCCTTCATG
CKM	F: GTCCGTGGAAGCTCTCAACAG
	R: CAGAGGTGACACGGGCTTGT
CKMT2	F: AGCAAGGATCCACGCTTTTCT
	R: TCTGCCGATCCGATCTATGTT
HPRT1	F: GCAGTACAGCCCCAAAATGG
	R: AACAAAGTCTGGCCTGTATCCAA

F: forward; R: reverse.

and donkey anti-rabbit IgG (Alexa Fluor 488, ab150073) at 1:200. To detect and visualize VDAC with plectin the following primary and secondary antibodies were used: rabbit polyclonal antibodies for VDAC (kindly provided by Catherine Brenner) at 1:200, guinea pig polyclonal antibodies for plectin (PROGEN, GP21) at 1:250 and goat anti-rabbit IgG (DyLight 488, ab96895) at 1:200, goat anti-guinea pig IgG (Alexa Fluor 647, ab150187) at 1:250. Samples were incubated with secondary antibodies as described above at room temperature for 2 h and then washed with 2% BSA solution, PBS and finally with deionized water. The samples were treated with ProLong Gold antifade reagent (Life Technologies) supplemented with 4′,6-diamidino-2-phenylindole dihydrochloride (DAPI, Molecular Probes) for visualizing the cell nucleus and deposited on glass coverslips for observation with confocal microscope (Olympus FluoView FV 10i-W).

2.5. ^1H NMR spectroscopy

For NMR analysis, heart muscle was frozen and powdered in liquid nitrogen. The powder was weighted and subjected to a methanol:water (2:1) extraction. Overnight lyophilized sample material was reconstituted in 0.5 mL of phosphate buffer (100 mM, pH 7.4). Thereafter, the sample was mixed with 4,4-dimethyl-4-silapentane-1-sulfonic acid (DSS, 1 mM)) in D_2O standard solution in ratio 9:1. The liquid amounts were determined gravimetrically. All experiments were performed at room temperature (25 °C) in 256 scans on a Bruker Avance III 800.13 MHz spectrometer equipped with a triple resonance inversed (TXI) probe. Chemical shifts were referenced and all concentrations calculated as a fold change compared to the DSS (0.1 mM) internal standard signal.

2.6. Determination of enzymatic activities

Pieces of muscles were snap frozen in liquid nitrogen and stored at −80 °C. The samples were allowed to thaw at 0 °C and homogenized in the medium containing the following: EDTA (1 mM), DTT (1 mM), glucose (10 mM), $MgCl_2$ (5 mM), HEPES (5 mM), Triton X-100(0.1%) and leupeptin (5 μg/mL), at pH 8 (maintained by NaOH) by Ultra-Turrax T25 homogenizer (IKA, Germany) on ice.

After homogenization the homogenates were left on ice for 1 h to allow complete extraction of the enzymes. Measurement of HK activity was performed using a spectrophotometer Lambda 900 (Perkin Elmer, U.S.) in solution containing Tris–HCl (50 mM), glucose (20 mM), DTT (0.3) mM, NADP (0.6 mM), MgATP (2 mM), glucose-6-phosphate dehydrogenase (G6PD) (2 IU/mL), pH 7.6, adjusted at 25 °C. The rate of NADPH formation was monitored after addition of homogenate at 340 nm [58]. For CK activity measurements solution containing glucose (20 mM), AMP (20 mM), DTT (0.3 mM), magnesium acetate (3 mM), MgADP (1 mM), NADP (1 mM), Tris-HCl (50 mM) (pH 7.4, 25 °C), HK (2 IU/mL), and G6PD (2 IU/mL) at 25 °C was used. After stabilization of the optical density, the reaction was started by adding 20 mM PCr and the rate of NADPH formation was registered [59]. AK activity

measurements were performed in solution containing Tris-HCl (20 mM) (pH 8, at 30 °C), KCl (15 mM), DTT (0.33 mM), NADH (0.24 mM), PEP (0.8 mM), ATP (1 mM), lactate dehydrogenase (3 IU/mL) and PK 6 (IU/mL). After registration of the basal ATPase activity, AMP (1.3 mM) was added and from the following changes in NADH oxidation rates at 340 nm, the AK activity was calculated [59].

2.7. Gene expression study

Total RNA was isolated by using the RNeasy Mini Kit (Qiagen). Genomic DNA wipeout and reverse transcription was performed by using Quantitect® Reverse Transcription Kit (Qiagen) according to manufacturer's protocol (Quantitect® Reverese Transcription Handbook, 2005). Real-time PCR amplification was carried out with mouse gene-specific primers (Proligo, France and Oligomer OY, Finland, Table 1) using QuantiTect SYBR Green PCR Kit (Qiagen, Germany). The process of collecting fluorescence data during PCR was performed by StepOnePlus™ real-Time PCR Instrument (Applied Biosystems, USA). The relative target quantity in samples was determined by the comparative threshold cycle (ΔCτ, ΔΔCτ) method [60]. Measurements were normalized to multiple endogenous control genes: ACTB, B2M or HPRT1. The relative quantity of target in each sample was assessed by comparing normalized target quantity in each sample to normalized target quantity in the reference sample.

2.8. Statistical analysis

Results are expressed as the mean ± standard error of the mean (SEM). To determine statistical significance between age groups, one-way analysis of variance (ANOVA) test was performed and p values < .05 were considered significant.

The proton NMR spectra of all samples (one sample corresponds to one mouse) were subjected to principal component analysis on Mestrenova version 12.

3. Results

3.1. Alterations in kinetic profile and substrate preferences (Km(ADP) and SUIT protocols)

In skeletal and cardiac muscles a contiguous energy supply for ATPases in myofibrils and ion channels is crucial for muscle work. In oxidative muscles the predominant site of the ATP synthesis is the mitochondrion where proton gradient is formed by ETS and the ADP phosphorylation is regulated by MI supercomplex.

The capability of Wfs1 KO and WT muscle cell mitochondria to generate ATP was followed using oxygraphic measurements with (1) SUIT (substrate-uncoupler-inhibitor-titration) protocol [56], (2) substrate-inhibitor protocol to determine the individual capacity of CI- and CII–linked ET, and (3) classical ADP-titration protocol to determine the kinetic constants like apparent Michaelis-Menten constant for ADP (Km (ADP)) and the maximal respiration rate (V_{max}). With these protocols the respiration linked to different pathways of the ETS can be followed simultaneously to the preference of the pathways to specific substrates.

In the SUIT protocol, P + M were first inserted as CI–linked substrates, and thereafter ADP was added to activate OXPHOS in mitochondria (V_{ADP}). Subsequently, glutamate was injected to detect the effect of different CI-linked substrates on OXPHOS (V_{GLUT}). We observed that the Leak respiration (oxygen consumption without adenylates) in these conditions was statistically higher in Wfs1-deficient soleus, RF and GW muscles but not in the cardiac muscle (Fig. 2A).

In the presence of P + M and ADP, the CI–linked OXPHOS was significantly different only in GW muscle where both the V_{ADP} and V_{GLUT} values were lower in Wfs1 KO animals compared to WT (Table 2). After addition of S (CII – linked substrate) the increase in respiration rate was significantly higher in Wfs1 KO mice GW muscle in

(a)

(b)
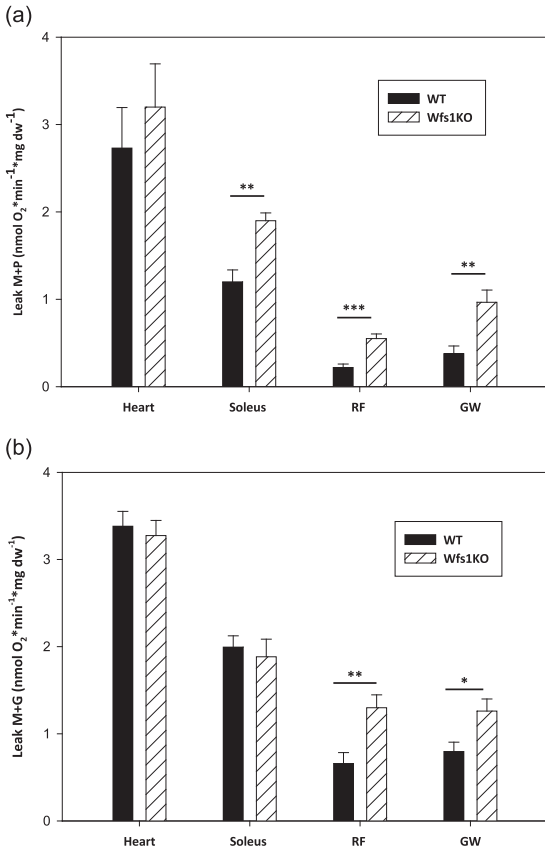
Fig. 2. Determination of the Leak respiration with different complex I substrates

Basal leak respiration (oxygen consumption rate without adenylates) in the heart, *m. soleus*, *m. rectus femoris* (RF) and *m. gastrocnemius* white (GW) fibers of Wfs1 KO and wild type (WT) mice with (**a**) pyruvate (P, 5mM) and malate (M, 2mM) and (**b**) glutamate (G, 5mM) and M as substrates. Respiration rates are represented as nmol O2*min^{-1}*mg dw^{-1}; *p < 0.05, ** p < 0.01, ***p < 0.001; n = 6-10

Table 2

Oxygen consumption rates (V) in the GW muscles of Wfs1-deficient (Wfs1 KO) and wild-type (WT) mice as measured according to the substrate-uncoupler-inhibitor titration protocol. The V_{Succ}-V_{Glut} represents increase in the respiration rate due to the addition of the CII-linked substrate of the ETS.

	WT	Wfs1 KO
ADP 2 mM	1.57 ± 0.15	0.68 ± 0.22**
Glutamate 5 mM	1.84 ± 0.14	0.86 ± 0.19**
Succinate 10 mM	2.48 ± 0.22	2.48 ± 0.25
ADP 5 mM	2.70 ± 0.27	2.76 ± 0.27
FCCP	2.68 ± 0.26	2.70 ± 0.28
Rotenone 2.5 μM	1.55 ± 0.22	1.75 ± 0.27
Antimycin A 10 μM	0.26 ± 0.04	0.26 ± 0.16
Complex IV	5.42 ± 0.87	4.01 ± 0.37
V_{Succ}-V_{Glut}	0.64 ± 0.26	1.63 ± 0.28**

Values are represented as the mean ± SEM, ** p < .01, (n = 6–10) compared to WT.

Table 3

Relative ratio of CII- versus CI–linked oxygen consumption rate in electron transport system of Wfs1-deficient (Wfs1 KO) and wild-type (WT) mice muscles.

Type of muscle	V(CII)/V(CI)	
	WT	Wfs1 KO
Heart	1.31 ± 0.12	1.00 ± 0.05
Soleus	0.77 ± 0.05	1.44 ± 0.07***
Rectus femoris	0.56 ± 0.01	0.86 ± 0.08*

Values are represented as the mean ± SEM. * p < .05, *** p < .001 compared to wild type (n = 6–10).

comparison with WT (Table 2). Similar tendency was observed in the other glycolytic muscle, RF but the changes were not statistically significant (data not shown). With substrate-inhibitor protocol, where after registering CI – dependent oxygen consumption rate, CI was inhibited with rotenone and then S was added, an increase in the ratio of CII-linked to CI–dependent respiration was detected in the soleus and RF muscles of Wfs1 KO compared to WT (Table 3). These results indicate a shift from CI- to CII-induced respiration in skeletal muscles of Wfs1 KO animals as a characteristic of pathological alterations.

We observed interesting shifts in substrate preferences in our experiments. As described above, with M + P as CI–linked substrates, the basal Leak respiration was significantly higher in Wfs1-deficient soleus, RF and GW muscles but not in the cardiac muscle (Fig. 2A). In the second set of experiments measuring oxygen consumption kinetics we used G + M as CI–linked substrates and detected a higher Leak respiration in glycolytic RF and GW muscles of Wfs1 KO mice compared to WT (Fig. 2B). In parallel, the maximal CI–linked respiration rate in the presence of P + M was significantly lower only in GW in Wfs1 KO mice (Table 2), while with G + M as CI–linked substrates the decrease in oxygen consumption was statistically significant in all studied muscles of Wfs1 KO mice compared to WT (Fig. 3).

In the measurements of oxygen consumption kinetics, using G + M as CI-linked substrates, exogenous ADP was added stepwise until the maximal respiration rate was achieved. In these conditions, as mentioned above, the maximal oxygen consumption rate was significantly
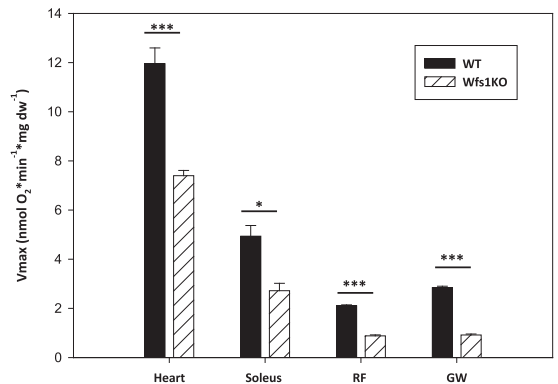
Fig. 3. Maximal oxygen consumption rates with glutamate and malate

Maximal oxygen consumption rates (V_{max}) in Wfs1KO and wild type (WT) mice heart, *m. soleus*, *m. rectus femoris* (RF) and *m. gastrocnemius* white (GW) fibers with glutamate (G, 5mM) and malate (M, 2mM) as substrates. V_{max} is determined from the measurements for Michaelis-Menten coefficient calculation. Respiration rates are represented as nmol O$_2$*min^{-1}*mg dw^{-1}; ***p < 0.001; n = 6-10

Table 4

Michaelis-Menten constant Km(ADP) values in the muscles of Wfs1-deficient (Wfs1 KO) and wild-type (WT) animals with (+Cr) and without (−Cr) activation of creatine kinase pathway.

Km(ADP)			
Type of muscle		- Cr	+ Cr
Heart	WT	101.6 ± 21.3	42.7 ± 5.0
	Wfs1 KO	54.2 ± 5.2	41.4 ± 3.0
Soleus	WT	463 ± 78.9	62.4 ± 15.4
	Wfs1 KO	482 ± 78.2	50.3 ± 16.8
RF	WT	6.45 ± 0,64	–
	Wfs1 KO	18.99 ± 3.15	–
GW	WT	10.36 ± 1.02	–
	Wfs1 KO	12.64 ± 2.29	–

Values are represented as $nmolO_2*min^{-1}*mg\ dw^{-1}$, means ± SEM are shown n = 6–10. RF- *M. rectus* femoris, GW- m. Gastrocnemius white.

lower in all measured Wfs1 KO mice muscle fibers compared to WT animals (Fig. 3). In parallel, Km(ADP) values did not show prominent kinetic differences between Wfs1 KO and WT skeletal muscle fibers (Table 4). However in the cardiac muscle fibers we detected a decrease in the Km(ADP) value (100 versus 50 μM ADP in WT and Wfs1 KO respectively), but in the presence of Cr, mimicking better physiological conditions, Km(ADP) values in the study group and WT animals were similar.

In conclusion, the results of oxygraphic measurements, characterizing ETS revealed increased Leak respiration in both GW and RF glycolytic skeletal muscles in the presence of M + G, as well as increased Leak respiration in the soleus, RF and GW muscle fibers in the presence of M + P. The maximal CI-dependent oxygen consumption rate in the presence of G + M decreased in all followed Wfs1 KO muscles compared to WT. In the presence of P + M, a decrease in the CI-linked ADP-stimulated respiration rate was detectable only in Wfs1 KO GW muscle compared to WT. These results indicate some alterations in glutamate metabolism, having no influence on the metabolism of pyruvate. In addition, in GW muscle the CII-linked respiration was significantly higher in Wfs1 KO muscle compared to WT. A similar shift was also detected in the soleus and RF muscles when the capacities of ETS complexes were measured independently.

These measurements were performed in conditions where energy transfer pathways from mitochondrion to ATPases in the cell were not activated. To investigate how the transport of the energy from mitochondrion to ATP-ases influences OXPHOS, we next investigated the three most important systems for energy facilitation in skeletal muscles.

3.2. Energy transfer pathways

Intracellular transfer of ATP from mitochondria to ATPases is impeded; thus, special energy transfer pathways are essential for maintaining steady energy balance at different ATP consumption sites in the cell. Facilitated transport of metabolites is especially important in oxidative muscle cells like the heart and soleus, where most of the ATP is synthesized in mitochondria; alteration in these pathways has immediate influence on the cellular metabolism as a whole. It has been demonstrated that the main energy transport system in the oxidative skeletal and heart muscles is the CK/PCr pathway [40,45,61], followed by the AK pathway [38,62]. In oxidative muscle cells, one of the manifestations of the effectiveness of the CK pathway is the increased affinity of mitochondria toward ADP (decrease in the Km(ADP) value) when the pathway is activated. In glycolytic GW and RF muscles the Km (ADP) value is low because there is no impediment for the ADP/ATP through the VDAC in the OMM. Therefore, it is not possible to determine the role of CK transfer with this method in these muscles. The effect of activation of CK pathway on Km(ADP) value was detected in the mutant and WT soleus and WT heart muscle fibers (Table 4). The
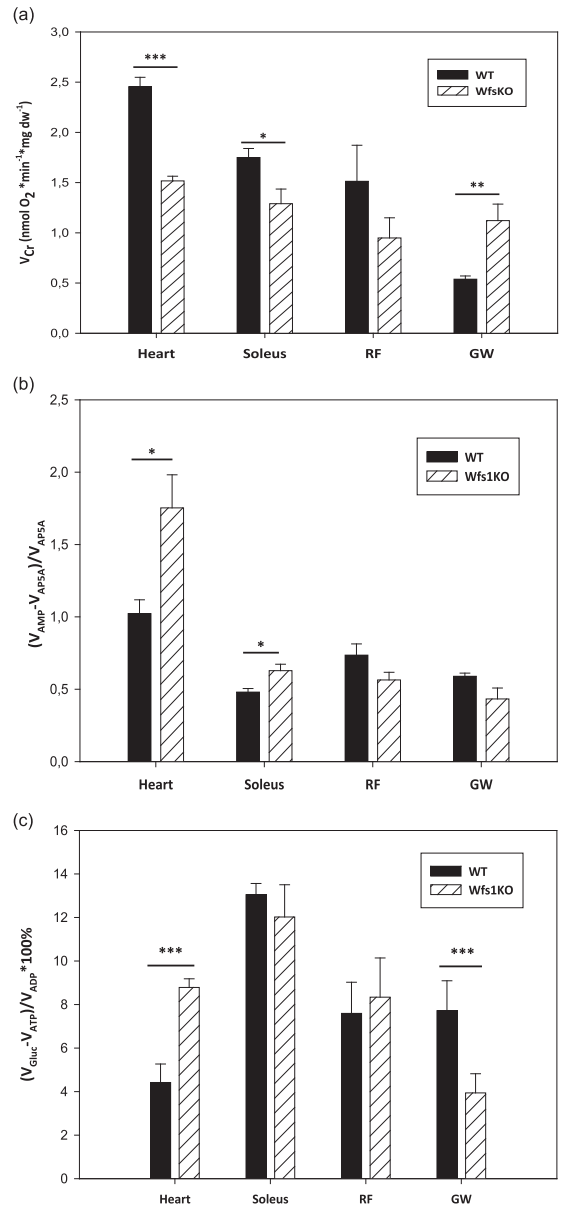
Fig. 4. Quantification of functional coupling between OXPHOS and energy transfer pathways

(**a**) Oxygen consumption rates measured with the maximal activation of the creatine kinase pathway. Respiration rates are represented in nmol $O_2*min^{-1}*mg\ dw^{-1}$.

(**b**) Functional coupling of oxygen consumption with adenylate kinase (AK) pathway is represented as AK index (IAK) calculated as IAK = $(V_{AMP} − V_{AP5A})/V_{AP5A}$ where V_{AMP} is oxygen consumption rate at the maximal activation of AK system and V_{AP5A} in the presence of AK inhibitor.

(**c**) Functional coupling of hexokinase (HK) to OXPHOS. The glucose index (GI) was calculated as $(V_{GLUC} − V_{ATP}) / (V_{ADP})*100\%$ where $(V_{GLUC} − V_{ATP})$ is the increase in the oxygen consumption rate in response to addition of 10mM glucose and V_{ADP} is the respiration rate in the presence of 2mM ADP; *p < 0.05, ** p < 0.01, ***p < 0.001; n=6-10

Table 5

Enzyme activities of Wfs1-deficient (Wfs1 KO) and wild-type (WT) mice muscles. Values are represented as nmol*min^{-1}*mg ww^{-1} ($n = 5$–8).

Enzyme	Type of muscle	WT	Wfs1 KO
Creatine kinase	Heart	262.5 ± 32.6	304.1 ± 16.7
	Soleus muscle	870.8 ± 101.4	443.3 ± 32.6 **
	Rectus femoris muscle	3072.1 ± 180.2	1579.2 ± 224.6 ***
	Gastrocnemius muscle	3495.4 ± 226.5	3088.1 ± 142.9
Adenylate kinase	Heart	176.0 ± 28.5	179.8 ± 22.8
	Soleus muscle	350.8 ± 18.5	196.0 ± 10.9***
	Rectus femoris muscle	399.8 ± 37.6	205.4 ± 48.9 **
	Gastrocnemius muscle	636.9 ± 60.8	654.8 ± 43.9
Hexokinase	Heart	7.2 ± 0.5	8.0 ± 0.7
	Soleus muscle	3.80 ± 0.11	3.43 ± 0.10 *
	Rectus femoris muscle	1.53 ± 0.09	2.14 ± 0.18 **
	Gastrocnemius muscle	2.58 ± 0.12	2.85 ± 0.05

Values are represented as the means ± SEM. * $p < .05$, ** $p < .01$, *** $p < .001$ compared to wild type.

Km(ADP) value in the heart fibers of Wfs1 KO animals was already lower without Cr, so we observed no further significant decrease as a response to the CK pathway activation (Table 4).

In the second protocol we used PK/PEP system for trapping all ADP generated by ATPases. Under these conditions, the registered oxygen consumption is directly dependent only on the ADP/ATP circulation incorporated in the MI and CK transfer system. The maximal Cr activated OXPHOS rate (V_{Cr}) in Wfs1 KO oxidative muscle (heart and soleus) fibers was decreased compared to WT and the alteration was more pronounced in the heart muscle (Fig. 4A). In contrast, in glycolytic GW the V_{Cr} was higher in fibers of Wfs1 KO mice than in WT. There was some decrease in V_{Cr} in RF muscle but the change was not significant (Fig. 4A).

In parallel, the total CK enzyme activities of in the wolframin-deficient soleus and RF muscle were ~2 times decreased but there were no differences detected in the heart and GW compared to WT tissues (Table 5). Recent proteomic results also showed no change of CK isoenzyme levels in the wolframin-deficient heart [63]. Consequently, lower oxygen consumption rate with activated creatine kinase pathway in Wfs1-deficient heart (Fig. 4A) could be mostly caused by the weakened interaction between mitochondrial CK and ANT and thereby impaired MI function.

Additionally, a study of the abundance of CK isoforms in RF demonstrated lower muscle-type CK isoform (CK-MM) mRNA level of Wfs1-deficient mice than in their WT littermates (Table 6). As CK-MM is known to be functionally coupled with ER Ca^{2+}-ATPase [64], the capability of CK-MM to phosphorylate ADP, produced by myofibrillar or ER ATPases, can be reduced and thereby induce local ATP deficiency. It leads to the impairment of muscle contraction and the other ER-linked energy-consuming processes. However, here we found that the expression of mitochondrial CK coding gene CKMT2 did not differ significantly ($p = .213$) between these two groups (Table 6).

Table 6

Relative mRNA levels of CK isoforms in M. rectus femoris of Wfs1-deficient (Wfs1 KO) and wild-type mice (WT).

	CKB	CKM	CKMT2
WT mice,	0.03 ± 0.01	199.0 ± 38.9	2.42 ± 0.43
Wfs1 KO mice,	0.04 ± 0.01	93.5 ± 9.5 *	3.42 ± 0.61

Values are represented as the means ± SEM. * $p < .05$ compared to wild type ($n = 6$).

The other main energy pathway in muscle cells is AK pathway. In Fig. 4B, the AK activation was presented as maximal AK oxygen consumption relative to the oxygen consumption independent of the AK system - AK Index (see 2.3.3. Methods). In oxidative, heart and soleus muscles there is a significant increase in the AK Index value in the fibers of Wfs1 KO mice compared to the WT fibers (Fig. 4B). Nevertheless, in soleus muscle the activity measurements of the tissue homogenates demonstrated a significant decrease in the AK activity (Table 5). This controversy needs future study, but it could be explained by the different approach of the experiments. In the enzyme activity evaluation, all the AK isoforms located in the tissue were included, while in the presented oxygraphic measurements only the AK, connected with transfer of high-energy phosphates from mitochondria to ATPases were followed. In glycolytic muscles, GW and RF, no significant change was detected in AK Index; however, we observed a trend toward decreased AK index in both muscles. Additionally, when looking at the total AK activity measurements, the decrease in AK activity in Wfs1 KO mice RF muscle was statistically significant (Table 5).

In addition, we measured the relative contribution of AK isoforms to the overall AK-related oxygen consumption flux using a protocol developed in our laboratory [52,55]. The role of cytosolic (AK1) isoform varies from ~60% in soleus to ~80% in heart muscle (Table S1 in supplements); however, despite some increase in the contribution of AK1 isoform in the GW muscle Wfs1 KO mice, the differences between Wfs1-deficient and WT mice muscles were not statistically significant.

The third investigated energy transfer system is the glycolytic pathway. These data are represented as the glucose index (GI) calculated as the ratio of the relative increase in OXPHOS rate due to the glucose addition to the maximal respiration rate with exogenous ADP. The GI characterizes the functional coupling of OXPHOS with glycolysis. According to our results, there are some interesting shifts in the GI values: in the oxidative heart muscle of the Wfs1 KO animals the GI is higher compared to WT; in the glycolytic GW muscle fibers, the normally high GI value decreases in KO animals (Fig. 4C). In parallel, the total HK activity in heart and GW muscle of Wfs1 KO animals were similar to wild type (Table 5).

Taking together, the alterations in the AK related oxygen consumption in the cardiac and soleus muscle cells are the opposite of those taking place with CK-related respiration (Fig. 4). Consequently, in the oxidative muscles of Wfs1 KO animals the role of CK energy transfer system is decreasing and at the same time, functional coupling of mitochondria with AK is increasing when compared to the muscles of WT animals. These shifts from one energy transfer pathway to the other may indicate a compensatory mechanism in energy metabolism. As the CK pathway activity is lower in oxidative muscle cells of Wfs1 KO animals, the AK and HK pathway may help to manage the energy flow from mitochondrion to the ATPases, especially in the cardiac muscle. Increase in the GI value in the cardiac muscle cells is registered during aging of the rat heart cardiomyocytes [65]. In the cardiomyocytes of young healthy animals the GI is very low, around 1%; during aging it increases to 8.2% at the age of 1.5 years.

3.3. H NMR studies of the heart muscle

Metabolites in tissue water soluble extracts of 4–6 month mice were determined using ^{1}H NMR spectroscopy. The total creatine content of KO animals was not different from that of the WT. The principal component analysis of proton NMR spectra did not reveal any systematic differences between the two mouse genotypes. We also calculated the values of six abundant metabolites: glucose, lactate, alanine, glutamine, glutamate and taurine (Supplementary Table 2). The concentrations of these metabolites were similar as presented before by Zervou et al. 2016 [66]. We did not find any statistically significant differences between the KO and WT groups. Our results are in good accordance with the study by Porosk et al. (2017) were they compared the heart metabolome of six month old Wfs1 KO and WT mice [67]. Therefore, the
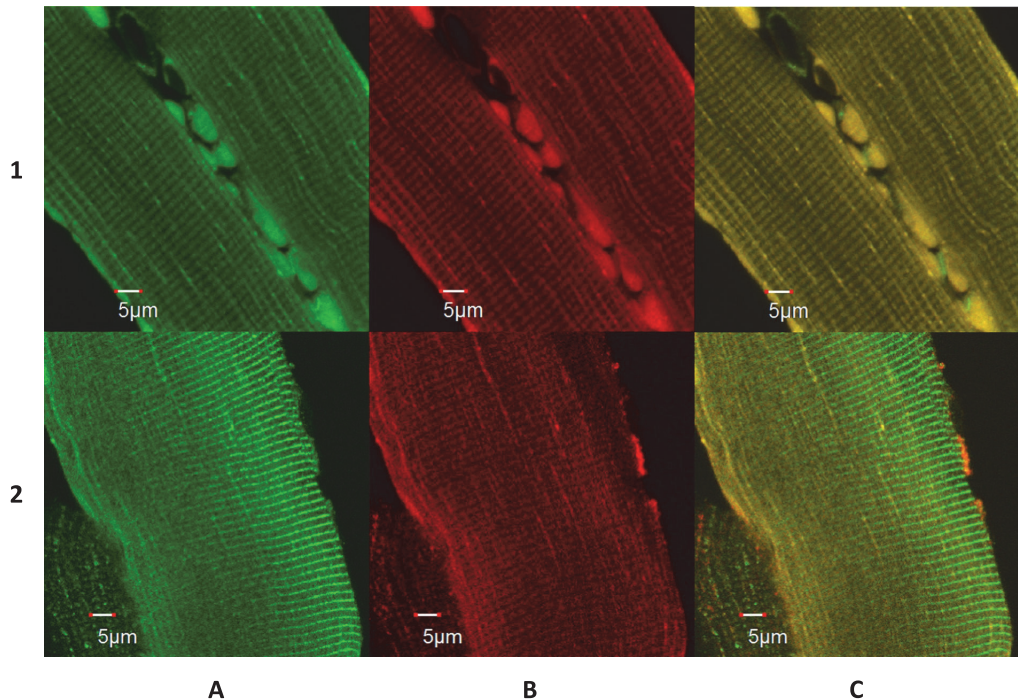
Fig. 5. Evaluation of the interaction between mitochondria and tubulin
Representative colocalization (C) pattern of (A) mitochondria (marked as VDAC1 (sc32064)Cy3 - red) and (B) βII-tubulin component of the α/β tubulin hetero-dimeres (beta2TUB (ab170931)Al488 - green) in WT (1) and Wfs1KO (2) soleus muscles. There is a tendency to decrease the colocalization between mitochondria and tubulin; calculated Pearson's coefficients are 0.93 and 0.54 for WT and for Wfs1KO, respectively.

alterations in the regulation of CK pathway could be a significant sign of functional disturbances in the cardiac muscle energy metabolism.

3.4. Structural changes - confocal microscopy

The energy metabolism regulation in the muscle cell mitochondria is directly dependent on the functional interaction of mitochondrial VDAC with cytoskeletal proteins, one of which is probably β-tubulin component of the free αβ-tubulin heterodimers [41,68,69]. According to our visual and manual observations the skeletal muscles of WFS1 KO mice are softer and more delicate then WT muscles. However, the animals have no difficulties to manage their movement in captivated/cage conditions. We used confocal microscopy to follow if this observation is accompanied with changes in the structure of the muscle cell. We used antibodies for VDAC and βII-tubulin in one combination (Fig. 5) and VDAC with plectin in another. Some alterations were detected in calculated Pearson's coefficients in muscle fibers of Wfs1 KO animals compared to WT, but these changes could not be considered as significant in the given context. As the age of the animals in our experiments was 4–6 month, there is a possibility that more prominent changes could develop later in the course of the disease.

4. Discussion

Recently, several theories about the pathways of the WS and the possible roles of wolframin have been presented. The placement of the wolframin in the ER membrane has been demonstrated and the involvement of the protein in cell metabolism through homeostasis of Ca^{2+} has found most proponents. However, several questions still remain unanswered. A few studies have investigated the effects of WS in

the muscle tissue, specifically in the bioenergetic metabolism. Some patient reviews indicate that the incidences of congenital heart defects are significantly higher among WS patients [33,34]. However, large functional alterations have been not detected in all patients. A possible reason for the lower number of reports about changes in the muscle tissues in WS patients could be that more emphasis is placed on the pathological conditions that emerge first in the disease process (e.g. pancreatic β-cell and neuronal changes) and thus affect the life quality in higher extent. Furthermore, as the life expectancy of the WS patients is reduced, smaller changes in physiology may occur unnoticed. However, to understand the mechanisms and roles of the wolframin protein, different tissues should be studied.

In this study, by studying 4–6 month old Wfs1 KO and WT mice, we detected some regulatory kinetic alterations in the apparent affinity of exogenous ADP to mitochondrion and some decline in the colocalization pattern between mitochondria and tubulin in soleus muscle of Wfs1 KO mice. Therefore, we may conclude that there are no critical structural changes in muscle cells and the functional interactions between mitochondria and cytoskeleton are generally intact. However, we observed significant changes in several aspects of OXPHOS and in the functional properties of the electron transport system and pathways, transporting high energy bond to the ATPases.

With both substrate combinations used for CI–linked respiration, increase in the Leak or basal Leak respiration was detected in the glycolytic muscles in Wfs1 KO compared to WT mice. This value demonstrates oxygen consumption in the non-phosphorylating conditions, i.e. proton leak through the IMM, across lipid bilayers without ATP-synthase activation. This result indicates inefficiency of the OXPHOS system and may be a sign of the functional changes in the IMM. These findings are in accordance with the research of Eimre et al. (2018) [70]

as they found an increase in the Leak respiration in the RF muscle of aged, 9–12 month old mice together with increased uncoupler protein 2 mRNA levels. In addition, they found that the citrate synthase activity and amount of ETS subunits as well as mitochondrial proteins was increased in the glycolytic RF muscle, while no important alteration was detected in oxidative cardiac and soleus muscle of Wfs1 KO compared to WT mice. Moreover, it has been demonstrated that the basal Leak respiration is related to the amount of ANT and other anion carrier proteins in mitochondria [71], but not with the activity of these protein complexes [72]. Thus, the increase in the Leak respiration could be connected to the alterations in the IMM composition or increase in the ANT abundance, which could be caused by an increase in the number of MI in mitochondria as an adaptive response to the less efficient ATP production in the Wfs1 KO animals.

In all the muscle types studied, we observed that the maximal ADP-dependent respiration rate with G + M was lower in the Wfs1 KO animals compared to WT. Interestingly, when P + M was used as CI-linked substrate, we found no significant differences between Wfs1 KO and WT. These results indicate that the wolframin deficiency has caused some alterations in the cell which have influence on the glutamate but not on the pyruvate metabolism. WS is characterized by increased ER stress, decrease in the number of mitochondria-ER connecting sites, and disturbances in Ca^{2+} homeostasis. These changes could have an influence on the activity of protein complexes regulating glutamate metabolism in mitochondria such as glutamate-aspartate antiporter (AGC) and 2-oxoglutarate-malate transporter. It has been demonstrated that Ca^{2+} related alterations in AGC1 (which is also expressed in the cardiac and skeletal muscle) is one of the causes of the autism spectrum disorder [73]. As the alterations in Ca^{2+} metabolism have also been detected in WS, these changes may also have an influence on the glutamate-related oxygen consumption rate here. Furthermore, in a study of cardiac cells with induced ER stress, Prola et al. (2019) detected a decrease in the glutamate- and succinate- but not in pyruvate-induced respiration. They concluded that fatty acid oxidation pathway in mitochondria is down-regulated in cells with ER stress while relative oxidation of pyruvate is increased [74]. These results are in a good accordance with the current study as we found that the GI was increased in the heart fibers of Wfs1 KO mice compared to WT.

The transport of high energy bond from mitochondria to ATPases is a crucial part of the energy provision. Our study demonstrated that there are several alterations in the pathways responsible for energy trafficking. We found an important shift taking place in the heart muscle of the Wfs1 KO mice. In healthy cardiac muscle cells the CK has a leading role in the transport of the phosphoryl group to ATPases. In the cardiac cells of Wfs1 KO animals the oxygen consumption rate of the creatine stimulated respiration is decreasing, while the role of the secondary AK pathway is increasing. Simultaneously, the functional interaction with glycolytic enzymes, represented as the glucose index, is higher in cardiac muscle of the Wfs1 KO animals. In glycolytic GW muscle, a contrary shift is taking place: in WT GW muscle, high GI was determined, but it was decreased significantly in the GW fibers of Wfs1 KO mice. In parallel, there was a significant increase in the CK pathway–related respiration in the wolframin deficient animals. Similar alterations in the pathway preferences are detected in the aging heart muscle [65] and in pathological conditions such as cancer [48]. These changes indicate possible compensatory mechanisms as a response to altered metabolism in the muscle cells: a decrease in the CK pathway is balanced by an increase in the AK system in the heart muscle. Similarly, in GW muscle a shift from glycolytic to CK pathway is taking place.

Using ^{1}H NMR, we detected no significant alterations in the metabolites profile of Wfs1 KO animals. This relative stability may be achieved due to the compensatory mechanism in the energy transfer pathways which enable to continue the muscle work at lower efficiency. We speculate that the problems might arise during in vivo conditions when the workload of the muscle has to be increased.

The results of our study indicate adaptations in the bioenergetic metabolism of the muscles to the alterations caused by the Wfs1 deficiency. We observed no crucial structural alterations, but clear functional changes in the MI and energy transport were detected. It was visible that in some muscles a decrease in the one pathway was balanced by the increase in the activity of parallel pathway. There was no direct decrease in the CI–linked ET capacity, but rather change in the substrate preference profile, which might be caused by the alterations connected with ER stress. These results are in accordance with the study of skeletal muscle of young adults with type I diabetes, where no changes in mitochondrial content or distribution have been detected, but mitochondrial oxidative capacity has been shown to decrease [75].

It has been demonstrated that wolframin is highly expressed in the cardiac as well as in the skeletal muscles. There are some reports of atrial and ventricular arrhythmias and sinus tachycardia in the later stages of WS [35]; however, the extent of the impairment is significantly smaller in comparison with the ones that emerge earlier in the neurons and pancreatic β-cells. Adaptations in muscle tissue as a response to the wolframin deficiency, detected in our study, could explain the contradiction. Yet, as the WS-accompanied alterations in oxidative muscle cells are not essential, the role of wolframin might be more complex and include additional functions regulating Ca^{2+} homeostasis.

In sum, WS is a metabolic disease with complicated diagnostics. Several cases have been described where patients with WS are misdiagnosed and treated for diabetes for years [33,34]. Better mechanistic understanding of wolframin functions could enable the development of methods for earlier diagnosis of WS, and for possible treatments in order to postpone the manifestations of the disease such as optical nerve degradation or diabetes. Our results demonstrate that WS is a mitochondrial disease and monitoring functional alterations in striated muscle bioenergetics could be considered as one of the directions for the better understanding of wolframin functions and for developing improved diagnostic methods for WS.

Contributions

K.T. and M.P. designed, preformed and interpreted all oxygraphic experiments with input from J.A.-V., N.T. and N.P.; L.K. developed gene expression study protocols and analyzed and interpreted all of the quantitative RT-PCR data; I.R. conducted NMR spectroscopy and analyzed the data; I.S. and V.C. performed immunohistochemistry experiments and corresponding data analysis; M.E. determined enzyme activities; K.P. supplied Wfs1 KO mice and coordinated work from the University of Tartu; T.K. coordinated and supervised work from NICPB; K.T., M.P., and M.E. wrote the manuscript with help from J.A.-V. and T.K.

Declaration of Competing Interest

Authors declare no conflict of interest.

Acknowledgments

Appendix A. Supplementary data

Supplementary data to this article can be found online at https://

doi.org/10.1016/j.bbagen.2020.129523.

References

[1] T.G. Barrett, S.E. Bundey, A.R. Fielder, P.A. Good, Optic atrophy in Wolfram (DIDMOAD) syndrome, Eye (Lond) 11 (Pt 6) (1997) 882–888.

[2] T.G. Barrett, S.E. Bundey, Wolfram (DIDMOAD) syndrome, J. Med. Genet. 34 (1997) 838–841.

[3] L. Rigoli, F. Lombardo, C. Di Bella, Wolfram syndrome and WFS1 gene, Clin. Genet. 79 (2011) 103–117, https://doi.org/10.1111/j.1399-0004.2010.01522.x.

[4] F. Urano, Wolfram syndrome: diagnosis, management, and treatment, Curr. Diabetes Rep. 16 (2016) 6, , https://doi.org/10.1007/s11892-015-0702-6.

[5] B. Delprat, T. Maurice, C. Delettre, Wolfram syndrome: MAMs' connection? Cell Death Dis. 9 (2018) 364, , https://doi.org/10.1038/s41419-018-0406-3.

[6] R. Medlej, J. Wasson, P. Baz, S. Azar, I. Salti, J. Loiselet, A. Permutt, G. Halaby, Diabetes mellitus and optic atrophy: a study of Wolfram syndrome in the Lebanese population, J. Clin. Endocrinol. Metab. 89 (2004) 1656–1661, https://doi.org/10.1210/jc.2002-030015.

[7] K. Takeda, H. Inoue, Y. Tanizawa, Y. Matsuzaki, J. Oba, Y. Watanabe, K. Shinoda, Y. Oka, WFS1 (Wolfram syndrome 1) gene product: predominant subcellular localization to endoplasmic reticulum in cultured cells and neuronal expression in rat brain, Hum. Mol. Genet. 10 (2001) 477–484, https://doi.org/10.1093/hmg/10.5.477.

[8] S. Hofmann, C. Philbrook, K.D. Gerbitz, M.F. Bauer, Wolfram syndrome: structural and functional analyses of mutant and wild-type wolframin, the WFS1 gene product, Hum. Mol. Genet. 12 (2003) 2003–2012, https://doi.org/10.1093/hmg/ddg214.

[9] S.G. Fonseca, M. Fukuma, K.L. Lipson, L.X. Nguyen, J.R. Allen, Y. Oka, F. Urano, WFS1 is a novel component of the unfolded protein response and maintains homeostasis of the endoplasmic reticulum in pancreatic beta-cells, J. Biol. Chem. 280 (2005) 39609–39615, https://doi.org/10.1074/jbc.M507426200.

[10] D. Takei, H. Ishihara, S. Yamaguchi, T. Yamada, A. Tamura, H. Katagiri, Y. Maruyama, Y. Oka, WFS1 protein modulates the free Ca(2+) concentration in the endoplasmic reticulum, FEBS Lett. 580 (2006) 5635–5640, https://doi.org/10.1016/j.febslet.2006.09.007.

[11] S. Lu, K. Kanekura, T. Hara, J. Mahadevan, L.D. Spears, C.M. Oslowski, R. Martinez, M. Yamazaki-Inoue, M. Toyoda, A. Neilson, P. Blanner, C.M. Brown, C.F. Semenkovich, B.A. Marshall, T. Hershey, A. Umezawa, P.A. Greer, F. Urano, A calcium-dependent protease as a potential therapeutic target for Wolfram syndrome, Proc. Natl. Acad. Sci. U. S. A. 111 (2014) E5292–E5301, https://doi.org/10.1073/pnas.1421055111.

[12] M. Zatyka, C. Ricketts, G. da Silva Xavier, J. Minton, S. Fenton, S. Hofmann-Thiel, G.A. Rutter, T.G. Barrett, Sodium-potassium ATPase 1 subunit is a molecular partner of Wolframin, an endoplasmic reticulum protein involved in ER stress, Hum. Mol. Genet. 17 (2008) 190–200, https://doi.org/10.1093/hmg/ddm296.

[13] A.A. Osman, M. Saito, C. Makepeace, M.A. Permutt, P. Schlesinger, M. Mueckler, Wolframin expression induces novel ion channel activity in endoplasmic reticulum membranes and increases intracellular calcium, J. Biol. Chem. 278 (2003) 52755–52762, https://doi.org/10.1074/jbc.M310331200.

[14] M. Cagalinec, M. Liiv, Z. Hodurova, M.A. Hickey, A. Vaarmann, M. Mandel, A. Zeb, V. Choubey, M. Kuum, D. Safiulina, E. Vasar, V. Veksler, A. Kaasik, Role of mitochondrial dynamics in neuronal development: mechanism for Wolfram syndrome, PLoS Biol. 14 (2016) e1002511, , https://doi.org/10.1371/journal.pbio.1002511.

[15] J.R. Porter, T.G. Barrett, Monogenic syndromes of abnormal glucose homeostasis: clinical review and relevance to the understanding of the pathology of insulin resistance and beta cell failure, J. Med. Genet. 42 (2005) 893–902, https://doi.org/10.1136/jmg.2005.030791.

[16] H. Ishihara, S. Takeda, A. Tamura, R. Takahashi, S. Yamaguchi, D. Takei, T. Yamada, H. Inoue, H. Soga, H. Katagiri, Y. Tanizawa, Y. Oka, Disruption of the WFS1 gene in mice causes progressive beta-cell loss and impaired stimulus-secretion coupling in insulin secretion, Hum. Mol. Genet. 13 (2004) 1159–1170, https://doi.org/10.1093/hmg/ddh125.

[17] T. Yamada, H. Ishihara, A. Tamura, R. Takahashi, S. Yamaguchi, D. Takei, A. Tokita, C. Satake, F. Tashiro, H. Katagiri, H. Aburatani, J. Miyazaki, Y. Oka, WFS1-deficiency increases endoplasmic reticulum stress, impairs cell cycle progression and triggers the apoptotic pathway specifically in pancreatic beta-cells, Hum. Mol. Genet. 15 (2006) 1600–1609, https://doi.org/10.1093/hmg/ddl081.

[18] Y. Ohta, A. Taguchi, T. Matsumura, H. Nakabayashi, M. Akiyama, K. Yamamoto, R. Fujimoto, R. Suetomi, A. Yanai, K. Shinoda, Y. Tanizawa, Clock gene dysregulation induced by chronic ER stress disrupts beta-cell function, EBioMedicine 18 (2017) 146–156, https://doi.org/10.1016/j.ebiom.2017.03.040.

[19] S. Morikawa, T. Tajima, A. Nakamura, K. Ishizu, T. Ariga, A novel heterozygous mutation of the WFS1 gene leading to constitutive endoplasmic reticulum stress is the cause of Wolfram syndrome, Pediatr. Diabetes 18 (2017) 934–941, https://doi.org/10.1111/pedi.12513.

[20] T.M. Strom, K. Hortnagel, S. Hofmann, F. Gekeler, C. Scharfe, W. Rabl, K.D. Gerbitz, T. Meitinger, Diabetes insipidus, diabetes mellitus, optic atrophy and deafness (DIDMOAD) caused by mutations in a novel gene (wolframin) coding for a predicted transmembrane protein, Hum. Mol. Genet. 7 (1998) 2021–2028.

[21] H. Luuk, S. Koks, M. Plaas, J. Hannibal, J.F. Rehfeld, E. Vasar, Distribution of Wfs1 protein in the central nervous system of the mouse and its relation to clinical symptoms of the Wolfram syndrome, J. Comp. Neurol. 509 (2008) 642–660, https://doi.org/10.1002/cne.21777.

[22] C. Angebault, J. Fauconnier, S. Patergnani, J. Rieusset, A. Danese, C.A. Affortit, J. Jagodzinska, C. Megy, M. Quiles, C. Cazevieille, J. Korchagina, D. Bonnet-Wersinger, D. Milea, C. Hamel, P. Pinton, M. Thiry, A. Lacampagne, B. Delprat, C. Delettre, ER-mitochondria cross-talk is regulated by the Ca(2+) sensor NCS1 and is impaired in Wolfram syndrome, Sci. Signal. 11 (2018), https://doi.org/10.1126/scisignal.aaq1380.

[23] M. Cagalinec, A. Zahradnikova, A. Zahradnikova Jr., D. Kovacova, L. Paulis, S. Kurekova, M. Hot'ka, J. Pavelkova, M. Plaas, M. Novotova, I. Zahradnik, Calcium signaling and contractility in cardiac myocyte of Wolframin deficient rats, Front. Physiol. 10 (2019) 172, https://doi.org/10.3389/fphys.2019.00172.

[24] S. Gharanei, M. Zatyka, D. Astuti, J. Fenton, A. Sik, Z. Nagy, T.G. Barrett, Vacuolar-type H+-ATPase V1A subunit is a molecular partner of Wolfram syndrome 1 (WFS1) protein, which regulates its expression and stability, Hum. Mol. Genet. 22 (2013) 203–217, https://doi.org/10.1093/hmg/dds400.

[25] S. Koks, R.W. Overall, M. Ivask, U. Soomets, M. Guha, E. Vasar, C. Fernandes, L.C. Schalkwyk, Silencing of the WFS1 gene in HEK cells induces pathways related to neurodegeneration and mitochondrial damage, Physiol. Genomics 45 (2013) 182–190, https://doi.org/10.1152/physiolgenomics.00122.2012.

[26] S. Hofmann, R. Bezold, M. Jaksch, B. Obermaier-Kusser, S. Mertens, P. Kaufhold, W. Rabl, W. Hecker, K.D. Gerbitz, Wolfram (DIDMOAD) syndrome and Leber hereditary optic neuropathy (LHON) are associated with distinct mitochondrial DNA haplotypes, Genomics 39 (1997) 8–18, https://doi.org/10.1006/geno.1996.4474.

[27] D. Pilz, O.W. Quarrell, E.W. Jones, Mitochondrial mutation commonly associated with Leber's hereditary optic neuropathy observed in a patient with Wolfram syndrome (DIDMOAD), J. Med. Genet. 31 (1994) 328–330, https://doi.org/10.1136/jmg.31.4.328.

[28] A. Barrientos, J. Casademont, A. Saiz, F. Cardellach, V. Volpini, A. Solans, E. Tolosa, A. Urbano-Marquez, X. Estivill, V. Nunes, Autosomal recessive Wolfram syndrome associated with an 8.5-kb mtDNA single deletion, Am. J. Hum. Genet. 58 (1996) 963–970.

[29] A. Rotig, V. Cormier, P. Chatelain, R. Francois, J.M. Saudubray, P. Rustin, A. Munnich, Deletion of mitochondrial DNA in a case of early-onset diabetes mellitus, optic atrophy, and deafness (Wolfram syndrome, MIM 222300), J. Clin. Invest. 91 (1993) 1095–1098, https://doi.org/10.1172/JCI116267.

[30] M.J. Jackson, L.A. Bindoff, K. Weber, J.N. Wilson, P. Ince, K.G. Alberti, D.M. Turnbull, Biochemical and molecular studies of mitochondrial function in diabetes insipidus, diabetes mellitus, optic atrophy, and deafness, Diabetes Care 17 (1994) 728–733, https://doi.org/10.2337/diacare.17.7.728.

[31] E. Domenech, M. Gomez-Zaera, V. Nunes, Study of the WFS1 gene and mitochondrial DNA in Spanish Wolfram syndrome families, Clin. Genet. 65 (2004) 463–469, https://doi.org/10.1111/j.1399-0004.2004.00249.x.

[32] A.D. Baron, G. Brechtel, P. Wallace, S.V. Edelman, Rates and tissue sites of non-insulin- and insulin-mediated glucose uptake in humans, Am. J. Phys. 255 (1988) E769–E774, https://doi.org/10.1152/ajpendo.1988.255.6.E769.

[33] M.A. Ganie, B.A. Laway, S. Nisar, M.M. Wani, M.L. Khurana, F. Ahmad, S. Ahmed, P. Gupta, I. Ali, I. Shabir, A. Shadan, A. Ahmed, S. Tufail, Presentation and clinical course of Wolfram (DIDMOAD) syndrome from North India, Diabet. Med. 28 (2011) 1337–1342, https://doi.org/10.1111/j.1464-5491.2011.03377.x.

[34] H.A. Korkmaz, K. Demir, F. Hazan, M. Yildiz, O.N. Elmas, B. Ozkan, Association of Wolfram syndrome with Fallot tetralogy in a girl, Arch. Argent. Pediatr. 114 (2016) e163–e166, https://doi.org/10.5546/aap.2016.eng.e163.

[35] B.T. Kinsley, M. Swift, R.H. Dumont, R.G. Swift, Morbidity and mortality in the Wolfram syndrome, Diabetes Care 18 (1995) 1566–1570, https://doi.org/10.2337/diacare.18.12.1566.

[36] V. Saks, A.V. Kuznetsov, M. Gonzalez-Granillo, K. Tepp, N. Timohhina, M. Karu-Varikmaa, T. Kaambre, P. Dos Santos, F. Boucher, R. Guzun, Intracellular energetic units regulate metabolism in cardiac cells, J. Mol. Cell. Cardiol. 52 (2012) 419–436, https://doi.org/10.1016/j.yjmcc.2011.07.015.

[37] M. Vendelin, N. Béraud, K. Guerrero, T. Andrienko, A.V. Kuznetsov, J. Olivares, L. Kay, V.A. Saks, Mitochondrial regular arrangement in muscle cells: a "crystal-like" pattern, Am. J. Physiol. Cell Physiol. 288 (2005) C757–C767, https://doi.org/10.1152/ajpcell.00281.2004.

[38] P.P. Dzeja, A. Terzic, Phosphotransfer networks and cellular energetics, J. Exp. Biol. 206 (2003) 2039–2047, https://doi.org/10.1242/jeb.00426.

[39] N. Timohhina, R. Guzun, K. Tepp, C. Monge, M. Varikmaa, H. Vija, P. Sikk, T. Kaambre, D. Sackett, V. Saks, Direct measurement of energy fluxes from mitochondria into cytoplasm in permeabilized cardiac cells in situ: some evidence for mitochondrial interactosome, J. Bioenerg. Biomembr. 41 (2009) 259–275, https://doi.org/10.1007/s10863-009-9224-8.

[40] K. Tepp, I. Shevchuk, V. Chekulayev, N. Timohhina, A.V. Kuznetsov, R. Guzun, V. Saks, T. Kaambre, High efficiency of energy flux controls within mitochondrial interactosome in cardiac intracellular energetic units, Biochim. Biophys. Acta 1807 (2011) 1549–1561, https://doi.org/10.1016/j.bbabio.2011.08.005.

[41] M. Puurand, K. Tepp, N. Timohhina, J. Aid, I. Shevchuk, V. Chekulayev, T. Kaambre, Tubulin betaII and betaIII isoforms as the regulators of VDAC channel permeability in health and disease, Cells 8 (2019), https://doi.org/10.3390/cells8030239.

[42] K. Mado, V. Chekulayev, I. Shevchuk, M. Puurand, K. Tepp, T. Kaambre, On the role of tubulin, plectin, desmin, and vimentin in the regulation of mitochondrial energy fluxes in muscle cells, Am. J. Physiol. Cell Physiol. 316 (2019) C657–C667, https://doi.org/10.1152/ajpcell.00303.2018.

[43] A. Klepinin, L. Ounpuu, K. Mado, L. Truu, V. Chekulayev, M. Puurand, I. Shevchuk, K. Tepp, A. Planken, T. Kaambre, The complexity of mitochondrial outer membrane permeability and VDAC regulation by associated proteins, J. Bioenerg. Biomembr. 50 (2018) 339–354, https://doi.org/10.1007/s10863-018-9765-9.

[44] V.A. Saks, T. Kaambre, P. Sikk, M. Eimre, E. Orlova, K. Paju, A. Piirsoo, F. Appaix, L. Kay, V. Regitz-Zagrosek, E. Fleck, E. Seppet, Intracellular energetic units in red muscle cells, Biochem. J. 356 (2001) 643–657, https://doi.org/10.1042/

bj3560643.

[45] V. Saks, U. Schlattner, M. Tokarska-Schlattner, T. Wallimann, R. Bagur, S. Zorman, M. Pelosse, P.D. Santos, F. Boucher, T. Kaambre, R. Guzun, Systems level regulation of cardiac energy fluxes via metabolic cycles: role of Creatine, phosphotransfer pathways, and AMPK Signaling, Springer Ser. Biophys. 16 (2014) 261–320, https://doi.org/10.1007/978-3-642-38505-6_11.

[46] R. Guzun, T. Kaambre, R. Bagur, A. Grichine, Y. Usson, M. Varikmaa, T. Annann, K. Tepp, N. Timohhina, I. Shevchuk, V. Chekulayev, F. Boucher, P. Dos Santos, U. Schlattner, T. Wallimann, A.V. Kuznetsov, P. Dzeja, M. Aliev, V. Saks, Modular organization of cardiac energy metabolism: energy conversion, transfer and feedback regulation, Acta Physiol. 213 (2015) 84–106, https://doi.org/10.1111/apha.12287.

[47] V. Chekulayev, K. Mado, I. Shevchuk, A. Koit, A. Kaldma, A. Klepinin, N. Timohhina, K. Tepp, M. Kandashvili, L. Ounpuu, K. Heck, L. Truu, A. Planken, V. Valvere, T. Kaambre, Metabolic remodeling in human colorectal cancer and surrounding tissues: alterations in regulation of mitochondrial respiration and metabolic fluxes, Biochem. Biophys. Rep. 4 (2015) 111–125, https://doi.org/10.1016/j.bbrep.2015.08.020.

[48] A. Kaldma, A. Klepinin, V. Chekulayev, K. Mado, I. Shevchuk, N. Timohhina, K. Tepp, M. Kandashvili, M. Varikmaa, A. Koit, M. Planken, K. Heck, L. Truu, A. Planken, V. Valvere, E. Rebane, T. Kaambre, An in situ study of bioenergetic properties of human colorectal cancer: the regulation of mitochondrial respiration and distribution of flux control among the components of ATP synthasome, Int. J. Biochem. Cell Biol. 55 (2014) 171–186, https://doi.org/10.1016/j.biocel.2014.09.004.

[49] M. Puurand, N. Peet, A. Piirsoo, M. Peetsalu, J. Soplepmann, M. Sirotkina, A. Peetsalu, A. Hemminki, E. Seppet, Deficiency of the complex I of the mitochondrial respiratory chain but improved adenylate control over succinate-dependent respiration are human gastric cancer-specific phenomena, Mol. Cell. Biochem. 370 (2012) 69–78, https://doi.org/10.1007/s11010-012-1399-3.

[50] H. Luuk, M. Plaas, S. Raud, J. Innos, S. Sutt, H. Lasner, U. Abramov, K. Kurrikoff, S. Koks, E. Vasar, Wfs1-deficient mice display impaired behavioural adaptation in stressful environment, Behav. Brain Res. 198 (2009) 334–345, https://doi.org/10.1016/j.bbr.2008.11.007.

[51] A.V. Kuznetsov, V. Veksler, F.N. Gellerich, V. Saks, R. Margreiter, W.S. Kunz, Analysis of mitochondrial function in situ in permeabilized muscle fibers, tissues and cells, Nat. Protoc. 3 (2008) 965–976, https://doi.org/10.1038/nprot.2008.61.

[52] M. Puurand, K. Tepp, A. Klepinin, L. Klepinina, I. Shevchuk, T. Kaambre, Intracellular energy-transfer networks and high-resolution respirometry: a convenient approach for studying their function, Int. J. Mol. Sci. 19 (2018), https://doi.org/10.3390/ijms19102933.

[53] M. Varikmaa, R. Bagur, T. Kaambre, A. Grichine, N. Timohhina, K. Tepp, I. Shevchuk, V. Chekulayev, M. Metsis, F. Boucher, V. Saks, A.V. Kuznetsov, R. Guzun, Role of mitochondria-cytoskeleton interactions in respiration regulation and mitochondrial organization in striated muscles, Biochim. Biophys. Acta 1837 (2014) 232–245, https://doi.org/10.1016/j.bbabio.2013.10.011.

[54] R. Guzun, M. Gonzalez-Granillo, M. Karu-Varikmaa, A. Grichine, Y. Usson, T. Kaambre, K. Guerrero-Roesch, A. Kuznetsov, U. Schlattner, V. Saks, Regulation of respiration in muscle cells in vivo by VDAC through interaction with the cytoskeleton and MtCK within mitochondrial interactosome, Biochim. Biophys. Acta 1818 (2012) 1545–1554, https://doi.org/10.1016/j.bbamem.2011.12.034.

[55] A. Klepinin, L. Ounpuu, R. Guzun, V. Chekulayev, N. Timohhina, K. Tepp, I. Shevchuk, U. Schlattner, T. Kaambre, Simple oxygraphic analysis for the presence of adenylate kinase 1 and 2 in normal and tumor cells, J. Bioenerg. Biomembr. 48 (2016) 531–548, https://doi.org/10.1007/s10863-016-9687-3.

[56] D. Pesta, E. Gnaiger, High-resolution respirometry: OXPHOS protocols for human cells and permeabilized fibers from small biopsies of human muscle, Methods Mol. Biol. 810 (2012) 25–58, https://doi.org/10.1007/978-1-61779-382-0_3.

[57] V.A. Saks, V.I. Veksler, A.V. Kuznetsov, L. Kay, P. Sikk, T. Tiivel, L. Tranqui, J. Olivares, K. Winkler, F. Wiedemann, W.S. Kunz, Permeabilized cell and skinned fiber techniques in studies of mitochondrial function in vivo, Mol. Cell. Biochem. 184 (1998) 81–100.

[58] R. Paasuke, M. Eimre, A. Piirsoo, N. Peet, L. Laada, L. Kadaja, M. Roosimaa, M. Paasuke, A. Martson, E. Seppet, K. Paju, Proliferation of human primary myoblasts is associated with altered energy metabolism in dependence on ageing in vivo and in vitro, Oxidative Med. Cell. Longev. 2016 (2016) 8296150, https://doi.org/10.1155/2016/8296150.

[59] E. Seppet, M. Eimre, N. Peet, K. Paju, E. Orlova, M. Ress, S. Kovask, A. Piirsoo, V.A. Saks, F.N. Gellerich, S. Zierz, E.K. Seppet, Compartmentation of energy metabolism in atrial myocardium of patients undergoing cardiac surgery, Mol. Cell. Biochem. 270 (2005) 49–61, https://doi.org/10.1007/s11010-005-3780-y.

[60] K.J. Livak, T.D. Schmittgen, Analysis of relative gene expression data using real-time quantitative PCR and the 2(−Delta Delta C(T)) method, Methods 25 (2001) 402–408, https://doi.org/10.1006/meth.2001.1262.

[61] V. Saks, T. Kaambre, R. Guzun, T. Anmann, P. Sikk, U. Schlattner, T. Wallimann, M. Aliev, M. Vendelin, The creatine kinase phosphotransfer network: thermodynamic and kinetic considerations, the impact of the mitochondrial outer membrane and modelling approaches, Subcell. Biochem. 46 (2007) 27–65.

[62] P.P. Dzeja, K. Hoyer, R. Tian, S. Zhang, E. Nemutlu, M. Spindler, J.S. Ingwall, Rearrangement of energetic and substrate utilization networks compensate for chronic myocardial creatine kinase deficiency, J. Physiol. 589 (2011) 5193–5211, https://doi.org/10.1113/jphysiol.2011.212829.

[63] M. Eimre, S. Kasvandik, M. Ivask, S. Koks, Proteomic dataset of wolframin-deficient mouse heart and skeletal muscles, Data in Brief 21 (2018) 616–619, https://doi.org/10.1016/j.dib.2018.10.015.

[64] A.M. Rossi, H.M. Eppenberger, P. Volpe, R. Cotrufo, T. Wallimann, Muscle-type MM creatine kinase is specifically bound to sarcoplasmic reticulum and can support Ca2+ uptake and regulate local ATP/ADP ratios, J. Biol. Chem. 265 (1990) 5258–5266.

[65] K. Tepp, N. Timohhina, M. Puurand, A. Klepinin, V. Chekulayev, I. Shevchuk, T. Kaambre, Bioenergetics of the aging heart and skeletal muscles: modern concepts and controversies, Ageing Res. Rev. 28 (2016) 1–14, https://doi.org/10.1016/j.arr.2016.04.001.

[66] S. Zervou, X. Yin, A.A. Nabeebaccus, B.A. O'Brien, R.L. Cross, D.J. McAndrew, R.A. Atkinson, T.R. Eykyn, M. Mayr, S. Neubauer, C.A. Lygate, Proteomic and metabolomic changes driven by elevating myocardial creatine suggest novel metabolic feedback mechanisms, Amino Acids (2016) 1–13, https://doi.org/10.1007/s00726-016-2236-x.

[67] R. Porosk, A. Terasmaa, R. Mahlapuu, U. Soomets, K. Kilk, Metabolomics of the Wolfram syndrome 1 gene (Wfs1) deficient mice, OMICS 21 (2017) 721–732, https://doi.org/10.1089/omi.2017.0143.

[68] M. Karu-Varikmaa, M. Saaremäe, P. Sikk, T. Käämbre, M. Metsis, V. Saks, Regulation of mitochondrial respiration by different tubulin isoforms in vivo, Biophys. J. 100 (2011) 459a.

[69] T.K. Rostovtseva, S.M. Bezrukov, VDAC inhibition by tubulin and its physiological implications, Biochim. Biophys. Acta 1818 (2012) 1526–1535, https://doi.org/10.1016/j.bbamem.2011.11.004.

[70] M. Eimre, K. Paju, N. Peet, L. Kadaja, M. Tarrend, S. Kasvandik, J. Seppet, M. Ivask, E. Orlova, S. Koks, Increased Mitochondrial Protein Levels and Bioenergetics in the Musculus Rectus Femoris of Wfs1-Deficient Mice, Oxidative Medicine and Cellular Longevity, v2018, (2018), https://doi.org/10.1155/2018/3175313 12p.

[71] M. Jastroch, A.S. Divakaruni, S. Mookerjee, J.R. Treberg, M.D. Brand, Mitochondrial proton and electron leaks, Essays Biochem. 47 (2010) 53–67, https://doi.org/10.1042/bse0470053.

[72] M.D. Brand, J.L. Pakay, A. Ocloo, J. Kokoszka, D.C. Wallace, P.S. Brookes, E.J. Cornwall, The basal proton conductance of mitochondria depends on adenine nucleotide translocase content, Biochem. J. 392 (2005) 353–362, https://doi.org/10.1042/BJ20050890.

[73] V. Napolioni, A.M. Persico, V. Porcelli, L. Palmieri, The mitochondrial aspartate/glutamate carrier AGC1 and calcium homeostasis: physiological links and abnormalities in autism, Mol. Neurobiol. 44 (2011) 83–92, https://doi.org/10.1007/s12035-011-8192-2.

[74] A. Prola, Z. Nichtova, J. Pires Da Silva, J. Piquereau, K. Monceaux, A. Guilbert, M. Gressette, R. Ventura-Clapier, A. Garnier, I. Zahradnik, M. Novotova, C. Lemaire, Endoplasmic reticulum stress induces cardiac dysfunction through architectural modifications and alteration of mitochondrial function in cardiomyocytes, Cardiovasc. Res. 115 (2019) 328–342, https://doi.org/10.1093/cvr/cvy197.

[75] C.M.F. Monaco, M.C. Hughes, S.V. Ramos, N.E. Varah, C. Lamberz, F.A. Rahman, C. McGlory, M.A. Tarnopolsky, M.P. Krause, R. Laham, T.J. Hawke, C.G.R. Perry, Altered mitochondrial bioenergetics and ultrastructure in the skeletal muscle of young adults with type 1 diabetes, Diabetologia 61 (2018) 1411–1423, https://doi.org/10.1007/s00125-018-4602-6.

Appendix 2

Publication II
Tepp, K., Aid-Vanakova, J., Puurand, M., Timohhina, N., Reinsalu, L., Tein, K., Plaas, M., Shevchuk, I., Terasmaa, A., & Kaambre, T. (2022). Wolframin deficiency is accompanied with metabolic inflexibility in rat striated muscles. Biochem Biophys Rep, 30, 101250. https://doi.org/10.1016/j.bbrep.2022.101250

Wolframin deficiency is accompanied with metabolic inflexibility in rat striated muscles

Kersti Tepp [a,*,1], Jekaterina Aid-Vanakova [a,b,1], Marju Puurand [a], Natalja Timohhina [a], Leenu Reinsalu [a,b], Karin Tein [a,c], Mario Plaas [c], Igor Shevchuk [a], Anton Terasmaa [a], Tuuli Kaambre [a]

[a] Laboratory of Chemical Biology, National Institute of Chemical Physics and Biophysics, Akadeemia tee 23, 12618, Tallinn, Estonia
[b] Department of Chemistry and Biotechnology, School of Science, Tallinn University of Technology, Ehitajate tee 5, 12618, Tallinn, Estonia
[c] Institute of Biomedicine and Translational Medicine, Laboratory Animal Centre, University of Tartu, 14B Ravila Street, Tartu, 50411, Estonia

ABSTRACT

The protein wolframin is localized in the membrane of the endoplasmic reticulum (ER), influencing Ca2+ metabolism and ER interaction with mitochondria, but the exact role of the protein remains unclear. Mutations in Wfs1 gene cause autosomal recessive disorder Wolfram syndrome (WS). The first symptom of the WS is diabetes mellitus, so accurate diagnosis of the disease as WS is often delayed. In this study we aimed to characterize the role of the Wfs1 deficiency on bioenergetics of muscles. Alterations in the bioenergetic profiles of Wfs1-exon-5-knock-out (Wfs1KO) male rats in comparison with their wild-type male littermates were investigated using high-resolution respirometry, and enzyme activity measurements. The changes were followed in oxidative (cardiac and soleus) and glycolytic (rectus femoris and gastrocnemius) muscles. There were substrate-dependent alterations in the oxygen consumption rate in Wfs1KO rat muscles. In soleus muscle, decrease in respiration rate was significant in all the followed pathways. The relatively small alterations in muscle during development of WS, such as increased mitochondrial content and/or increase in the OxPhos-related enzymatic activity could be an adaptive response to changes in the metabolic environment. The significant decrease in the OxPhos capacity is substrate dependent indicating metabolic inflexibility when multiple substrates are available.

1. Introduction

The protein wolframin consists of 890 amino acids, and is located in the membrane of endoplasmic reticulum (ER) with nine *trans*-membrane domains [1–3]. Wolframin regulates Ca^{2+} homeostasis, has influence on the formation of mitochondria-associated ER membrane (MAM) and affects Ca^{2+} transport between mitochondria and ER [4–6]. Alterations in intracellular wolframin content are associated with ER stress and activation of the Unfolded Protein Response (UPR) [7–16]. However, the exact mechanism of wolframin function is still not clear [8,17–20].

Mutations in the wolframin coding WFS1 gene cause autosomal recessive disorder Wolfram syndrome 1 (WS1) [21–23]. Usually WS starts with *diabetes mellitus* (DM, mostly during the first decade of the life), followed by optic atrophy (OA, in the beginning of the second decade), *diabetes insipidus (DI)* and deafness (D); therefore acronym

DIDMOAD is used. Defects in the CDGSH Iron Sulfur Domain 2 (CISD2, or ERIS (endoplasmic reticulum intermembrane small protein or WFS2) gene, cause progression of illness with symptoms alike WS1, named Wolframin Syndrome type 2 (WS2, approximately 5–10% of the WS cases) [24,25]. However, till now a direct functional interaction between CISD2 and wolframin has not been detected [26,27].

WS first symptom, glucose intolerance, is due to the progressive loss of pancreatic β-cells. This, and simultaneous neuronal tissue degeneration is initiated by ER stress, UPR activation and altered Ca^{2+} homeostasis [28,29]. WS is a rare disease and is doubtlessly underdiagnosed, as after DM symptoms appear, diabetes and its complications are primarily targeted [30].

ER works in close functional interaction with mitochondria. Several symptoms of WS have common features with mitochondrial diseases like Friedreich ataxia and Leber's hereditary optic neuropathy (LHON)

[31–33]. Direct mitochondrial DNA (mtDNA) deletions have been observed only in some of WS patients, but the altered regions vary and do not occur in most WS cases [33–36].

Besides nerve and β-cells, the content of the wolframin is high in the heart and skeletal muscles [2]. The role of the wolframin as Ca²⁺ metabolism regulator, and the fact that these muscles relay mostly on mitochondrial energy metabolism should cause strong alterations in the heart and oxidative muscle cells of WS patients. Also, development of the insulin resistance and diabetes in WS patients should be accompanied by changes in both skeletal and heart muscles mitochondria as is described in patients with similar symptoms without WS [31,37]. It is necessary to clarify what modifications have taken place in the bioenergetic profile of skeletal and heart muscle cells in wolframin deficiency. Severe skeletal muscle dysfunction, and shift in muscle type have been detected in WS2 [24,25,38]. In the case of WS1 the reported alterations in the skeletal muscles are milder, if at all, and appear in a later stage of the disease. Structural defects in heart muscle of the WS1 patients is noticed in somewhat higher percentage than in average population but it is not prevailing in all patients [30,39–41]. However, it has been shown that WFS1-deficient rat left ventricle cardiomyocytes had increased contractility (both amplitude and duration of the contraction) due to the prolonged cytosolic calcium transients [18]. Also, a higher relative incidence of sinus tachycardia and atrioventricular arrhythmias has been shown in WS patients [42].

In our previous study we investigated alterations in mitochondrial metabolism of Wfs1KO mice muscles and found decreased and less coupled NADH-linked ADP-stimulated respiration in comparison with wild type (WT) littermates [43]. These alterations are largely substrate-dependent. In Wfs1KO mice muscles the maximal mitochondrial respiration in the presence of Glutamate (Glut) and Malate (Mal) as respiratory system complex I (CI)-linked substrates was decreased in all studied muscle types, accompanied with significantly increased Leak respiration in glycolytic muscles. With Mal and Pyruvate (Pyr) as substrates the increased Leak was detected only in glycolytic muscles (rectus femoris (RF)) and white gastrocnemius (GW)) and decrease in CI linked oxygen consumption was significant only in GW [43,44]. Decrease in adenylate and creatine kinase enzymatic activities of skeletal muscles of wolframin-deficient glucose-intolerant animals and changes in coupling of these enzymes to oxidative phosphorylation (OxPhos) suggest the reconfiguration of energy transport networks and thus could affect muscle performance at higher workloads [43].

Alterations in substrate preferences, detected in WFS1KO mice muscles, agree with the described incapability to use certain available substrates, metabolic inflexibility in diabetes and other metabolic diseases [45]. In diabetic heart, even in hyperglycemic situation, heart muscle cells mostly use fatty acids (FA) [46,47]. In the contrary, the failing heart is metabolically inflexible with increased glucose metabolism [47]. In the skeletal muscle cells of individuals with type-2 diabetes glucose oxidation is elevated and FA usage reduced [48,49].

The extent and severity of the alterations due to the WS in a specific cell type seems not to be directly related to the wolframin content of the cells. Therefore it is possible that some cells have developed adaptation mechanisms to overcome the wolframin deficiency. Knowledge of these means could give us valuable information for the development of better medication for WS. Also, WS1-specific change in the energy metabolism of muscle cells helps to clarify the role of wolframin in cells in different tissues to enable more precise medication.

Generation and characterization of rat model of Wolfram syndrome (Wfs1-exon-5 KO, Wfs1KO), used in this study was described earlier [50]; exon 5 of Wfs1 gene is deleted in this model and results in appearance of WS symptoms [50]. This is a loss of function model and the order of appearance of WS symptoms is similar to the WS development in humans. First, a decrease in glucose-stimulated insulin release is detected from 3 month of age in this Wfs1KO rat model, glucose intolerance progresses with age and culminates with severe hyperglycemia and insulin dependent diabetes mellitus at the age of 12 months [50].

From this age also brainstem and optic nerve neurodegeneration is observed. Diabetes mellitus and optic nerve atrophy appears in childhood or puberty for most of human WS patients, while in the rat model WS symptoms appear after sexual maturity. Drawing of direct parallels from rat studies to human patients must always be done with caution, such limitation is inherent for any animal model of human disease. However, this is unlikely to affect conclusion of this study on the role of Wfs1 on muscle bioenergetics.

The aim of our research is to determine the alterations in bioenergetics profile of the wolframin deficient muscle and clarify the role of the wolframin in the muscle energy metabolism.

2. Methods

2.1. Laboratory animals and chemicals

In all the experiments we used wild type (WT) male Wistar rats and their Wfs1-deficient male littermates (age 8–9 months). Wfs1-deficient rats were generated by deletion of exon 5 in Wfs1 gene resulting in loss of 27 amino acids from the Wfs1 protein, and loss of function of the protein [50]. Breeding and genotyping of the rats were performed at the Laboratory Animal Centre of the Institute of Biomedicine and Translational Medicine, University of Tartu. The rats were housed under standard laboratory conditions (at constant temperature 22 °C and a 12:12 h light/dark cycle with free access to food and water). Animal experiments were approved by the Estonian National Board of Animal Experiments (protocol nr. 114 from 13.10.2017) in accordance with the European Communities Directive (86/609/EEC).

Only ultra-pure chemicals suitable for molecular biology and work with cell cultures were used in experiments. All chemicals were purchased from Fluka and Sigma-Aldrich (Saint Louis, MO, USA).

2.2. Preparation of skinned muscle fibers

For fiber preparation animals were anaesthetized by intraperitoneal injection of ketamine (75 mg/kg) and dexmedetomidin (1 mg/kg), decapitated. Permeabilized fibers were prepared from the heart, *m. soleus*, GW and RF according to the methods described previously [51]. The cells' sarcolemma was permeabilized by saponin treatment (50 μg/mL) for 30 min at 4 °C. Fibers were washed in Mitomedium B solution: EGTA (0.5 mM), MgCl₂.6H₂O (3.0 mM), K-lactobionate (60 mM), KH₂PO₄ (3.0 mM), taurine (20 mM), HEPES (20 mM), sucrose (110 mM), dithiothreitol (DTT, 0.5 mM), bovine serum albumin (BSA, 5 mg/ml)) at pH 7.1 supplemented with leupeptin (5 μM) for the protection of cytoskeletal proteins from lysosomal proteolysis and kept in the same solution at 4 °C under constant stirring until used for experiments.

2.3. Measurements of oxygen consumption

All measurements of oxygen consumption were performed by a high-resolution respirometry instrument Oxygraph-2K (OROBOROS Instruments, Innsbruck, Austria). Experiments were carried out at 25 °C in the Mitomedium B solution [52], supplemented with BSA (5 mg/mL) under continuous magnetic stirring. The permeabilized fiber was weighted and inserted into the oxygraphic chamber with respiration media (Mitomedium B solution) supplemented with respiratory substrates according to the protocol. The measured oxygen consumption rates are presented as nmolO₂/min per mg wet weight.

2.4. Respiratory complexes protocol (RC)

In order to compare the individual capacity of the ETS complexes in relation to two substrate pathways, the classical protocol for measurement of respiratory complexes was applied. All the concentrations presented in the following protocols are final concentrations in the oxygraphic camber.

Permeabilized muscle fibers were inserted into an oxygraph chamber filled with Mitomedium B solution supplemented with Mal (2 mM). First either Glut (Protocol 1A) or Pyr (Protocol 1B) was added to record basal Leak respiration in the absence of adenylates. Then in both protocols ADP (2 mM) was added and the respiratory capacity of ETS complex I (CI) was measured. After inhibition of CI with rotenone (Rot, 2.5 μM) the activity of complex II (CII) was determined in the presence of CII-dependent substrate, succinate (Suc, 10 mM). Then ETS complex III was inhibited with Antimycin A (AntA, 10 μM) and addition of N,N,N′, N′-tetramethyl-p-phenylenediamine (TMPD; 1 mM) demonstrates maximal capacity of complex IV (CIV). Finally, addition of NaCN (1 mM) inhibited cytochrome oxidase (COX) and blocked electron transport; as a result it allowed detecting residual oxygen consumption due to TMPD oxidation reaction.

2.5. Substrate-uncoupler-inhibitor titration (SUIT) protocols

To clarify the task of separate substrate branches of OxPhos and maximal respiratory capacity in the presence of multiple substrates, following modified SUIT protocols were used [53].

The SUIT-1 protocol was applied to determine the role of FA oxidation linked OxPhos independently from glucose-linked pathway. In this protocol firstly Mal and octanoyl carnitine (Oct, 0.2 mM) were injected into the chamber to register basal Leak oxygen consumption, after that ADP (2 mM) was added to stimulate phosphorylation system. To complement the system with substrate from glycolytic pathway, Pyr (5 mM) was inserted. In order to detect maximal capacity of CI, Glut (5 mM) was added into the chamber. Addition of Suc (10 mM) allowed to measure the ADP-dependent respiration when electrons are fed simultaneously to the ETS via CI and CII. Subsequent addition of ADP (final concentration of 5 mM) allowed controlling the limitations in the efficiency of ATP synthase [54]. The maximal capacity of the ETS was evaluated with titration of uncoupler carbonyl cyanide-4-(trifluoromethoxy) phenylhydrazone (FCCP) until saturation of respiration was reached. Subsequent inhibition of CI by Rot (2.5 μM) allowed to determine the CII-linked electron transfer capacity. Inhibition of Complex III (CIII) by AntA (10 μM) allowed to determine the residual oxygen consumption.

In the third, SUIT-2 protocol, to control whether the contribution of glycolytic substrate pathway could have inhibitory influence on the ETS, the substrates were presented in reverse way. First Mal with Pyr was introduced, then, after registration of Leak respiration, ADP-dependent oxygen consumption was determined. Next, Oct was injected and combined CI-substrate linked respiration was detected. Maximum CI-linked oxygen consumption rate was measured with the Glut. At the end, the CII-linked substrate Suc was added to activate ETS CII-dependent respiration.

In the fourth, SUIT-3 protocol, maximal capacity of glucose-linked substrate pathway was determined independently from FA pathway. First Mal with Pyr was introduced into the chamber, then, after registration of Leak respiration, ADP-dependent oxygen consumption was determined. After that, maximum rate of NADH-linked oxygen consumption was measured with the Glut. Then, in the presence of CII-linked substrate Suc joint CI and CII-dependent respiration was registered. Finally, the capacity of ETS was evaluated by titration with FCCP.

2.6. Energy transfer pathways

To determine the alterations in the energy transfer pathways, the influence of AK or CK pathway activation on the mitochondrial respiration was measured. For that, after injection of substrates Mal and Glut, ATP-ases were activated with MgATP (2 mM in oxidative and 0.1 mM on glycolytic muscles). After that, addition of 10 mM Cr or 2 mM AMP activated the respective pathways and an increase in respiratory rate indicates an association between the respective energy transfer network and OxPhos [52].

2.7. Determination of enzymatic activities

2.7.1. Preparation of cell lysates

Pieces of muscles were snap frozen in liquid nitrogen and stored at −80 °C. Tissues were grinded in liquid nitrogen with pestle and homogenized in the Tris-HCl (pH = 8.1), the medium containing KCl (0.9 M), glucose (10 mM), MgCl$_2$ (20 mM), EDTA-Na$_2$ (10 mM), Triton X-100 (0.25%) and leupeptin (5 μg/mL), at pH 8 using a Retsch Mixer Mill (Retsch) at 25 Hz for 2 min, then centrifuged at 12,000 rcf for 20 min at 4 °C. The supernatants were used for enzymatic assays. Protein concentrations were determined by Pierce BCA Protein Assay Kit according to the manufacturer recommendations using bovine serum albumin (BSA) as a standard.

2.7.2. Measurements of activities

Determination of HK activity was performed using a spectrophotometer (PerkinElmer, U.S.) in solution containing Tris–HCl (50 mM), KCl (45 mM), NaH$_2$PO$_4$ (1 mM), EDTA-Na$_2$ (0.5 mM), MgCl$_2$ (7.7 mM) glucose (4.2 mM), NADP (0.6 mM), MgATP (6.7 mM), glucose-6-phosphate dehydrogenase (G6PD) (1 IU/mL), adjusted at 25 °C. The rate of NADPH formation was monitored after addition of homogenate at 340 nm [55].

ETS Complex I activity was measured with spectrophotometer (PerkinElmer, U.S.) from homogenates in phosphate buffer (100 mM, pH 7.4) comprising NADH, Coenzyme Q1 stock B, KCN, and NaN$_3$ ca. 100 s. At the end rotenone was added to record rotenone insensitive activity of the preparation [56].

Citrate synthase activity was measured spectrophotometrically in cell lysates at 25 °C with a FLUOstar Omega microplate reader. Citrate synthase (CS) activity was determined by measuring the rate of thionitrobenzoic acid production at 412 nm [57].

2.8. DNA extraction and mitochondrial DNA (mtDNA) copy number

DNA was isolated from frozen rat muscle tissue samples using PureLinkTM Genomic DNA Mini Kit (Invitrogen, USA) according to the instructions provided by the manufacturer. DNA concentrations and quality were measured using the BioSpec-Nano spectrophotometer (Shimadzu, Japan).

The DNA from muscles was used to determine the mitochondrial DNA copy number by the comparison of mitochondrial and nuclear DNA measured by real-time PCR using the Rat Mitochondrial DNA Copy Number Kit (MCN2) (Detroit R&D, USA). The manufacturer's instructions were followed to prepare samples for PCR and to calculate the mtDNA copy number relative to nucDNA.

3. Results

In this study we determined alterations in the bioenergetic profile of the two oxidative (heart, soleus) and two glycolytic (RF and GW) muscles of the 8–9 month old Wfs1 deficient rats in comparison to WT littermates. To characterize alterations in the ETS profile, we measured sequential activation of ETS complexes and ADP-dependent oxygen consumption rate. We evaluated flexibility of OxPhos with different substrate combinations to switch between glucose-linked (Pyr) and FA (Oct) substrates.

First we determined oxygen consumption capacity for respiratory chain complexes CI, CII and CIV individually (RC protocol, Fig. 1), using respective substrates/inhibitors (two alternative CI-linked substrate combinations: Mal with Glut and Mal with Pyr). We did not register any statistically significant alteration in Wfs1KO muscles in comparison with WT animals for either substrate combination (Table 1 in Supplements).

Next we applied SUIT protocols where multiple ETS complexes are activated simultaneously, a situation which is more in line with *in vivo* conditions. At the beginning of the SUIT-1 protocol respiration is supported only by the FA pathway with Oct. In this state in the heart muscle
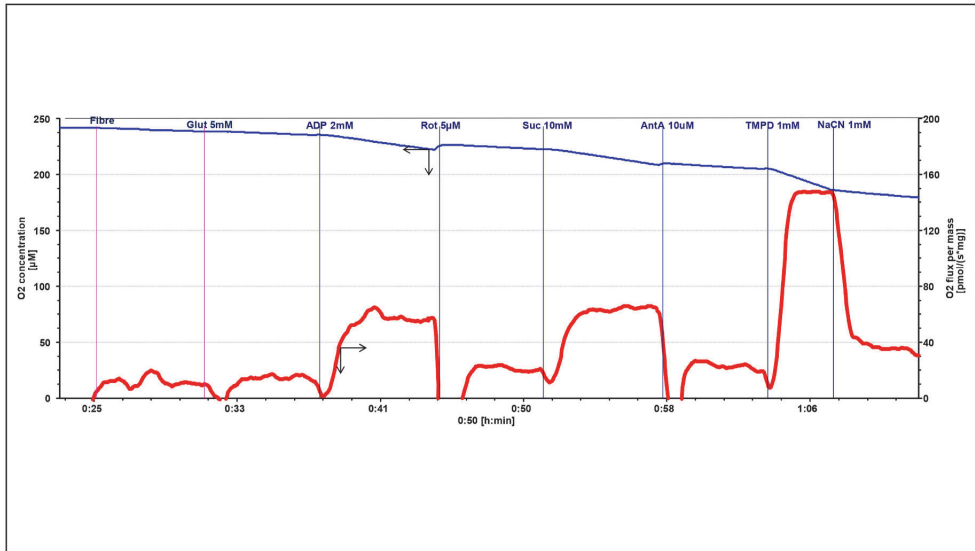
Fig. 1. Representative trace of oxygraphic measurement. Analysis of the individual respiratory chain complexes activities.
After insertion of the muscle fiber into the oxygraphic chamber we added CI – linked substrate glutamate (Glut, 5 mM; malate (2 mM) is in the medium), and the basal oxygen consumption rate without adenylates (Leak) is visible. Then the addition of ADP (2 mM) activates ATP-Synthase (maximal respiration via complex I (CI)). Thereafter, we inhibited CI with its specific inhibitor rotenone (Rot, 5 μM), added succinate (Succ, 10 mM) and registered maximal oxygen consumption capacity through CII. After insertion of antimycin A, (AntA, 10 μM), an inhibitor of complex III, we injected N,N,N',N'-tetramethyl-p-phenylenediamine (TMPD, 1 mM) and ascorbate (5 mM) to activate cytochrome c oxidase associated oxygen consumption, demonstrating the theoretical maximal respiration rate. Thereafter, we added Na cyanide (NaCN) to inhibit cytochrome c oxidase. Blue line – oxygen concentration in the medium, red line – oxygen consumption rate.

Table 1
Enzymatic activities of the wolframin-deficient (Wfs1KO) and wild type (WT) rat heart, m. soleus, m. rectus femoris (RF) and m. gastrocnemius white (GW) fibers.

Enzyme	Muscle	WT		Wfs1KO	
Citrate synthase μmol/mg	Heart	156.3	±9.8	156.9	±9.0
protein	Sol	44.3	±2.5	63.1	±5.7*
	RF	15.4	±0.9	17.1	±0.9
	GW	19.0	±2.3	29.0	±2.8**
Hexokinase μmol/mg protein	Heart	53.7	±2.6	60.3	±2.3
	Sol	28.1	±0.7	32.8	±0.5
	RF	8.2	±0.5	8.9	±0.5
	GW	7.9	±0.5	8.1	±0.5
Complex I μmol/mg protein	Heart	438.0	±26.6	489.2	±51.4
	Sol	190.4	±7.3	220.2	±14.8
	RF	11.9	±0.9	20.6	±1.8**
Complex I/CS	Heart	2.8	±0.2	3.1	±0.4
	Sol	4.3	±0.3	3.5	±0.4
	RF	0.8	±0.1	1.2	±0.1*

**p < 0.01; *p < 0.05; n = 6–10.

there was no difference in FA-linked respiration rate between WT and Wfs1KO. In contrast, in soleus, which also represents oxidative striated muscle, there was a clear decline in the respiratory rate with Oct in Wfs1KO animal (Fig. S1 in Supplements). Following the protocol, CI-linked respiration was then activated. Registered maximal CI-linked respiration and maximal OxPhos (CI + CII) were significantly reduced in both oxidative muscles of Wfs1KO compared to the WT (p=<0.01 (Fig. 2); and p=<0.01 (Fig. S1 in Supplements);), for heart and soleus, respectively). In the normal heart, the sequential addition of substrates was followed by an increase in respiration rate and peaked at the highest level in the presence of the uncoupler (Fig. S1 in Supplements), reflecting the plasticity and the ability of mitochondrial energy metabolism to use different substrates simultaneously. This plasticity appears to be altered in Wfs1KO animals and expresses as loss in efficiency to use

glucose-linked carbon sources if mitochondria are already switched to FA oxidation. At the same time, when the same protocol was applied to glycolytic muscles there was no significant differences in the OxPhos rates in a situation when FA oxidation were activated before glucose-linked pathway of Wfs1KO in comparison with WT.

We determined whether the decrease in the respiration rate with the glucose-linked substrate in oxidative muscle was caused by the FA pathway that inhibited utilisation of other CI-linked substrates with SUIT-2 protocol. We activated the pathways in the reversed order where the glucose-linked substrate, Pyr was added first. At these conditions no significant alteration was detected in Wfs1KO heart muscle (Fig. 2, Fig. S1 in Supplements) suggesting that FA pathway activation was the one that inhibited the glucose-linked pathway in the SUIT1 protocol. However, the OxPhos rates of the Wfs1KO soleus muscle are significantly decreased regardless of the order of added substrates (p=<0.01, Fig. 2; Table 1 in Supplements).

In glycolytic muscles, the maximal OxPhos capacity of the RF with SUIT2 protocol was lower in Wfs1KO rat (p < 0.05), whereas in the Wfs1KO GW muscle the CI-linked and maximal OxPhos capacity was even increased compared to WT (p < 0.05 and p < 0.01 respectively; Fig. 2). To the contrary of the WT RF muscle, in GW the addition of Oct after Pyr did not increase the respiration rates of WT and Wfs1KO rat GW to the level at which they reached when the substrates were added in reversed order (Fig. 2).

We used SUIT-3 protocol to determine alterations in the use of the glucoses-linked substrate pathway. In the heart muscle there was no significant differences in the ETS capacity between Wfs1KO and WT when Pyr was used as a substrate. Again, reduced OxPhos rate was registered in soleus muscle of Wfs1KO rat (p < 0.01), and no significant change were observed in the ETS capacity in glycolytic muscles of Wfs1KO animals (Fig. 2).

When comparing different substrate introduction orders within one muscle type only, some tendencies can be observed. In WT heart muscle
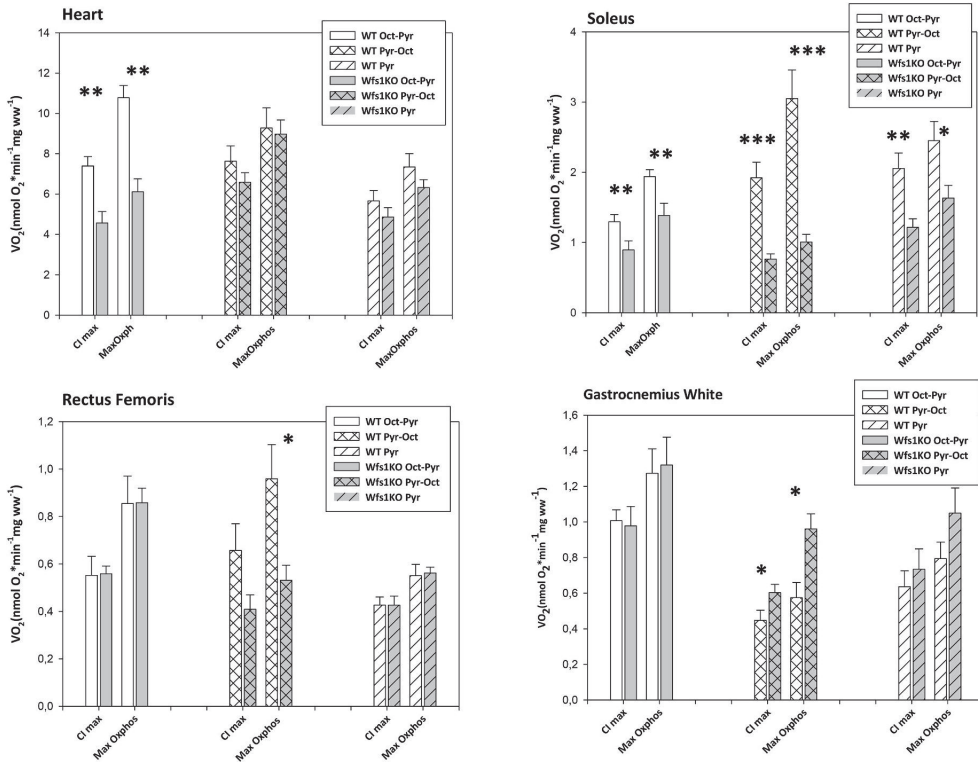
Fig. 2. OxPhos capacity through CI and maximal OxPhos values with simultaneously activated CI and CII - linked substrate pathways. Maximal oxygen consumption rates with CI- linked substrates (CI) and in the presence of simul
-taneously
activated complex I (CI) and CII-linked substrates (Max OxPhos) in wolframin-deficient (Wfs1KO) and wild type (WT) rat heart, m. s
oleus, m. r
ectus femoris (RF) and m. g
astrocnemius white (GW) fibers. In order to investigate the influence of multiple substrate pathways to the respiratory capacity, we used CI-linked substrates in variable order: in SUIT1 protocol (Oct-Pyr), first we inserted fatty acid - octanoyl carnitine (Oct, 0.2 mM), then added glucose-linked pathway substrate pyruvate (Pyr, 5 mM), para id="fspara0065">mM). In SUIT2 protocol (Pyr-Oct) first Pyr was introduced, then we added Oct, followed by Glut. In SUIT3 (Pyr) protocol we first injected Pyr and then Glut. In all the protocols malate (Mal, 2 mM) was in the medium and succinate (10 mM) was used as CII-linked substrate. Respiration rates are represented as nmol O2*min-1*mg ww-1; ***p <
0.001; **p <
0.01; *
p < 0.05; n = 6–
10.

the maximal OxPhos capacity as well as CI-linked respiration rate is higher with SUIT1 and SUIT2 protocol (with Oct; $p < 0.05$) than with SUIT3 (without Oct). In case of Wfs1KO heart muscle the highest oxygen consumption rate was detected with SUIT2 protocol (Pyr added first) in comparison with SUIT1 and SUIT3 ($p < 0.05$), indicating the alterations in fatty acid pathway. In WT glycolytic RF muscle there is a tendency to achieve higher maximal oxygen consumption rate in the presence of Oct and Pyr than with Pyr alone ($p < 0.05$). In contrast, in Wfs1KO RF muscle the OxPhos rates with SUIT2 as well as SUIT3 (just Pyr) protocol are lower in comparison with the situation when the fatty acid pathway is activated first, followed by Pyr (SUIT1 protocol ($p < 0.05$)), indicating an inhibitory effect of glycolysis-linked pathway on FA pathway.

To determine whether the fall in the oxygen consumption rate present with CI-linked substrates in heart, soleus and RF muscle were caused by a possible decrease in CI enzymatic activity the corresponding measurements were performed. No significant difference was found between WT and Wfs1KO muscle (Table 1). Also, in order to check for

alterations in the initial metabolic processing of intracellular glucose, we measured HK activity but no difference in Wfs1KO muscle was found (Table 1).

To assess differences in the amount of muscle tissue mitochondria the measurements of citrate synthase (CS) activity were performed. Significantly higher CS activity was detected in the GW and soleus muscle of Wfs1KO in comparison with WT and a similar trend was observed in RF, while there were no changes in heart muscle (Table 1). We also measured mtDNA content relative to nuclear DNA to determine whether the relatively unchanged respiratory capacity in the heart muscle was also consistent with unchanged mitochondrial content. Slightly higher mtDNA content was detected in WFS1KO rat heart muscle in comparison with WT.

Additionally, we performed oxygraphic measurements to identify possible modifications in energy transfer pathways in Wfs1KO muscles. We did not find any substantial alterations in parameters characterizing coupling between AK and CK energy transfer pathways and OxPhos

(Table S2 in Supplements).

4. Discussion

Heart and skeletal muscle cells have high wolframin abundance [2]. However, functional impact of Wfs1 deficiency in muscles is poorly studied. Ataxia and respiratory problems of WS patients are assumed to be directly related with neurodegeneration, not to the alterations in muscle metabolism. Though, there are few reports demonstrating altered cardiac function in WS patients e.g. incidences of cardiac murmurs [30,58]. One case was documented in Tunisia - a patient with moderate WS is accompanied with cardiomyopathy [59]. Disturbed cardiac calcium signalling and cardiac function was also reported in a rat model of WS [18]. Our aim was to determine bioenergetics profile of Wfs1 deficient heart and skeletal muscles.

In this study, 8–9 month old Wfs1KO rats were used. Previous research has shown that glucose intolerance and defective insulin secretion develops at the age of 7 month while basal blood and urine glucose levels are still normal [50]. The age was chosen to avoid artifacts related to elevated blood glucose. In order to investigate the alterations in muscles of different metabolic type we used two oxidative (heart and soleus) and two glycolytic (RF and GW) muscles.

The bioenergetic profile of a tissue is characterized via measurement of mitochondrial oxygen consumption, which depends on two main substrate delivery pathways: FA oxidation and glycolysis-linked pathway. Every cell has its substrate pathway preference, but in healthy tissue most of the cell types are able to shift between the substrates according to the metabolic situation. Inflexibility between these pathways is a hallmark in several metabolic diseases [45,47]. Similarly, decrease in the activity of some of the respiratory system complexes could be partly compensated by another. For example, increased CII activity accompanied with decreased CI one, is described in several tissues during aging and in the case of pathology [60–63].

Our study did not detect significant increase in the Leak oxygen consumption, indicating that functionality of the inner mitochondrial membrane of the muscles is not extensively altered in Wfs1 deficiency. Also, there were no significant alterations in maximal oxygen consumption capacity of individual respiratory complexes in oxidative muscles.

In Wfs1KO heart muscle the main alteration was inhibitory effect of activated FA pathway to the glucose-linked pathway usage. Our results are compatible with the previous knowledge that the energy production in the insulin resistant heart cells cannot effectively switch from FA to glucose-linked metabolism and rely primarily on FA oxidation, even in hyperglycaemic state [37,46,47]. Wfs1KO rats have insulin deficiency, while insulin sensitivity is not altered. Thus, these changes in heart muscle bioenergetics can be caused by insulin deficiency or Wfs1 deficiency, but not by insulin insensitivity. Interestingly, when the substrates are introduced in reversed order and the glucose-linked substrate pathway is activated before FA pathway, there was no difference between Wfs1KO and WT in the heart muscle fibre. The relatively small alteration in the heart muscle oxygen consumption could be explained by slightly increased mtDNA relative to nucDNA ratio in the heart muscle of Wfs1KO animals, indicating elevated mitochondrial content in Wfs1KO rats' heart (Table S2 in Supplements). Similar results have been demonstrated in mice genetic model of type-1 diabetes [64].

In other oxidative muscle *m. soleus*, there was a significant decrease in the respiratory capacity of Wfs1KO animals with all substrate combinations and it was not related to the order in which the substrates were presented. Higher CS activity in Wfs1KO soleus muscle also suggests an adaptive increase in the number of mitochondria in response to a decrease in ETS capacity. However, these changes do not appear to be sufficient to maintain OxPhos level similar to that in WT. The activity of CI in both oxidative muscles does not differ between Wfs1KO and WT rat, so the declined OxPhos capacity in these tissues is not related to the decreased activity of this ETS complex.

In both glycolytic muscles studied, we found slightly higher individual RC complexes respiratory rates in Wfs1KO muscles which is accompanied with increased CS activity of tissue.

In contrast to the heart muscle, Wfs1KO RF muscle display an inhibitory effect of glucose-linked pathway on FA usage. Similar phenomena, elevated glucose oxidation and reduced FA usage, is described also in the skeletal muscle cells of individuals with type-2 diabetes and other metabolic diseases [48,49,65]. The bioenergetics profile of Wfs1KO GW muscle indicates adaptive rearrangements in tissue level, as both CS activity and therefore also oxygen consumption rates per tissue mass have increased. Similar changes in muscle fibre type were described in RF muscle of Wfs1 deficient mice [44].

Altogether, the most common alteration in the bioenergetics of the muscle cells, caused by the wolframin deficiency is metabolic inflexibility in substrate usage (Fig. 3).

In Wfs1KO heart muscle the glucose-linked pathway is impaired when the FA pathway is activated first. But in glycolytic RF muscle, the activation of glucose-linked pathway blocks the FA usage. Interestingly, in oxidative soleus muscle the decrease in the OxPhos capacity is irrespective to the substrate pathway, while in glycolytic GW, higher CS activity preserves the OxPhos capacity in Wfs1KO muscle. Similar shift is visible in glycolytic RF muscle where in Wfs1KO muscle has higher CI activity than in WT.
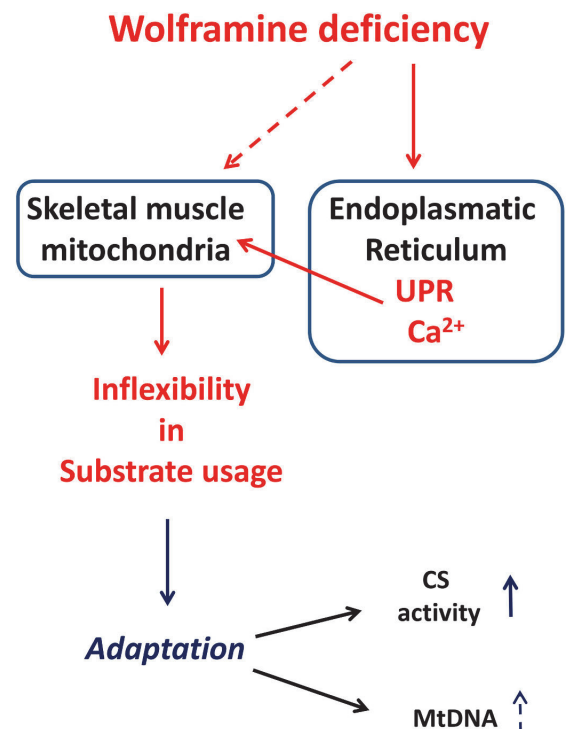

Fig. 3. Alterations in the bioenergetics profile in the rat muscle due to the WFS1 deficiency Wolframin
-deficiency alters Ca2+ metabolism and unfolded protein response (UPR) in endoplasmic reticulum. This initiates abnormalities in the OxPhos substrate use profile, leading to a loss of metabolic flexibility. The relatively small alterations like an increased mitochondrial content and/or increase in the
activities of some OxPhos-related enzymes
in skeletal and heart muscle during development of WS could be may be adaptive changes initiated by alterations in the metabolic environment:.
MtDNA – mitochondrial DNA; CS - citrate synthase.

This study demonstrates that the lack of wolframin doesn't cause universal changes in different muscles. However, deficiency of this protein contributes to the development of metabolic inflexibility in striated muscle tissue. In addition, the ability of mitochondria to use different substrate simultaneously is impaired. It remains to be investigated whether such metabolic inflexibility contributes to WS associated neuronal loss.

Author contributions

Conceptualization, Kersti Tepp, Jekaterina Aid-Vanakova and Anton Terasmaa; Formal analysis, Kersti Tepp; Investigation, Kersti Tepp, Jekaterina Aid-Vanakova, Marju Puurand, Natalja Timohhina, Leenu Reinsalu and Karin Tein; Methodology, Kersti Tepp and Jekaterina Aid-Vanakova; Resources, Mario Plaas; Supervision, Tuuli Kaambre; Visualization, Igor Shevchuk; Writing – original draft, Kersti Tepp and Jekaterina Aid-Vanakova; Writing – re-view & editing, Marju Puurand, Karin Tein, Mario Plaas, Anton Terasmaa and Tuuli Kaambre. All authors have read and agreed to the manuscript.

Declaration of competing interest

The authors declare that they have no known competing financial interests or personal relationships that could have appeared to influence the work reported in this paper.

Acknowledgments

Appendix A. Supplementary data

Supplementary data to this article can be found online at https://doi.org/10.1016/j.bbrep.2022.101250.

References

[1] K. Takeda, H. Inoue, Y. Tanizawa, Y. Matsuzaki, J. Oba, Y. Watanabe, K. Shinoda, Y. Oka, WFS1 (Wolfram syndrome 1) gene product: predominant subcellular localization to endoplasmic reticulum in cultured cells and neuronal expression in rat brain, Hum. Mol. Genet. 10 (2001) 477–484, https://doi.org/10.1093/hmg/10.5.477.

[2] S. Hofmann, C. Philbrook, K.D. Gerbitz, M.F. Bauer, Wolfram syndrome: structural and functional analyses of mutant and wild-type wolframin, the WFS1 gene product, Hum. Mol. Genet. 12 (2003) 2003–2012, https://doi.org/10.1093/hmg/ddg214.

[3] L. Li, S. Venkataraman, S. Chen, H. Fu, Function of WFS1 and WFS2 in the central nervous system: implications for Wolfram syndrome and alzheimer's disease, Neurosci. Biobehav. Rev. 118 (2020) 775–783, https://doi.org/10.1016/j.neubiorev.2020.09.011.

[4] M. Cagalinec, M. Liiv, Z. Hodurova, M.A. Hickey, A. Vaarmann, M. Mandel, A. Zeb, V. Choubey, M. Kuum, D. Safiulina, E. Vasar, V. Veksler, A. Kaasik, Role of mitochondrial dynamics in neuronal development: mechanism for Wolfram syndrome, PLoS Biol. 14 (2016), e1002511, https://doi.org/10.1371/journal.pbio.1002511.

[5] B. Delprat, T. Maurice, C. Delettre, Wolfram syndrome: MAMs' connection? Cell Death Dis. 9 (2018) 364, https://doi.org/10.1038/s41419-018-0406-3.

[6] C. La Morgia, A. Maresca, G. Amore, L.L. Gramegna, M. Carbonelli, E. Scimonelli, A. Danese, S. Patergnani, L. Caporali, F. Tagliavini, V. Del Dotto, M. Capristo, F. Sadun, P. Barboni, G. Savini, S. Evangelisti, C. Bianchini, M.L. Valentino, R. Liguori, C. Tonon, C. Giorgi, P. Pinton, R. Lodi, V. Carelli, Calcium mishandling in absence of primary mitochondrial dysfunction drives cellular pathology in Wolfram Syndrome, Sci. Rep. 10 (2020) 4785, https://doi.org/10.1038/s41598-020-61735-3.

[7] H. Ishihara, S. Takeda, A. Tamura, R. Takahashi, S. Yamaguchi, D. Takei, T. Yamada, H. Inoue, H. Soga, H. Katagiri, Y. Tanizawa, Y. Oka, Disruption of the WFS1 gene in mice causes progressive beta-cell loss and impaired stimulus-secretion coupling in insulin secretion, Hum. Mol. Genet. 13 (2004) 1159–1170, https://doi.org/10.1093/hmg/ddh125.

[8] T. Yamada, H. Ishihara, A. Tamura, R. Takahashi, S. Yamaguchi, D. Takei, A. Tokita, C. Satake, F. Tashiro, H. Katagiri, H. Aburatani, J. Miyazaki, Y. Oka, WFS1-deficiency increases endoplasmic reticulum stress, impairs cell cycle progression and triggers the apoptotic pathway specifically in pancreatic beta-cells, Hum. Mol. Genet. 15 (2006) 1600–1609, https://doi.org/10.1093/hmg/ddl081.

[9] Y. Ohta, A. Taguchi, T. Matsumura, H. Nakabayashi, M. Akiyama, K. Yamamoto, R. Fujimoto, R. Suetomi, A. Yanai, K. Shinoda, Y. Tanizawa, Clock gene dysregulation induced by chronic ER stress disrupts beta-cell function, EBioMedicine 18 (2017) 146–156, https://doi.org/10.1016/j.ebiom.2017.03.040.

[10] S. Morikawa, T. Tajima, A. Nakamura, K. Ishizu, T. Ariga, A novel heterozygous mutation of the WFS1 gene leading to constitutive endoplasmic reticulum stress is the cause of Wolfram syndrome, Pediatr. Diabetes 18 (2017) 934–941, https://doi.org/10.1111/pedi.12513.

[11] J.R. Porter, T.G. Barrett, Monogenic syndromes of abnormal glucose homeostasis: clinical review and relevance to the understanding of the pathology of insulin resistance and beta cell failure, J. Med. Genet. 42 (2005) 893–902, https://doi.org/10.1136/jmg.2005.030791.

[12] S.G. Fonseca, M. Fukuma, K.L. Lipson, L.X. Nguyen, J.R. Allen, Y. Oka, F. Urano, WFS1 is a novel component of the unfolded protein response and maintains homeostasis of the endoplasmic reticulum in pancreatic beta-cells, J. Biol. Chem. 280 (2005) 39609–39615, https://doi.org/10.1074/jbc.M507426200.

[13] D. Takei, H. Ishihara, S. Yamaguchi, T. Yamada, A. Tamura, H. Katagiri, Y. Maruyama, Y. Oka, WFS1 protein modulates the free Ca(2+) concentration in the endoplasmic reticulum, FEBS Lett. 580 (2006) 5635–5640, https://doi.org/10.1016/j.febslet.2006.09.007.

[14] S. Lu, K. Kanekura, T. Hara, J. Mahadevan, L.D. Spears, C.M. Oslowski, R. Martinez, M. Yamazaki-Inoue, M. Toyoda, A. Neilson, P. Blanner, C.M. Brown, C.F. Semenkovich, B.A. Marshall, T. Hershey, A. Umezawa, P.A. Greer, F. Urano, A calcium-dependent protease as a potential therapeutic target for Wolfram syndrome, Proc. Natl. Acad. Sci. U. S. A. 111 (2014) E5292–E5301, https://doi.org/10.1073/pnas.1421055111.

[15] M. Zatyka, C. Ricketts, G. da Silva Xavier, J. Minton, S. Fenton, S. Hofmann-Thiel, G.A. Rutter, T.G. Barrett, Sodium-potassium ATPase 1 subunit is a molecular partner of Wolframin, an endoplasmic reticulum protein involved in ER stress, Hum. Mol. Genet. 17 (2008) 190–200, https://doi.org/10.1093/hmg/ddm296.

[16] A.A. Osman, M. Saito, C. Makepeace, M.A. Permutt, P. Schlesinger, M. Mueckler, Wolframin expression induces novel ion channel activity in endoplasmic reticulum membranes and increases intracellular calcium, J. Biol. Chem. 278 (2003) 52755–52762, https://doi.org/10.1074/jbc.M310331200.

[17] C. Angebault, J. Fauconnier, S. Patergnani, J. Rieusset, A. Danese, C.A. Affortit, J. Jagodzinska, C. Megy, M. Quiles, C. Cazevieille, J. Korchagina, D. Bonnet-Wersinger, D. Milea, C. Hamel, P. Pinton, M. Thiry, A. Lacampagne, B. Delprat, C. Delettre, ER-mitochondria cross-talk is regulated by the Ca(2+) sensor NCS1 and is impaired in Wolfram syndrome, Sci. Signal. 11 (2018), https://doi.org/10.1126/scisignal.aaq1380.

[18] M. Cagalinec, A. Zahradnikova, A. Zahradnikova Jr., D. Kovacova, L. Paulis, S. Kurekova, M. Hot'ka, J. Pavelkova, M. Plaas, M. Novotova, I. Zahradnik, Calcium signaling and contractility in cardiac myocyte of wolframin deficient rats, Front. Physiol. 10 (2019) 172, https://doi.org/10.3389/fphys.2019.00172.

[19] S. Gharanei, M. Zatyka, D. Astuti, J. Fenton, A. Sik, Z. Nagy, T.G. Barrett, Vacuolar-type H+-ATPase V1A subunit is a molecular partner of Wolfram syndrome 1 (WFS1) protein, which regulates its expression and stability, Hum. Mol. Genet. 22 (2013) 203–217, https://doi.org/10.1093/hmg/dds400.

[20] S. Koks, R.W. Overall, M. Ivask, U. Soomets, M. Guha, E. Vasar, C. Fernandes, L. C. Schalkwyk, Silencing of the WFS1 gene in HEK cells induces pathways related to neurodegeneration and mitochondrial damage, Physiol. Genom. 45 (2013) 182–190, https://doi.org/10.1152/physiolgenomics.00122.2012.

[21] T.G. Barrett, S.E. Bundey, A.R. Fielder, P.A. Good, Optic atrophy in Wolfram (DIDMOAD) syndrome, Eye 11 (Pt 6) (1997) 882–888.

[22] T.G. Barrett, S.E. Bundey, Wolfram (DIDMOAD) syndrome, J. Med. Genet. 34 (1997) 838–841.

[23] L. Rigoli, F. Lombardo, C. Di Bella, Wolfram syndrome and WFS1 gene, Clin. Genet. 79 (2011) 103–117, https://doi.org/10.1111/j.1399-0004.2010.01522.x.

[24] Z.Q. Shen, Y.L. Huang, Y.C. Teng, T.W. Wang, C.H. Kao, C.H. Yeh, T.F. Tsai, CISD2 maintains cellular homeostasis, Biochimica et biophysica acta, Mol. Cell Res. 1868 (2021) 118954, https://doi.org/10.1016/j.bbamcr.2021.118954.

[25] N.C. Chang, M. Nguyen, J. Bourdon, P.A. Risse, J. Martin, G. Danialou, R. Rizzuto, B.J. Petrof, G.C. Shore, Bcl-2-associated autophagy regulator Naf-1 required for maintenance of skeletal muscle, Hum. Mol. Genet. 21 (2012) 2277–2287, https://doi.org/10.1093/hmg/dds048.

[26] L. Rigoli, C. Di Bella, Wolfram syndrome 1 and Wolfram syndrome 2, Curr. Opin. Pediatr. 24 (2012) 512–517, https://doi.org/10.1097/MOP.0b013e328354ccdf.

[27] S. Amr, C. Heisey, M. Zhang, X.J. Xia, K.H. Shows, K. Ajlouni, A. Pandya, L.S. Satin, H. El-Shanti, R. Shiang, A homozygous mutation in a novel zinc-finger protein, ERIS, is responsible for Wolfram syndrome 2, Am. J. Hum. Genet. 81 (2007) 673–683, https://doi.org/10.1086/520961.

[28] T.T. Fischer, B.E. Ehrlich, Wolfram syndrome: a monogenic model to study diabetes mellitus and neurodegeneration, Curr. Opin. Physiol. 17 (2020) 115–123, https://doi.org/10.1016/j.cophys.2020.07.009.

[29] M.T. Pallotta, G. Tascini, R. Crispoldi, C. Orabona, G. Mondanelli, U. Grohmann, S. Esposito, Wolfram syndrome, a rare neurodegenerative disease: from pathogenesis to future treatment perspectives, J. Transl. Med. 17 (2019) 238, https://doi.org/10.1186/s12967-019-1993-1.

[30] R. Medlej, J. Wasson, P. Baz, S. Azar, I. Salti, J. Loiselet, A. Permutt, G. Halaby, Diabetes mellitus and optic atrophy: a study of Wolfram syndrome in the Lebanese population, J. Clin. Endocrinol. Metab. 89 (2004) 1656–1661, https://doi.org/10.1210/jc.2002-030015.

[31] M. Cnop, H. Mulder, M. Igoillo-Esteve, Diabetes in Friedreich ataxia, J. Neurochem. 126 (Suppl 1) (2013) 94–102, https://doi.org/10.1111/jnc.12216.

[32] F.V. Pallardo, G. Pagano, L.R. Rodriguez, P. Gonzalez-Cabo, A. Lyakhovich, M. Trifuoggi, Friedreich Ataxia: current state-of-the-art, and future prospects for mitochondrial-focused therapies, Transl. Res. : J. Lab. Clin. Med. 229 (2021) 135–141, https://doi.org/10.1016/j.trsl.2020.08.009.

[33] D. Pilz, O.W. Quarrell, E.W. Jones, Mitochondrial mutation commonly associated with Leber's hereditary optic neuropathy observed in a patient with Wolfram syndrome (DIDMOAD), J. Med. Genet. 31 (1994) 328–330, https://doi.org/10.1136/jmg.31.4.328.

[34] S. Hofmann, R. Bezold, M. Jaksch, B. Obermaier-Kusser, S. Mertens, P. Kaufhold, W. Rabl, W. Hecker, K.D. Gerbitz, Wolfram (DIDMOAD) syndrome and Leber hereditary optic neuropathy (LHON) are associated with distinct mitochondrial DNA haplotypes, Genomics 39 (1997) 8–18, https://doi.org/10.1006/geno.1996.4474.

[35] A. Barrientos, J. Casademont, A. Saiz, F. Cardellach, V. Volpini, A. Solans, E. Tolosa, A. Urbano-Marquez, X. Estivill, V. Nunes, Autosomal recessive Wolfram syndrome associated with an 8.5-kb mtDNA single deletion, Am. J. Hum. Genet. 58 (1996) 963–970.

[36] A. Rotig, V. Cormier, P. Chatelain, R. Francois, J.M. Saudubray, P. Rustin, A. Munnich, Deletion of mitochondrial DNA in a case of early-onset diabetes mellitus, optic atrophy, and deafness (Wolfram syndrome, MIM 222300), J. Clin. Invest. 91 (1993) 1095–1098, https://doi.org/10.1172/JCI116267.

[37] M. Makrecka-Kuka, E. Liepinsh, A.J. Murray, H. Lemieux, M. Dambrova, K. Tepp, M. Puurand, T. Kaambre, W.H. Han, P. de Goede, K.A. O'Brien, B. Turan, E. Tuncay, Y. Olgar, A.P. Rolo, C.M. Palmeira, N.T. Boardman, R.C.I. Wust, T. S. Larsen, Altered mitochondrial metabolism in the insulin-resistant heart, Acta Physiol. 228 (2020), e13430, https://doi.org/10.1111/apha.13430.

[38] Y.F. Chen, C.H. Kao, Y.T. Chen, C.H. Wang, C.Y. Wu, C.Y. Tsai, F.C. Liu, C.W. Yang, Y.H. Wei, M.T. Hsu, S.F. Tsai, T.F. Tsai, Cisd2 deficiency drives premature aging and causes mitochondria-mediated defects in mice, Gene Dev. 23 (2009) 1183–1194, https://doi.org/10.1101/gad.1779509.

[39] M.A. Ganie, B.A. Laway, S. Nisar, M.M. Wani, M.L. Khurana, F. Ahmad, S. Ahmed, P. Gupta, I. Ali, I. Shabir, A. Shadan, A. Ahmed, S. Tufail, Presentation and clinical course of Wolfram (DIDMOAD) syndrome from North India, Diabetic medicine, J. Br. Diabet. Assoc. 28 (2011) 1337–1342, https://doi.org/10.1111/j.1464-5491.2011.03377.x.

[40] H.A. Korkmaz, K. Demir, F. Hazan, M. Yildiz, O.N. Elmas, B. Ozkan, Association of Wolfram syndrome with Fallot tetralogy in a girl, Arch. Argent. Pediatr. 114 (2016) e163–166, https://doi.org/10.5546/aap.2016.eng.e163.

[41] L. Tranebjaerg, T. Barrett, N.D. Rendtorff, in: M.P. Adam, H.H. Ardinger, R. A. Pagon, S.E. Wallace, L.J.H. Bean, G. Mirzaa, A. Amemiya (Eds.), WFS1 Wolfram Syndrome Spectrum Disorder, GeneReviews((R)), Seattle (WA), 1993.

[42] B.T. Kinsley, M. Swift, R.H. Dumont, R.G. Swift, Morbidity and mortality in the Wolfram syndrome, Diabetes Care 18 (1995) 1566–1570, https://doi.org/10.2337/diacare.18.12.1566.

[43] K. Tepp, M. Puurand, N. Timohhina, J. Aid-Vanakova, I. Reile, I. Shevchuk, V. Chekulayev, M. Eimre, N. Peet, L. Kadaja, K. Paju, T. Kaambre, Adaptation of striated muscles to Wolframin deficiency in mice: alterations in cellular bioenergetics, Biochim. Biophys. Acta Gen. Subj. 1864 (2020) 129523, https://doi.org/10.1016/j.bbagen.2020.129523.

[44] M. Eimre, K. Paju, N. Peet, L. Kadaja, M. Tarrend, S. Kasvandik, J. Seppet, M. Ivask, E. Orlova, S. Koks, Increased mitochondrial protein levels and bioenergetics in the musculus rectus femoris of wfs1-deficient mice, Oxid. Med. Cell. Longev. 2018 (2018) 3175313, https://doi.org/10.1155/2018/3175313.

[45] J. Gambardella, A. Lombardi, G. Santulli, Metabolic flexibility of mitochondria plays a key role in balancing glucose and fatty acid metabolism in the diabetic heart, Diabetes 69 (2020) 2054–2057, https://doi.org/10.2337/dbi20-0024.

[46] M. Isfort, S.C. Stevens, S. Schaffer, C.J. Jong, L.E. Wold, Metabolic dysfunction in diabetic cardiomyopathy, Heart Fail. Rev. 19 (2014) 35–48, https://doi.org/10.1007/s10741-013-9377-8.

[47] R.L. Smith, M.R. Soeters, R.C.I. Wust, R.H. Houtkooper, Metabolic flexibility as an adaptation to energy Resources and requirements in health and disease, Endocr. Rev. 39 (2018) 489–517, https://doi.org/10.1210/er.2017-00211.

[48] B.H. Goodpaster, L.M. Sparks, Metabolic flexibility in health and disease, Cell Metabol. 25 (2017) 1027–1036, https://doi.org/10.1016/j.cmet.2017.04.015.

[49] D.E. Kelley, M. Mokan, J.A. Simoneau, L.J. Mandarino, Interaction between glucose and free fatty acid metabolism in human skeletal muscle, J. Clin. Invest. 92 (1993) 91–98, https://doi.org/10.1172/JCI116603.

[50] M. Plaas, K. Seppa, R. Reimets, T. Jagomae, M. Toots, T. Koppel, T. Vallisoo, M. Nigul, I. Heinla, R. Meier, A. Kaasik, A. Piirsoo, M.A. Hickey, A. Terasmaa, E. Vasar, Wfs1- deficient rats develop primary symptoms of Wolfram syndrome: insulin-dependent diabetes, optic nerve atrophy and medullary degeneration, Sci. Rep. 7 (2017) 10220, https://doi.org/10.1038/s41598-017-09392-x.

[51] A.V. Kuznetsov, V. Veksler, F.N. Gellerich, V. Saks, R. Margreiter, W.S. Kunz, Analysis of mitochondrial function in situ in permeabilized muscle fibers, tissues and cells, Nat. Protoc. 3 (2008) 965–976, https://doi.org/10.1038/nprot.2008.61.

[52] M. Puurand, K. Tepp, A. Klepinin, L. Klepinina, I. Shevchuk, T. Kaambre, Intracellular energy-transfer networks and high-resolution respirometry: a convenient approach for studying their function, Int. J. Mol. Sci. 19 (2018), https://doi.org/10.3390/ijms19102933.

[53] D. Pesta, E. Gnaiger, High-resolution respirometry: OXPHOS protocols for human cells and permeabilized fibers from small biopsies of human muscle, Methods Mol. Biol. 810 (2012) 25–58, https://doi.org/10.1007/978-1-61779-382-0_3.

[54] V.A. Saks, V.I. Veksler, A.V. Kuznetsov, L. Kay, P. Sikk, T. Tiivel, L. Tranqui, J. Olivares, K. Winkler, F. Wiedemann, W.S. Kunz, Permeabilized cell and skinned fiber techniques in studies of mitochondrial function in vivo, Mol. Cell. Biochem. 184 (1998) 81–100.

[55] R. Paasuke, M. Eimre, A. Piirsoo, N. Peet, L. Laada, L. Kadaja, M. Roosimaa, M. Paasuke, A. Martson, E. Seppet, K. Paju, Proliferation of Human Primary Myoblasts Is Associated with Altered Energy Metabolism in Dependence on Ageing in Vivo and in Vitro, Oxidative Medicine and Cellular Longevity, vol. 2016, 2016, p. 8296150, https://doi.org/10.1155/2016/8296150.

[56] M. Spinazzi, A. Casarin, V. Pertegato, M. Ermani, L. Salviati, C. Angelini, Optimization of respiratory chain enzymatic assays in muscle for the diagnosis of mitochondrial disorders, Mitochondrion 11 (2011) 893–904, https://doi.org/10.1016/j.mito.2011.07.006.

[57] A. Cormio, F. Guerra, G. Cormio, V. Pesce, F. Fracasso, V. Loizzi, P. Cantatore, L. Selvaggi, M.N. Gadaleta, The PGC-1alpha-dependent pathway of mitochondrial biogenesis is upregulated in type I endometrial cancer, Biochem. Biophys. Res. Commun. 390 (2009) 1182–1185, https://doi.org/10.1016/j.bbrc.2009.10.114.

[58] A. Kadayifci, Y. Kepekci, Y. Coskun, Y. Huang, Wolfram syndrome in a family with variable expression, Acta Med. 44 (2001) 115–118.

[59] N. Mezghani, M. Mnif, E. Mkaouar-Rebai, N. Kallel, I.H. Salem, N. Charfi, M. Abid, F. Fakhfakh, The mitochondrial ND1 m.3337G>A mutation associated to multiple mitochondrial DNA deletions in a patient with Wolfram syndrome and cardiomyopathy, Biochem. Biophys. Res. Commun. 411 (2011) 247–252, https://doi.org/10.1016/j.bbrc.2011.06.106.

[60] K. Tepp, M. Puurand, N. Timohhina, J. Adamson, A. Klepinin, L. Truu, I. Shevchuk, V. Chekulayev, T. Kaambre, Changes in the mitochondrial function and in the efficiency of energy transfer pathways during cardiomyocyte aging, Mol. Cell. Biochem. 432 (2017) 141–158, https://doi.org/10.1007/s11010-017-3005-1.

[61] A. Koit, I. Shevchuk, L. Ounpuu, A. Klepinin, V. Chekulayev, N. Timohhina, K. Tepp, M. Puurand, L. Truu, K. Heck, V. Valvere, R. Guzun, T. Kaambre, Mitochondrial respiration in human colorectal and breast cancer clinical material is regulated differently, Oxid. Med. Cell. Longev. (2017) 1372640, https://doi.org/10.1155/2017/1372640, 2017.

[62] A. Weber, H. Klocker, H. Oberacher, E. Gnaiger, H. Neuwirt, N. Sampson, I.E. Eder, Succinate accumulation is associated with a shift of mitochondrial respiratory control and HIF-1alpha upregulation in PTEN negative prostate cancer cells, Int. J. Mol. Sci. 19 (2018), https://doi.org/10.3390/ijms19072129.

[63] M. Gruno, N. Peet, A. Tein, R. Salupere, M. Sirotkina, J. Valle, A. Peetsalu, E. K. Seppet, Atrophic gastritis: deficient complex I of the respiratory chain in the mitochondria of corpus mucosal cells, J. Gastroenterol. 43 (2008) 780–788, https://doi.org/10.1007/s00535-008-2231-4.

[64] X. Shen, S. Zheng, V. Thongboonkerd, M. Xu, W.M. Pierce Jr., J.B. Klein, P. N. Epstein, Cardiac mitochondrial damage and biogenesis in a chronic model of type 1 diabetes, Am. J. Physiol. Endocrinol. Metab. 287 (2004) E896–E905, https://doi.org/10.1152/ajpendo.00047.2004.

[65] C.E. van den Brom, M.C. Huisman, R. Vlasblom, N.M. Boontje, S. Duijst, M. Lubberink, C.F. Molthoff, A.A. Lammertsma, J. van der Velden, C. Boer, D. M. Ouwens, M. Diamant, Altered myocardial substrate metabolism is associated with myocardial dysfunction in early diabetic cardiomyopathy in rats: studies using positron emission tomography, Cardiovasc. Diabetol. 8 (2009) 39, https://doi.org/10.1186/1475-2840-8-39.

Appendix 3

Publication III

Aid, J., Tanjeko, A. T., Serre, J., Eggelbusch, M., Noort, W., de Wit, G. M. J., van Weeghel, M., Puurand, M., Tepp, K., Gayan-Ramirez, G., Degens, H., Kaambre, T., & Wust, R. C. I. (2024). Smoking cessation only partially reverses cardiac metabolic and structural remodeling in mice. Acta Physiol (Oxf), 240(7), e14145. https://doi.org/10.1111/apha.14145

RESEARCH PAPER

Smoking cessation only partially reverses cardiac metabolic and structural remodeling in mice

Jekaterina Aid[1,2] | Ajime Tom Tanjeko[3,4] | Jef Serré[3] | Moritz Eggelbusch[2] | Wendy Noort[2] | Gerard M. J. de Wit[2] | Michel van Weeghel[5,6] | Marju Puurand[1] | Kersti Tepp[1] | Ghislaine Gayan-Ramirez[3] | Hans Degens[4,7] | Tuuli Käämbre[1] | Rob C. I. Wüst[2]

[1]Laboratory of Chemical Biology, National Institute of Chemical Physics and Biophysics, Tallinn, Estonia

[2]Laboratory of Myology, Department of Human Movement Sciences, Faculty of Behavioral and Movement Sciences, Amsterdam Movement Sciences, Vrije Universiteit Amsterdam, Amsterdam, The Netherlands

[3]Laboratory of Respiratory Diseases and Thoracic Surgery, Department of Chronic Diseases, and Metabolism, KU-Leuven, Leuven, Belgium

[4]Department of Life Sciences, Institute of Sport, Manchester Metropolitan University, Manchester, UK

[5]Laboratory Genetic Metabolic Diseases, Amsterdam UMC, Amsterdam Gastroenterology and Metabolism, Amsterdam Cardiovascular Sciences, University of Amsterdam, Amsterdam, The Netherlands

[6]Core Facility Metabolomics, Amsterdam UMC, University of Amsterdam, Amsterdam, The Netherlands

[7]Institute of Sport Science and Innovations, Lithuanian Sports University, Kaunas, Lithuania

Correspondence
Rob C. I. Wüst, Laboratory of Myology, Department of Human Movement Sciences, Faculty of Behavioral and Movement Sciences, Amsterdam Movement Sciences, Vrije Universiteit Amsterdam, Van der Boechorststraat 7, 1081 BT Amsterdam, The Netherlands.
Email: r.wust@vu.nl

Abstract

Aims: Active cigarette smoking is a major risk factor for chronic obstructive pulmonary disease that remains elevated after cessation. Skeletal muscle dysfunction has been well documented after smoking, but little is known about cardiac adaptations to cigarette smoking. The underlying cellular and molecular cardiac adaptations, independent of confounding lifestyle factors, and time course of reversibility by smoking cessation remain unclear. We hypothesized that smoking negatively affects cardiac metabolism and induces local inflammation in mice, which do not readily reverse upon 2-week smoking cessation.

Methods: Mice were exposed to air or cigarette smoke for 14 weeks with or without 1- or 2-week smoke cessation. We measured cardiac mitochondrial respiration by high-resolution respirometry, cardiac mitochondrial density, abundance of mitochondrial supercomplexes by electrophoresis, and capillarization, fibrosis, and macrophage infiltration by immunohistology, and performed cardiac metabolome and lipidome analysis by mass spectrometry.

Results: Mitochondrial protein, supercomplex content, and respiration (all $p < 0.03$) were lower after smoking, which were largely reversed within 2-week smoking cessation. Metabolome and lipidome analyses revealed alterations in

mitochondrial metabolism, a shift from fatty acid to glucose metabolism, which did not revert to control upon smoking cessation. Capillary density was not different after smoking but increased after smoking cessation ($p = 0.02$). Macrophage infiltration and fibrosis ($p < 0.04$) were higher after smoking but did not revert to control upon smoking cessation.

Conclusions: While cigarette-impaired smoking-induced cardiac mitochondrial function was reversed by smoking cessation, the remaining fibrosis and macrophage infiltration may contribute to the increased risk of cardiovascular events after smoking cessation.

KEYWORDS

cardiac metabolism, cardiac remodeling, fibrosis, inflammation, macrophages, smoking cessation

1 | INTRODUCTION

Cigarette smoking is a major risk factor for the development of chronic obstructive pulmonary disease (COPD)[1] and cardiovascular diseases,[2] all contributing to the higher mortality rate of current smokers. The risk for cardiovascular complications is even higher for ex-smokers and could be related to irreversible cumulative changes induced by exposure to cigarette smoke.[3,4] For instance, former heavy smokers have a higher prevalence of type 2 diabetes mellitus, left ventricular systolic dysfunction, coronary artery disease, and peripheral arterial disease, as well as higher circulating levels of serum C-reactive protein and interleukin-6 compared to never smokers.[3] Skeletal muscle adaptations, such as increased fatigue and cachexia, are often reported in patients with COPD,[5–7] but the link with smoking-induced cardiovascular disease is not well understood. Smokers often exhibit lower physical activity levels and a poor diet, lifestyle factors that in themselves are significant risk factors for cardiovascular complications.[8] Therefore, these confounding factors blur how smoking itself affects intracellular cardiac structure and function.

Many substances in cigarette smoke are known to impair oxygen transport to tissue and cellular metabolism.[4,7,9,10] In addition, smoking reduced mitochondrial respiration in murine skeletal muscles, caused skeletal muscle atrophy,[9] and increased macrophage infiltration in bronchoalveolar lavage fluid that all reverted to control values after 2 weeks of smoking cessation.[11,12] Smoking has also been associated with capillary rarefaction.[13] It is most likely that the effects of smoking on mitochondrial function and capillaries are not restricted to skeletal muscle but will have a similar impact on mitochondria in any tissue, including the brain and heart. Likewise, smoke-induced circulating inflammatory markers from lungs may also cause an altered cardiac metabolism, local inflammation, and fibrosis, which may contribute to the elevated risk of developing cardiovascular diseases[11,12] and systolic dysfunction in smokers.[14] However, whether cardiac muscle metabolism, inflammation, and fibrosis are affected by cigarette smoking and to what extent these are reversible by smoking cessation has not yet been explored.

Therefore, the objective of the study was to comprehensively assess the impact of exposure to cigarette smoking and smoking cessation of up to 2 weeks on cardiac muscle structure, local inflammation, and cardiac metabolism in mice. We hypothesized that smoking negatively affects cardiac metabolism and induces local inflammation and fibrosis. To investigate this, metabolome and lipidome analyses were performed to assess changes in cardiac metabolism upon smoking and smoking cessation.

2 | MATERIALS AND METHODS

2.1 | Animals and study design

The supplemental datasheet contains an extended Materials and Methods section, which is in line with good publishing practice in physiology.[15] All experimental procedures were approved by the Leuven Ethical Committee. The study design was as previously described.[11] Eight-week-old male C57Bl/6JolaH mice ($n = 44$) were randomly divided into four groups: one exposed to cigarette smoke for 14 weeks (SM); a group exposed to cigarette smoke for 13 weeks and 1-week cessation (SC1W); a group exposed to cigarette smoke for 12 weeks and 2-week cessation (SC2W); and a control group (CON) exposed to room air.[11]

2.2 | (Immuno-)histochemistry and western blotting

Connective tissue, capillary, nuclear densities, succinate dehydrogenase (SDH) activity, macrophage infiltration, GLUT4 translocation and cardiomyocyte cross-sectional area were assessed in cardiac sections. In a subgroup of 20 animals, protein content of subunits of all five OXPHOS complexes, DRP1, OPA1, and GLUT4 was determined.

2.3 | Mitochondrial respiration and supercomplex content

Mitochondrial respiration was measured in the apex using high-resolution respirometry. Mitochondrial supercomplexes were visualized by blue native gel electrophoresis.

2.4 | Metabolomic and lipidomic analysis

Metabolome and lipidome analyses were performed in the apex, and data were normalized to internal standards and tissue weight.

2.5 | Statistical analysis

Results are expressed as the mean $\pm$ SEM. Statistical analysis consisted of two parts because the smoking cessation groups had two interventions (smoking + cessation). First, statistical differences between control and smoking were assessed with an independent t-test, and the effect of smoke cessation compared to smoking was tested with a one-way analysis of variance (ANOVA). To test whether 2 weeks of smoke cessation was significantly different from control, an independent t-test was performed. A $p < 0.05$ was considered significant.

3 | RESULTS

3.1 | Body and heart mass and cardiomyocyte size

Body mass was lower after smoking (SM) compared to control (CON; Figure 1A), and gradually increased after smoking cessation.[11] Heart mass was not significantly different between smoking and controls (Figure 1B) but was higher after 2 weeks of smoking cessation (SC2W) compared to smoking animals. The heart-to-body mass ratio was higher after smoking (5.2 ± 0.1 vs. 4.1 ± 0.2 mg·g^{-1} in

control; $p < 0.001$) but did not change after smoking cessation. Cardiomyocyte cross-sectional area tended to be lower after smoking but did not increase after smoking cessation (Figure 1C,D).

3.2 | Cardiac fibrosis and capillary supply

Collagen content was higher in smoking than control and further increased after 1-week smoking cessation (Figure 1E,F). Although collagen content was not different between 2 weeks of smoking cessation (SC2W) and smoking, collagen content was still higher in SC2W compared to control. Capillary density was not different after smoking compared to control, but significantly increased after smoking cessation, and remained higher than control (Figure 1G,H).

3.3 | Nuclear density and infiltration of immune cells

We performed a hematoxylin and eosin stain to visualize cells and nuclei. There were no significant differences in cardiac nuclear density between smoking and control, but nuclear density was higher after 1 week of smoking cessation, but not after 2 weeks, compared to smoking (Figure 2A,B). We reasoned that these additional nuclei could be immune cells such as macrophages, and indeed, cigarette smoke exposure increased the concentration of infiltrated macrophages compared to control (Figure 2C,D), which remained elevated above control after smoking cessation ($p < 0.0001$). No signs of cardiac cell necrosis or cell death were observed.

3.4 | Mitochondrial function

To understand smoking-induced alterations in cardiac metabolism, we assessed mitochondrial respiration in the apex. Leak respiration with NADH substrates (Figure 3A), NADH (complex I)-linked respiration (Figure 3B) and complex II-linked respiration (Figure 3C) were not significantly different between groups. Oxidative phosphorylation capacity tended to be lower after smoking compared to control ($p = 0.056$), and significantly increased to control values after smoking cessation (Figure 3D). Uncoupling respiration was significantly lower after smoking and returned to control level after smoking cessation (Figure 3E). Normalized leak respiration was significantly higher after smoking, and returned to control levels after smoke
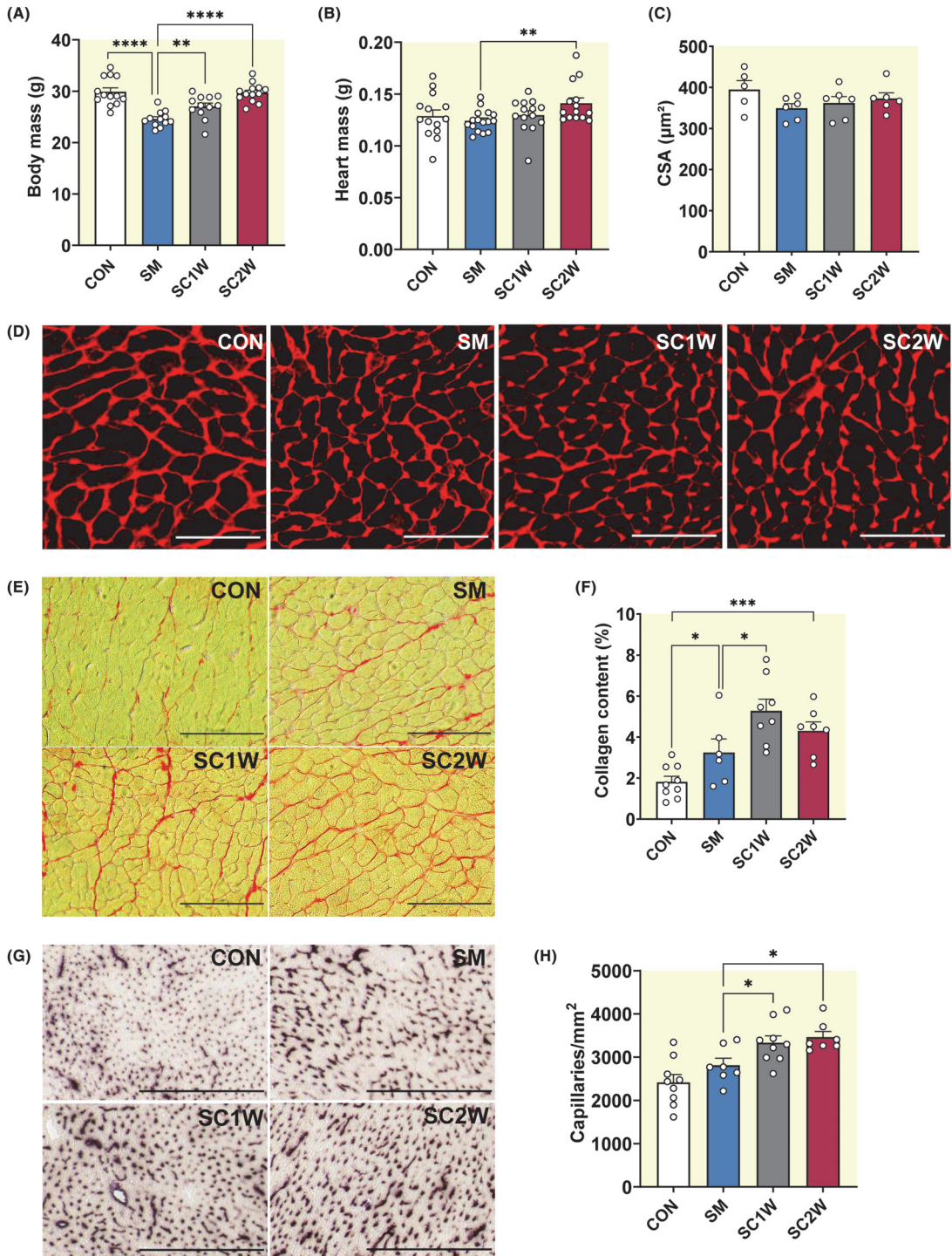
cessation, indicative of a relatively higher mitochondrial uncoupling during smoking. Excess capacity (oxidative phosphorylation / electron transport capacity) was significantly higher after smoking (0.91 ± 0.06) versus control (0.84 ± 0.08, $p = 0.018$), which tended to remain higher after 2 weeks of smoke cessation (0.90 ± 0.06, $p = 0.068$).

FIGURE 1 Body mass, heart mass, cross-sectional area of cardiomyocytes, fibrosis, and capillary density after smoking and smoking cessation in mice. (A) Body (CON $n=13$, SM $n=12$, SC1W $n=12$, SC2W $n=13$) and heart mass (B) of mice exposed to cigarette smoke (SM $n=16$), and after 1–2 weeks of smoking cessation (SC1W $n=14$, SC2W $n=14$), compared to control (CON $n=14$). (C) Cardiomyocyte cross-sectional area was not significantly different between groups (CON $n=5$, SM $n=6$, SC1W $n=6$, SC2W $n=6$). (D) Representative images of cell membranes (wheat germ agglutinin antibody). (E) Representative images of collagen. (F) Collagen content was higher after smoking and further increased after smoking cessation (CON $n=9$, SM $n=6$, SC1W $n=8$, SC2W $n=7$). (G) Representative images of cardiac capillaries. (H) Capillary density increased after 1 and 2 weeks of smoking cessation (CON $n=9$, SM $n=7$, SC1W $n=9$, SC2W $n=7$). Results are expressed as mean $\pm$ SEM. The corresponding significant p values are shown in the figures. Scale bar represents $100\,\mu m$ (D, E) or $250\,\mu m$ (G). SM versus CON and SC2W versus CON (unpaired two-tailed t-test); SC1W versus SM and SC2W versus SM (one-way ANOVA).

Mitochondrial complex I subunit NDUFB8 content was lower after smoking compared to control (Figure S1D,E) and remained lower after 2-week smoke cessation than in control ($p=0.011$). No group differences in protein level of subunits for complexes II and III and ATP synthase were observed (Figure S1F–I), although complex IV subunit MTCO1 level was lower after smoking compared to control (Figure S1H). SDH activity (Figure 3F,G) was reduced after smoking, and continued to decrease after 1-week smoke cessation, but recovered to smoking levels after 2-week cessation. No significant group differences were observed in the protein content of key players of mitochondrial fusion (OPA1) and fission (DRP1; Figure S1A–C).

We next tested whether mitochondrial supercomplex formation was affected by smoking and normalized after smoking cessation. For this, we isolated mitochondria and performed blue-native electrophoresis. Independent of mitochondrial content, smoking was associated with a lower content of high-molecular-weight mitochondrial supercomplexes, which was restored to control after 2 weeks of smoke cessation (Figure 3H). Moreover, the content of free mitochondrial complexes tended to be lower after smoking and were significantly lower after smoking cessation (Figure 3I). The normalized mitochondrial supercomplex content (relative to total complexes) was not significantly different between smoking and control (Figure 3J), indicating a proportional decrease in supercomplexes and free complexes after smoking. The normalized mitochondrial supercomplex content increased after smoke cessation.

3.5 | Metabolomics

Metabolomics was performed to understand how cigarette smoking and cessation affected cardiac metabolism. Metabolites with variable importance in projection (VIP) score >1.4 were used for enrichment pathway analysis (Table S1, Figure 4). Enrichment pathway analysis revealed alterations in nicotinate and nicotinamide metabolism, glycolysis, pentose phosphate metabolism and gluconeogenesis, branched-chain amino acids

degradation and nucleotide metabolism, mitochondrial beta-oxidation, and other lipid metabolism pathways.

Smoking and smoking cessation decreased the reduced form of nicotinamide mononucleotide (NMNH) in the nicotinamide adenine dinucleotide (NAD$^+$) pathway (Figure S2). Two-week smoking cessation increased NAD$^+$ and NADH levels compared to smoking. Higher metabolite concentrations related to glycolysis and gluconeogenesis suggested a higher glucose breakdown after 2-week smoking cessation compared to control (Figure S3). Metabolites in the pentose phosphate pathway (ribose 5-phosphate and sedoheptulose 7-phosphate) were lower after 2 weeks of smoke cessation than in control. Ophthalmic acid, a biomarker of oxidative stress, was higher after smoking and 2 weeks of smoke cessation (Figure S3).

After 1-week smoking cessation, the branched-chain amino acids, isoleucine, leucine, valine, and allantoin (Figure S4), and ADP-ribose (Figure S2) were decreased compared to smoking. Branched-chain amino-acid content did not restore to control level after 2 weeks of smoke cessation, apart from allantoin and ADP-ribose. Cardiac purine and pyrimidine contents were not significantly changed by smoking but were higher after 2-week smoke cessation compared to control (Figure S5). Metabolites of purine biosynthesis (inosinic acid (IMP) and hypoxanthine) were not altered by smoking but were lower after 2-week smoke cessation ($p=0.0208$ and $p=0.0059$, respectively).

3.6 | Lipidomics

Lipid profiling was performed on the apex of the heart to study whether smoking caused alteration in the lipid content and species (Figure S6A–D). Enrichment analysis identified various lipid classes to be differentially abundant between groups (Figures S6A–D and S7A–D). Although total triacylglycerol concentration in heart tissue was not significantly altered after smoking and smoking cessation, long-chain and very-long-chain highly unsaturated triacylglycerol concentrations were higher after 2 weeks of smoke cessation compared to control and smoking

(A)

(B)

(C)

(D)
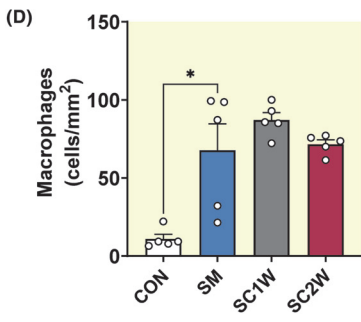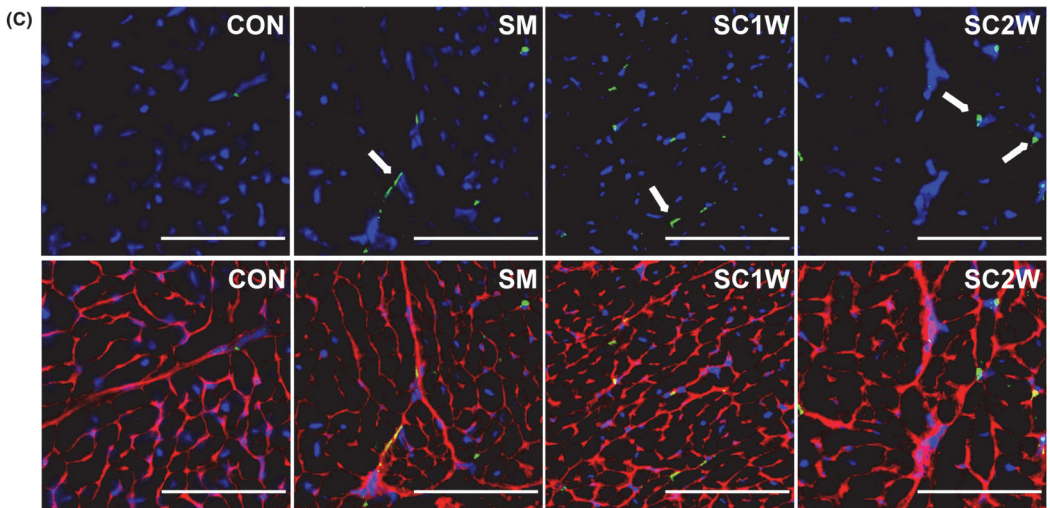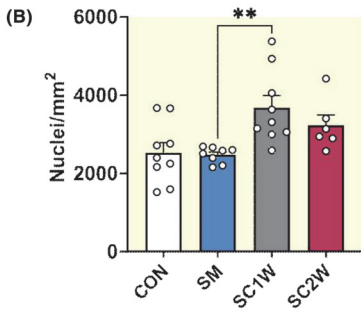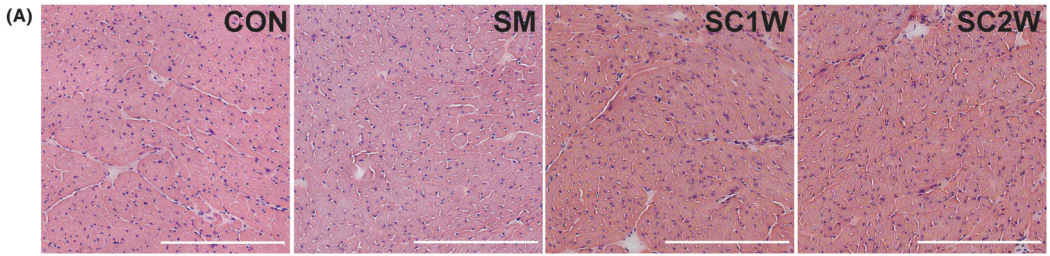
FIGURE 2 Nuclear density and macrophage infiltration of cardiac tissue after smoking and smoking cessation in mice. (A) Representative examples for hematoxylin and eosin staining in control (CON), smoking (SM), and 1–2 weeks of smoking cessation (SC1W and SC2W). (B) Nuclear density in cardiac tissue increased after smoking cessation (CON $n=9$, SM $n=8$, SC1W $n=9$, SC2W $n=6$). (C) Representative examples of macrophages (green), membranes (red), and nuclei (blue). Upper panel shows staining of cardiomyocyte nuclei and macrophages, and lower panel shows staining of cardiomyocyte membranes and nuclei and macrophages. White arrows show macrophages (upper panel). (D) Macrophage density was higher after smoking and smoking cessation. (CON $n=5$, SM $n=5$, SC1W $n=5$, SC2W $n=5$). Results are expressed as the mean ± SEM. Scale bar is 250 (A) or 50 μm (C). SM versus CON and SC2W versus CON (unpaired two-tailed t-test); SC1W versus SM and SC2W versus SM (one-way ANOVA).

(Figure 5), indicative of a lower breakdown or higher production of triacylglycerols after smoke cessation.

3.7 | Glucose transport

Our metabolome and lipidome analyses indicated that smoking cessation shifted metabolism from fatty acid oxidation toward glucose oxidation, possibly via an altered translocation of glucose transporter type 4 (GLUT4) from the cytosol to the cell membrane (Figure 6A). We therefore next determined whether there were differences in the membrane-associated GLUT4 in the mice that were fasted for >3 h. Smoking did not alter the fraction of GLUT4 associated with the cell membrane, but relatively more GLUT4 was translocated toward the cell membrane after smoking cessation (Figure 6C,D). No differences were observed in the amount of cell membrane that contained GLUT4. With western immunoblotting, we tested the hypothesis that GLUT4 protein concentration was different, but no group differences in overall GLUT4 protein concentration were observed (Figure 6C).

4 | DISCUSSION

We performed a detailed assessment of changes in cardiac structure and metabolism upon cigarette smoking and smoking cessation for up to 2 weeks in a mouse model of COPD. Cigarette smoking caused macrophage infiltration and fibrosis in the heart, which only partially recovered after smoking cessation. Surprisingly, smoking cessation—but not smoking itself—induced extensive capillary proliferation resulting in an increased capillary density. Smoking reduced maximal mitochondrial capacity that returned to control values after 2 weeks of smoking cessation. This was associated with quantitative and qualitative decrements in mitochondrial protein content, SDH activity, and mitochondrial supercomplex formation. Metabolome and lipidome analyses indicated a shift from fatty acid to glucose oxidation upon smoking cessation, which confirmed that cardiac metabolism only partially returns to control after smoking cessation.

4.1 | Cardiac atrophy, local inflammation, and fibrosis

We observed a lower cardiac weight and tendency for a lower fibre cross-sectional area after cigarette smoking. Extrapulmonary manifestations are often observed in COPD, and these results suggest that besides skeletal muscle atrophy and cachexia,[4–6] the cardiac muscle is not spared from smoking-induced atrophy. Currently, it is unclear what the cellular and molecular overlap is between the cardiac and skeletal muscle atrophy upon cigarette smoking and whether cardiac atrophy is similar to cachexia. We propose that the term "cardiac cachexia" should refer to cardiac alterations, rather than skeletal muscle cachexia in patients with chronic heart failure.[16]

Local and systemic inflammation likely contribute to the altered cardiac structure and function. Smoking was accompanied by macrophage infiltration into the heart which did not revert to control after smoking cessation. The infiltrations occurred predominantly around endothelial cells. This local endothelial inflammation may induce a higher endothelial permeability in cigarette smoke-exposed mice.[17] These tissue-infiltrating macrophages are involved in the clearance of dead, dysfunctional, and dying cells, as well as tissue remodeling and angiogenesis.[18]

Macrophage infiltration is also associated with a higher local concentration of pro-inflammatory cytokines, such as TNF-α, various interleukins, and TGF-β, negatively affecting cardiac metabolism,[19,20] and can also promote collagen production and fibrosis.[21] Indeed, the smoking-induced fibrosis did not recover after cigarette smoking cessation. Cardiac macrophage infiltration, higher fibrosis, and capillary density after smoking and smoking cessation indicate that local inflammation contributed to the structural changes in the heart, linked to a stiffened heart and diastolic dysfunction,[22] typical for heart failure with preserved ejection fraction often observed in COPD patients.

The lower cytosolic concentrations of branched-chain amino acids (BCAA; leucine, isoleucine, and valine) in the heart after smoking cessation can be related to an increased protein synthesis[23] upon smoking cessation, but
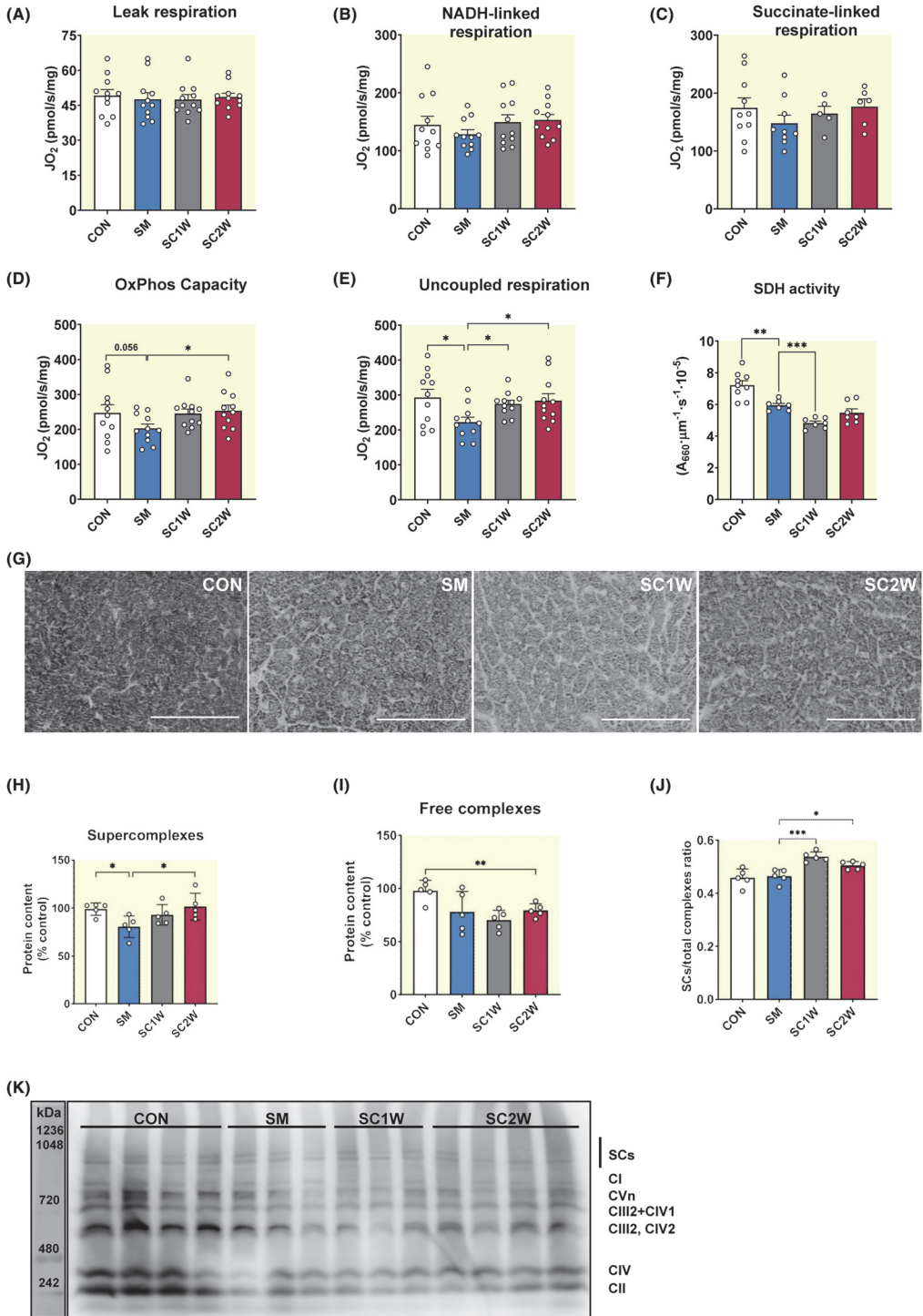
FIGURE 3 Cardiac maximal mitochondrial capacity is reduced with smoking and restored after smoking cessation. Succinate dehydrogenase activity depression in smoking and smoking cessation groups and supercomplex formation in the heart after smoking and smoking cessation in mice. (A) Leak respiration, (B) NADH (complex I) linked with pyruvate, malate, and glutamate, and (C) complex II-linked respiration (with succinate/rotenone) were not significantly different among control (CON), smoking (SM), and after 1–2 weeks smoking cessation (SC1W and SC2W). (D) Oxidative phosphorylation and (E) uncoupled respiration were lower in smoking compared to 2-week smoking cessation (CON $n = 11$, SM $n = 11$, SC1W $n = 11$, SC2W $n = 11$). (F) Lower succinate dehydrogenase (SDH) activity after smoking and both groups of smoking cessation compared to control (CON $n = 9$, SM $n = 7$, SC1W $n = 7$, SC2W $n = 7$). (G) Representative images of succinate dehydrogenase (SDH) activity staining. (H) Protein content of high-molecular-weight supercomplexes was lower after smoking and recovered after smoke cessation (CON $n = 5$, SM $n = 5$, SC1W $n = 5$, SC2W $n = 5$). (I) Free or low-molecular-weight complexes of CI-IV and ATPase synthase were lower in SC1W and SC2W. (J) Normalized supercomplex relative to total complex increased after smoke cessation. (K) Representative example of free mitochondrial complexes and complexes assembled in the supercomplex (SCs: $I + III_2 + II_n$, $I + III_2 + IV_1$). Results are expressed as mean $\pm$ SEM. Scale bar is 100 µm (G). SM versus CON and SC2W versus CON (unpaired two-tailed t-test); SC1W versus SM and SC2W versus SM (one-way ANOVA).

the fibre cross-sectional area did not enlarge. The discrepancy between the gains in heart weight without a concomitant change in cardiomyocyte size at smoking cessation is likely due to other factors than an elevated protein synthesis. Possibly, the increased cell infiltration and blood volume contribute to elevated heart weight after smoking and smoking cessation. Circulating inflammatory cytokines, such as tumor necrosis factor-α (TNF-α), also increase BCAA catabolism and leucine oxidation.[24] A declined BCAA content may therefore also be a consequence of continued elevated local inflammation rather than a reflection in protein synthesis.

We observed increased levels of purines and pyrimidines after 2-week smoking cessation. These changes in nucleotide abundance may contribute to metabolic derangements and ventricle dysfunction as similar changes are also seen in pulmonary arterial hypertension[25] and myocardial hypertrophy.[26] Metabolites connected to the uridine metabolism are involved in protein O-GlcNAcylation, which in turn is directly linked to insulin resistance.[27] Indeed, GLUT4 translocation to the cell membrane was altered, but future studies are required to fully understand how smoking and smoking cessation alter whole-body insulin resistance.

4.2 | Angiogenesis

While smoking has been linked to endothelial damage and a lower capillary-to-fibre ratio in skeletal muscle,[13] we did not observe a decreased capillary density in the heart of mice exposed to cigarette smoke. This discrepancy between smoking-induced changes in capillary density in skeletal muscle and cardiac muscle is perhaps due to the unceasing demand for oxygen and nutrients in the beating heart, while skeletal muscles are intermittently active. Surprisingly, capillary density increased after smoking cessation. We speculate that a smoking cessation-induced increase in the number of circulating endothelial progenitor cells[28] could stimulate neovascularization, further

facilitated by the sustained local inflammation and release of cytokines by local macrophages.

4.3 | Cardiac mitochondrial structure and function

Uncoupled respiration was lower after cigarette smoking but returned to control values after 2 weeks of smoking cessation. Likely, these results are explained by a combination of a lower mitochondrial protein content (evidenced by lower mitochondrial complexes I and IV content and SDH activity), less supercomplexes, and intrinsic impairments in the convergent electron flow within the mitochondria, indicated by the higher normalized NADH-linked respiration. Cigarette smoking directly impairs mitochondrial respiration and electron transport via inhibition of complex III and IV activity by carbon monoxide and other cigarette smoke compounds,[9,11] which may explain the impairments in the convergent electron flow into complex III. Smoking cessation alleviated this direct inhibition of mitochondrial respiration and improved maximal electron transport system capacity, likely due to alterations in the mitochondrial supercomplex formation, rather than adding more mitochondria per se, as mitochondrial protein content was only marginally affected by smoking and cessation. Interestingly, the time course of some adaptations, such as SDH activity and the protein content of some free complexes, was different from the smoking cessation-induced alterations in uncoupled respiration or amount of supercomplexes. The underlying reason for this is currently unclear.

We hypothesize that the intricate balance between disassembly and re-assembly of mitochondrial supercomplexes and novel protein synthesis from individual subunits is affected by smoking and smoking cessation, which partly explains the alteration of supercomplex content and overall mitochondrial respiration. This could explain the increased mitochondrial respiration, without obvious mitochondrial biogenesis. Nollet et al. (2023) indeed recently

showed that enhanced incorporation of complex I into respiratory supercomplexes improved the capacity to oxidize NADH and thereby increased NADH-linked respiration.[29] The formation of mitochondrial supercomplexes may reflect an adaptation to cope with oxidative stress, also inferred from our results of a higher ophthalmic acid (a marker of oxidative stress) observed in smoking and smoking cessation.[30]

The nicotinamide pathway was affected after smoking, as the precursor NMNH was lower after smoking despite similar NAD^{+} levels. Lower NAD^{+} levels are observed in several cardiovascular diseases, including atherosclerosis and heart failure with reduced and preserved ejection fraction.[31] NMNH, NAD^{+}, and NADH significantly increased after smoking cessation, indicative of an increased synthesis or a decreased degradation, since ribose-5-phosphate (a breakdown product of NAD[+][32]) was lower. These improvements in NAD^{+} metabolism contribute to improved mitochondrial function and redox signalling[33] after smoking cessation.
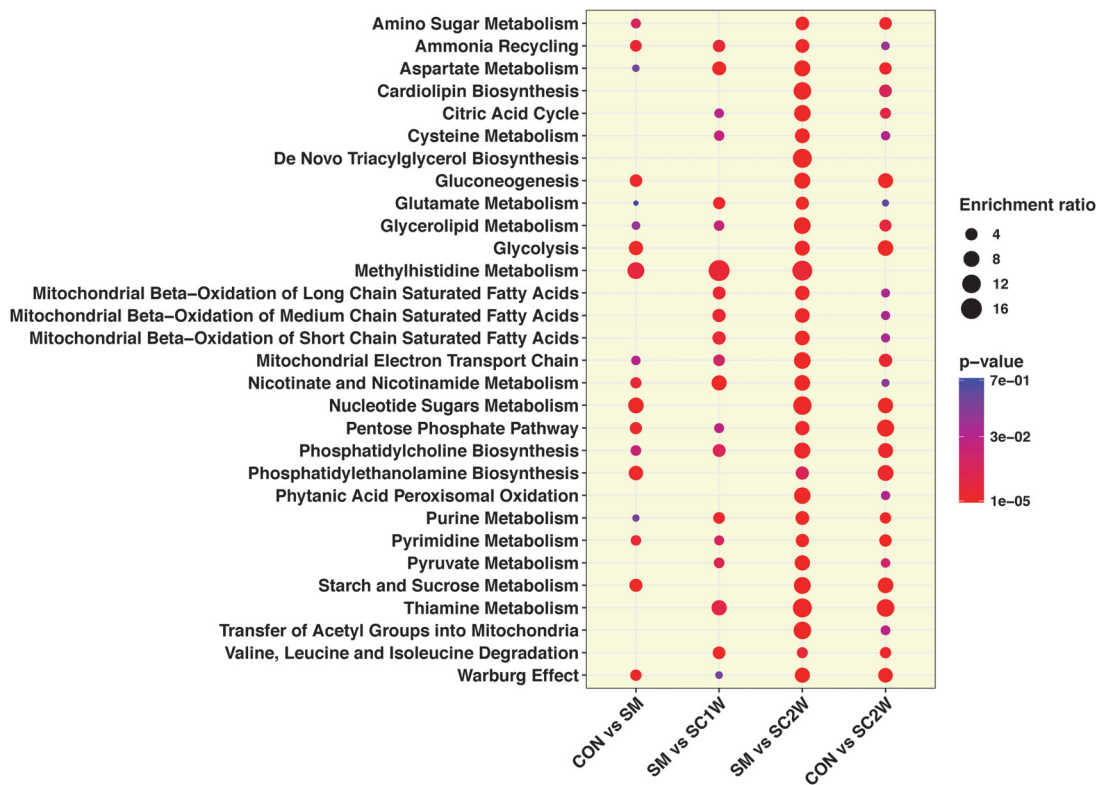

FIGURE 4 Top 30 metabolic pathways altered after smoking and smoking cessation in mice. Enrichment plot depicts several metabolic pathway alterations induced by smoking and smoking cessation. Metabolites were used with variable importance in projection (VIP) score >1.4 for control (CON $n = 5$), smoking (SM $n = 5$), and 1 to 2 weeks of smoking cessation (SC1W $n = 5$ and SC2W $n = 5$). The size of the dot represents enrichment ratio (metabolite count enriched in the pathway), and the color presents significance.
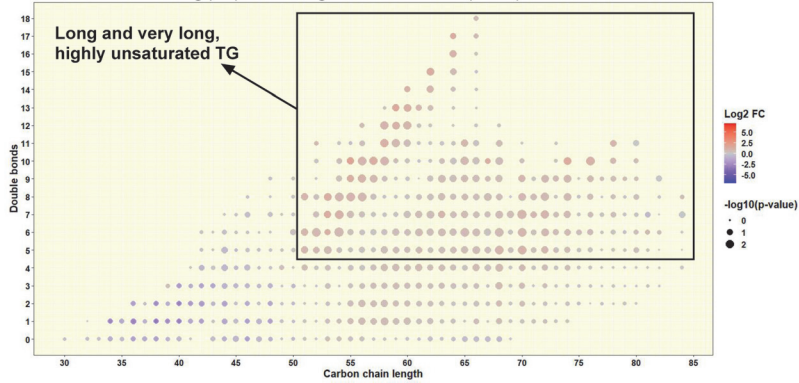
FIGURE 5 Effect of smoking and smoking cessation on triacylglycerols abundance in mice cardiac tissue. (A) Total triacylglycerols concentration in control (CON $n = 5$), smoking (SM $n = 5$), and 1- or 2-week smoking cessation groups (SC1W $n = 5$ and SC2W $n = 5$, respectively). SM versus CON and SC2W versus CON (unpaired two-tailed t-test); SC1W versus SM and SC2W versus SM (one-way ANOVA). (B-D) Comparison of long- and very-long-chain highly unsaturated triacylglycerols among control, smoking, and 2 weeks of smoking cessation. Triacylglycerols TG (51:5)–TG (84:18) were chosen for comparison. CON versus SM, SM versus SC2W, and CON versus SC2W (unpaired two-tailed t-test). (E-G) Dot-plot illustration of triacylglycerol saturation among control, smoking, and two weeks of smoking cessation. Results are expressed as mean $\pm$ SEM.
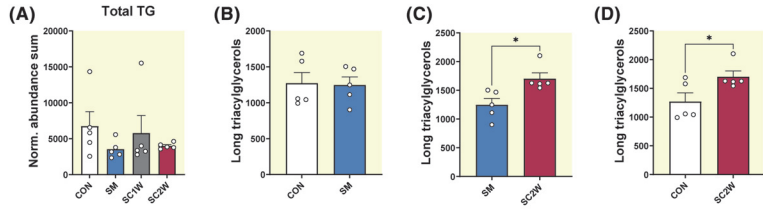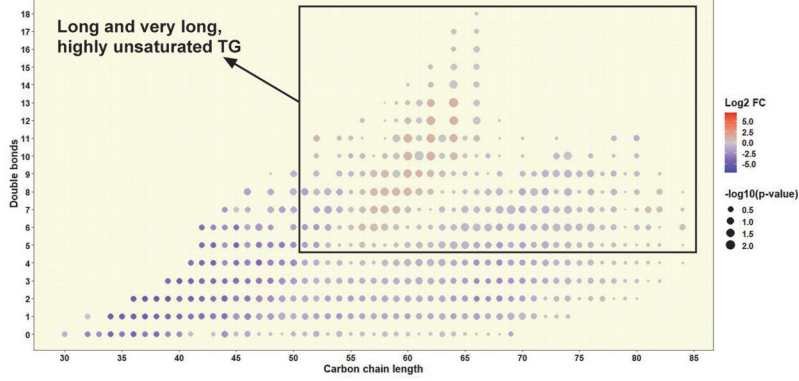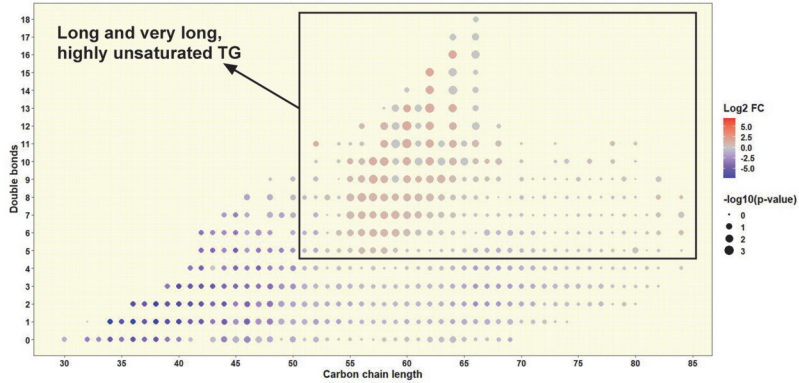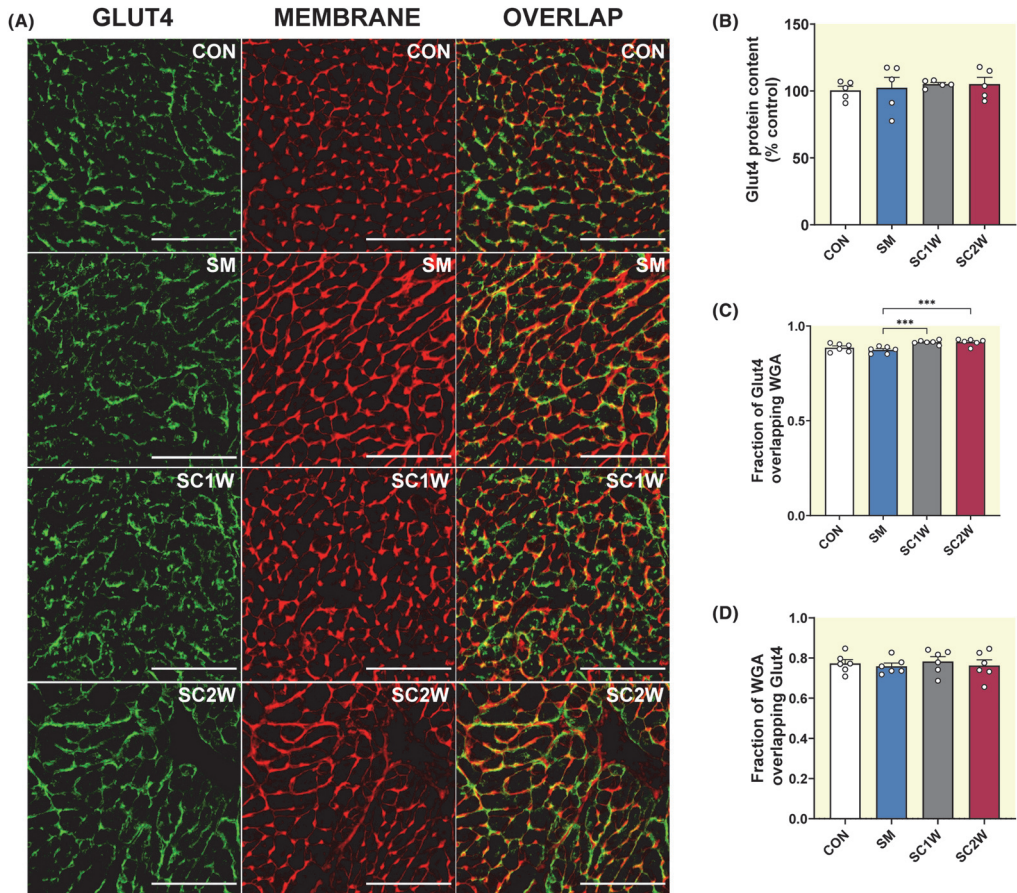
FIGURE 6 More glucose transporter type 4 (GLUT4) translocation at the cell membrane after smoking and smoking cessation in mice. (A) Representative images of heart sections stained with GLUT4 antibody. Left panel shows GLUT4 protein staining with GLUT4 antibody, middle panel shows membrane staining with WGA antibody, and right panel shows overlapping of GLUT4 and membrane staining. Scale bar is 100 μm. (B) Western blot analysis was used to measure protein content of GLUT4 (CON $n=5$, SM $n=5$, SC1W $n=5$, SC2W $n=5$). (C) Fraction of GLUT4 localized at the cell membrane increased after smoke cessation. (D) Fraction of membrane overlapping with GLUT4 in control (CON $n=6$), smoking (SM $n=6$), and 1- or 2-week smoking cessation (SC1W $n=6$, SC2W $n=6$). Results are expressed as mean ± SEM. SM versus SM versus CON and SC2W versus CON (unpaired two-tailed t-test); SC1W versus SM and SC2W versus SM (one-way ANOVA).

4.4 | Alterations in intracellular metabolism

Cardiomyocytes exhibit metabolic flexibility[34] and predominantly use fatty acids and glucose for ATP production.[34,35] Our metabolomics results are indicative of a shift away from fatty acid to glucose oxidation during smoking cessation, similar to that observed in cardiovascular diseases,[36] where metabolic inflexibility is observed.[34,35] We observed increased levels of various glycolytic intermediates, suggestive of a larger reliance on glucose oxidation after smoking cessation.[37] This was associated with a higher colocalization of GLUT4

at the plasma membrane after smoking cessation. Our lipidomic analysis confirmed a systematic increase in concentration of various long-chain highly unsaturated fatty acids after 2 weeks of smoking cessation, indicative of reduced fatty acid oxidation. These data confirm a cellular shift in metabolism toward glucose oxidation away from fatty acid oxidation. Why this particularly occurred during smoking cessation remains unknown but is in line with anecdotal evidence of glucose craving after smoking cessation. Whether this is a cardiac-specific adaptation or is associated with changes in whole-body change toward glucose oxidation deserves further study.

We observed long-chain and very-long-chain highly unsaturated triacylglycerols concentrations after 2 weeks of smoke cessation compared to control and smoking. Excess storage of triacylglycerols is associated with insulin resistance and mitochondrial abnormalities in skeletal muscle,[38,39] cardiac hypertrophy,[35] and ultimately a reduced ventricular function.[40] Serum triacylglycerol concentration is also higher in patients with COPD,[41] and serum diacylglycerols and triacylglycerols were negatively associated with skeletal muscle oxidative capacity in patients with severe COPD.[42] Since severity of COPD is negatively associated with plasma sphingolipid concentrations,[43] we also observed lower tissue concentrations of sphingomyelin SM(t33:0) and ceramide Cer(d44:3) in smoking compared to control. Furthermore, there were several ceramides and hexosylceramides with significantly lower concentrations after smoking cessation in comparison to control.

5 | Limitations of the study

Here, we highlight some limitations of this study that could be addressed in future studies. First, we did not measure systolic and diastolic function,[44] or local cardiac blood flow, to link our cellular and molecular alterations to cardiac function. The assessment of whole-body insulin sensitivity or glucose tolerance tests, as well as isotope-labelled substrate analyses, would have provided more depth into the whole-body and cardiac metabolic alterations upon smoking. Electron microscopy imaging of mitochondrial cristae and fragmentation was not performed[39] but could have added important new insights into the structural changes in mitochondrial morphology and function upon cigarette smoking and smoking cessation. Lastly, the contribution of the immune system was understudied, as the time course and exact nature of immune cell infiltration in the heart were something that we could not assess with the current study design.

6 | CONCLUSION

Here, we provide an in-depth analysis of the structural and metabolic alterations in the heart of mice exposed to cigarette smoke and follow the adjustments after smoking cessation, which were not enough to completely recover to the control level. Our cellular and molecular analyses show that smoking reduces maximal mitochondrial respiratory capacity and causes a metabolic shift away from fatty acid oxidation to glucose metabolism. These cellular adaptations are associated with alterations in antioxidant signalling, NAD^+ metabolism, and accumulation of long-chain unsaturated triacylglycerols. Smoking cessation normalized maximal mitochondrial capacity, partly due to increased assembly of mitochondrial supercomplexes. The local infiltration of macrophages confirms a local inflammatory environment that does not normalize after smoking cessation. The observation that cardiac fibrosis, local inflammation, and metabolic alterations remained after 2 weeks of smoking cessation could help to explain the increased risk for atherosclerosis, myocardial infarction, and arrhythmias in ex-smokers. These results contribute to a better understanding of the increased risk of cardiovascular diseases in patients with COPD and open the potential for finding new therapies to protect the heart during smoking and immediately after smoking cessation, as well as to develop new quit-smoking programs.

AUTHOR CONTRIBUTIONS
Rob C. I. Wüst: Conceptualization; investigation; funding acquisition; writing – original draft; writing – review and editing; project administration; supervision; visualization; formal analysis; methodology. **Jekaterina Aid:** Conceptualization; methodology; software; investigation; formal analysis; funding acquisition; visualization; writing – original draft; writing – review and editing. **Ajime Tom Tanjeko:** Conceptualization; investigation; writing – review and editing; project administration. **Jef Serré:** Conceptualization; investigation; writing – review and editing. **Moritz Eggelbusch:** Investigation; formal analysis; visualization; writing – review and editing; methodology. **Wendy Noort:** Investigation; visualization; formal analysis; methodology; writing – review and editing. **Gerard M. J. de Wit:** Methodology; investigation; writing – review and editing. **Michel van Weeghel:** Writing – review and editing; visualization; investigation. **Marju Puurand:** Funding acquisition; writing – review and editing; supervision; conceptualization. **Kersti Tepp:** Funding acquisition; writing – review and editing; supervision; conceptualization. **Ghislaine Gayan-Ramirez:** Conceptualization; methodology; investigation; supervision; project administration; writing – review and editing; funding acquisition. **Hans Degens:** Conceptualization; investigation; methodology; writing – review and editing; project administration; supervision. **Tuuli Käämbre:** Writing – review and editing; funding acquisition; supervision; conceptualization.

CONFLICT OF INTEREST STATEMENT

The authors do not declare conflicts of interest.

DATA AVAILABILITY STATEMENT

Data and material are available upon request from the corresponding author.

ORCID

Jekaterina Aid https://orcid.org/0000-0003-4533-7179
Ajime Tom Tanjeko https://orcid.org/0000-0002-8779-8929
Jef Serré https://orcid.org/0000-0002-9562-3416
Moritz Eggelbusch https://orcid.org/0000-0002-4006-4063
Wendy Noort https://orcid.org/0000-0002-3578-7611
Michel van Weeghel https://orcid.org/0000-0002-4916-2866
Marju Puurand https://orcid.org/0000-0002-0083-3390
Kersti Tepp https://orcid.org/0000-0001-7367-6632
Ghislaine Gayan-Ramirez https://orcid.org/0000-0001-9652-7437
Hans Degens https://orcid.org/0000-0001-7399-4841
Tuuli Käämbre https://orcid.org/0000-0001-5755-4694
Rob C. I. Wüst https://orcid.org/0000-0003-3781-5177

REFERENCES

1. Lundback B, Lindberg A, Lindstrom M, et al. Not 15 but 50% of smokers develop COPD?—Report from the obstructive lung disease in Northern Sweden studies. *Respir Med.* 2003;97(2):115-122.
2. Axson EL, Ragutheeswaran K, Sundaram V, et al. Hospitalisation and mortality in patients with comorbid COPD and heart failure: a systematic review and meta-analysis. *Respir Res.* 2020;21(1):54.
3. Ahmed AA, Patel K, Nyaku MA, et al. Risk of heart failure and death after prolonged smoking cessation: role of amount and duration of prior smoking. *Circ Heart Fail.* 2015;8(4):694-701.
4. Degens H, Gayan-Ramirez G, van Hees HW. Smoking-induced skeletal muscle dysfunction: from evidence to mechanisms. *Am J Respir Crit Care Med.* 2015;191(6):620-625.
5. Sanders KJ, Kneppers AE, van de Bool C, Langen RC, Schols AM. Cachexia in chronic obstructive pulmonary disease: new insights and therapeutic perspective. *J Cachexia Sarcopenia Muscle.* 2016;7(1):5-22.
6. Wüst RCI, Degens H. Factors contributing to muscle wasting and dysfunction in COPD patients. *Int J Chron Obstruct Pulmon Dis.* 2007;2(3):289-300.
7. Wüst RCI, Morse CI, de Haan A, Rittweger J, Jones DA, Degens H. Skeletal muscle properties and fatigue resistance in relation to smoking history. *Eur J Appl Physiol.* 2008;104(1):103-110.
8. Booth FW, Gordon SE, Carlson CJ, Hamilton MT. Waging war on modern chronic diseases: primary prevention through exercise biology. *J Appl Physiol (1985).* 2000;88(2):774-787.
9. Gosker HR, Langen RC, Bracke KR, et al. Extrapulmonary manifestations of chronic obstructive pulmonary disease in a mouse model of chronic cigarette smoke exposure. *Am J Respir Cell Mol Biol.* 2009;40(6):710-716.
10. Wüst RC, Jaspers RT, van der Laarse WJ, Degens H. Skeletal muscle capillarization and oxidative metabolism in healthy smokers. *Appl Physiol Nutr Metab.* 2008;33(6):1240-1245.
11. Ajime TT, Serre J, Wüst RCI, et al. Two weeks of smoking cessation reverse cigarette smoke-induced skeletal muscle atrophy and mitochondrial dysfunction in mice. *Nicotine Tob Res.* 2021;23(1):143-151.
12. Darabseh MZ, Maden-Wilkinson TM, Welbourne G, et al. Fourteen days of smoking cessation improves muscle fatigue resistance and reverses markers of systemic inflammation. *Sci Rep.* 2021;11(1):12286.
13. Nogueira L, Trisko BM, Lima-Rosa FL, et al. Cigarette smoke directly impairs skeletal muscle function through capillary regression and altered myofibre calcium kinetics in mice. *J Physiol.* 2018;596(14):2901-2916.
14. Hendriks T, van Dijk R, Alsabaan NA, van der Harst P. Active tobacco smoking impairs cardiac systolic function. *Sci Rep.* 2020;10(1):6608.
15. Jensen BL, Persson PB. Good publication practice in physiology 2021. *Acta Physiol (Oxf).* 2022;234(1):e13741.
16. Loncar G, Springer J, Anker M, Doehner W, Lainscak M. Cardiac cachexia: hic et nunc. *J Cachexia Sarcopenia Muscle.* 2016;7(3):246-260.
17. Mazzone P, Tierney W, Hossain M, Puvenna V, Janigro D, Cucullo L. Pathophysiological impact of cigarette smoke exposure on the cerebrovascular system with a focus on the blood-brain barrier: expanding the awareness of smoking toxicity in an underappreciated area. *Int J Environ Res Public Health.* 2010;7(12):4111-4126.
18. Oishi Y, Manabe I. Macrophages in inflammation, repair and regeneration. *Int Immunol.* 2018;30(11):511-528.
19. Shi A, Hillege MMG, Wüst RCI, Wu G, Jaspers RT. Synergistic short-term and long-term effects of TGF-beta1 and 3 on collagen production in differentiating myoblasts. *Biochem Biophys Res Commun.* 2021;547:176-182.
20. Eggelbusch M, Shi A, Broeksma BC, et al. The NLRP3 inflammasome contributes to inflammation-induced morphological and metabolic alterations in skeletal muscle. *J Cachexia Sarcopenia Muscle.* 2022;13(6):3048-3061.
21. McDonald LT, Zile MR, Zhang Y, et al. Increased macrophage-derived SPARC precedes collagen deposition in myocardial fibrosis. *Am J Physiol Heart Circ Physiol.* 2018;315(1):H92-H100.
22. Gonzalez A, Lopez B, Ravassa S, San Jose G, Diez J. The complex dynamics of myocardial interstitial fibrosis in heart failure. Focus on collagen cross-linking. *Biochim Biophys Acta Mol Cell Res.* 2019;1866(9):1421-1432.
23. Petersen AM, Magkos F, Atherton P, et al. Smoking impairs muscle protein synthesis and increases the expression of myostatin and MAFbx in muscle. *Am J Physiol Endocrinol Metab.* 2007;293(3):E843-E848.
24. Holecek M. Branched-chain amino acids in health and disease: metabolism, alterations in blood plasma, and as supplements. *Nutr Metab (Lond).* 2018;15:33.

25. Prisco SZ, Rose L, Potus F, et al. Excess protein O-GlcNAcylation links metabolic derangements to right ventricular dysfunction in pulmonary arterial hypertension. *Int J Mol Sci*. 2020;21(19):7278.

26. Swain JL, Sabina RL, Peyton RB, Jones RN, Wechsler AS, Holmes EW. Derangements in myocardial purine and pyrimidine nucleotide metabolism in patients with coronary artery disease and left ventricular hypertrophy. *Proc Natl Acad Sci U S A*. 1982;79(2):655-659.

27. Yki-Jarvinen H, Virkamaki A, Daniels MC, McClain D, Gottschalk WK. Insulin and glucosamine infusions increase O-linked N-acetyl-glucosamine in skeletal muscle proteins in vivo. *Metabolism*. 1998;47(4):449-455.

28. Kondo T, Hayashi M, Takeshita K, et al. Smoking cessation rapidly increases circulating progenitor cells in peripheral blood in chronic smokers. *Arterioscler Thromb Vasc Biol*. 2004;24(8):1442-1447.

29. Nollet EE, Duursma I, Rozenbaum A, et al. Mitochondrial dysfunction in human hypertrophic cardiomyopathy is linked to cardiomyocyte architecture disruption and corrected by improving NADH-driven mitochondrial respiration. *Eur Heart J*. 2023;44(13):1170-1185.

30. Anwar MR, Saldana-Caboverde A, Garcia S, Diaz F. The Organization of Mitochondrial Supercomplexes is modulated by oxidative stress in vivo in mouse models of mitochondrial encephalopathy. *Int J Mol Sci*. 2018;19(6):1582.

31. Tong D, Schiattarella GG, Jiang N, et al. NAD(+) repletion reverses heart failure with preserved ejection fraction. *Circ Res*. 2021;128(11):1629-1641.

32. Dolle C, Rack JG, Ziegler M. NAD and ADP-ribose metabolism in mitochondria. *FEBS J*. 2013;280(15):3530-3541.

33. Yaku K, Okabe K, Nakagawa T. NAD metabolism: implications in aging and longevity. *Ageing Res Rev*. 2018;47:1-17.

34. Smith RL, Soeters MR, Wüst RCI, Houtkooper RH. Metabolic flexibility as an adaptation to energy resources and requirements in health and disease. *Endocr Rev*. 2018;39(4):489-517.

35. Makrecka-Kuka M, Liepinsh E, Murray AJ, et al. Altered mitochondrial metabolism in the insulin-resistant heart. *Acta Physiol (Oxf)*. 2020;228(3):e13430.

36. McGarrah RW, Crown SB, Zhang GF, Shah SH, Newgard CB. Cardiovascular Metabolomics. *Circ Res*. 2018;122(9):1238-1258.

37. Tulen CBM, Wang Y, Beentjes D, et al. Dysregulated mitochondrial metabolism upon cigarette smoke exposure in various human bronchial epithelial cell models. *Dis Model Mech*. 2022;15(3):dmm049247.

38. Kelley DE, Goodpaster BH. Skeletal muscle triglyceride. An aspect of regional adiposity and insulin resistance. *Diabetes Care*. 2001;24(5):933-941.

39. Eggelbusch M, Charlton BT, Bosutti A, et al. The impact of bed rest on human skeletal muscle metabolism. *Cell Rep Med*. 2024;5(1):101372.

40. Ge F, Hu C, Hyodo E, et al. Cardiomyocyte triglyceride accumulation and reduced ventricular function in mice with obesity reflect increased long chain fatty acid uptake and de novo fatty acid synthesis. *J Obes*. 2012;2012:205648.

41. Xuan L, Han F, Gong L, et al. Association between chronic obstructive pulmonary disease and serum lipid levels: a meta-analysis. *Lipids Health Dis*. 2018;17(1):263.

42. Li R, Adami A, Chang CC, Tseng CH, Hsiai TK, Rossiter HB. Serum Acylglycerols inversely associate with muscle oxidative capacity in severe COPD. *Med Sci Sports Exerc*. 2021;53(1):10-18.

43. Bowler RP, Jacobson S, Cruickshank C, et al. Plasma sphingolipids associated with chronic obstructive pulmonary disease phenotypes. *Am J Respir Crit Care Med*. 2015;191(3):275-284.

44. Wüst RCI, Coolen BF, Held NM, et al. The antibiotic doxycycline impairs cardiac mitochondrial and contractile function. *Int J Mol Sci*. 2021;22(8):4100.

SUPPORTING INFORMATION

Additional supporting information can be found online in the Supporting Information section at the end of this article.

Curriculum vitae

Personal data

Name:	Jekaterina Aid
Date of birth:	28.04.1984
Place of birth:	Tallinn, Estonia
Citizenship:	Estonian

Contact data

E-mail:	jekaterina.aid@gmail.com

Education

2018–2024	Tallinn University of Technology, PhD study, Department of Chemistry and Biotechnology
2011–2015	University of Tartu, M.Sc. in Gene Technology
2003–2011	University of Tartu, B.Sc. in Molecular Biology
1991–2003	Tallinn Karjamaa gymnasium

Language competence

Russian	Native Speaker
English	Fluent
Estonian	Fluent

Professional employment

2018–present	National Institute of Chemical Physics and Biophysics, Tallinn, Estonia, Junior Researcher
2016–2018	Institute of Agricultural and Environmental Sciences, Estonian University of Life Science, Tartu, Estonia, Junior Researcher
2014–2016	Synlab Eesti OÜ, Tallinn, Estonia, Analyst of Cytology in Gynaecology

Workshops

2019	Laboratory Animal Science, Estonian University of Life Sciences
2019	Basic Science Summer School, European Accreditation Council for Continuing Medical Education, European Society of Cardiology
2018	Multivariate Data Analysis Using PC-ORD, Estonian University of Life Sciences
2018	Molecular methods for detection of food- and waterborne pathogens, University of Helsinki, Faculty of Veterinary Medicine
2017	Sustainable insect management and disease control based on RNAi technology, University of Helsinki, Department of Agricultural Sciences
2017	Molecular Biology in Animal Sciences, Estonian University of Life Sciences
2015	Cervical cancer diagnostics – prevention and current status. Association of Estonian Biomedical Laboratory Scientists, Tallinn, Estonia

2015	Cervical cancer diagnostics – What is New? Estonian Society for Laboratory Medicine and Estonian Society for Colposcopy, Tallinn, Estonia
2014	Gynaecologic cytology; allergy. Association of Estonian Biomedical Laboratory Scientists, Tallinn, Estonia
2014	Gynaecologic cytology. Association of Estonian Biomedical Laboratory Scientists, Tartu, Estonia

Honours and Awards

2021	Conference award for the best poster presentation at SPS2021, Meeting of the Scandinavian Physiological Society, Stockholm, Sweden

Publications

Aid, J., Tanjeko, A. T., Serre, J., Eggelbusch, M., Noort, W., de Wit, G. M. J., van Weeghel, M., Puurand, M., Tepp, K., Gayan-Ramirez, G., Degens, H., Kaambre, T., & Wust, R. C. I. (2024). Smoking cessation only partially reverses cardiac metabolic and structural remodeling in mice. Acta Physiol (Oxf), 240(7), e14145. https://doi.org/10.1111/apha.14145

Tepp, K., Aid-Vanakova, J., Puurand, M., Timohhina, N., Reinsalu, L., Tein, K., Plaas, M., Shevchuk, I., Terasmaa, A., & Kaambre, T. (2022). Wolframin deficiency is accompanied with metabolic inflexibility in rat striated muscles. Biochem Biophys Rep, 30, 101250. https://doi.org/10.1016/j.bbrep.2022.101250

Tepp, K., Puurand, M., Timohhina, N., Aid-Vanakova, J., Reile, I., Shevchuk, I., Chekulayev, V., Eimre, M., Peet, N., Kadaja, L., Paju, K., & Kaambre, T. (2020). Adaptation of striated muscles to Wolframin deficiency in mice: Alterations in cellular bioenergetics. Biochim Biophys Acta Gen Subj, 1864(4), 129523. https://doi.org/10.1016/j.bbagen.2020.129523

Puurand, M., Tepp, K., Timohhina, N., Aid, J., Shevchuk, I., Chekulayev, V., & Kaambre, T. (2019). Tubulin betaII and betaIII Isoforms as the Regulators of VDAC Channel Permeability in Health and Disease. Cells, 8(3). https://doi.org/10.3390/cells8030239

Elulookirjeldus

Isikuandmed

Nimi:	Jekaterina Aid
Sünniaeg:	28.04.1984
Sünnikoht:	Tallinn, Eesti
Kodakondsus:	Eesti

Kontaktandmed

E-post:	jekaterina.aid@gmail.com

Hariduskäik

2018–2024	Tallinna Tehnikaülikool, Ph.D, Keemia ja Biotehnoloogia Instituut
2011–2015	Tartu Ülikool, M.Sc. geenitehnoloogias
2003–2011	Tartu Ülikool, B.Sc. molekulaarbioloogias
1991–2003	Tallinna Karjamaa gümnaasium

Keelteoskus

Vene keel	Emakeel
Inglise keel	Kõrgtase
Eesti keel	Kõrgtase

Teenistuskäik

2018–...	Keemilise ja bioloogilise füüsika instituut, nooremteadur
2016–2018	Eesti Maaülikool, Põllumajandus- ja keskkonnainstituut, nooremteadur
2014–2016	Synlab Eesti OÜ, tsütoloogia laborant

Täiendõpe

2019	Katseloomateadus, Maaülikool
2019	Alus-teaduste Suvekool, Euroopa Akrediteerimisnõukogu Jätkuva Meditsiinilise Hariduse jaoks, Euroopa Kardioloogide Selts
2018	Mitmemõõtmeline Andmeanalüüs PC-ORD abil, Eesti Maaülikool
2018	Molekulaarsed meetodid toidu- ja veepõhiste patogeenide tuvastamiseks, Helsingi Ülikool, Veterinaarmeditsiini Teaduskond
2017	Säästlik putukate tõrje ja haiguste kontroll RNAi tehnoloogia põhjal, Helsingi Ülikool, Põllumajandusteaduste Osakond
2017	Molekulaarbioloogia loomateadustes, Eesti Maaülikool
2015	Emakakaela diagnoostika – ennetus ja hetkeolukord, MTÜ Eesti Bioanalüütikute Ühing
2015	Emakakaelavähi diagnostika – mis on uut, Eesti Laborimeditsiini Ühing ja Eesti Kolposkoopia Ühing
2014	Vulva ja vulva haigused, atüüpiline endomeetrium, allergia, MTÜ Eesti Bioanalüütikute Ühing
2014	Güneko-tsütoloogia, MTÜ Eesti Bioanalüütikute Ühing

Teaduspreemiad ja tunnustused

2021   Konverentsiauhind   parima   poster   ettekande   eest
                rahvusvahelisel   konverentsil   SPS2021,   Skandinaavia
                Füsioloogia Seltsi koosolek, Stockholm, Rootsi

Publikatsioonid

Aid, J., Tanjeko, A. T., Serre, J., Eggelbusch, M., Noort, W., de Wit, G. M. J., van Weeghel, M., Puurand, M., Tepp, K., Gayan-Ramirez, G., Degens, H., Kaambre, T., & Wust, R. C. I. (2024). Smoking cessation only partially reverses cardiac metabolic and structural remodeling in mice. Acta Physiol (Oxf), 240(7), e14145. https://doi.org/10.1111/apha.14145

Tepp, K., Aid-Vanakova, J., Puurand, M., Timohhina, N., Reinsalu, L., Tein, K., Plaas, M., Shevchuk, I., Terasmaa, A., & Kaambre, T. (2022). Wolframin deficiency is accompanied with metabolic inflexibility in rat striated muscles. Biochem Biophys Rep, 30, 101250. https://doi.org/10.1016/j.bbrep.2022.101250

Tepp, K., Puurand, M., Timohhina, N., Aid-Vanakova, J., Reile, I., Shevchuk, I., Chekulayev, V., Eimre, M., Peet, N., Kadaja, L., Paju, K., & Kaambre, T. (2020). Adaptation of striated muscles to Wolframin deficiency in mice: Alterations in cellular bioenergetics. Biochim Biophys Acta Gen Subj, 1864(4), 129523. https://doi.org/10.1016/j.bbagen.2020.129523

Puurand, M., Tepp, K., Timohhina, N., Aid, J., Shevchuk, I., Chekulayev, V., & Kaambre, T. (2019). Tubulin betaII and betaIII Isoforms as the Regulators of VDAC Channel Permeability in Health and Disease. Cells, 8(3). https://doi.org/10.3390/cells8030239